On the Shift Invariance of Max Pooling Feature Maps in CNN

joint work with H. Leterme, K. Alahari et V. Perrier

Kévin Polisano

Convolutional neural networks

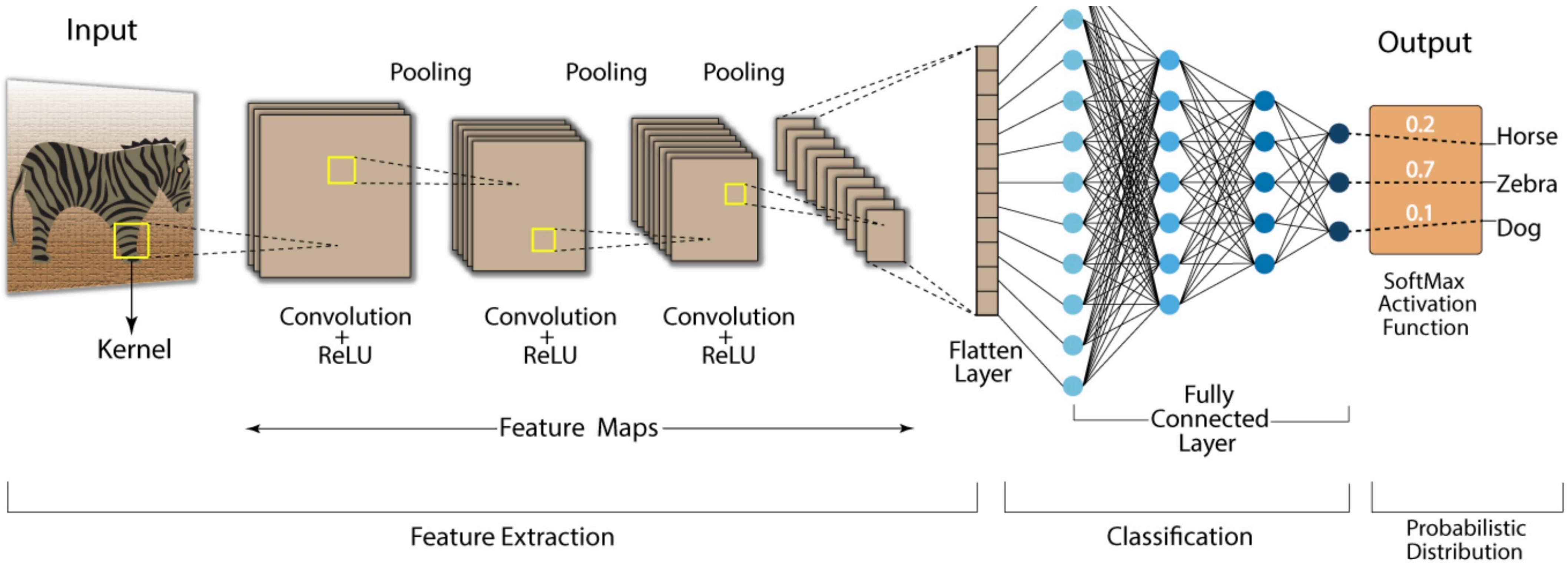

Source : https://developersbreach.com/convolution-neural-network-deep-learning/

Convolutional neural networks

- Image classification: feature vectors are fed into a linear classifier

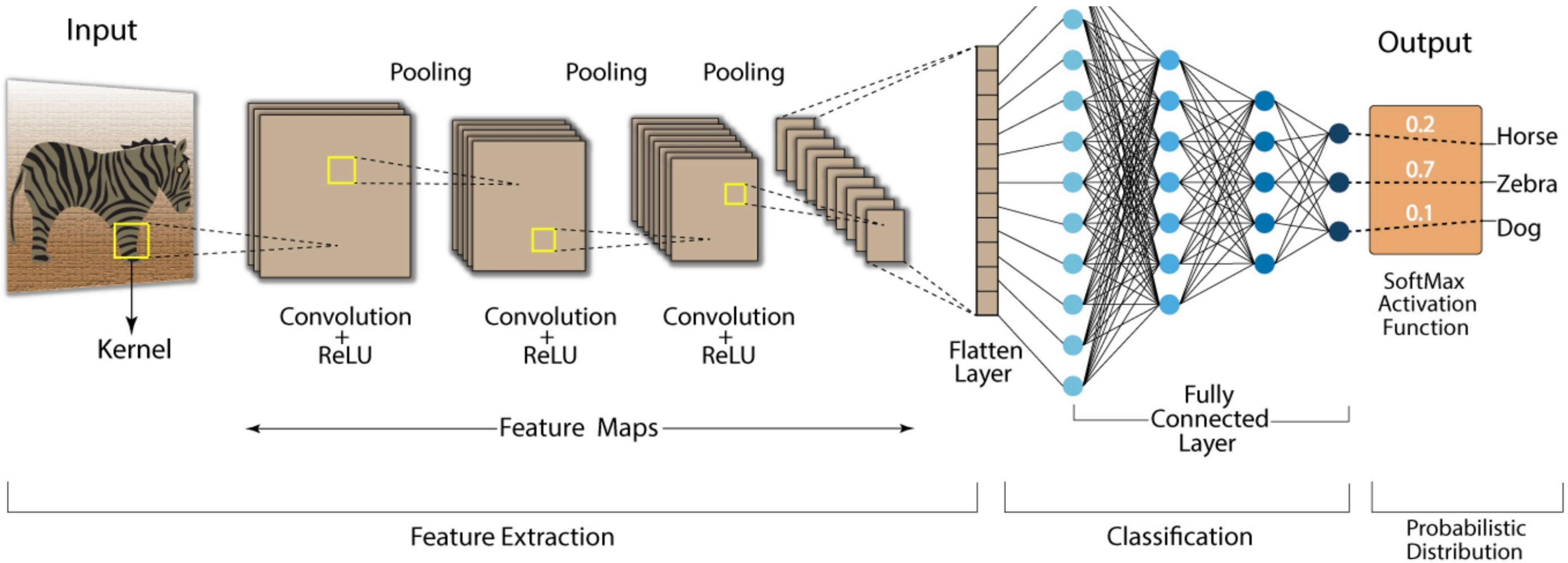

Source : https://developersbreach.com/convolution-neural-network-deep-learning/

Convolutional neural networks

- Image classification: feature vectors are fed into a linear classifier
- Desired property of CNN: to remain invariant to small translations

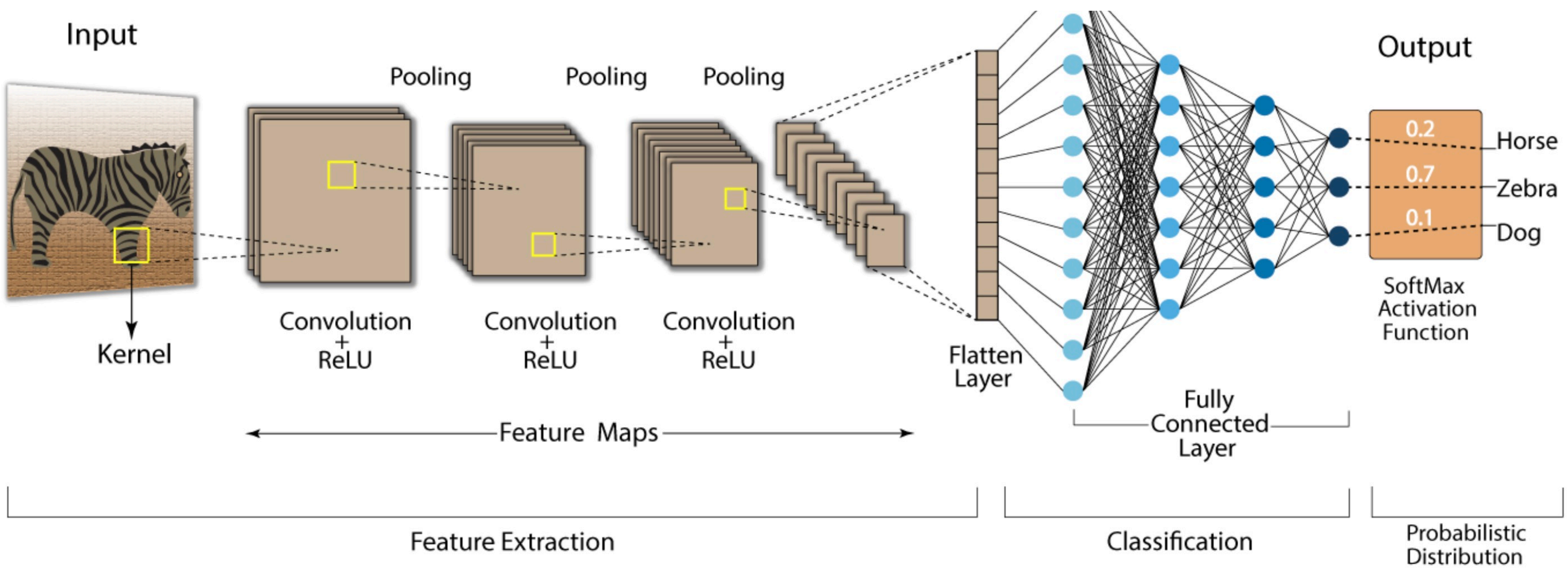

Source : https://developersbreach.com/convolution-neural-network-deep-learning/

Convolutional neural networks

- Image classification: feature vectors are fed into a linear classifier

- Desired property of CNN: to remain invariant to small translations

- Are extracted features maps stable to translations?

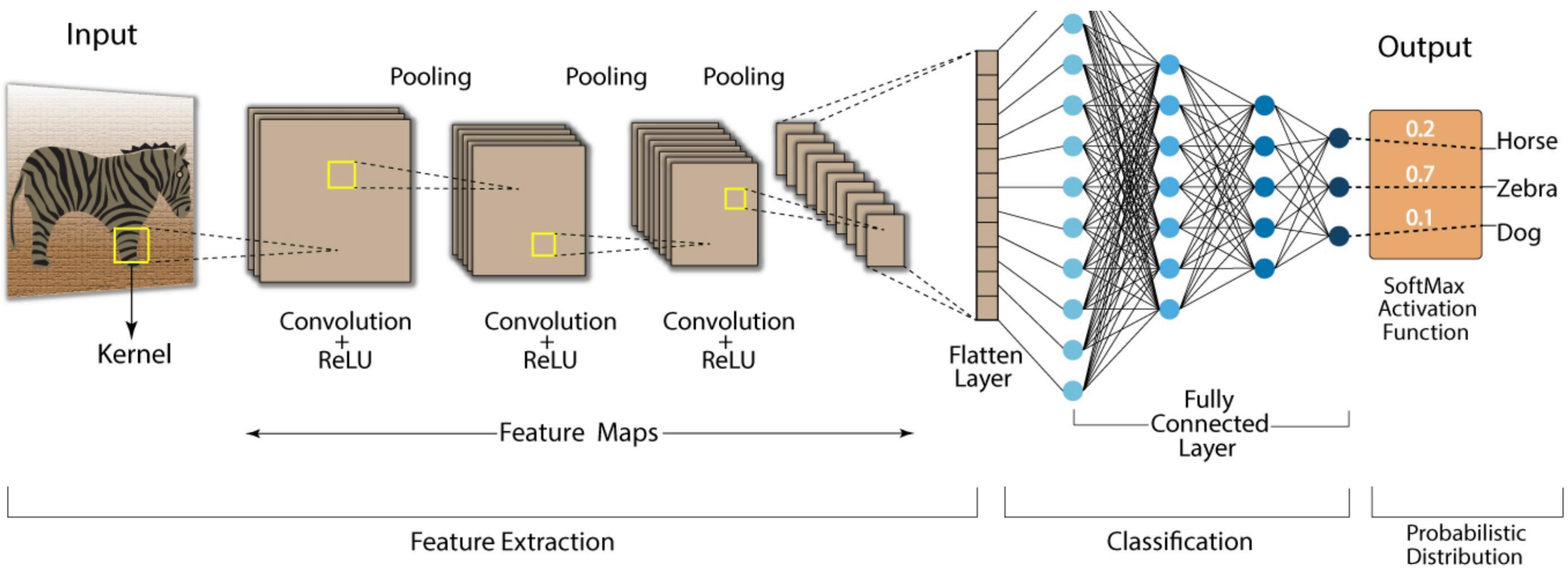

Source : https://developersbreach.com/convolution-neural-network-deep-learning/

Are CNNs shift-invariant?

My cat Ada

Are CNNs shift-invariant?

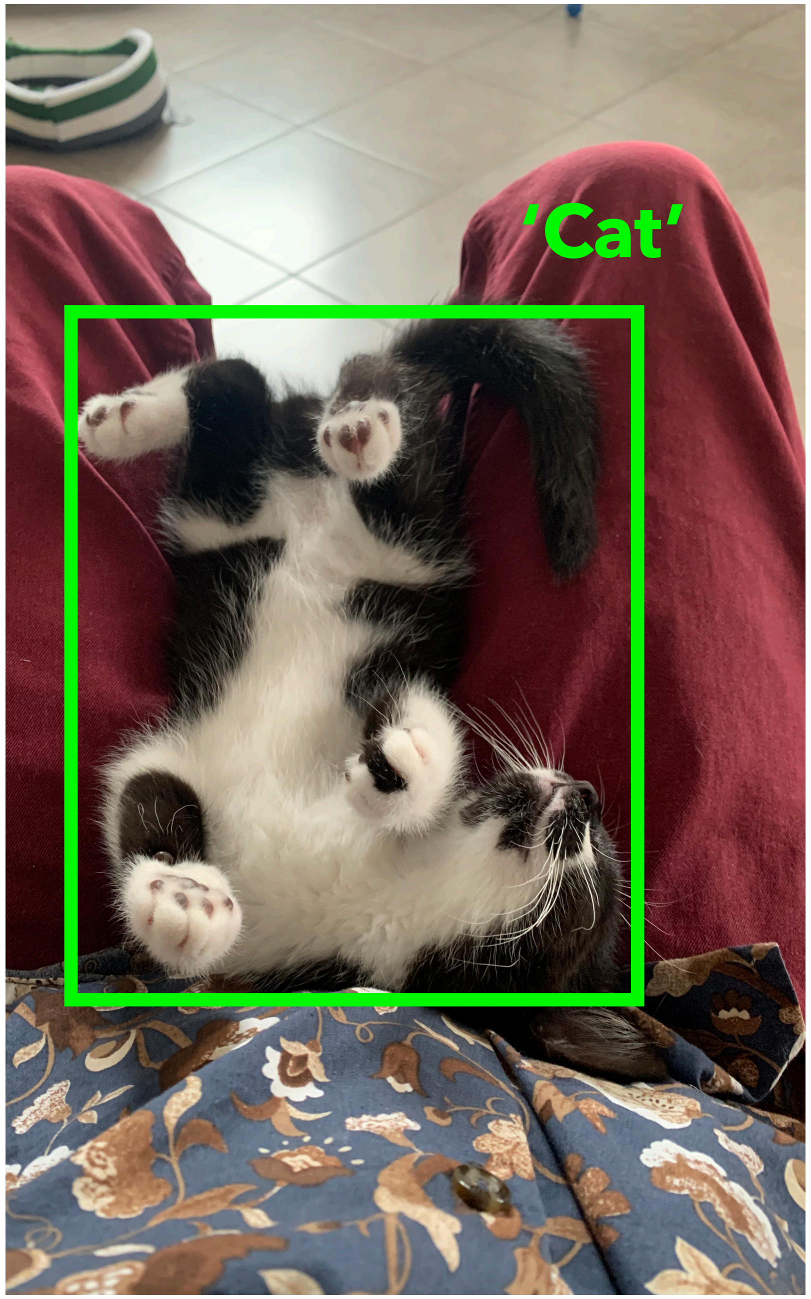

Are CNNs shift-invariant?

Are CNNs shift-invariant?

Are CNNs shift-invariant?

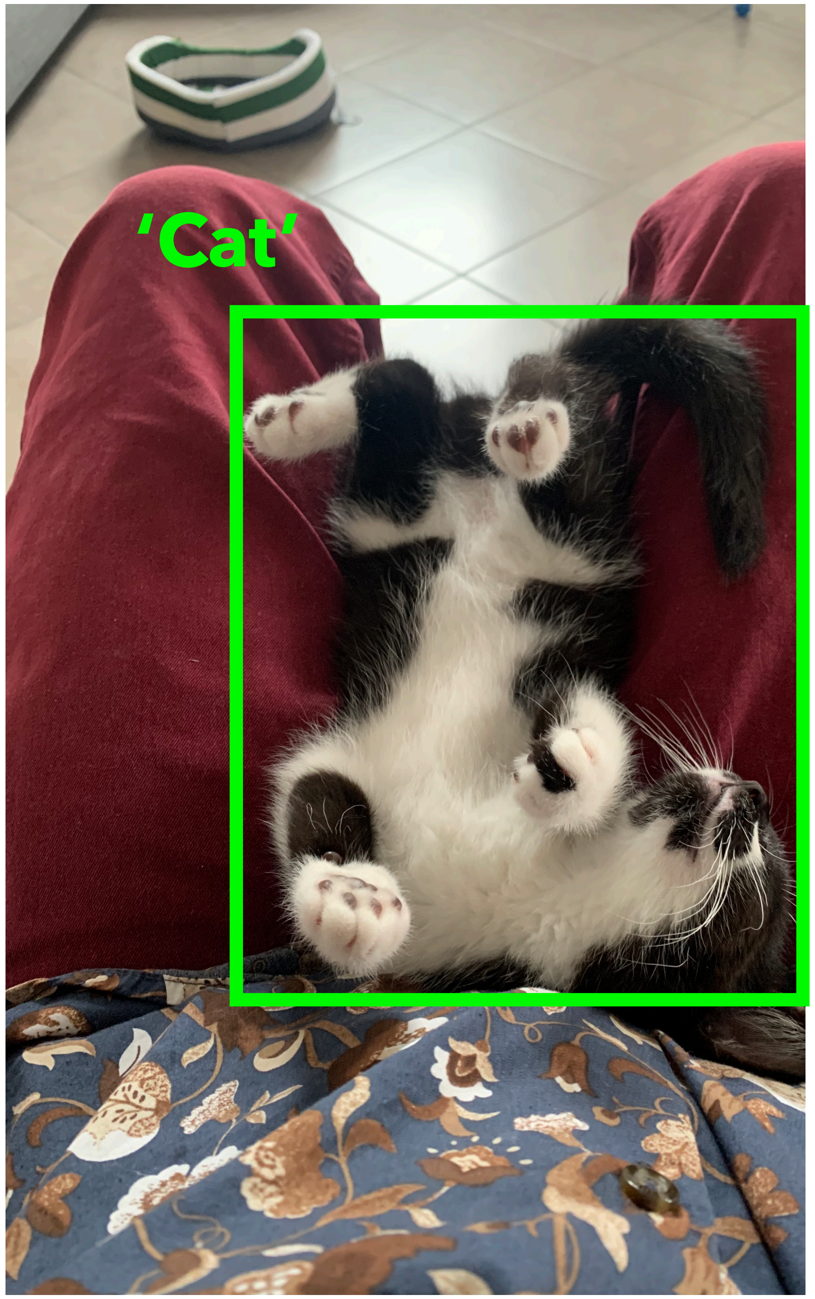

Are CNNs shift-invariant?

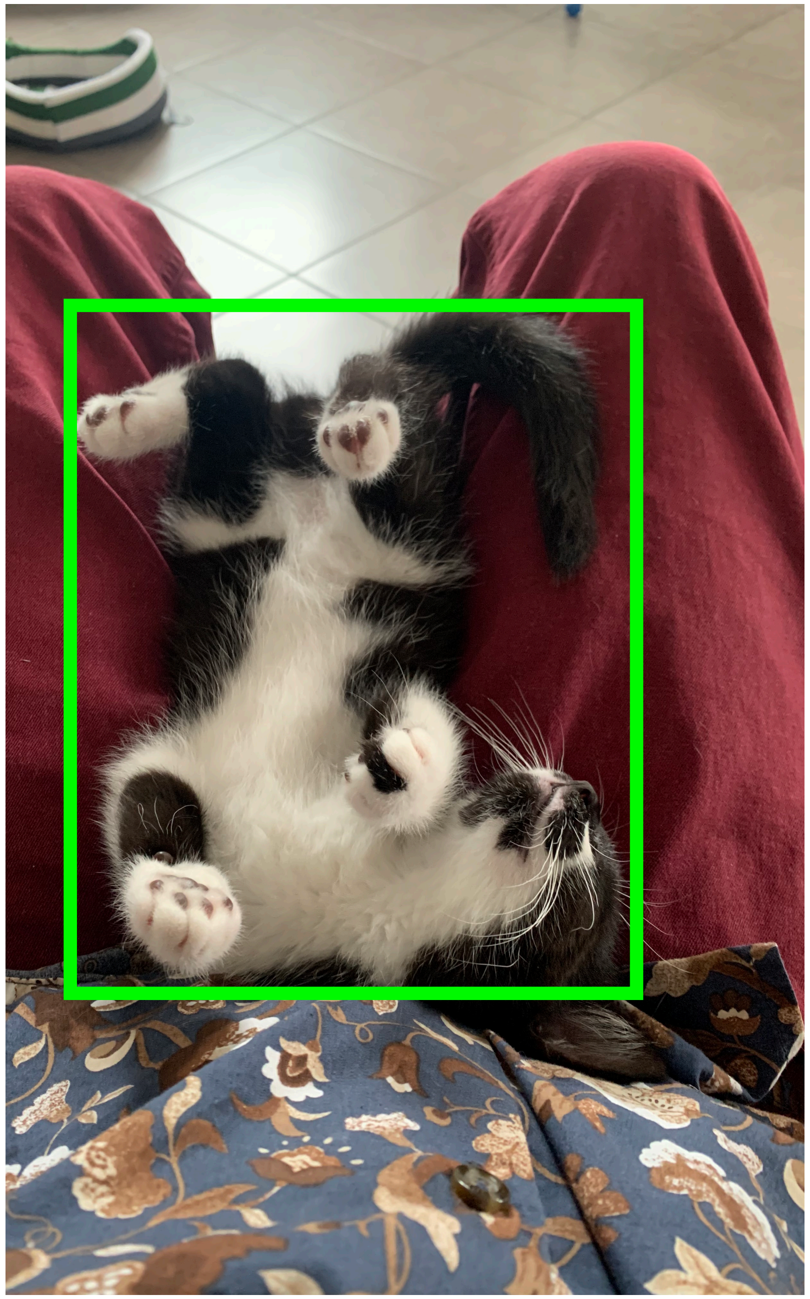

Are CNNs shift-invariant?

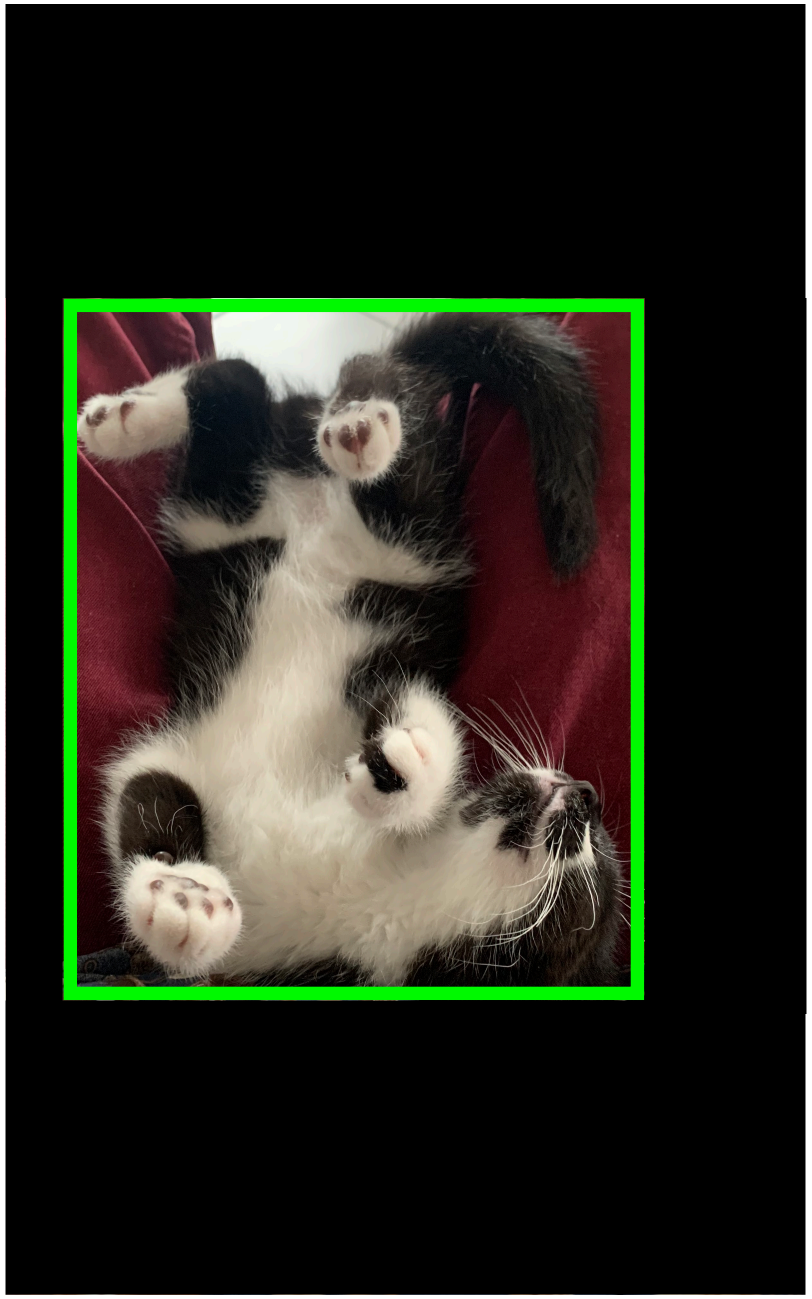

Are CNNs shift-invariant?

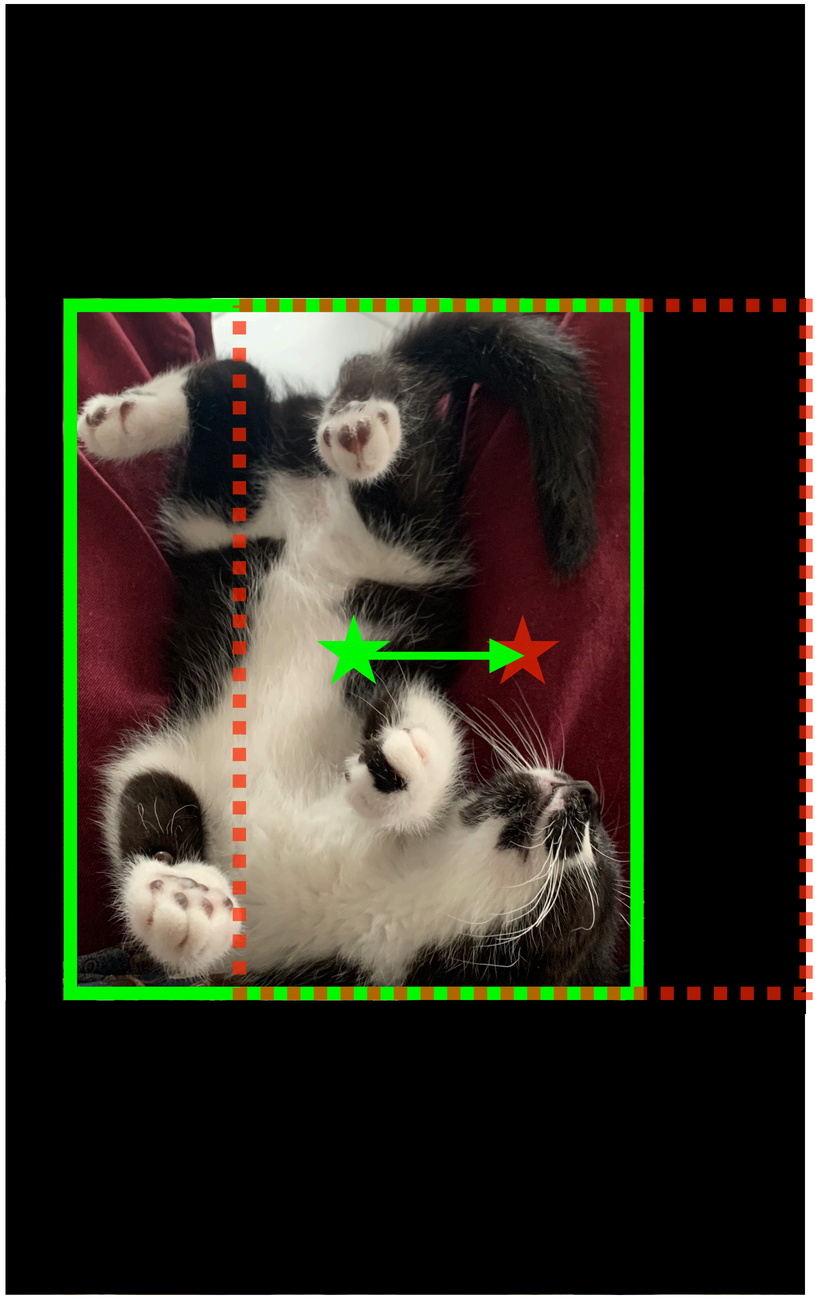

Are CNNs shift-invariant?

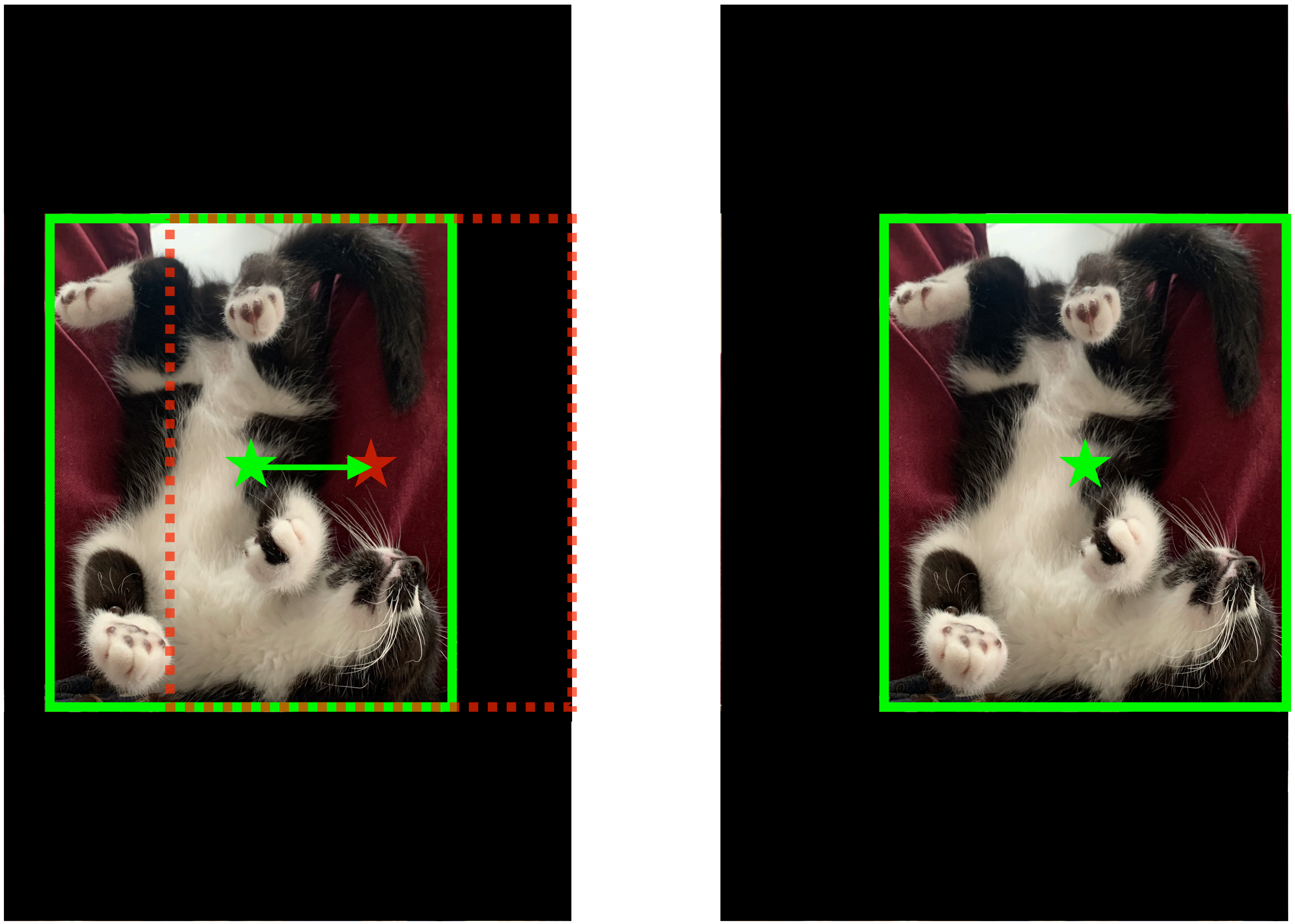

Are CNNs shift-invariant?

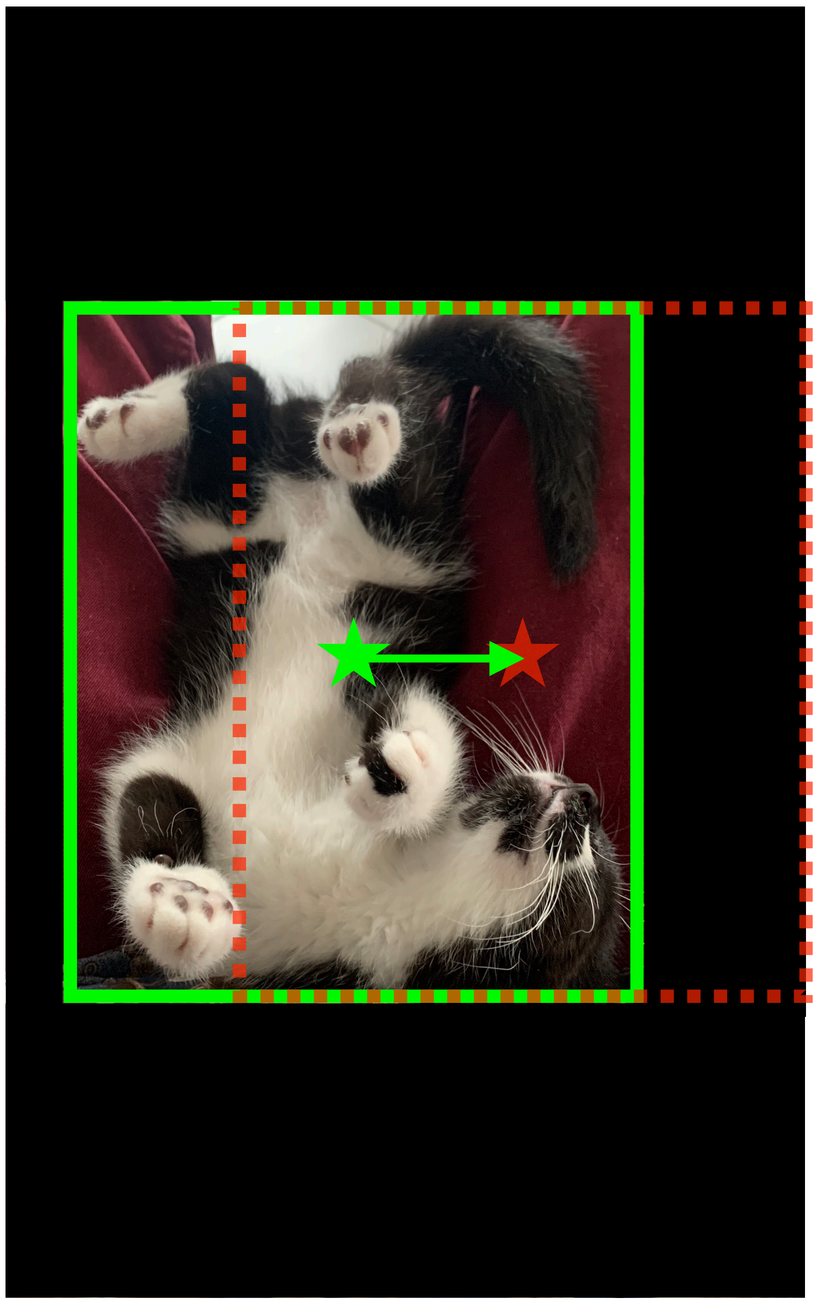

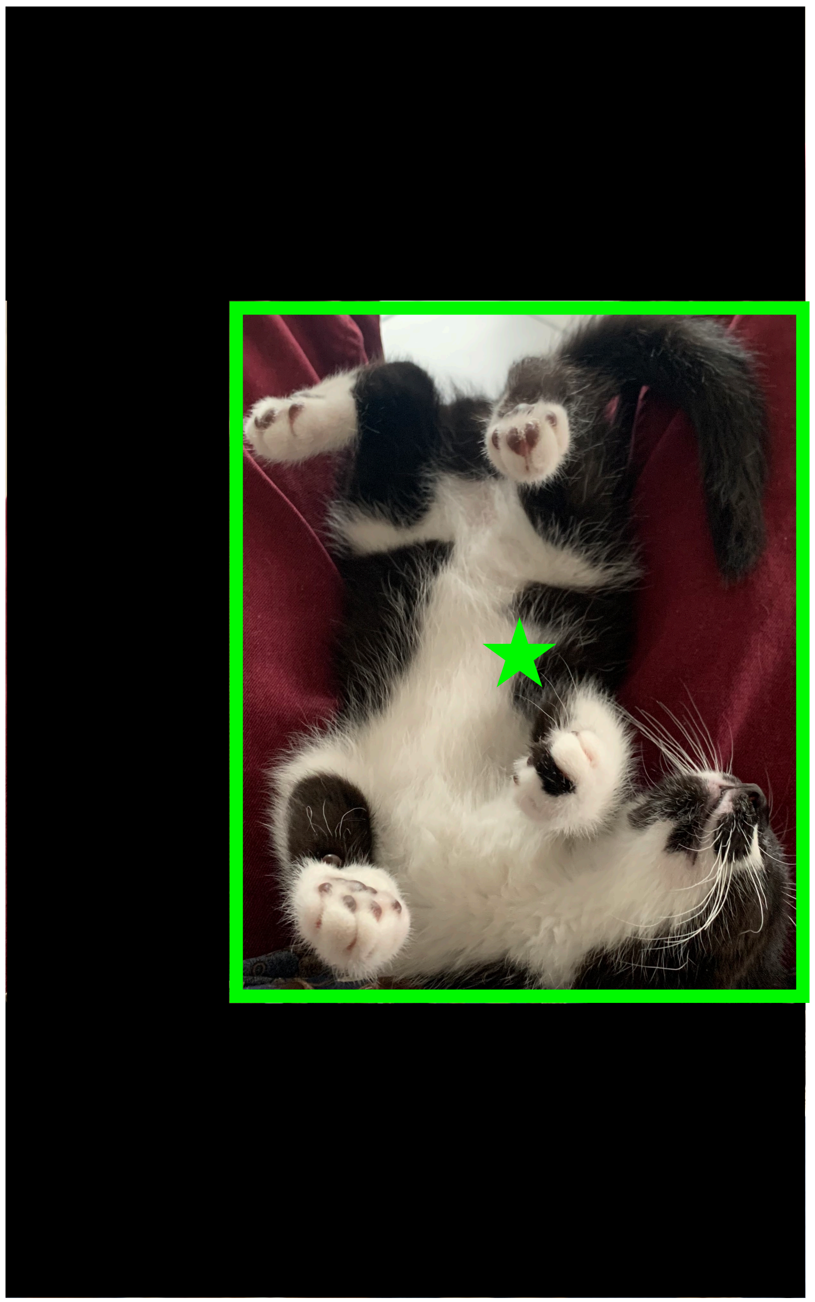

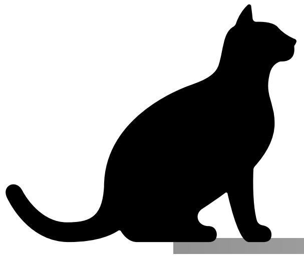

Shift invariance

Input image X | Shifted input $\mathcal{T}_{\boldsymbol{v}}\mathrm{X}$

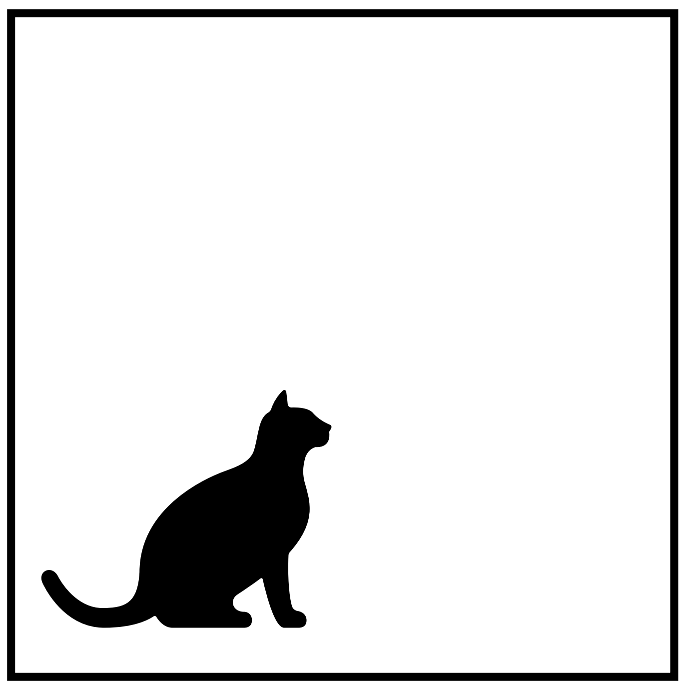

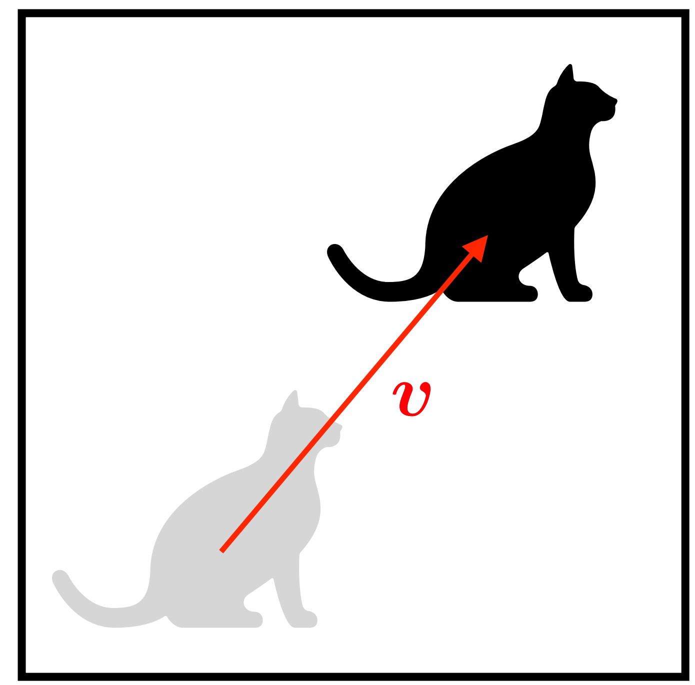

Output $f(\mathrm{X}) = 1$ | Output $f(\mathcal{T}_{\boldsymbol{v}}\mathrm{X}) = 1$

Shift invariance

Input image X Shifted input $\mathcal{T}_{\boldsymbol{v}}\mathrm{X}$

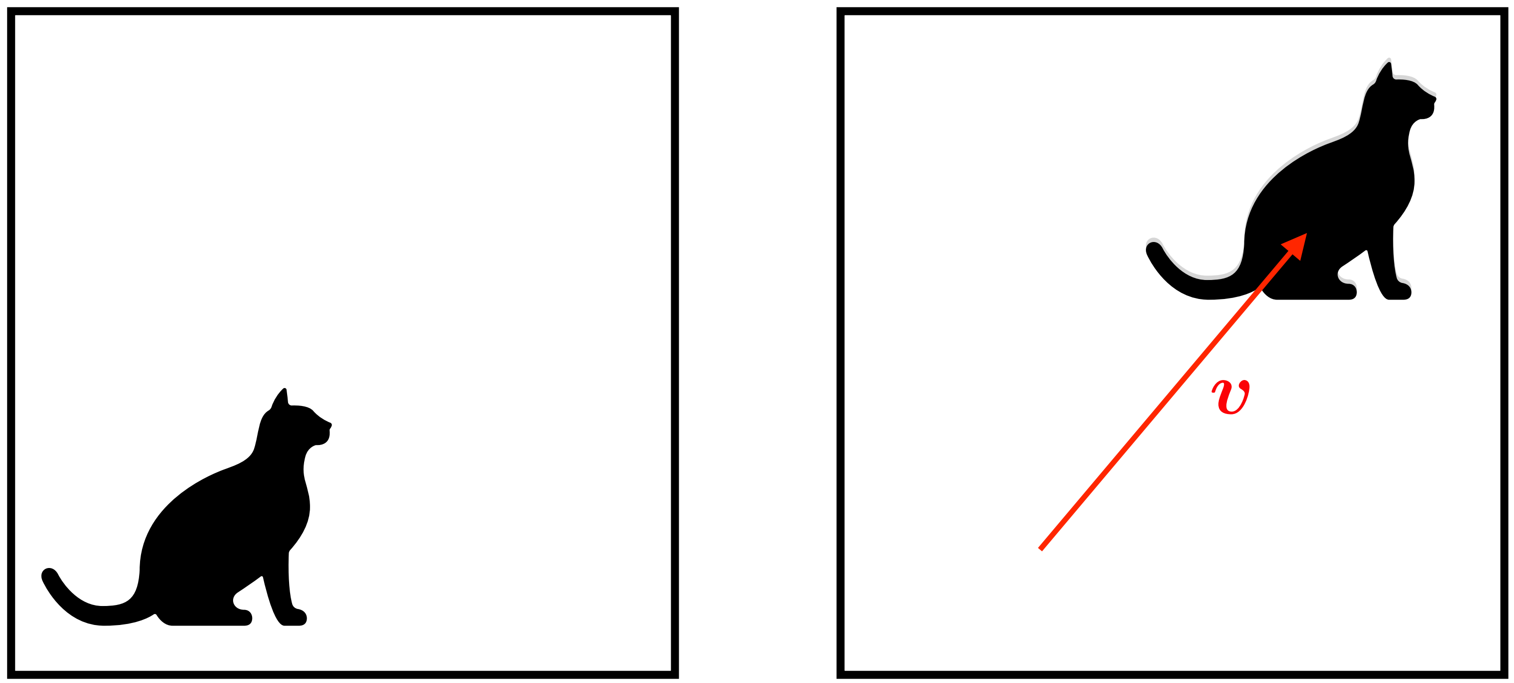

Output $f(\mathrm{X}) = 1$ Output $f(\mathcal{T}_{\boldsymbol{v}}\mathrm{X}) = 1$

How to make CNNs shift-invariant?

- **Trained invariance** by data augmentation

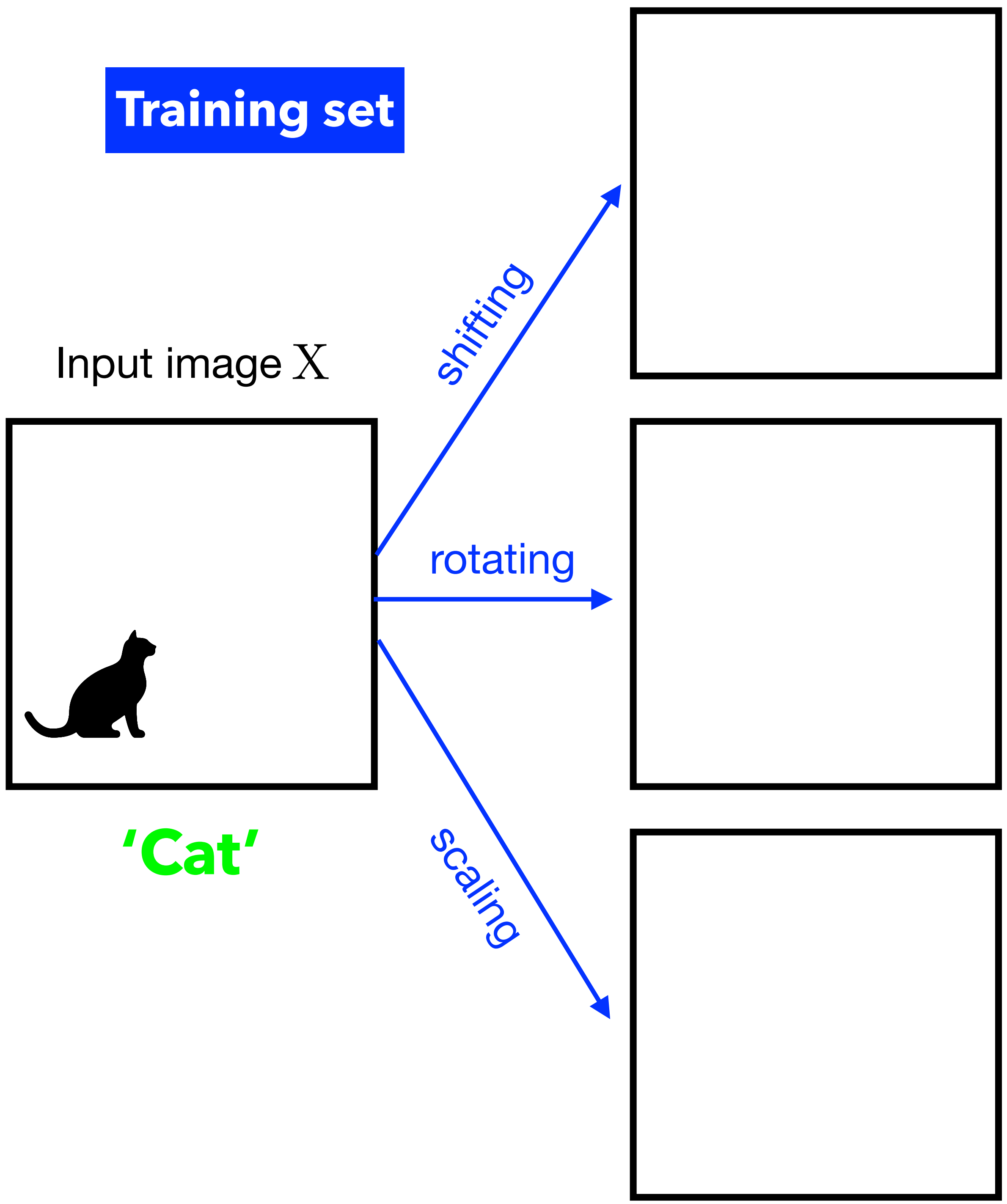

How to make CNNs shift-invariant?

- **Trained invariance** by data augmentation

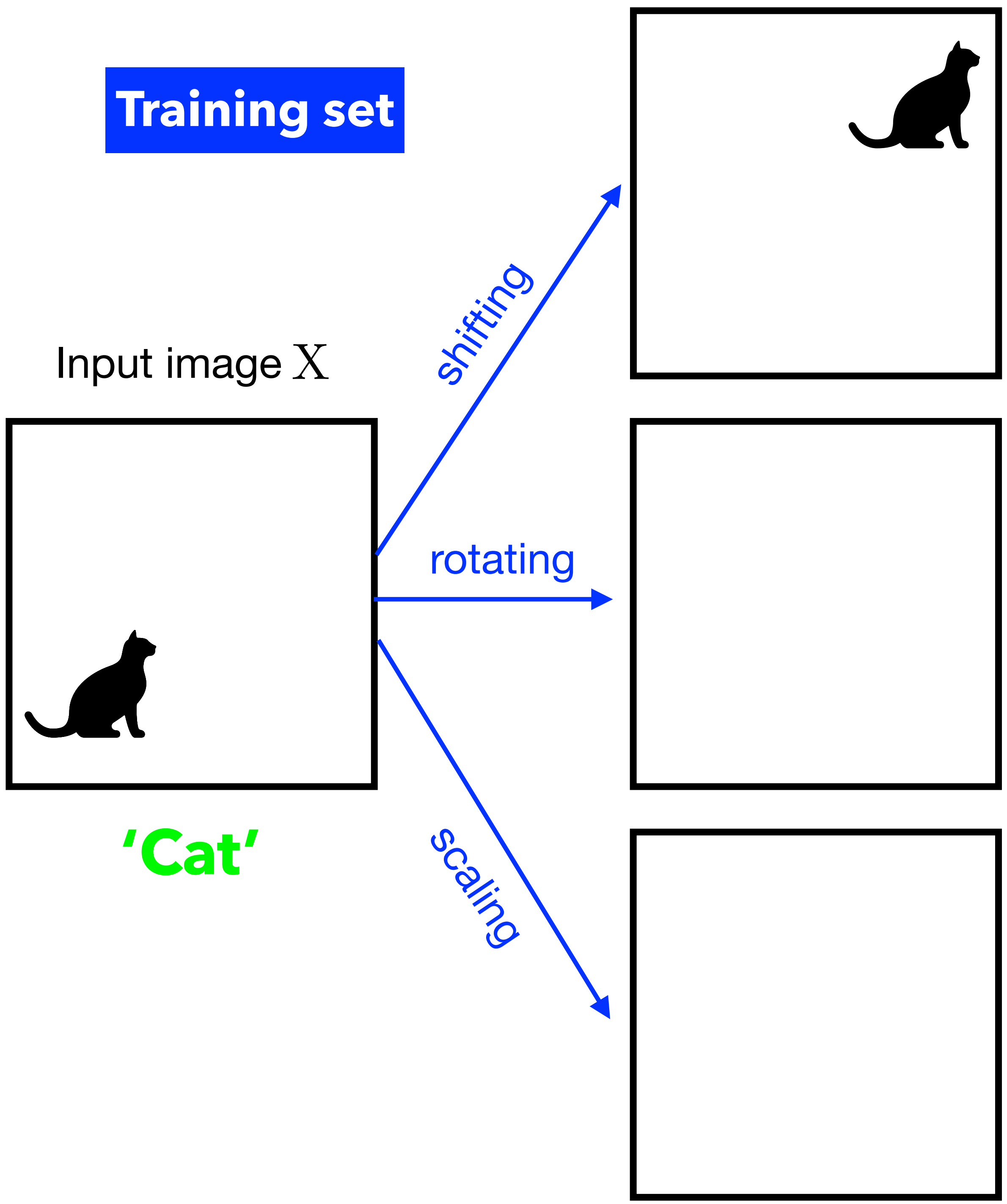

How to make CNNs shift-invariant?

- **Trained invariance** by data augmentation

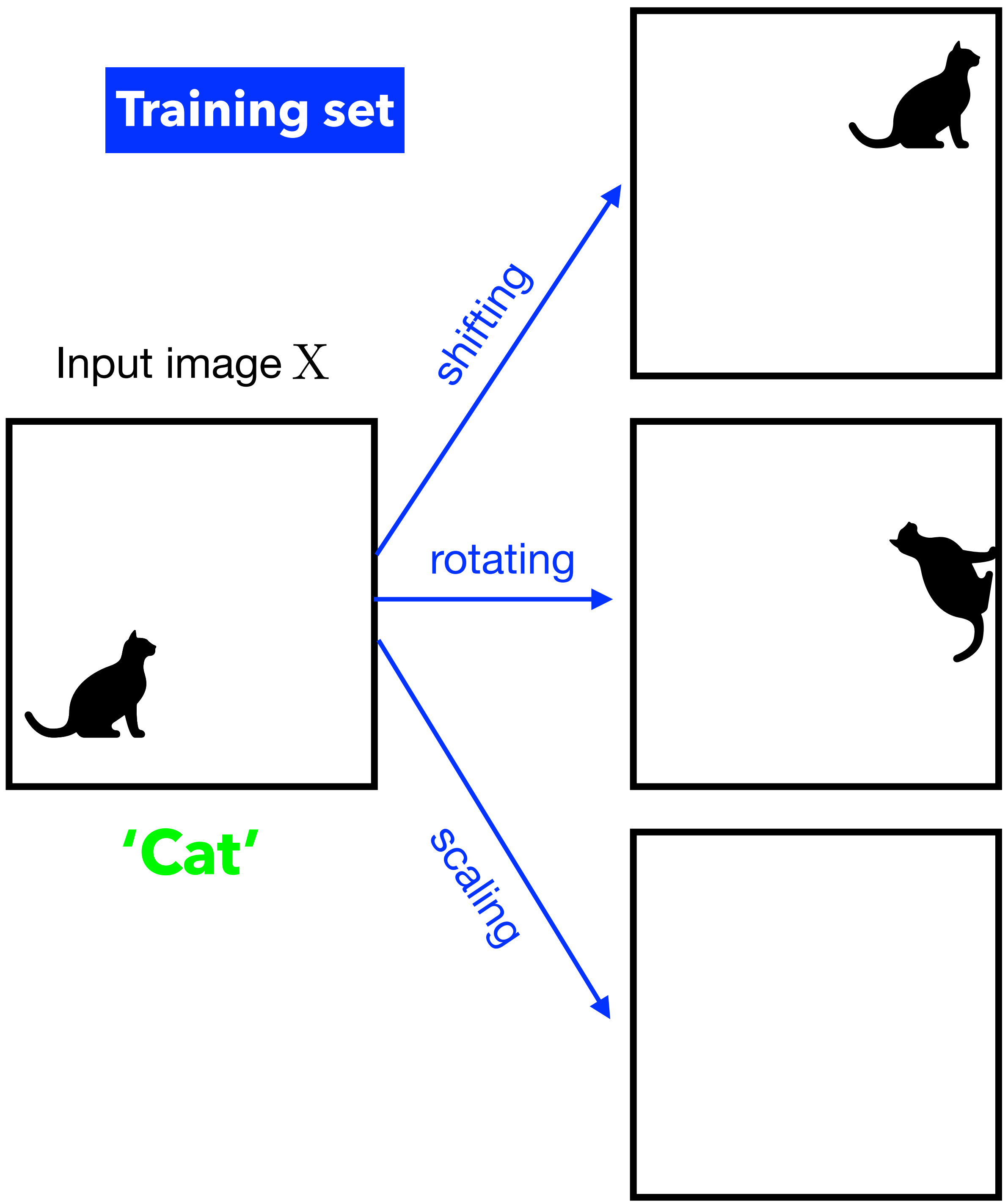

How to make CNNs shift-invariant?

- **Trained invariance** by data augmentation

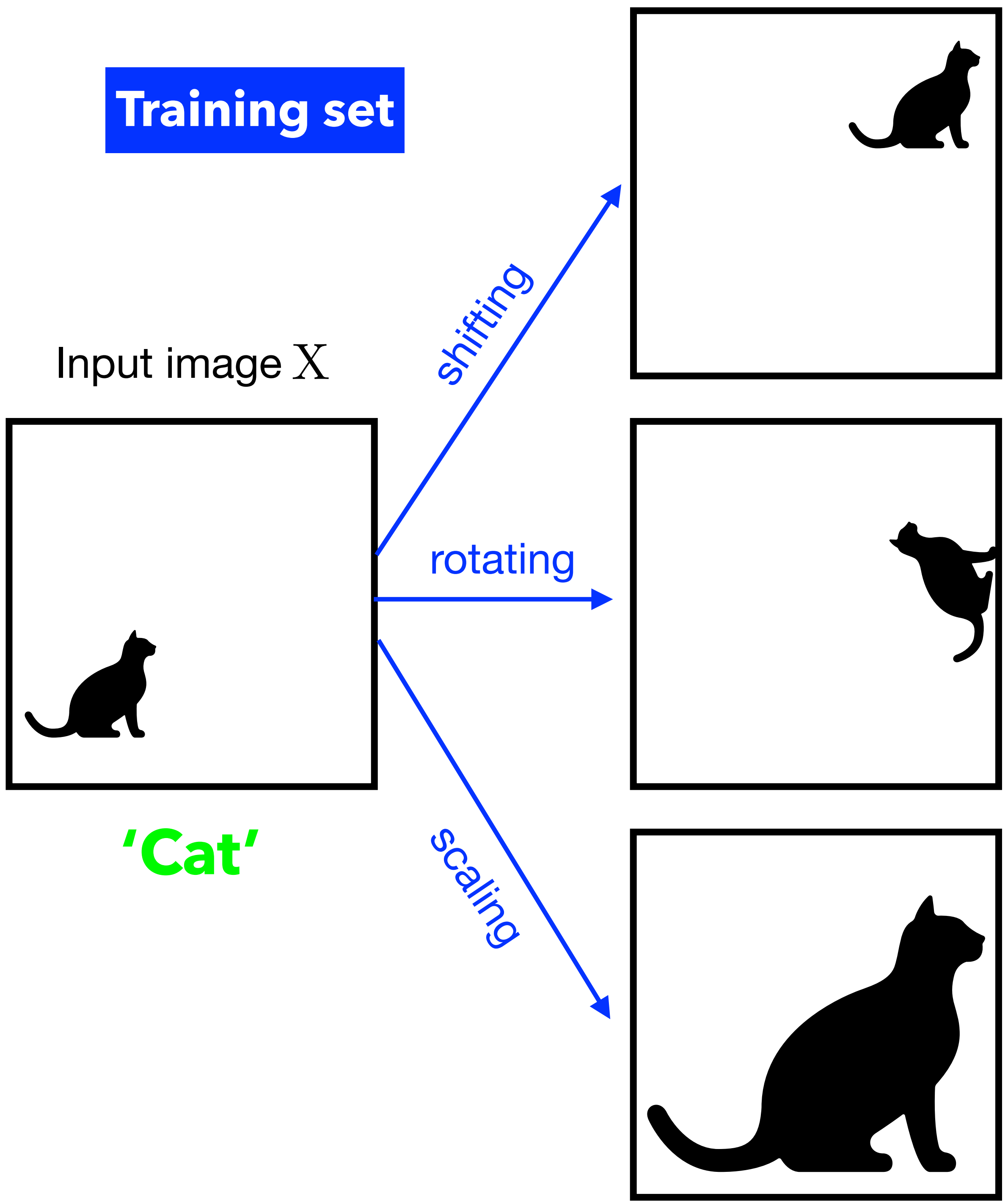

How to make CNNs shift-invariant?

- **Trained invariance** by data augmentation

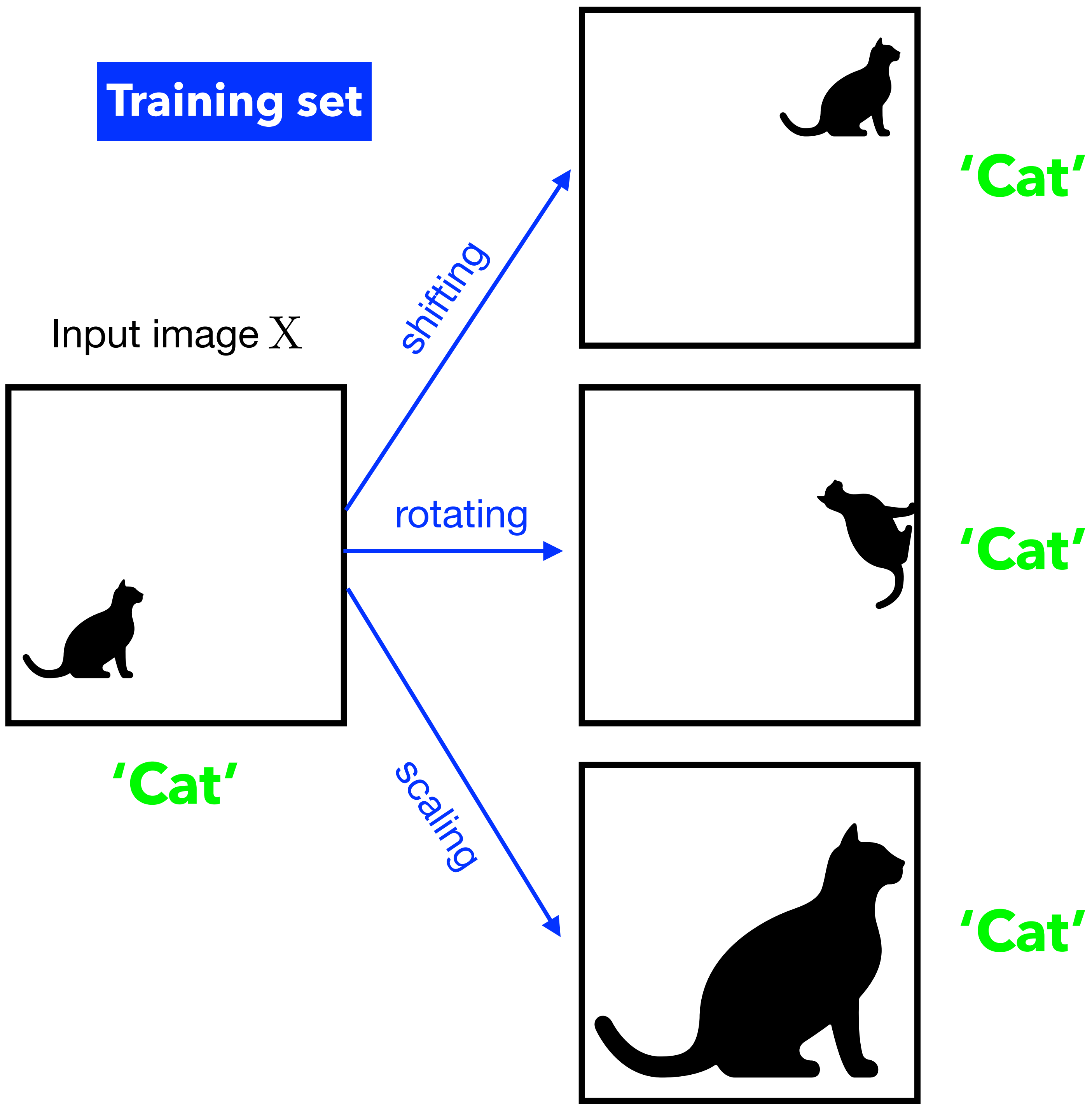

How to make CNNs shift-invariant?

- **Trained invariance** by data augmentation

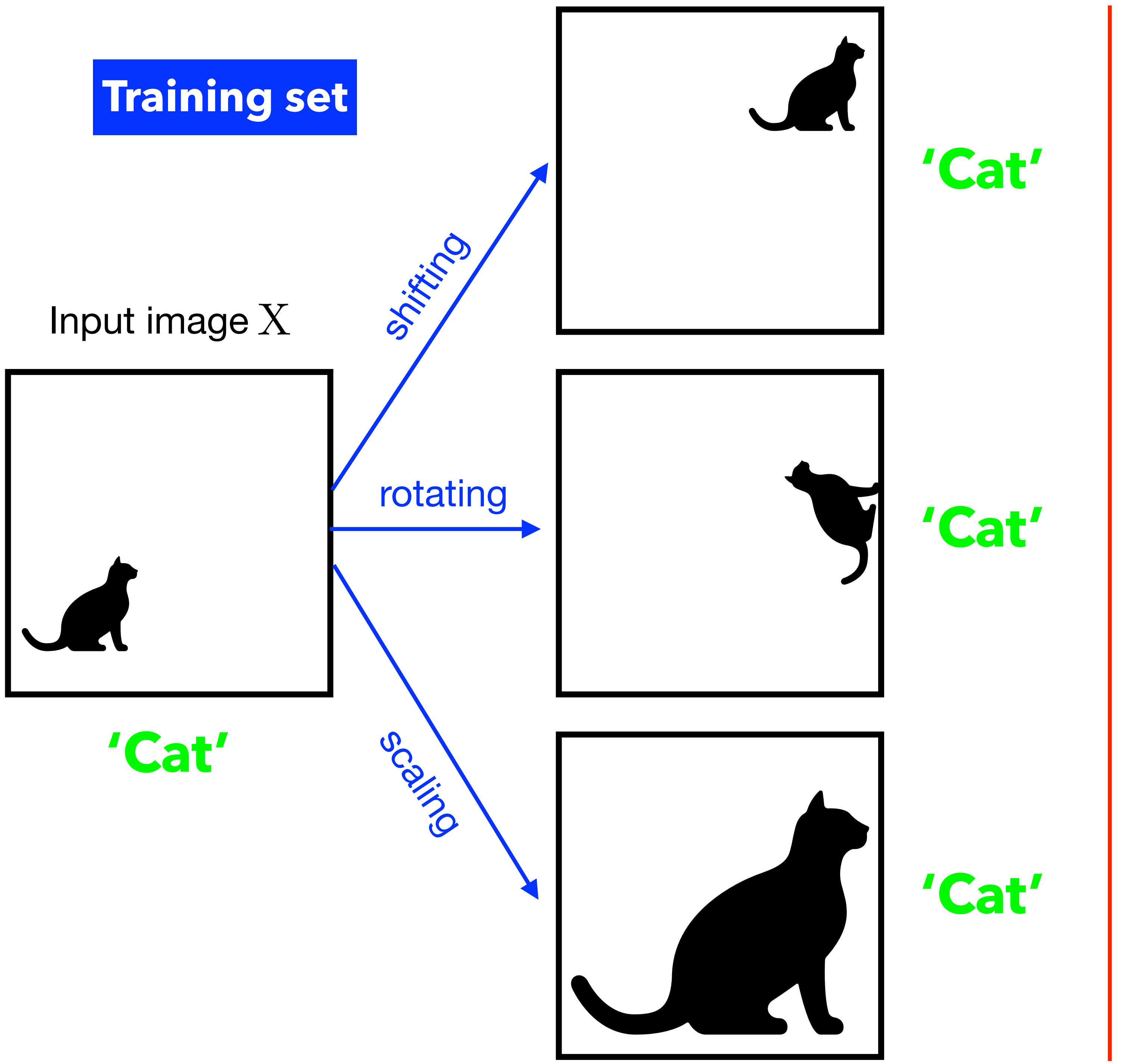

How to make CNNs shift-invariant?

- **Trained invariance** by data augmentation

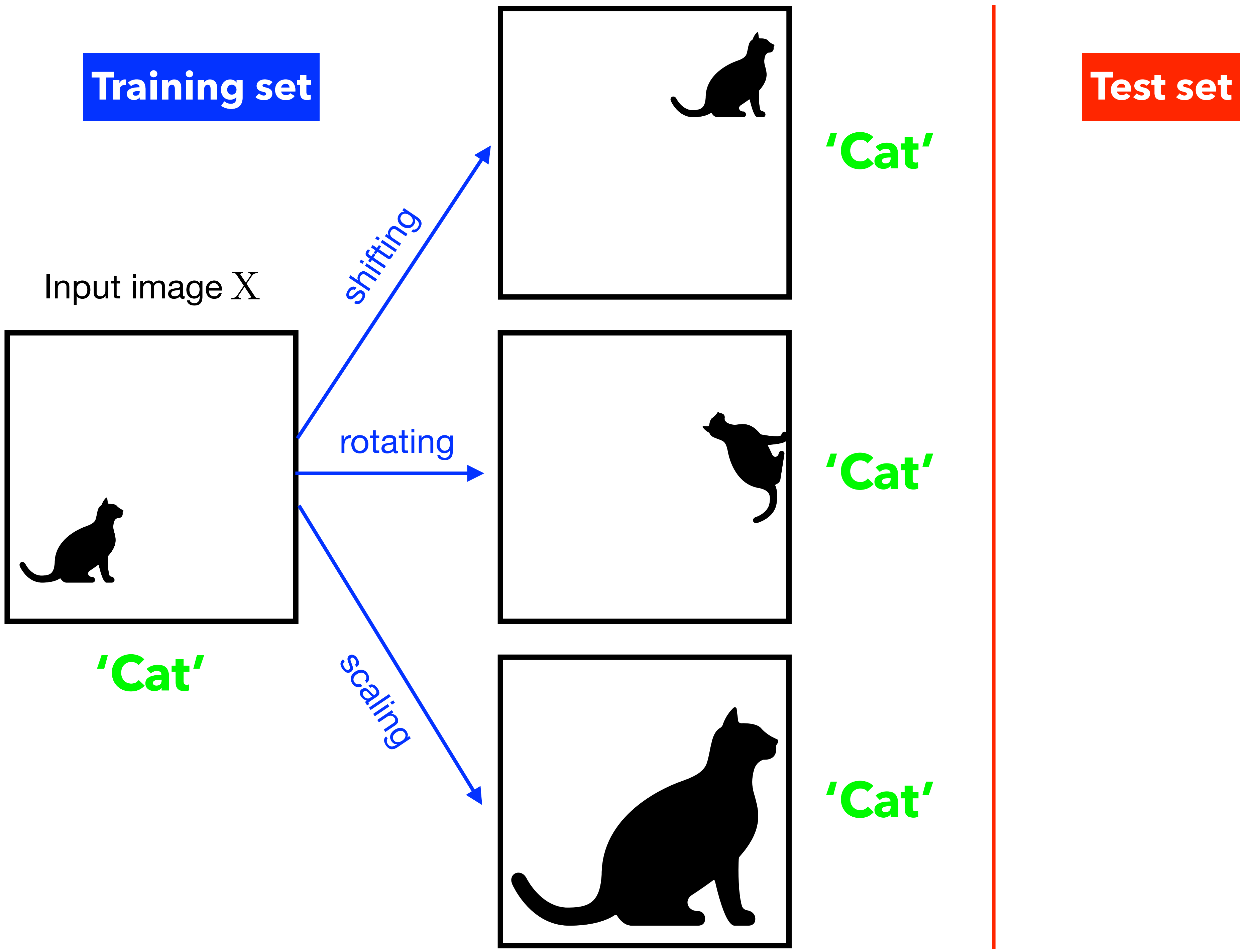

How to make CNNs shift-invariant?

- **Trained invariance** by data augmentation

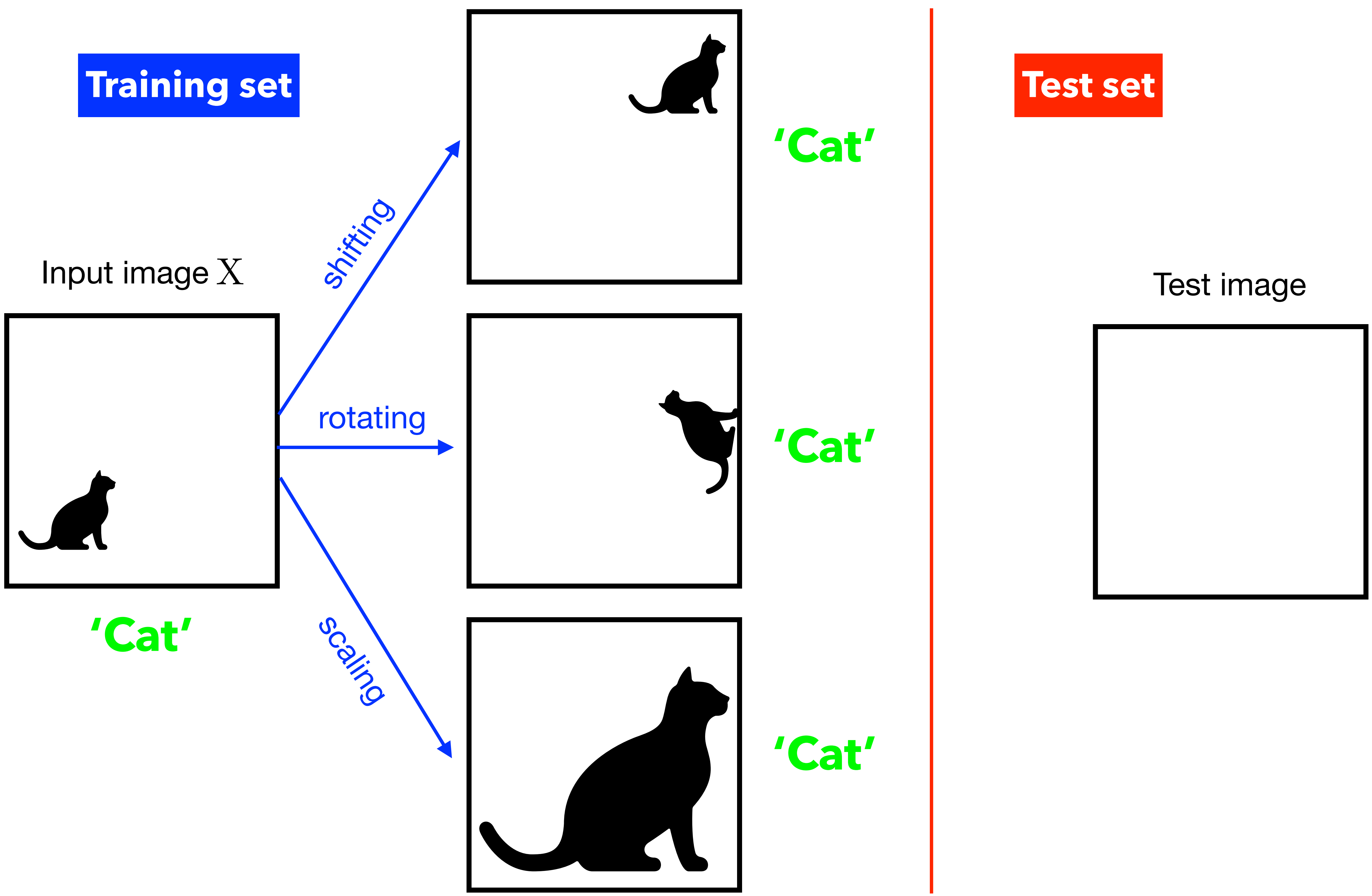

How to make CNNs shift-invariant?

- **Trained invariance** by data augmentation

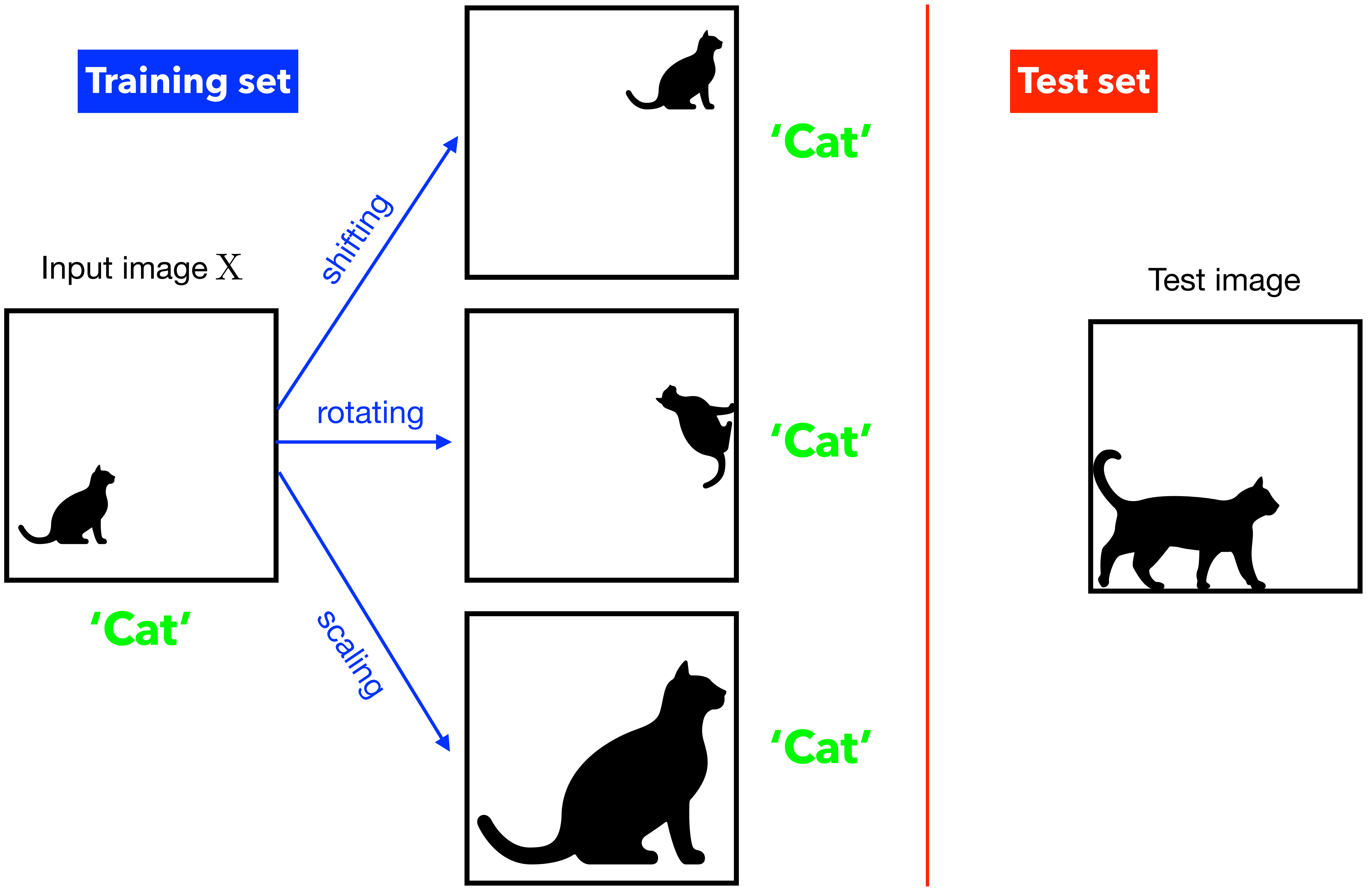

How to make CNNs shift-invariant?

- **Trained invariance** by data augmentation

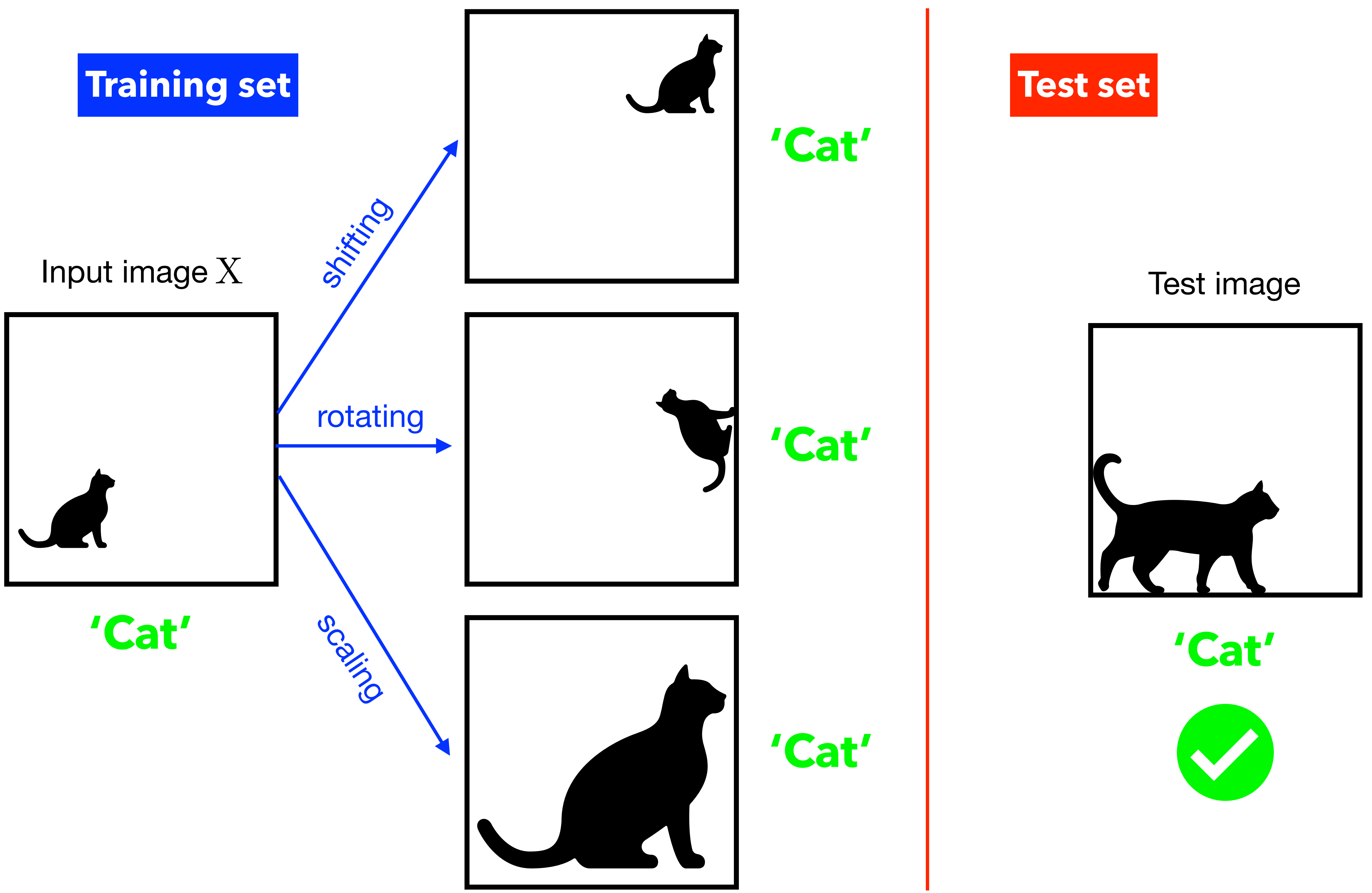

How to make CNNs shift-invariant?

- **Online invariance** at one-to-many locations

Training set

Input image X

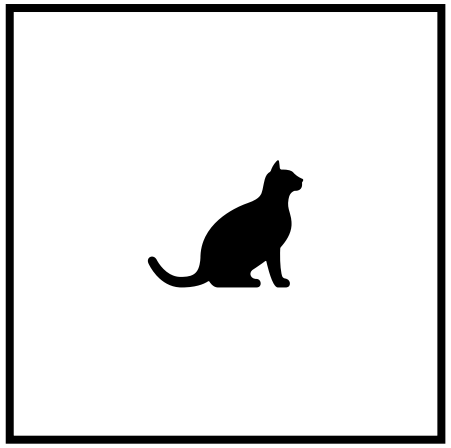

'Cat'

Input image X

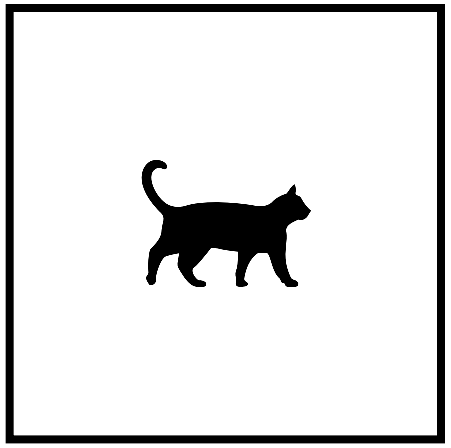

'Cat'

How to make CNNs shift-invariant?

- **Online invariance** at one-to-many locations

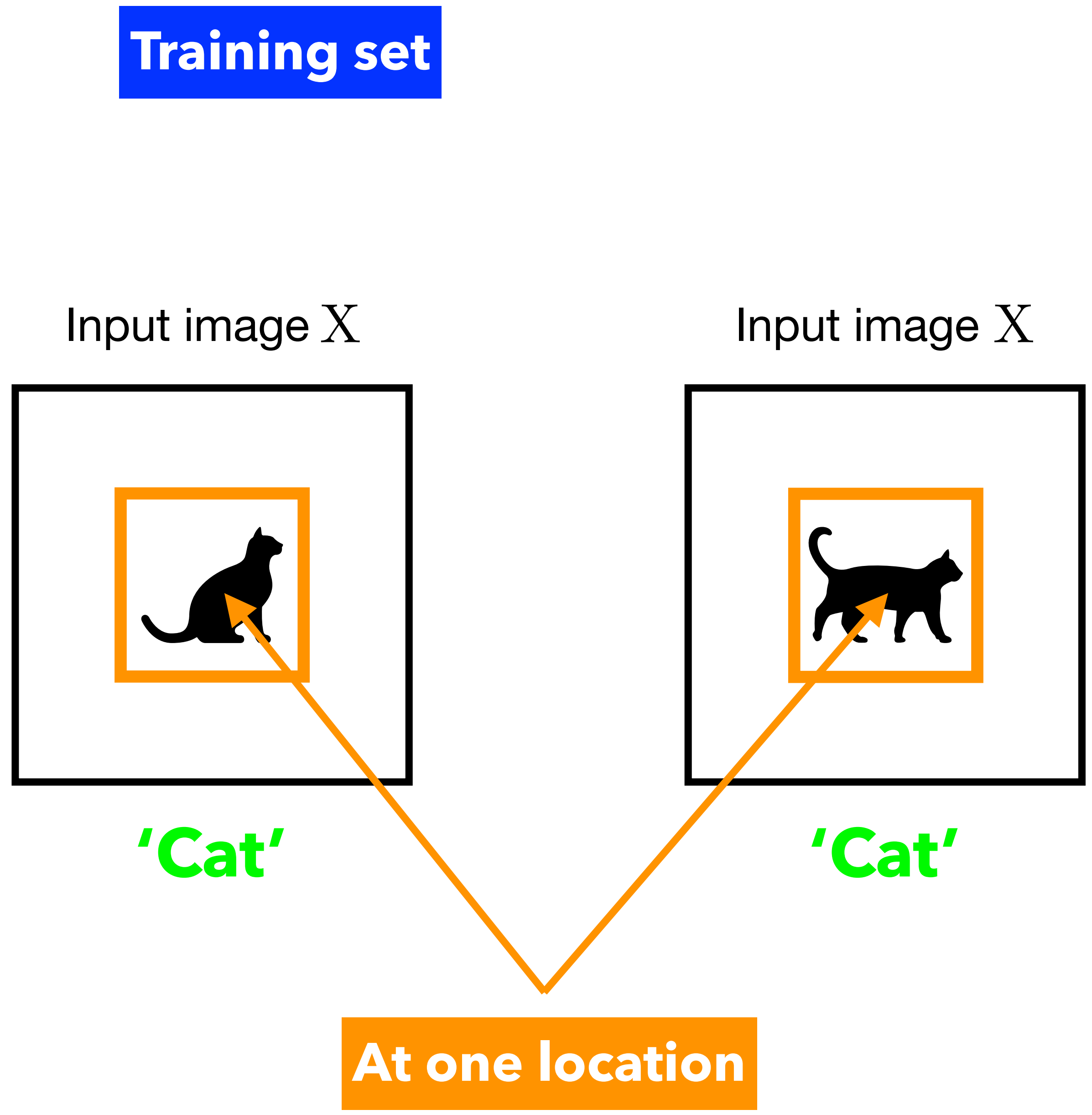

How to make CNNs shift-invariant?

- **Online invariance** at one-to-many locations

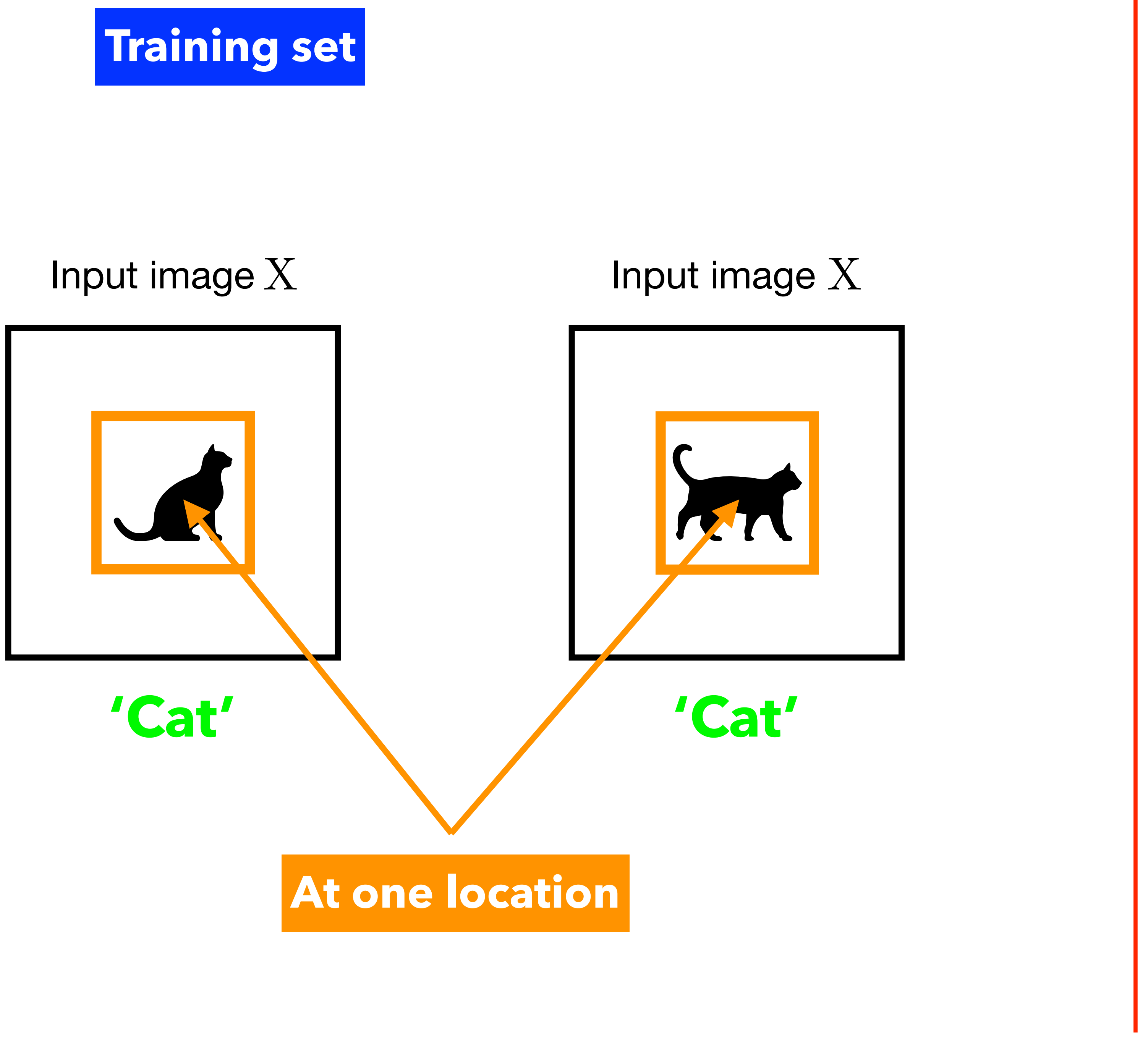

How to make CNNs shift-invariant?

- **Online invariance** at one-to-many locations

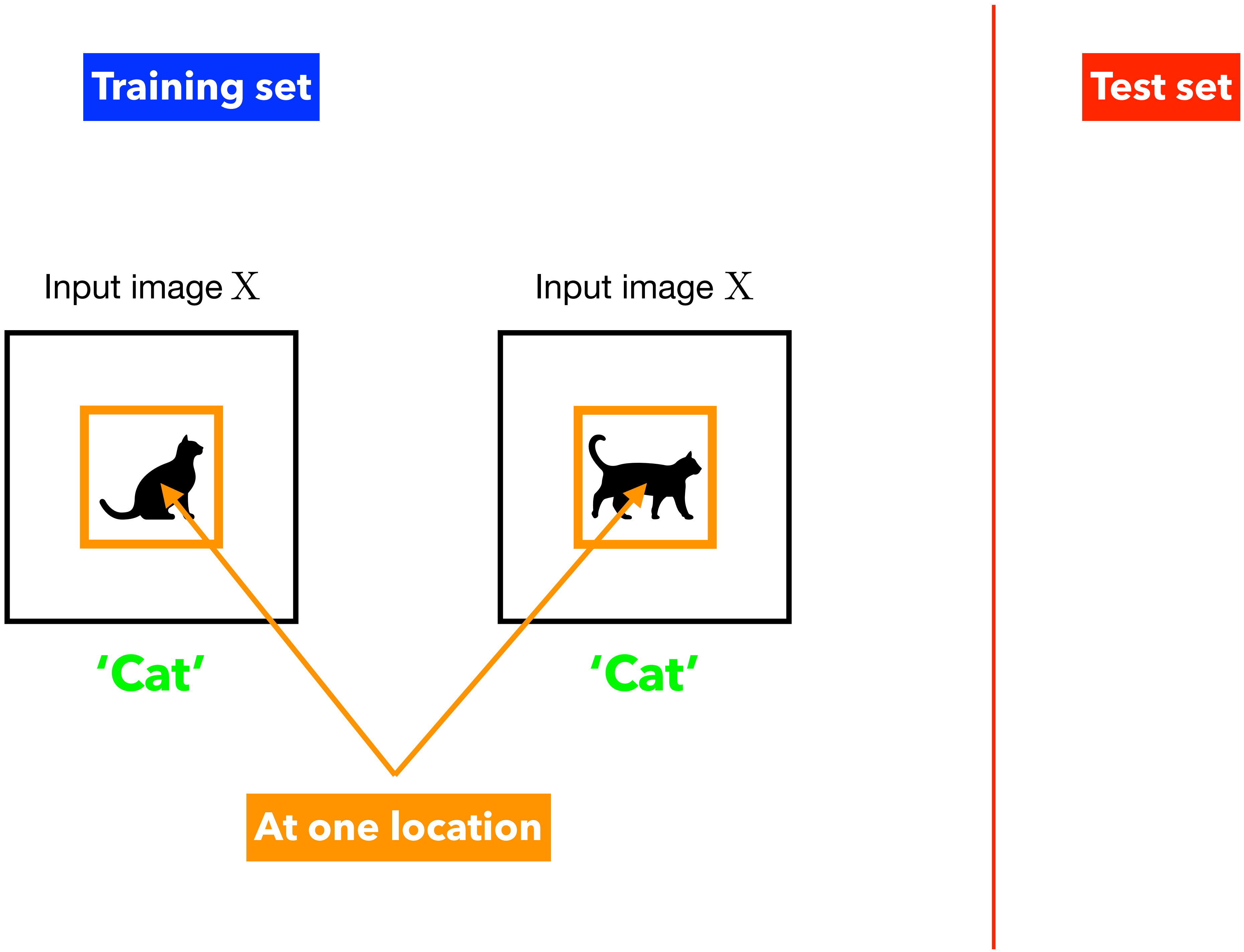

How to make CNNs shift-invariant?

- **Online invariance** at one-to-many locations

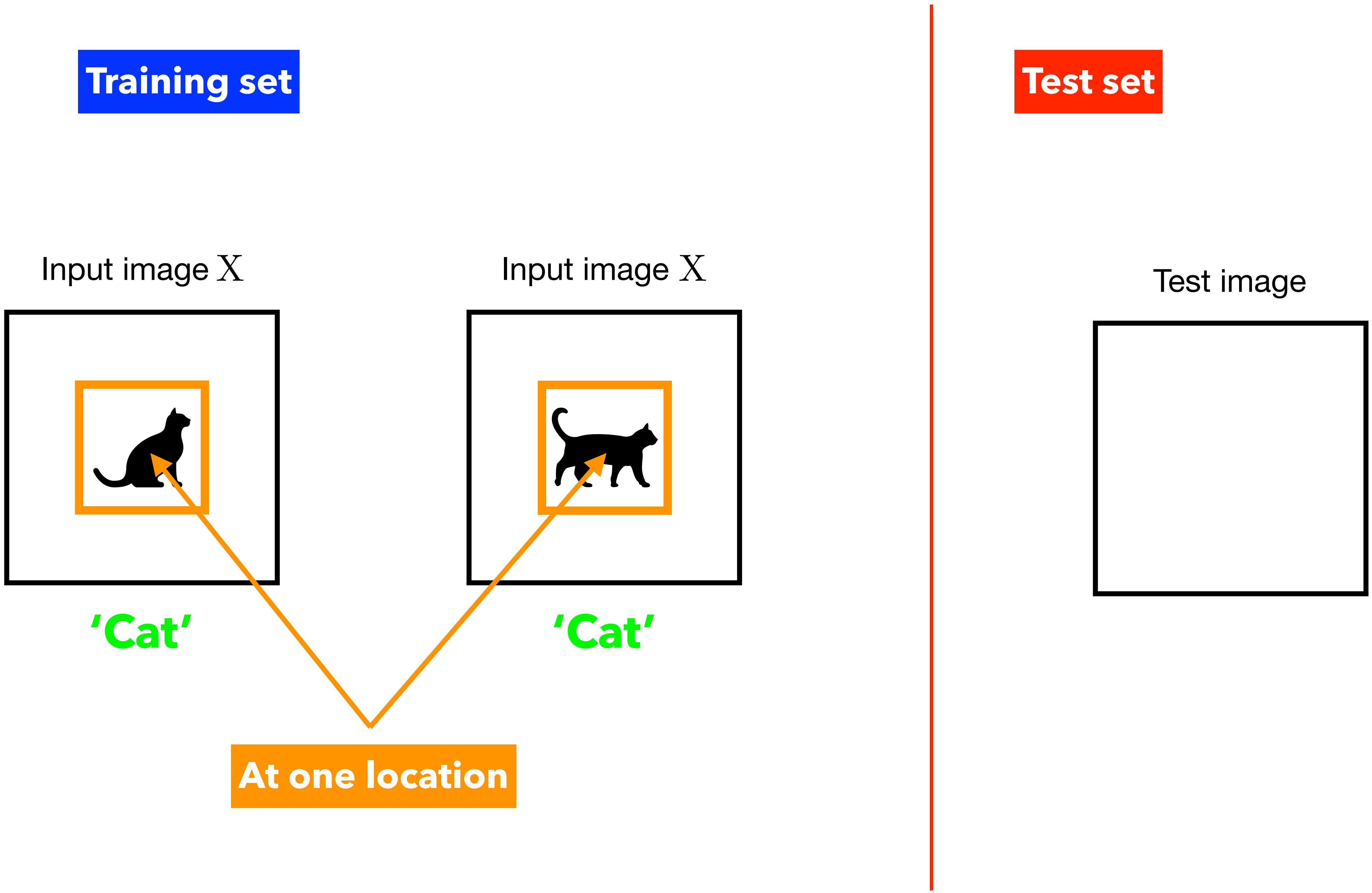

How to make CNNs shift-invariant?

- **Online invariance** at one-to-many locations

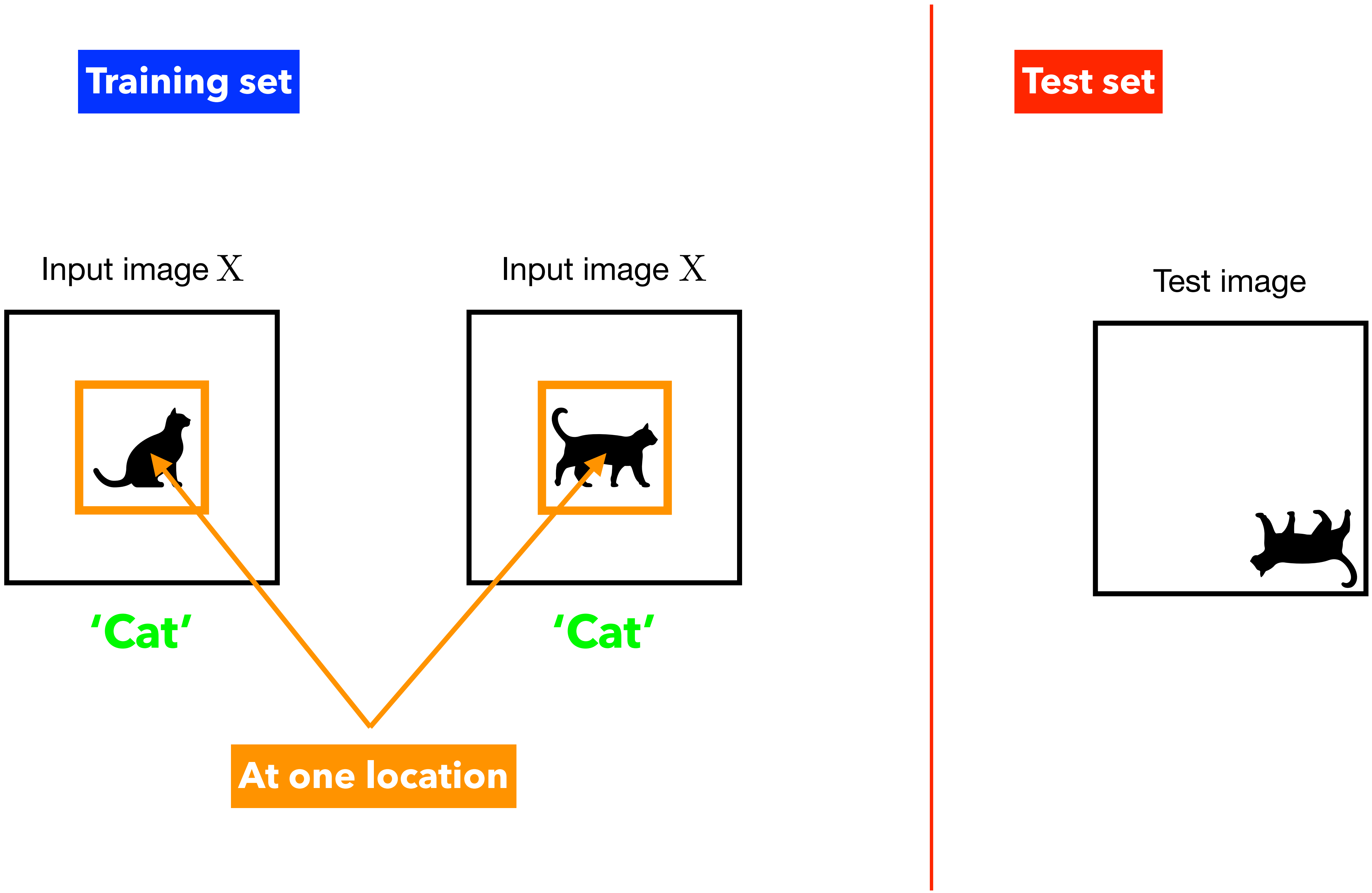

How to make CNNs shift-invariant?

- **Online invariance** at one-to-many locations

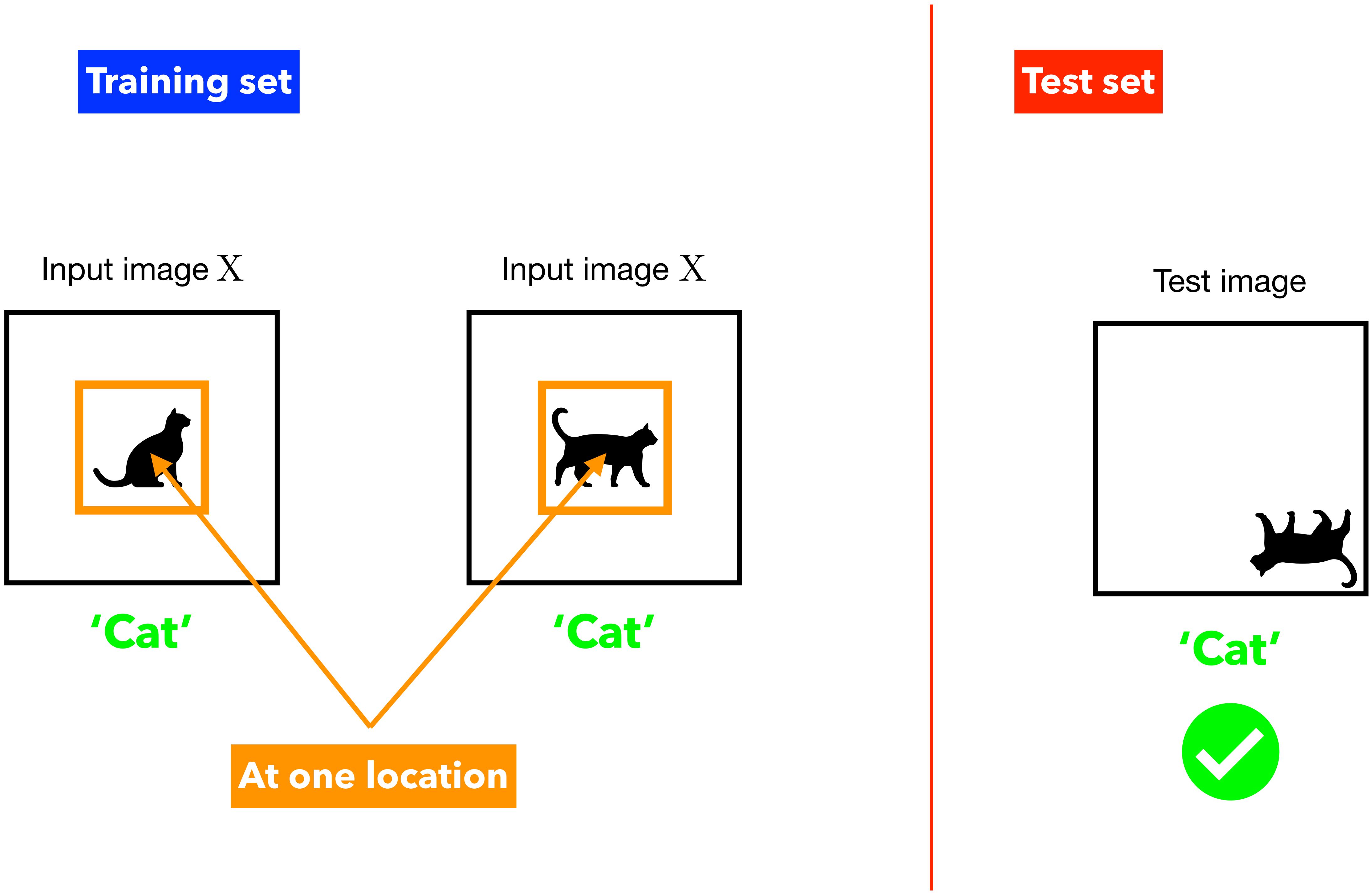

How to make CNNs shift-invariant?

- **Architectural online invariance**

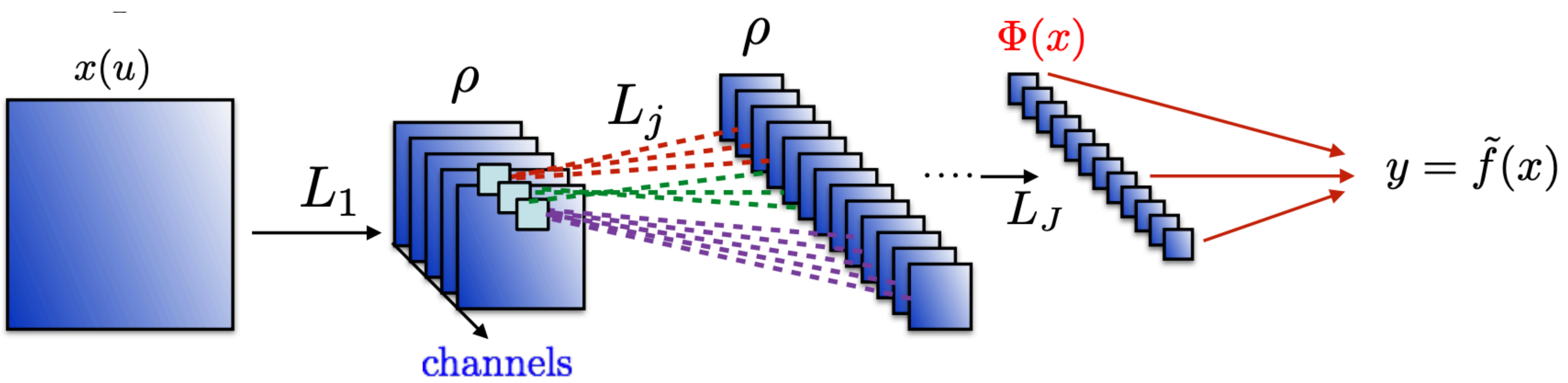

$$\Phi(\mathcal{T}_v x) \approx \Phi(x)$$

- What kind of linear and non-linear operators to consider?
- Are extracted features maps stable to translations?

How to make CNNs shift-invariant?

- **Architectural online invariance**

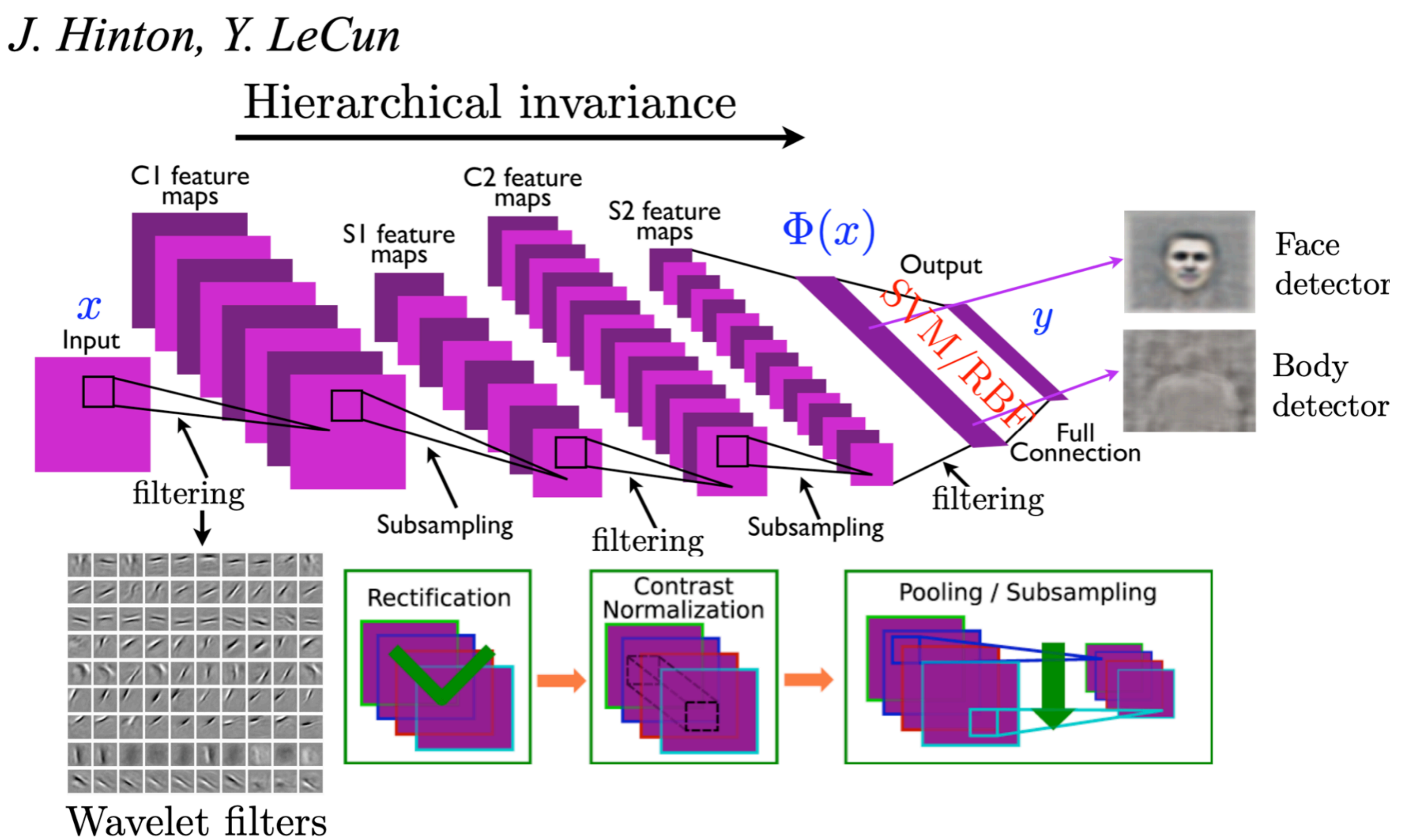

Inductive biases

- Multichanneling
- Weight sharing
- Locality
- Downsampling

Convolutional layers in CNN

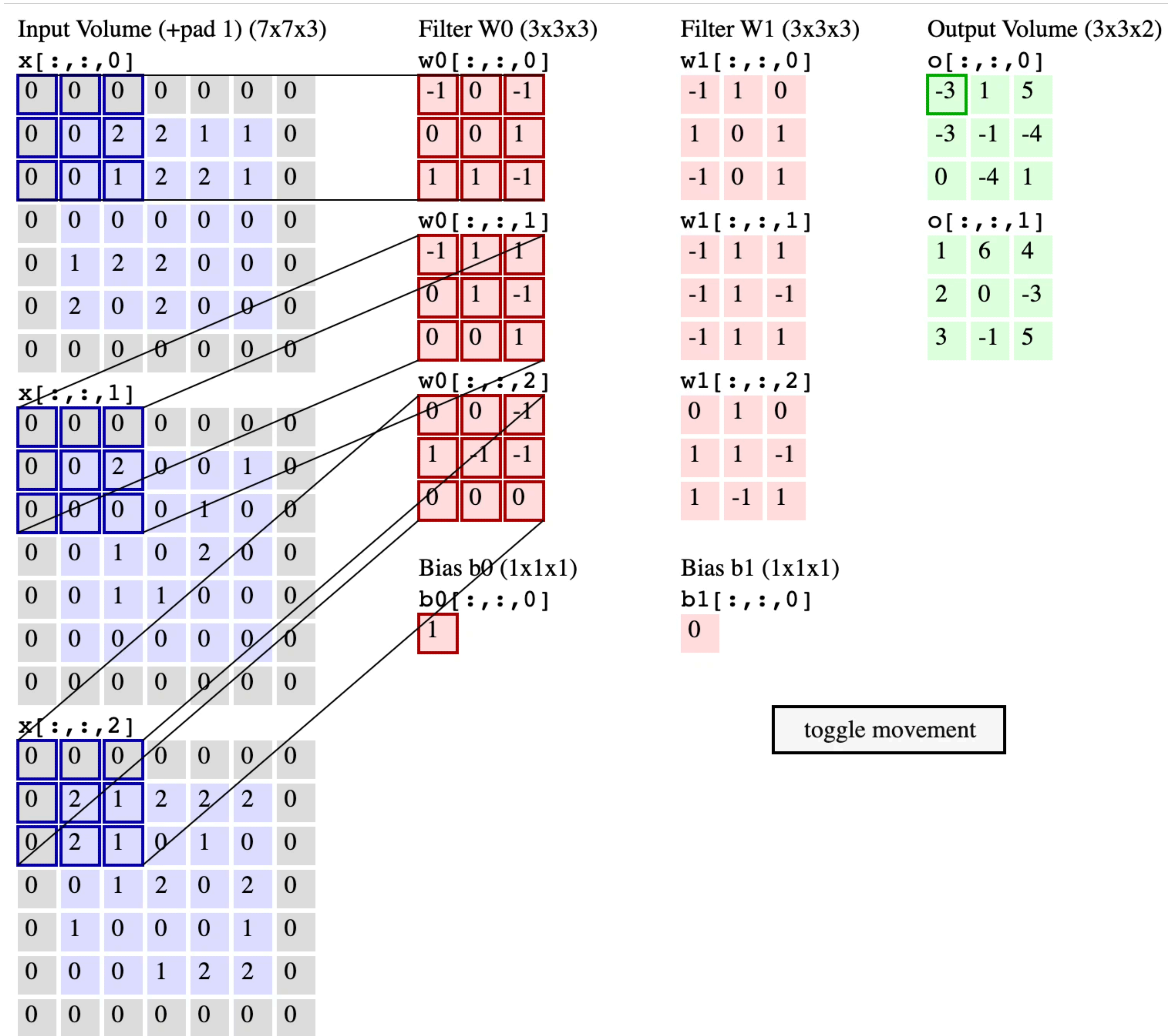

Source : https://cs231n.github.io/convolutional-networks/

Convolutional layers in CNN

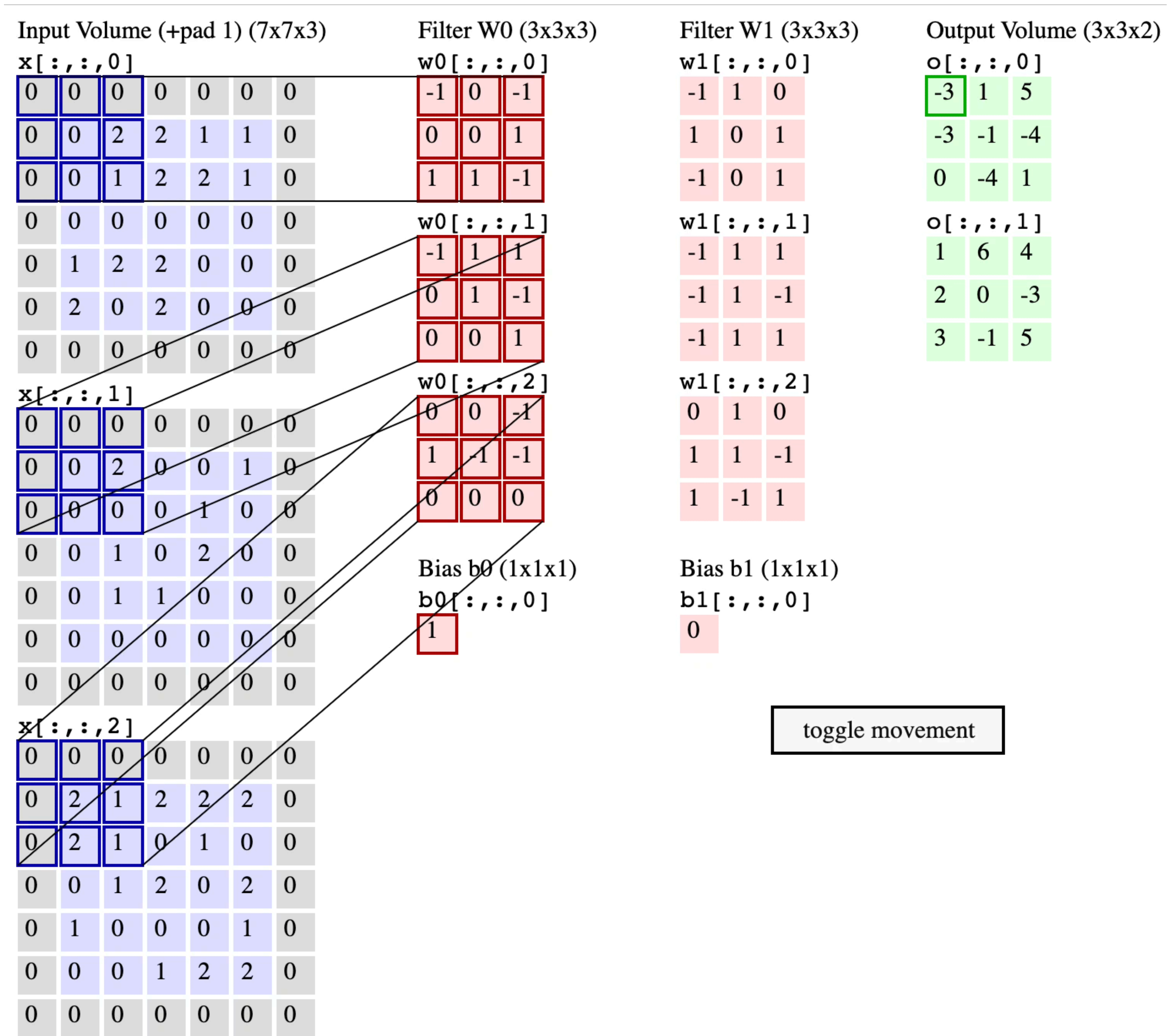

Source : https://cs231n.github.io/convolutional-networks/

Convolution & Max Pooling invariance ?

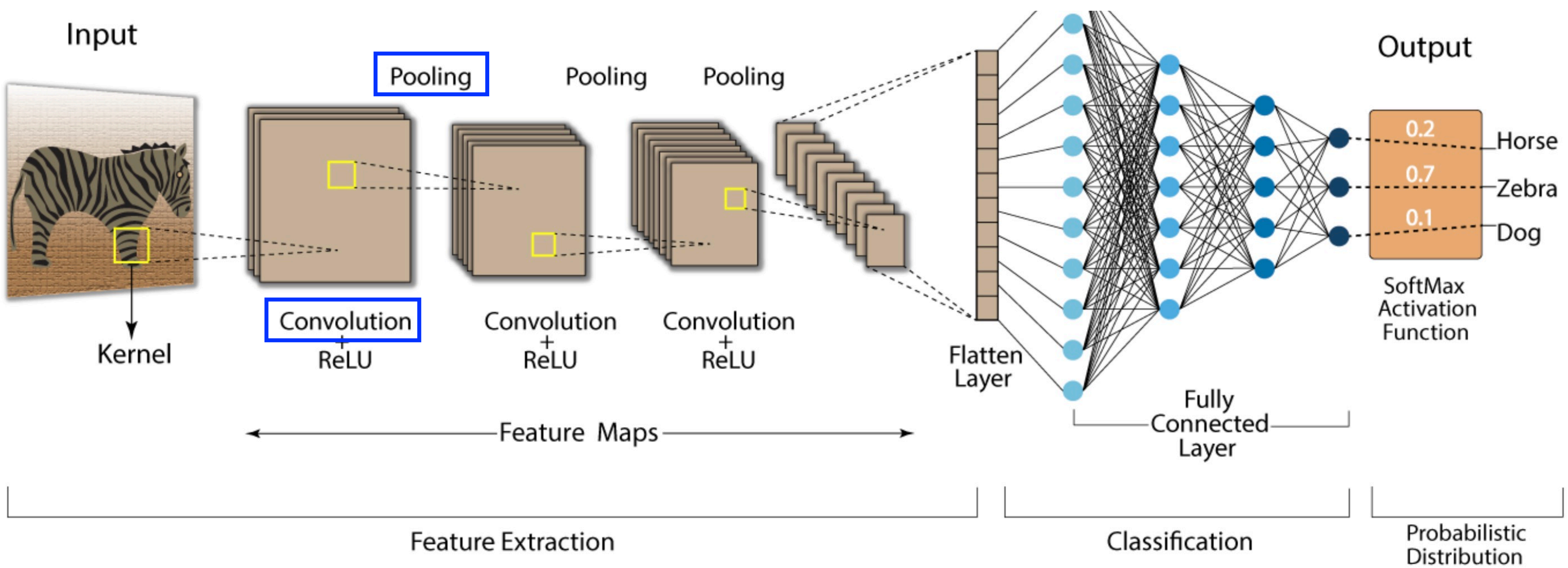

Source : https://developersbreach.com/convolution-neural-network-deep-learning/

Shift invariance

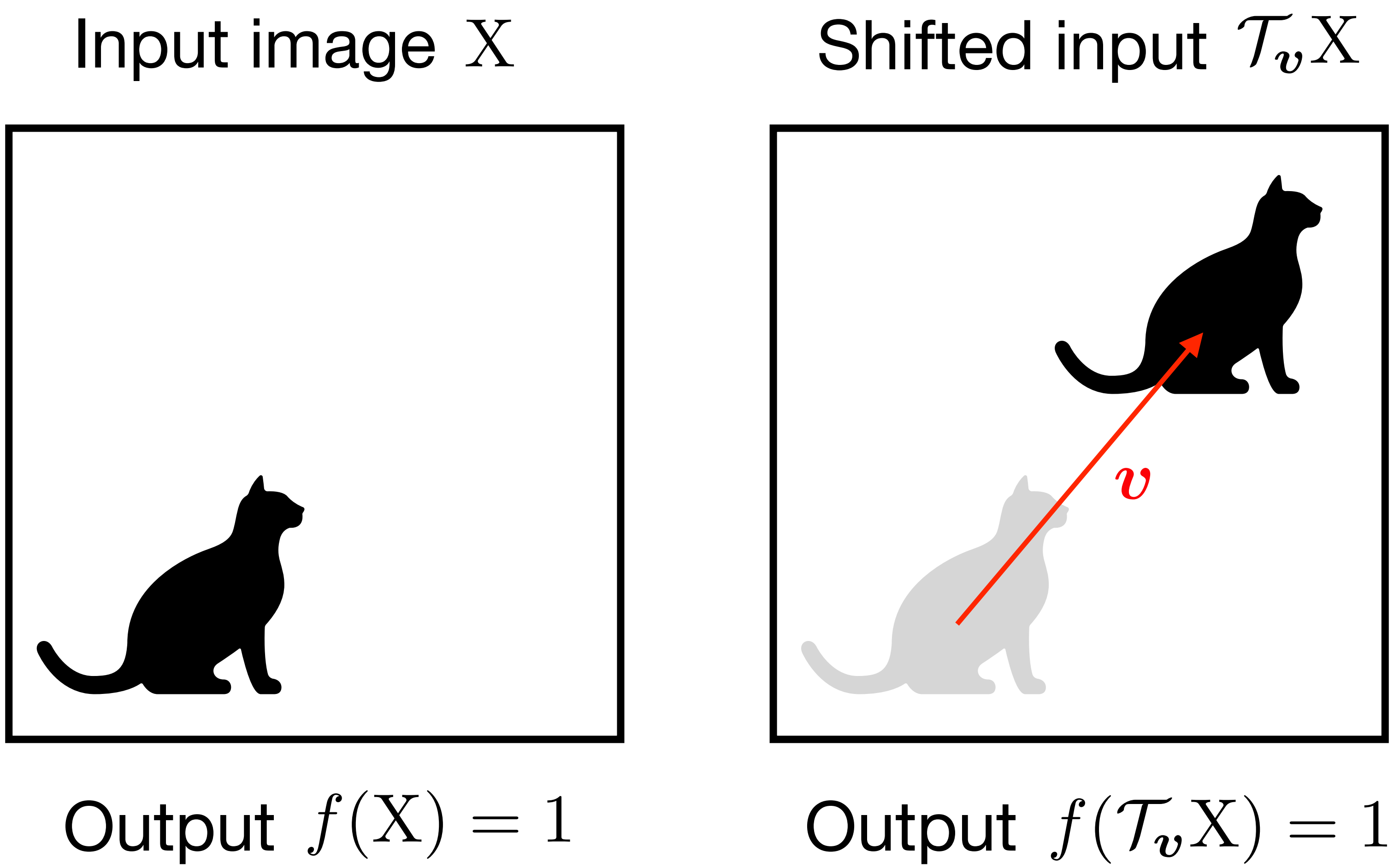

Shift invariance

Input image X

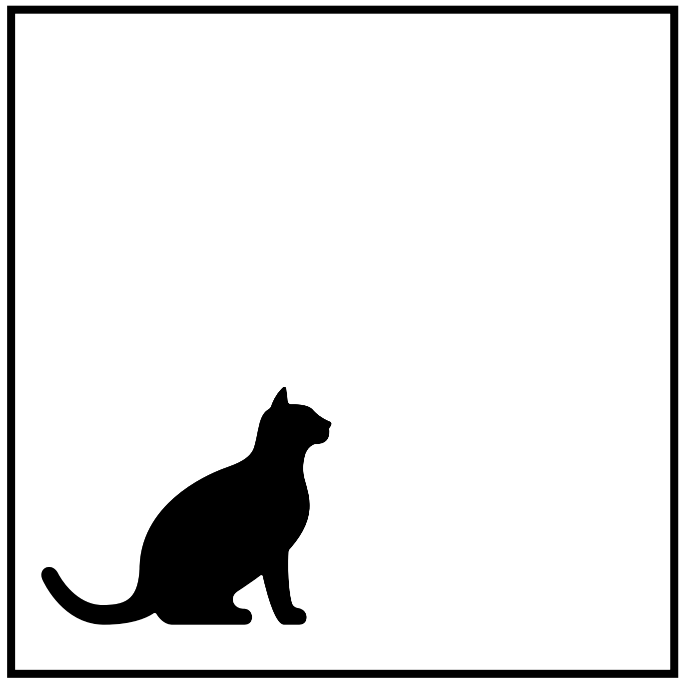

Output $f(\mathrm{X}) = 1$

Shifted input $\mathcal{T}_{\boldsymbol{v}}\mathrm{X}$

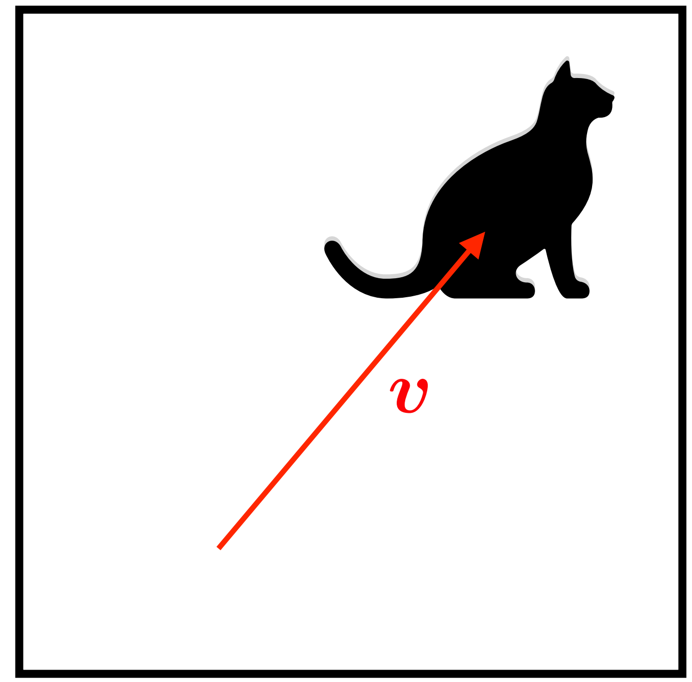

Output $f(\mathcal{T}_{\boldsymbol{v}}\mathrm{X}) = 1$

Shift invariance

Input image X Shifted input $\mathcal{T}_{\boldsymbol{v}}\mathrm{X}$

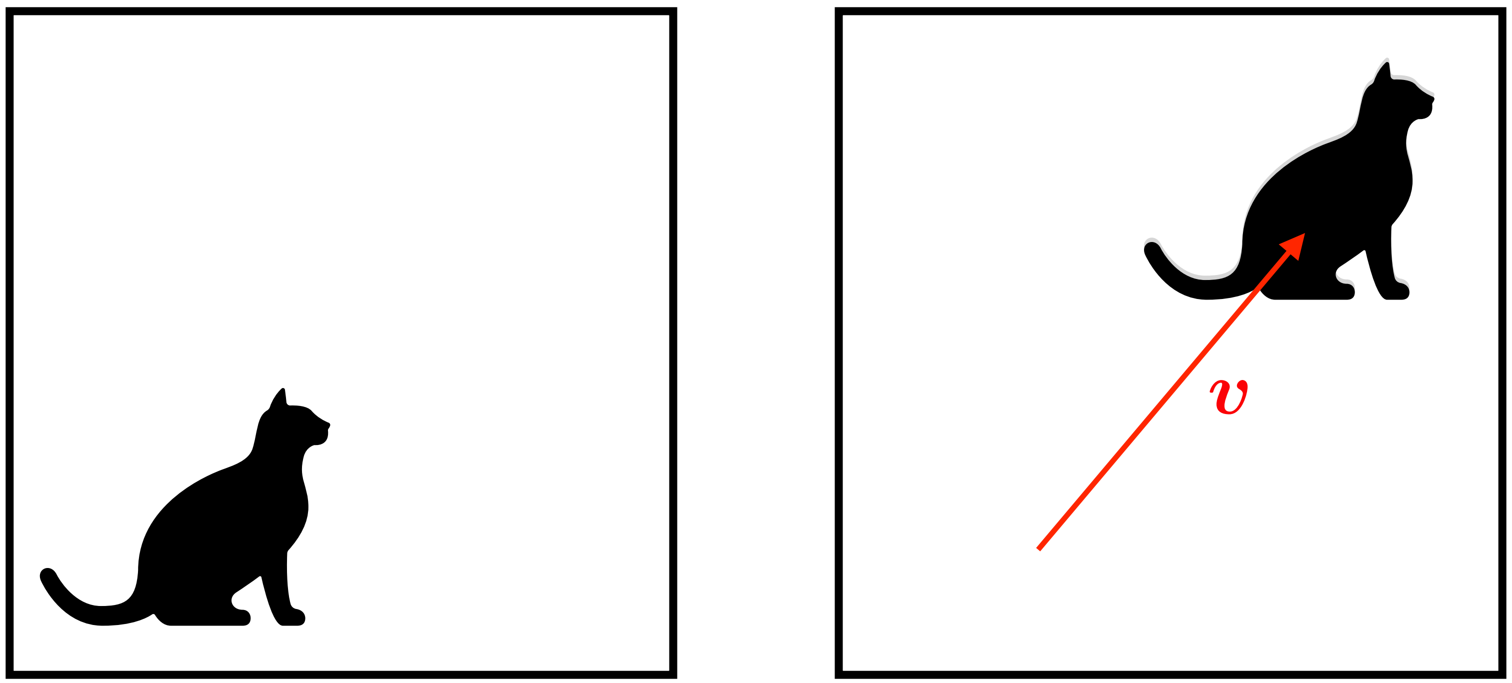

Output $f(\mathrm{X}) = 1$ Output $f(\mathcal{T}_{\boldsymbol{v}}\mathrm{X}) = 1$

Shift invariance ≠ Equivariance

Shift equivariance

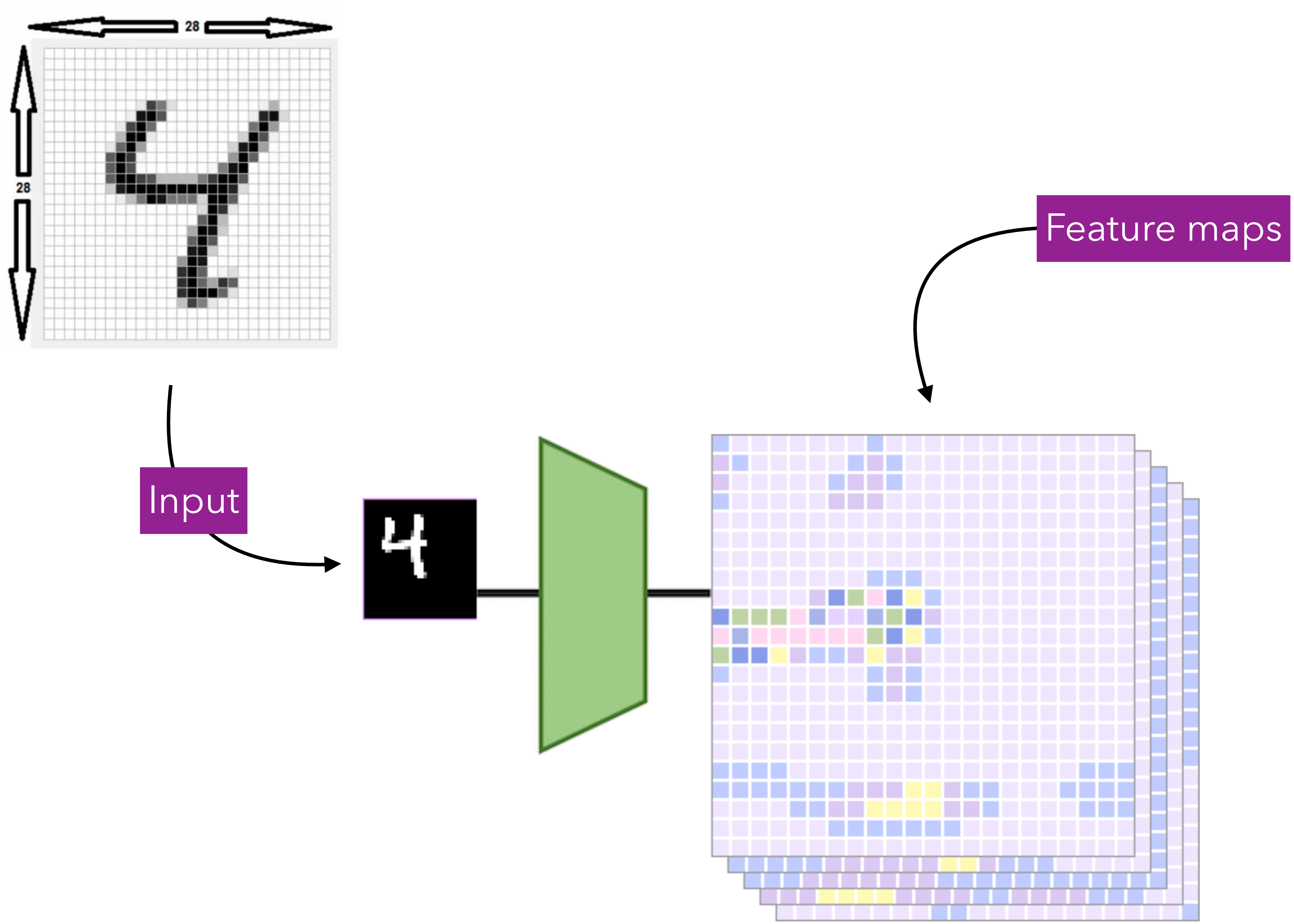

Shift equivariance

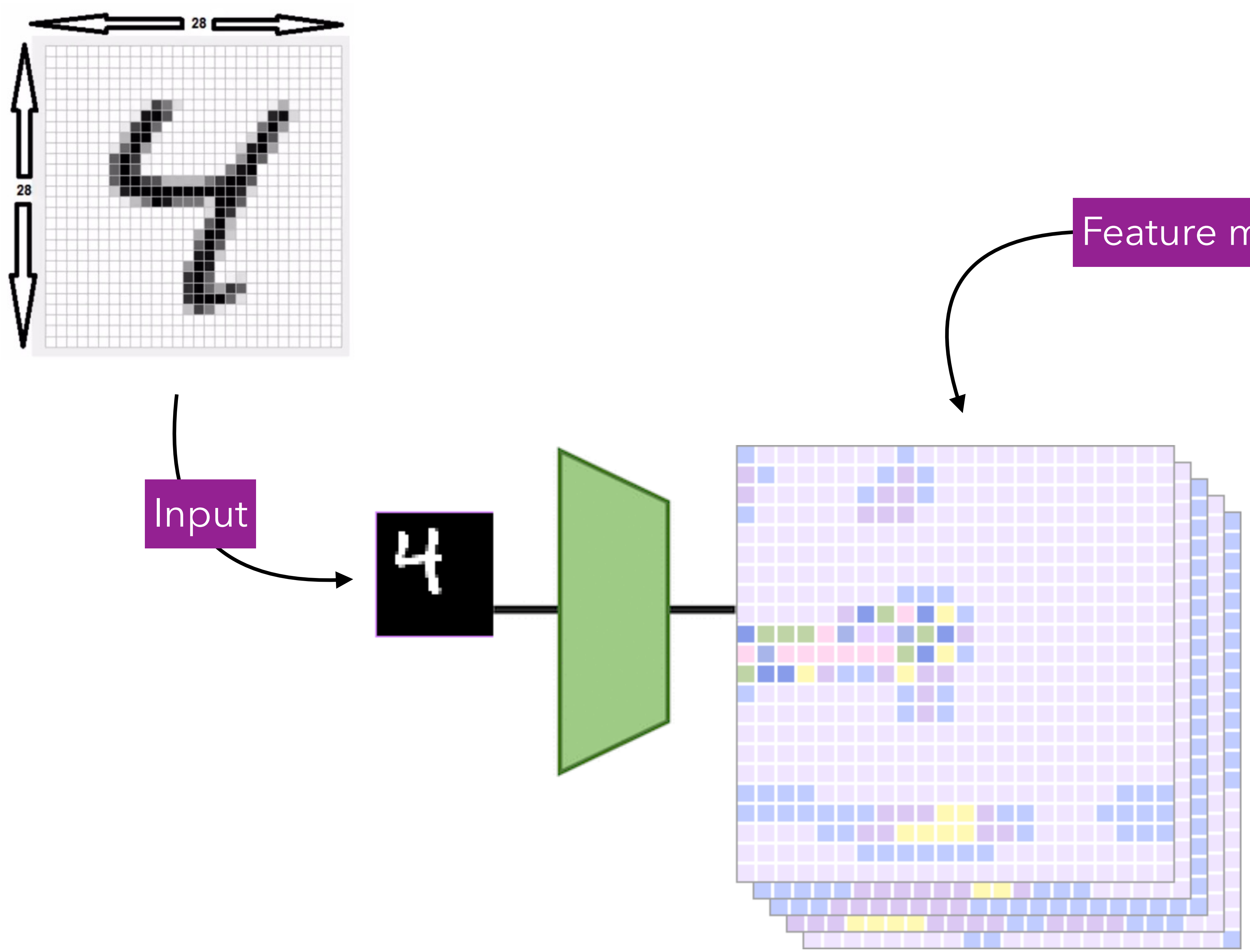

Shift equivariance

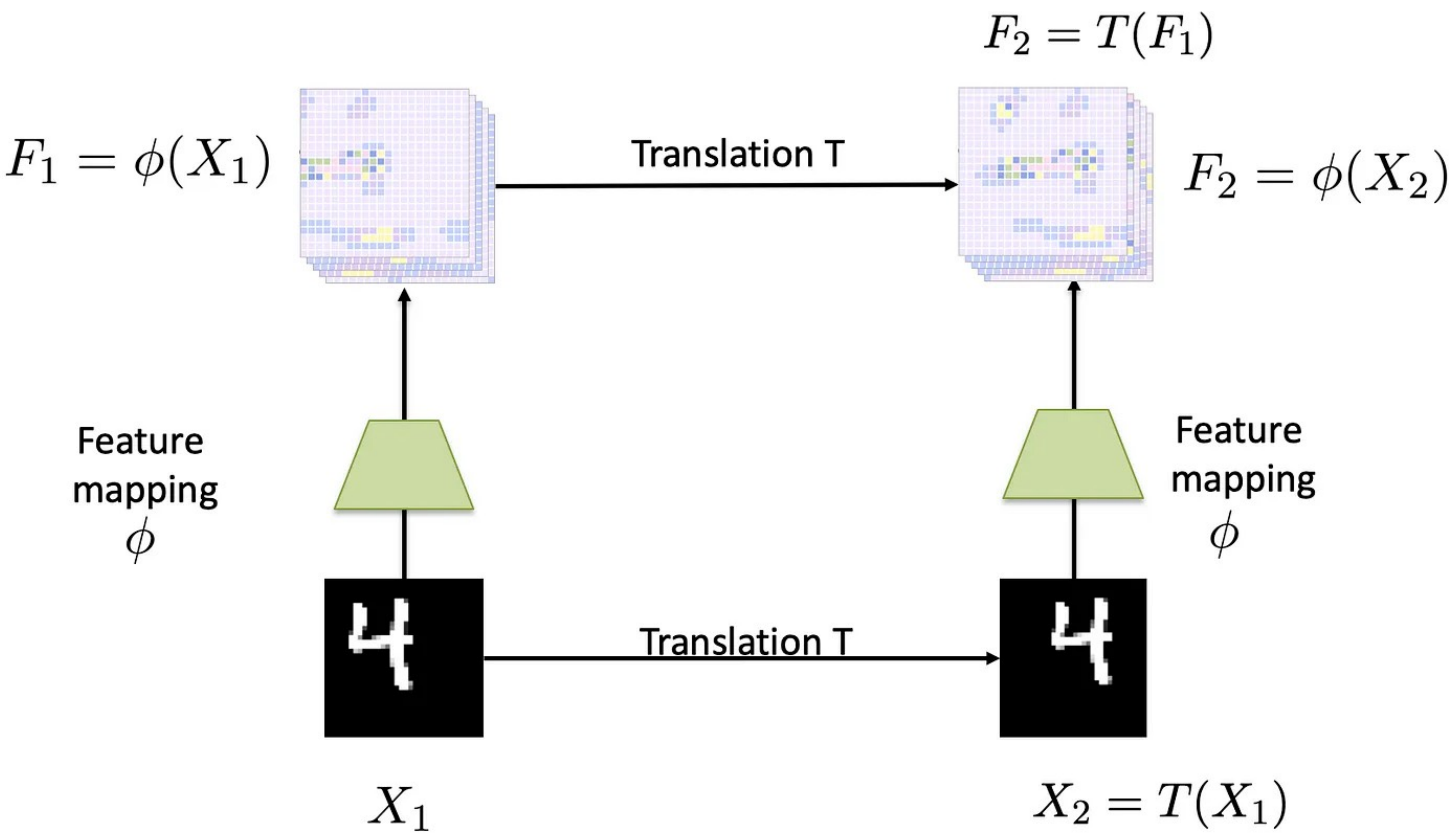

Source : https://chriswolfvision.medium.com/what-is-translation-equivariance-and-why-do-we-use-convolutions-to-get-it-6f18139d4c59

Convolutions are shift-equivariant

Convolutions are shift-equivariant

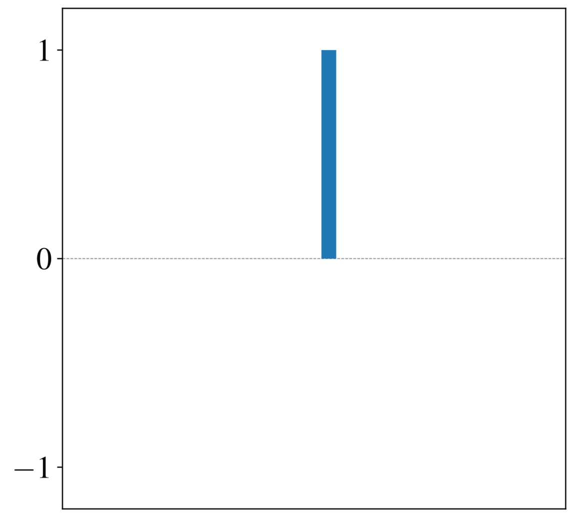

Input signal

Convolutions are shift-equivariant

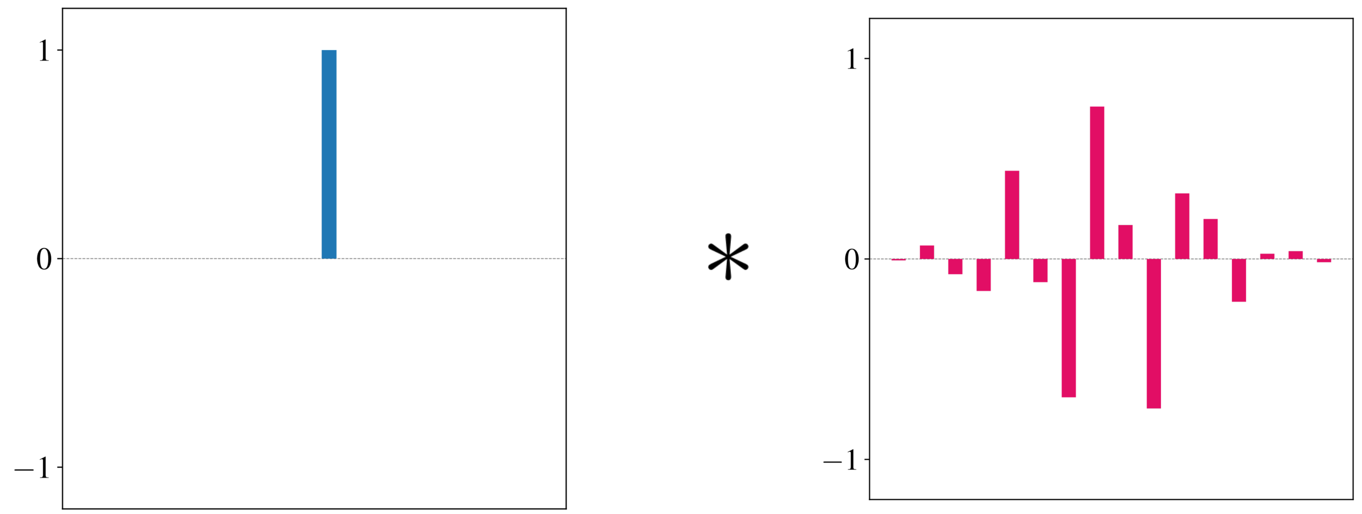

Input signal

Band-pass
convolution kernel

Convolutions are shift-equivariant

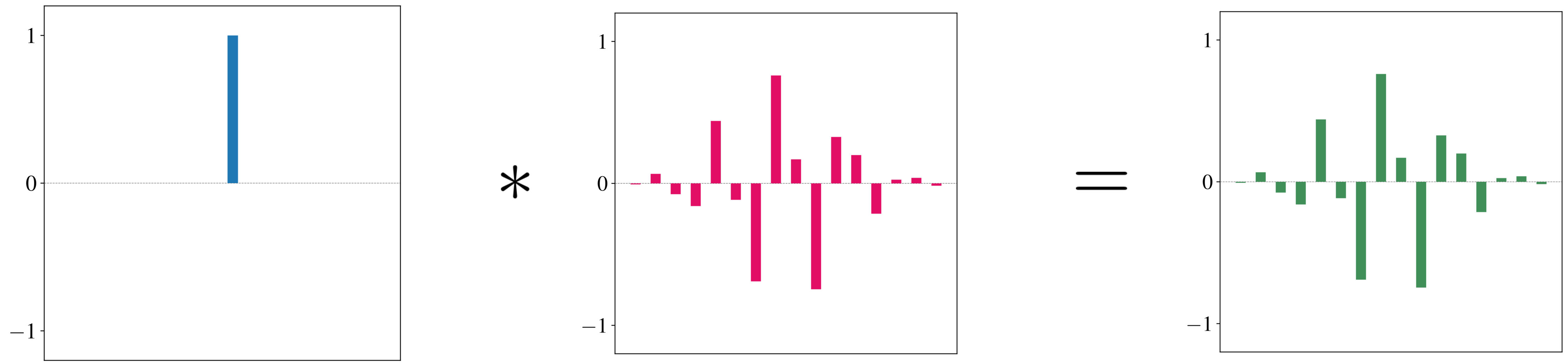

Input signal

Band-pass
convolution kernel

Output signal

Convolutions are shift-equivariant

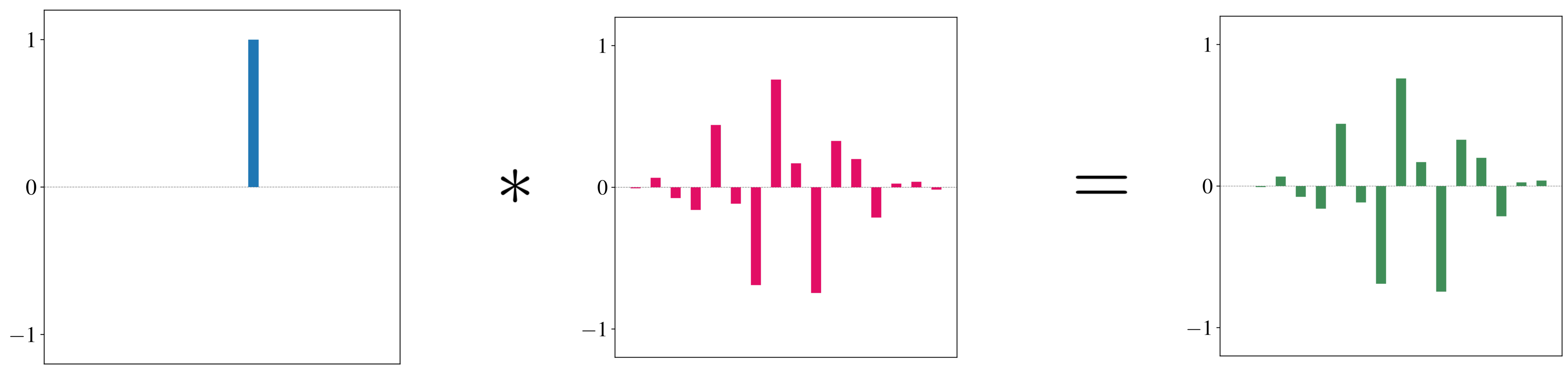

Input signal

Band-pass
convolution kernel

Output signal

Convolutions are shift-equivariant

Shift **equivariance**, or **covariance**

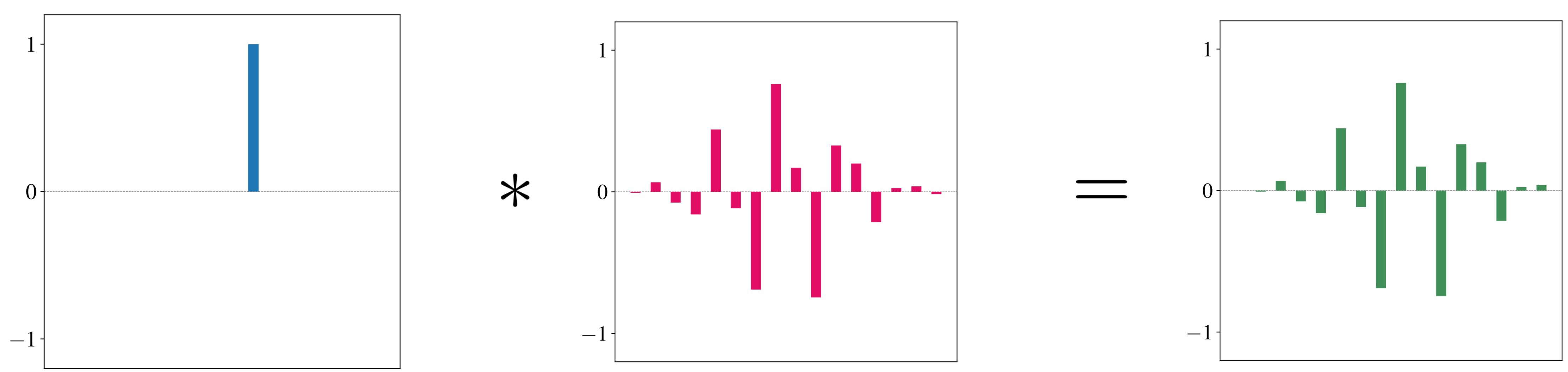

Input signal

Band-pass
convolution kernel

Output signal

Convolutions are shift-equivariant

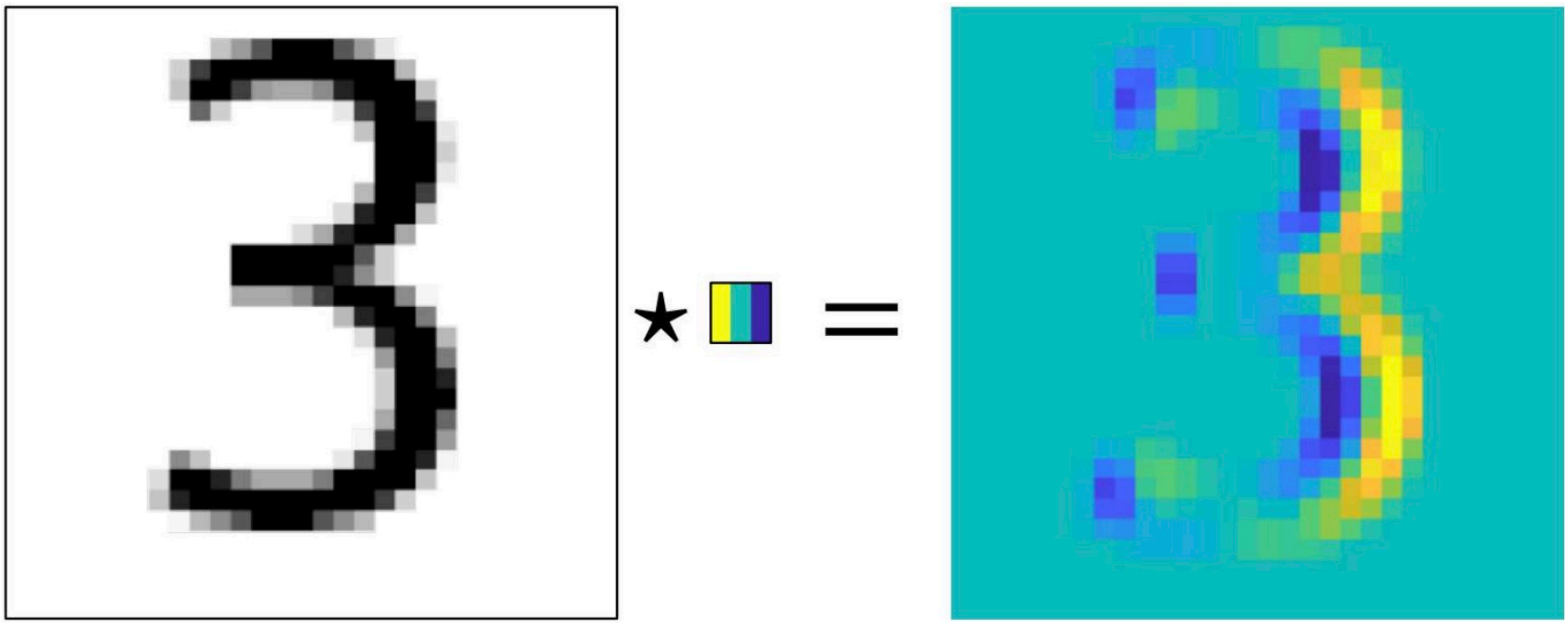

Source : https://www.doc.ic.ac.uk/~bkainz/teaching/DL/notes/equivariance.pdf

Convolutions are shift-equivariant

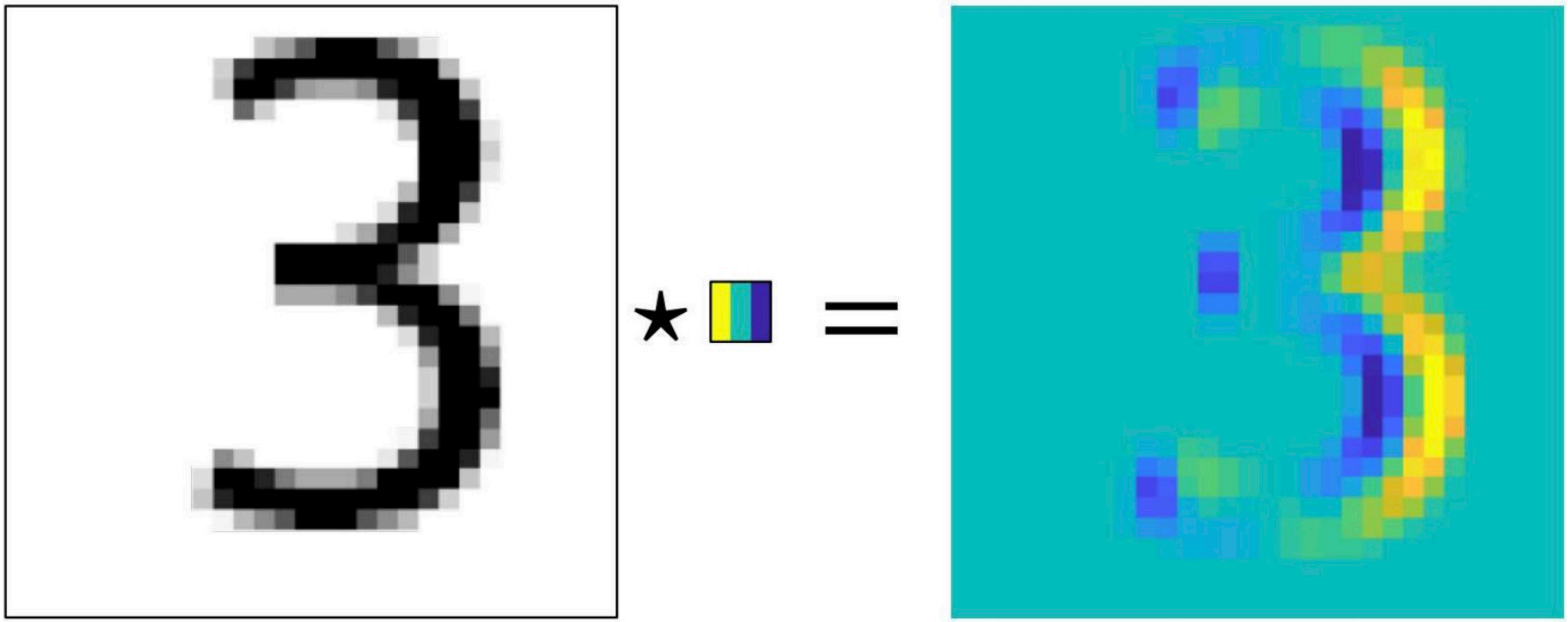

Source : https://www.doc.ic.ac.uk/~bkainz/teaching/DL/notes/equivariance.pdf

Max pooling layers

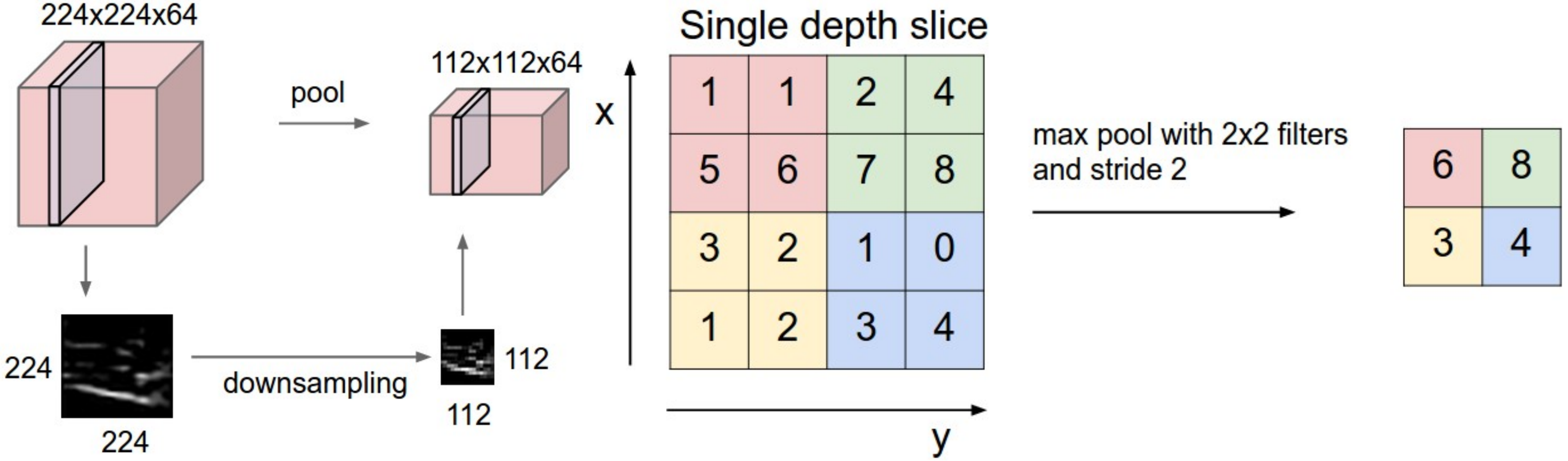

Source : https://cs231n.github.io/convolutional-networks/

Convolutions are followed by a max pooling

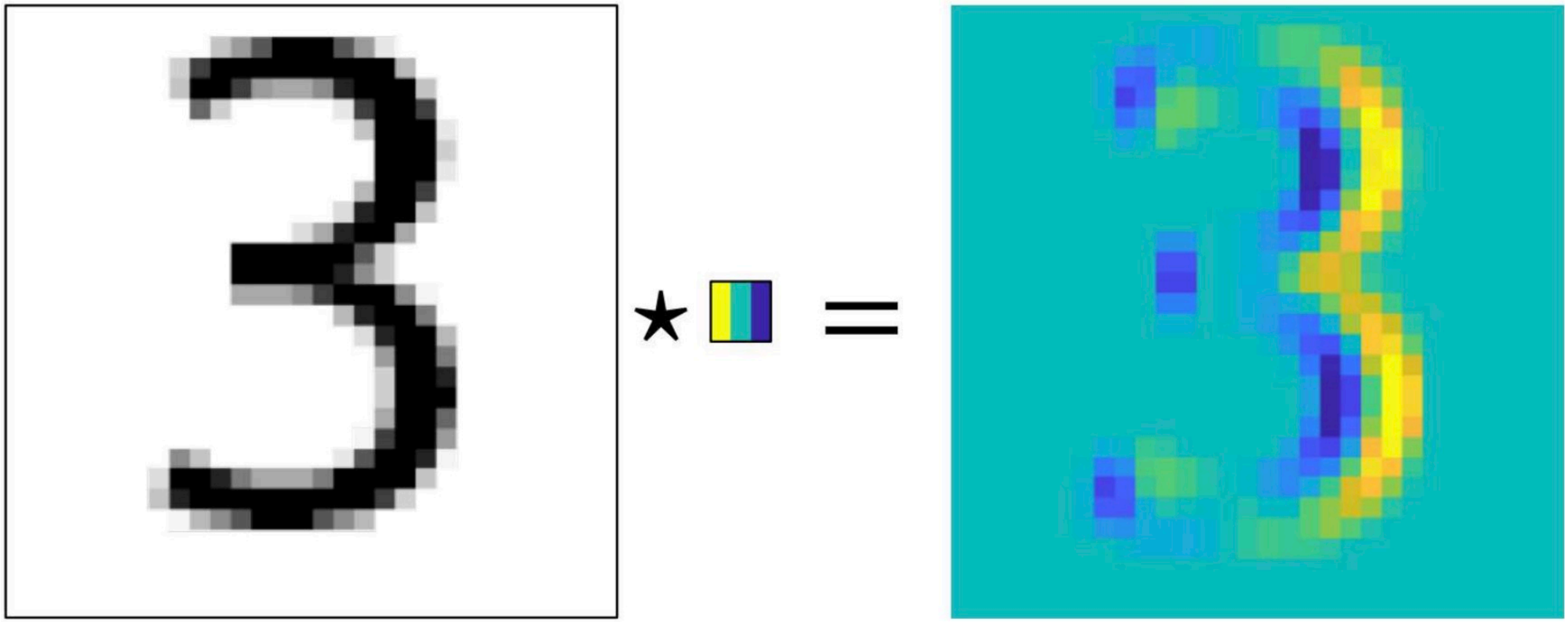

Source : https://www.doc.ic.ac.uk/~bkainz/teaching/DL/notes/equivariance.pdf

Convolutions are followed by a max pooling

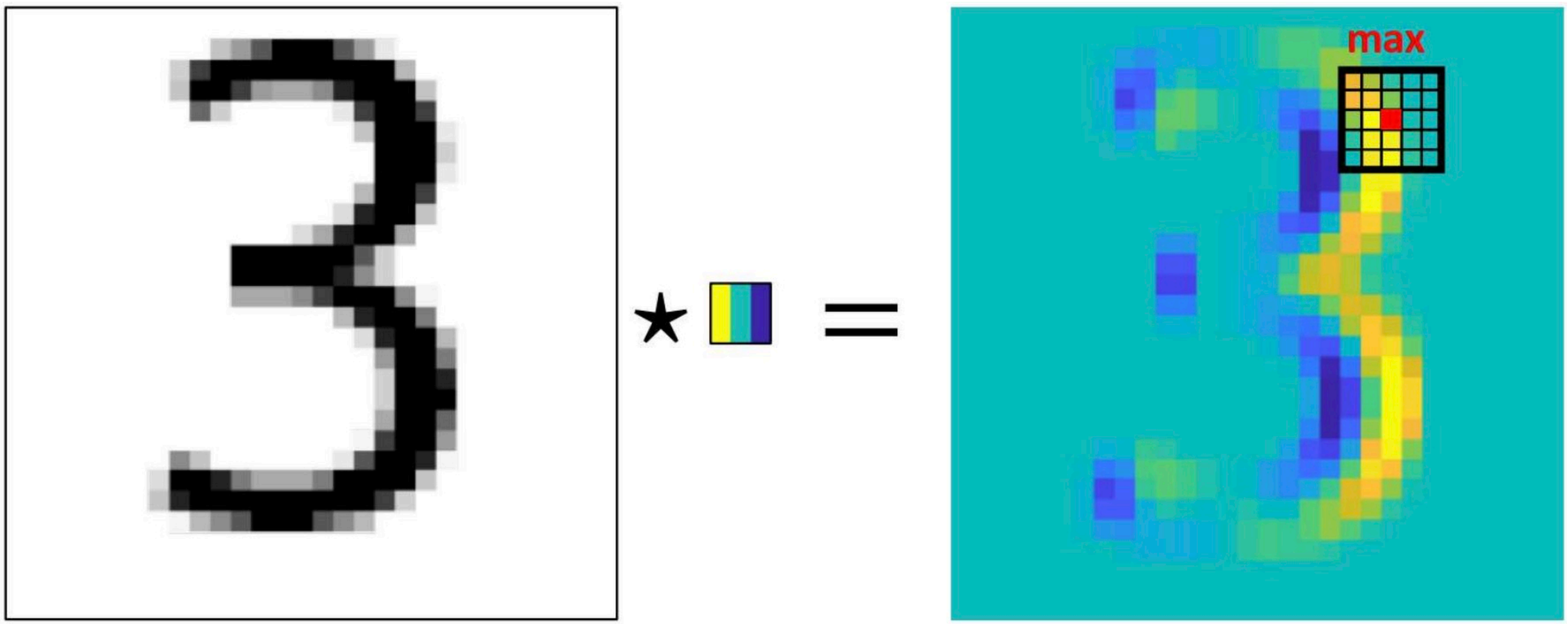

Max pooling builds up shift-invariance

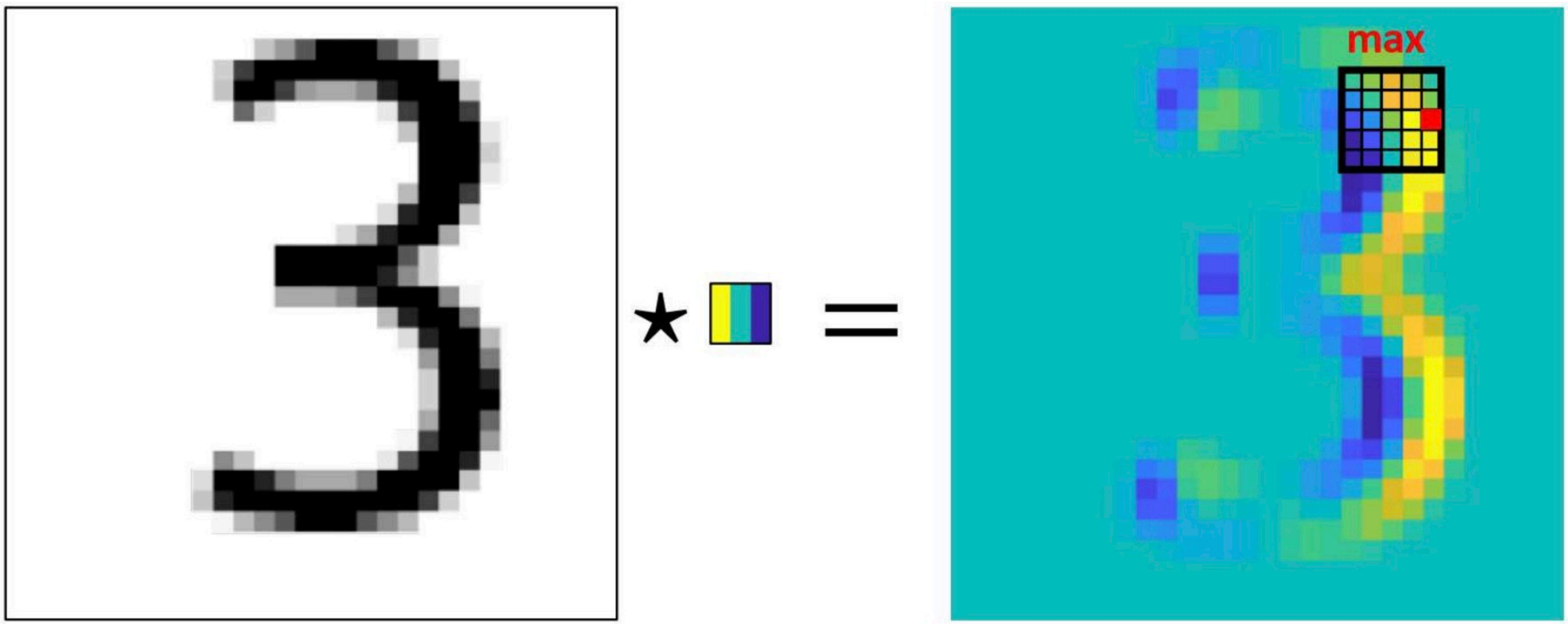

Invariance studies in CNN

Invariance studies in CNN

- The **scattering transform** builds shift-invariant feature vectors:

$$\Phi(x) := S_J x = \begin{pmatrix} x \star \phi_{2^J} \\ |x \star \psi_{\lambda_1}| \star \phi_{2^J} \\ ||x \star \psi_{\lambda_1}| \star \psi_{\lambda_2}| \star \phi_{2^J} \\ |||x \star \psi_{\lambda_1}| \star \psi_{\lambda_2}| \star \psi_{\lambda_3}| \star \phi_{2^J} \\ \vdots \end{pmatrix}_{\lambda_1, \lambda_2, \lambda_3, \ldots}$$

Invariance studies in CNN

- The **scattering transform** builds shift-invariant feature vectors:

$$\Phi(x) := S_J x = \begin{pmatrix} x \star \phi_{2^J} \\ |x \star \psi_{\lambda_1}| \star \phi_{2^J} \\ ||x \star \psi_{\lambda_1}| \star \psi_{\lambda_2}| \star \phi_{2^J} \\ |||x \star \psi_{\lambda_1}| \star \psi_{\lambda_2}| \star \psi_{\lambda_3}| \star \phi_{2^J} \\ \vdots \end{pmatrix}_{\lambda_1, \lambda_2, \lambda_3, \ldots}$$

J. Bruna and S. Mallat, "Invariant scattering convolution networks," IEEE Trans. Pattern Anal. Mach. Intell., vol. 35, no. 8, pp. 1872–1886, 2013.

Invariance studies in CNN

- The **scattering transform** builds shift-invariant feature vectors:

$$\Phi(x) := S_J x = \begin{pmatrix} x \star \phi_{2^J} \\ |x \star \psi_{\lambda_1}| \star \phi_{2^J} \\ ||x \star \psi_{\lambda_1}| \star \psi_{\lambda_2}| \star \phi_{2^J} \\ |||x \star \psi_{\lambda_1}| \star \psi_{\lambda_2}| \star \psi_{\lambda_3}| \star \phi_{2^J} \\ \vdots \end{pmatrix}_{\lambda_1, \lambda_2, \lambda_3, \ldots}$$

- **General deep convolutional neural networks** also become more translation invariant with increasing network depth (proved in the *continuous framework*).

J. Bruna and S. Mallat, “Invariant scattering convolution networks,” IEEE Trans. Pattern Anal. Mach. Intell., vol. 35, no. 8, pp. 1872–1886, 2013.

Invariance studies in CNN

- The **scattering transform** builds shift-invariant feature vectors:

$$\Phi(x) := S_J x = \begin{pmatrix} x \star \phi_{2^J} \\ |x \star \psi_{\lambda_1}| \star \phi_{2^J} \\ ||x \star \psi_{\lambda_1}| \star \psi_{\lambda_2}| \star \phi_{2^J} \\ |||x \star \psi_{\lambda_1}| \star \psi_{\lambda_2}| \star \psi_{\lambda_3}| \star \phi_{2^J} \\ \vdots \end{pmatrix}_{\lambda_1, \lambda_2, \lambda_3, \dots}$$

- **General deep convolutional neural networks** also become more translation invariant with increasing network depth (proved in the *continuous framework*).

J. Bruna and S. Mallat, "Invariant scattering convolution networks," IEEE Trans. Pattern Anal. Mach. Intell., vol. 35, no. 8, pp. 1872–1886, 2013.

T. Wiatowski and H. Bölcskei, A Mathematical Theory of Deep Convolutional Neural Networks for Feature Extraction, IEEE Transactions on Information Theory, 64 (2018), pp. 1845–1866

Invariance studies in CNN

- These results do not fully extend to the ***discrete framework***

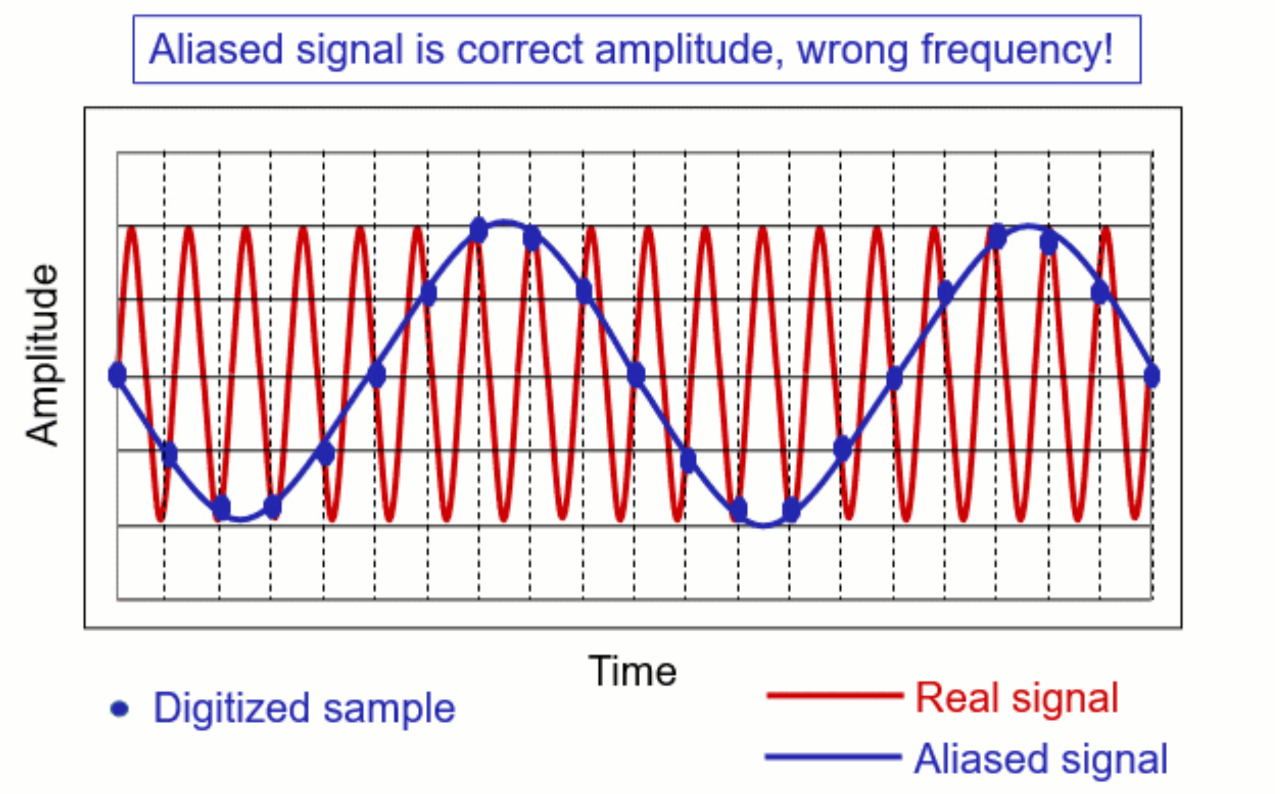

Source : https://community.sw.siemens.com/s/article/data-acquisition-anti-aliasing-filters

Invariance studies in CNN

- These results do not fully extend to the ***discrete framework***
- **Strided** convolution and pooling operators may greatly diverge from shift invariance, due to **aliasing** when subsampling high-frequency signals

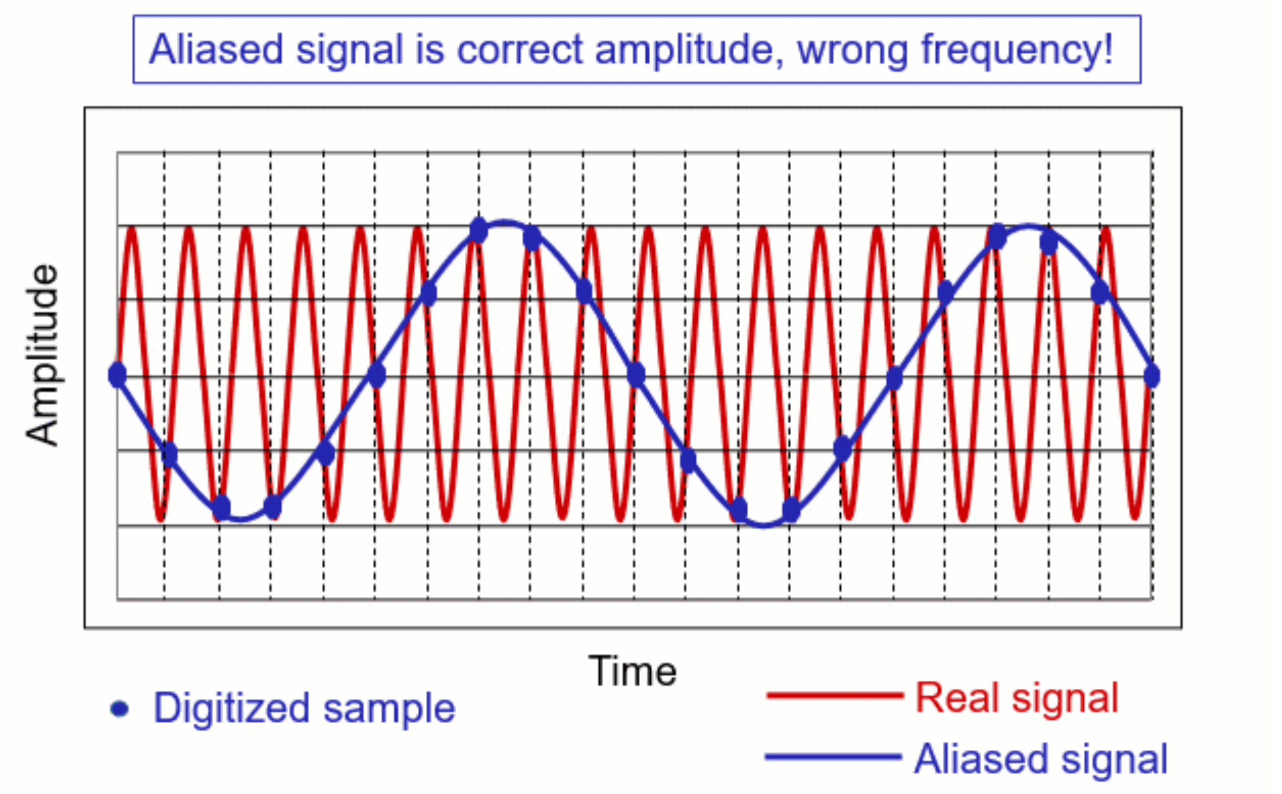

Source : https://community.sw.siemens.com/s/article/data-acquisition-anti-aliasing-filters

Invariance studies in CNN

- These results do not fully extend to the ***discrete framework***
- **Strided** convolution and pooling operators may greatly diverge from shift invariance, due to **aliasing** when subsampling high-frequency signals

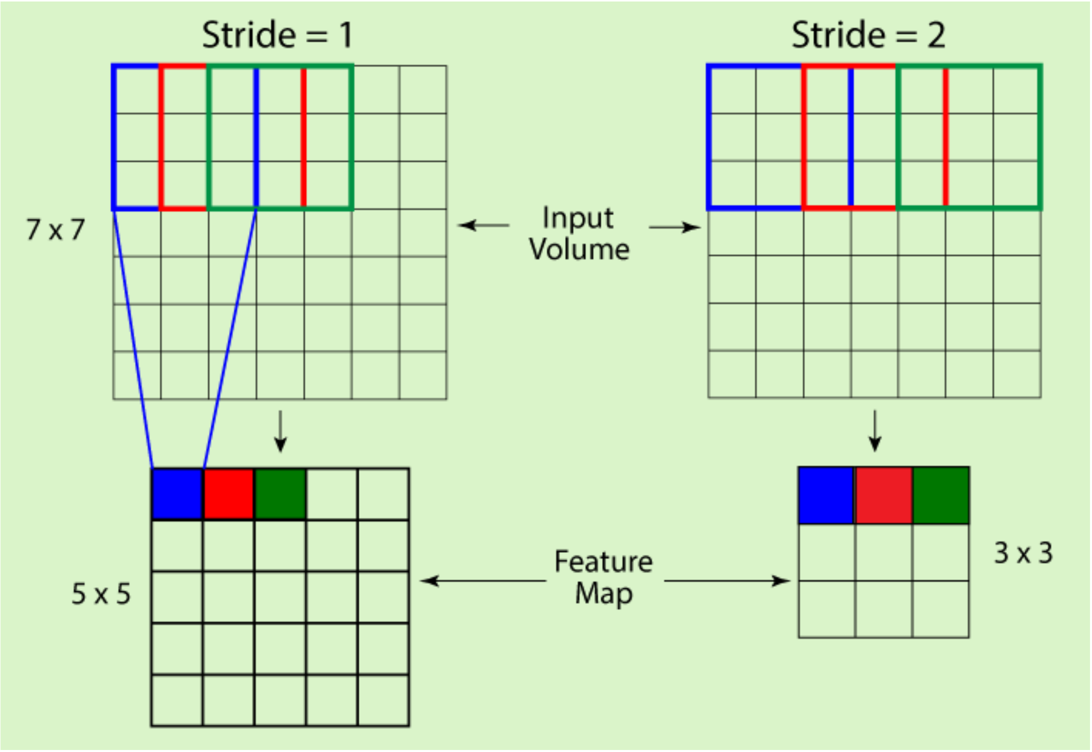

Source : https://developersbreach.com/convolution-neural-network-deep-learning/

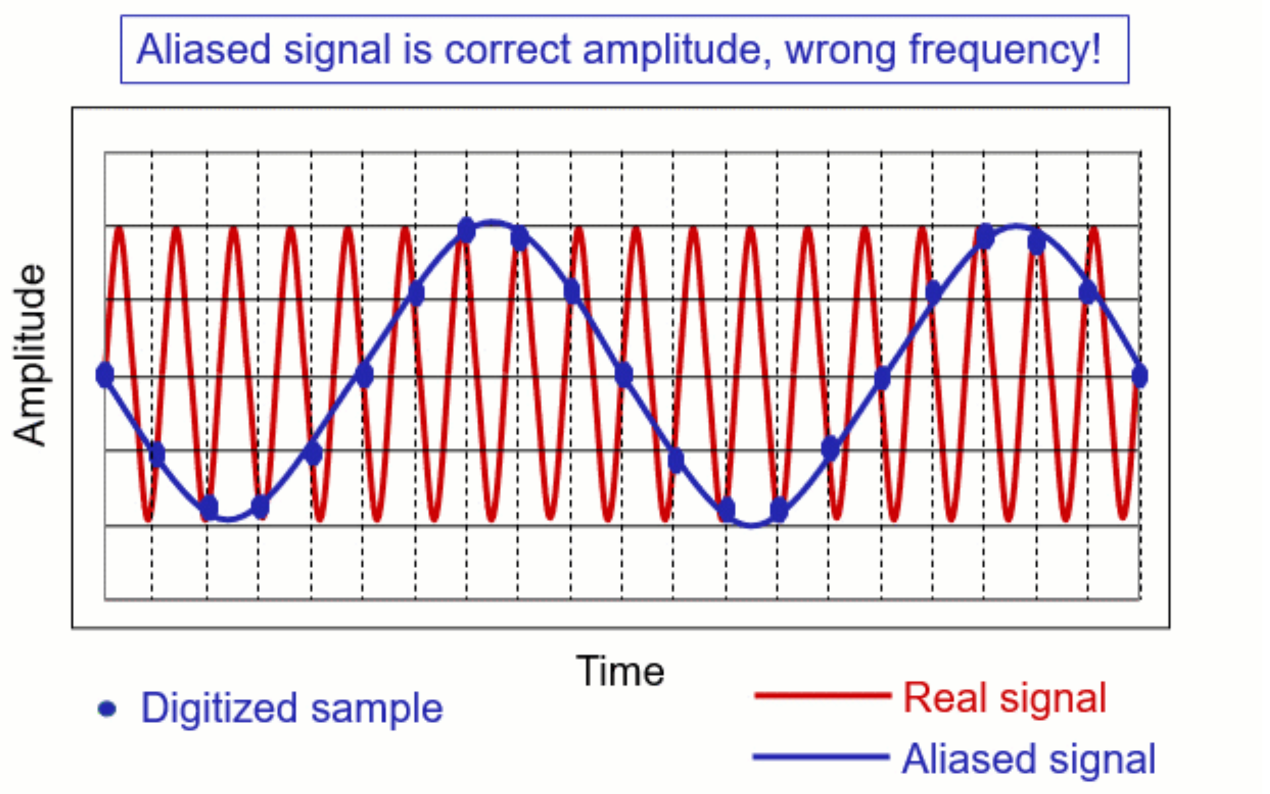

Source : https://community.sw.siemens.com/s/article/data-acquisition-anti-aliasing-filters

Invariance studies in CNN

- These results do not fully extend to the ***discrete framework***
- **Strided** convolution and pooling operators may greatly diverge from shift invariance, due to **aliasing** when subsampling high-frequency signals

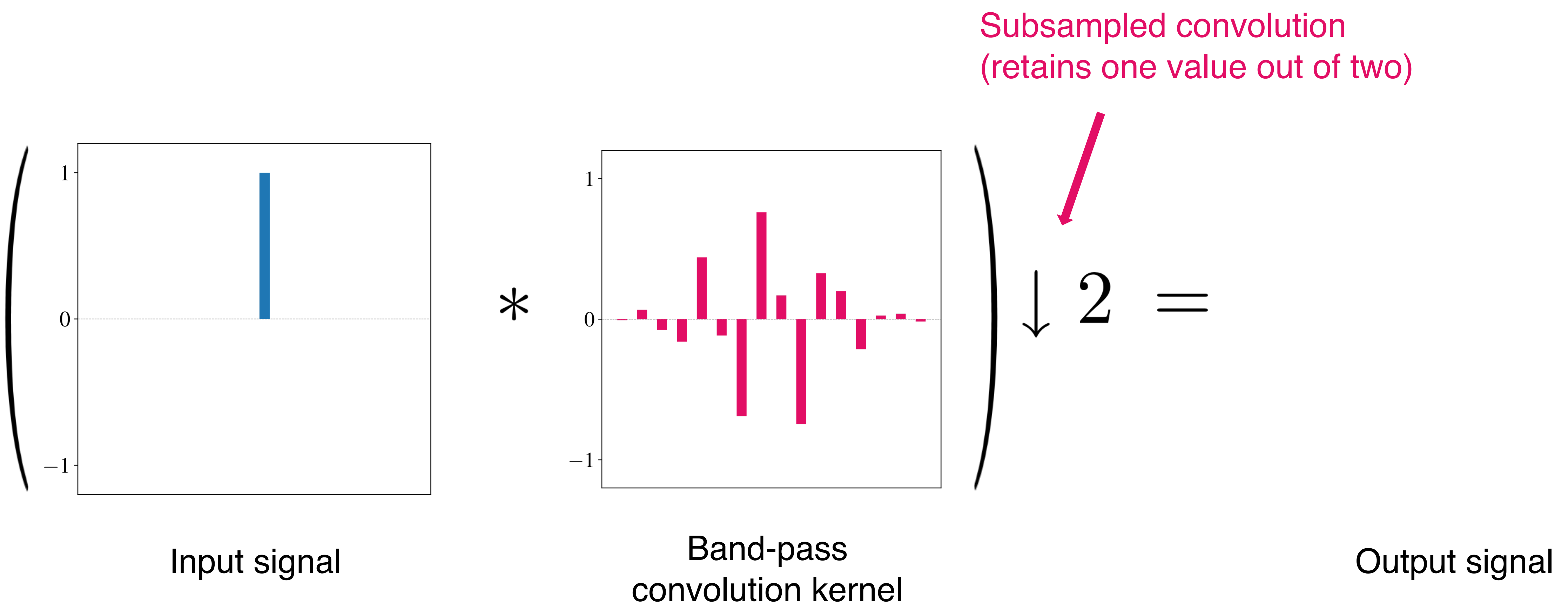

Invariance studies in CNN

- These results do not fully extend to the ***discrete framework***
- **Strided** convolution and pooling operators may greatly diverge from shift invariance, due to **aliasing** when subsampling high-frequency signals

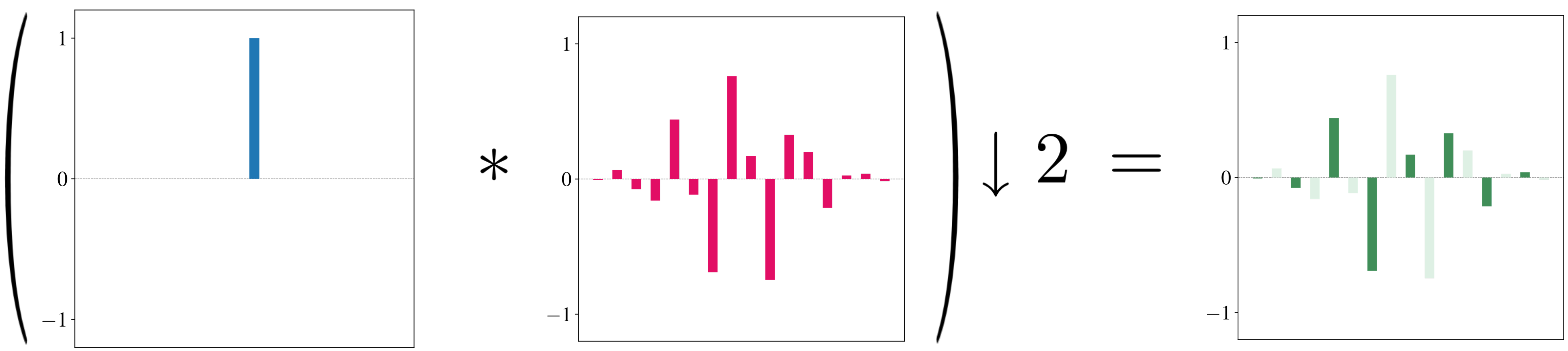

Input signal

Band-pass
convolution kernel

Output signal

Invariance studies in CNN

- These results do not fully extend to the ***discrete framework***
- **Strided** convolution and pooling operators may greatly diverge from shift invariance, due to **aliasing** when subsampling high-frequency signals

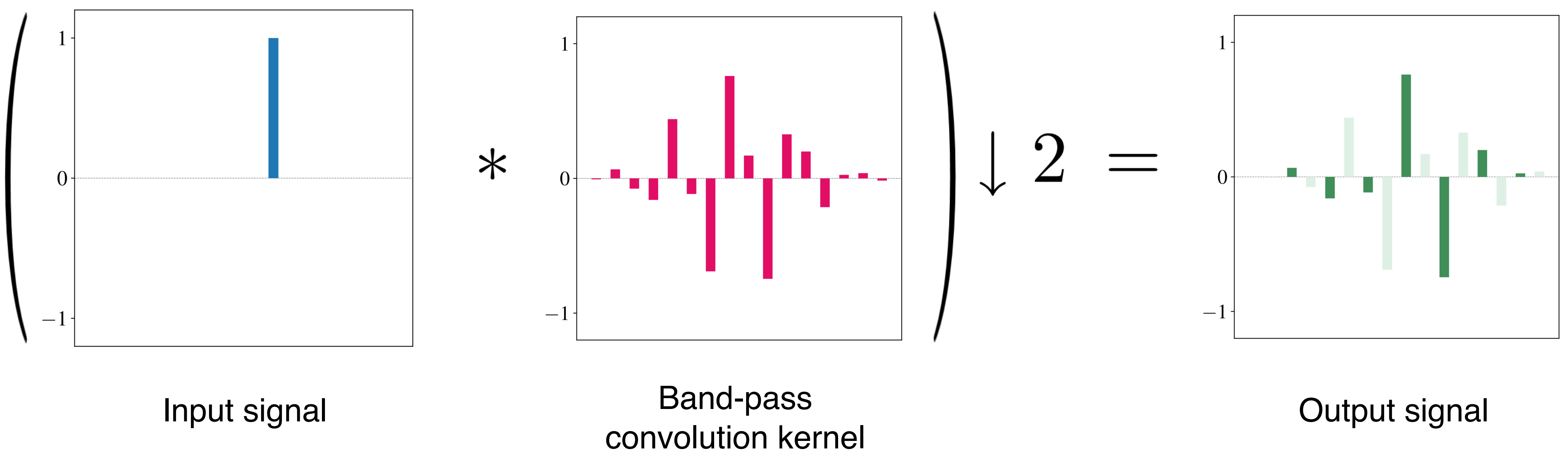

Invariance studies in CNN

- These results do not fully extend to the ***discrete framework***
- **Strided** convolution and pooling operators may greatly diverge from shift invariance, due to **aliasing** when subsampling high-frequency signals

Subsampling a high-frequency signal
→ **Aliasing effect**
→ **Instability to small input shifts**

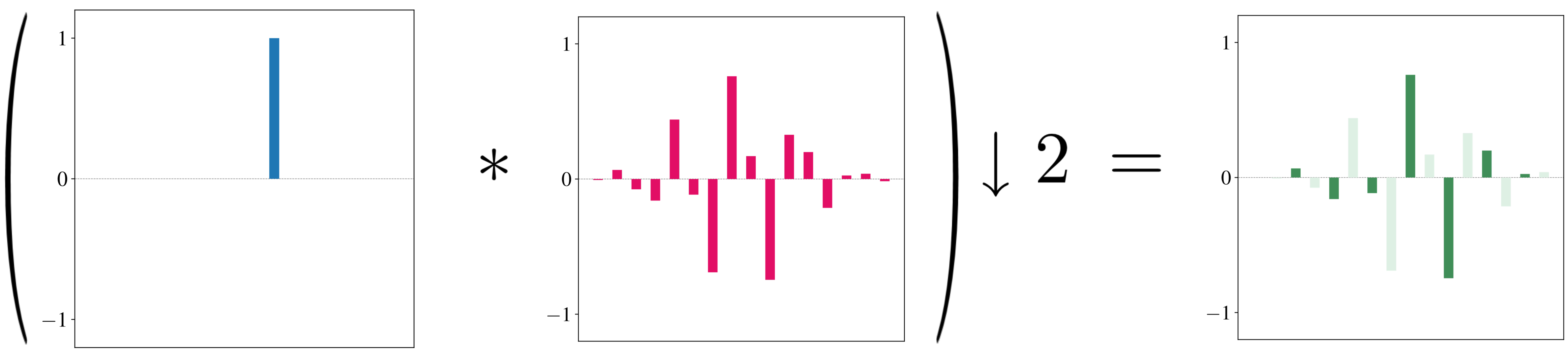

Input signal

Band-pass convolution kernel

Output signal

Invariance studies in CNN

- These results do not fully extend to the ***discrete framework***
- **Strided** convolution and pooling operators may greatly diverge from shift invariance, due to **aliasing** when subsampling high-frequency signals

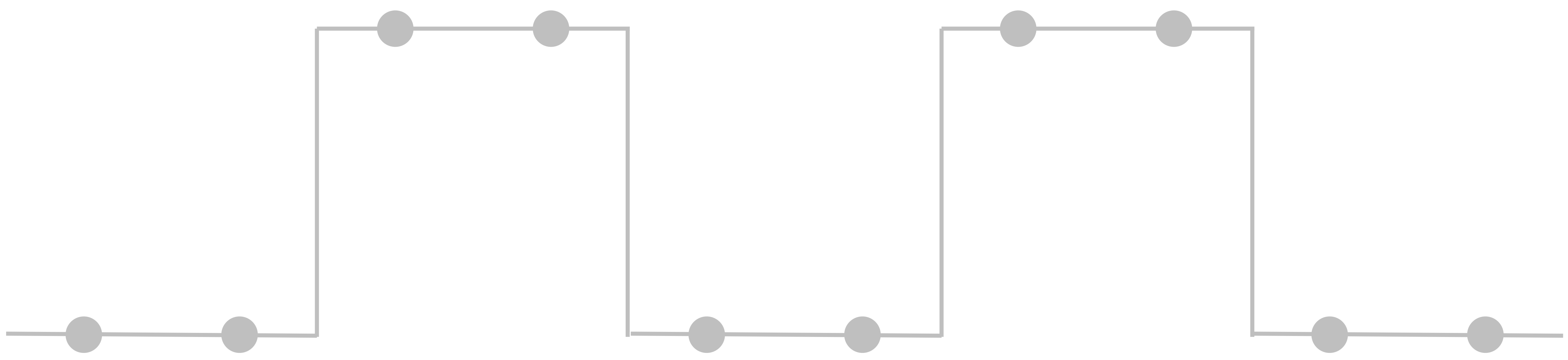

R. Zhang, Making Convolutional Networks Shift-Invariant Again, in International Conference on Machine Learning, 2019.

A. Azulay and Y. Weiss, Why do deep convolutional networks generalize so poorly to small image transformations?, Journal of Machine Learning Research, 2019.

Invariance studies in CNN

- These results do not fully extend to the ***discrete framework***
- **Strided** convolution and pooling operators may greatly diverge from shift invariance, due to **aliasing** when subsampling high-frequency signals

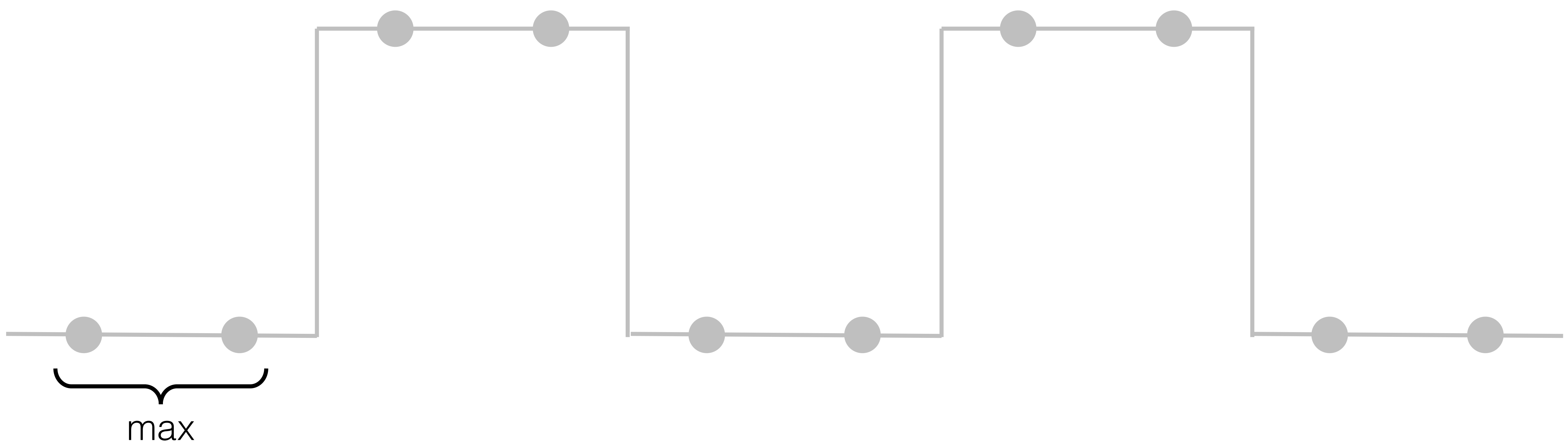

R. Zhang, Making Convolutional Networks Shift-Invariant Again, in International Conference on Machine Learning, 2019.

A. Azulay and Y. Weiss, Why do deep convolutional networks generalize so poorly to small image transformations?, Journal of Machine Learning Research, 2019.

Invariance studies in CNN

- These results do not fully extend to the ***discrete framework***

- **Strided** convolution and pooling operators may greatly diverge from shift invariance, due to **aliasing** when subsampling high-frequency signals

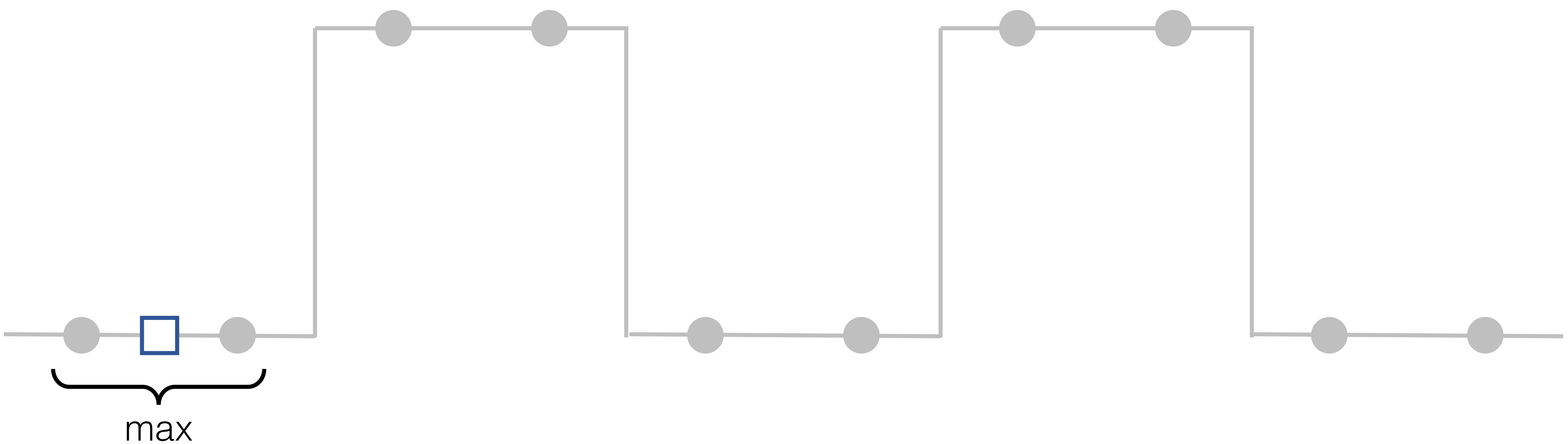

R. Zhang, Making Convolutional Networks Shift-Invariant Again, in International Conference on Machine Learning, 2019.

A. Azulay and Y. Weiss, Why do deep convolutional networks generalize so poorly to small image transformations?, Journal of Machine Learning Research, 2019.

Invariance studies in CNN

- These results do not fully extend to the ***discrete framework***

- **Strided** convolution and pooling operators may greatly diverge from shift invariance, due to **aliasing** when subsampling high-frequency signals

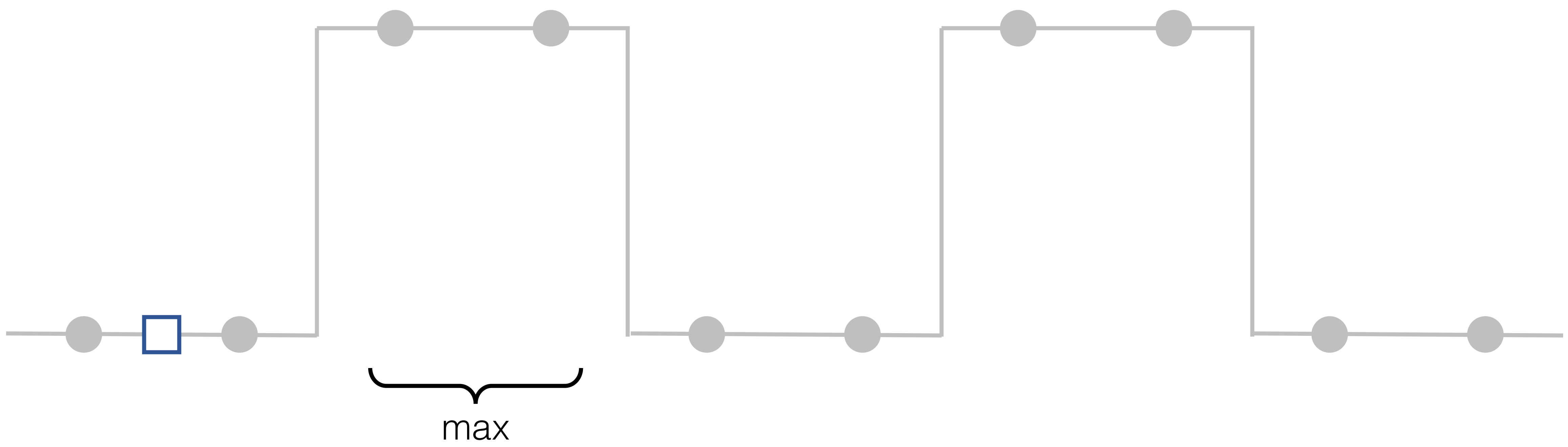

R. Zhang, Making Convolutional Networks Shift-Invariant Again, in International Conference on Machine Learning, 2019.

A. Azulay and Y. Weiss, Why do deep convolutional networks generalize so poorly to small image transformations?, Journal of Machine Learning Research, 2019.

Invariance studies in CNN

- These results do not fully extend to the ***discrete framework***
- **Strided** convolution and pooling operators may greatly diverge from shift invariance, due to **aliasing** when subsampling high-frequency signals

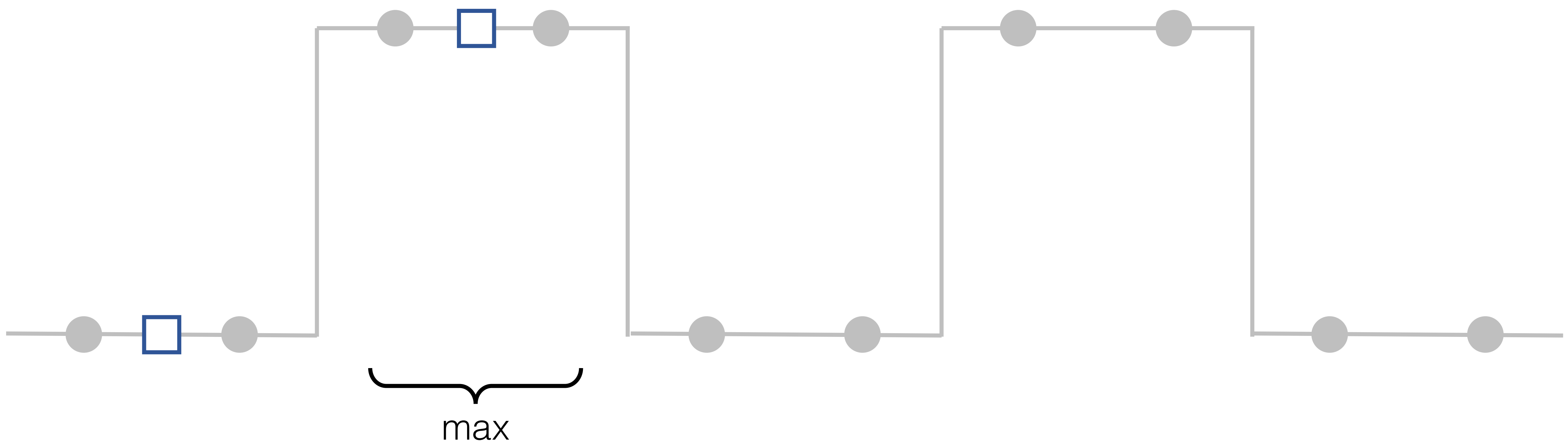

R. Zhang, Making Convolutional Networks Shift-Invariant Again, in International Conference on Machine Learning, 2019.

A. Azulay and Y. Weiss, Why do deep convolutional networks generalize so poorly to small image transformations?, Journal of Machine Learning Research, 2019.

Invariance studies in CNN

- These results do not fully extend to the ***discrete framework***
- **Strided** convolution and pooling operators may greatly diverge from shift invariance, due to **aliasing** when subsampling high-frequency signals

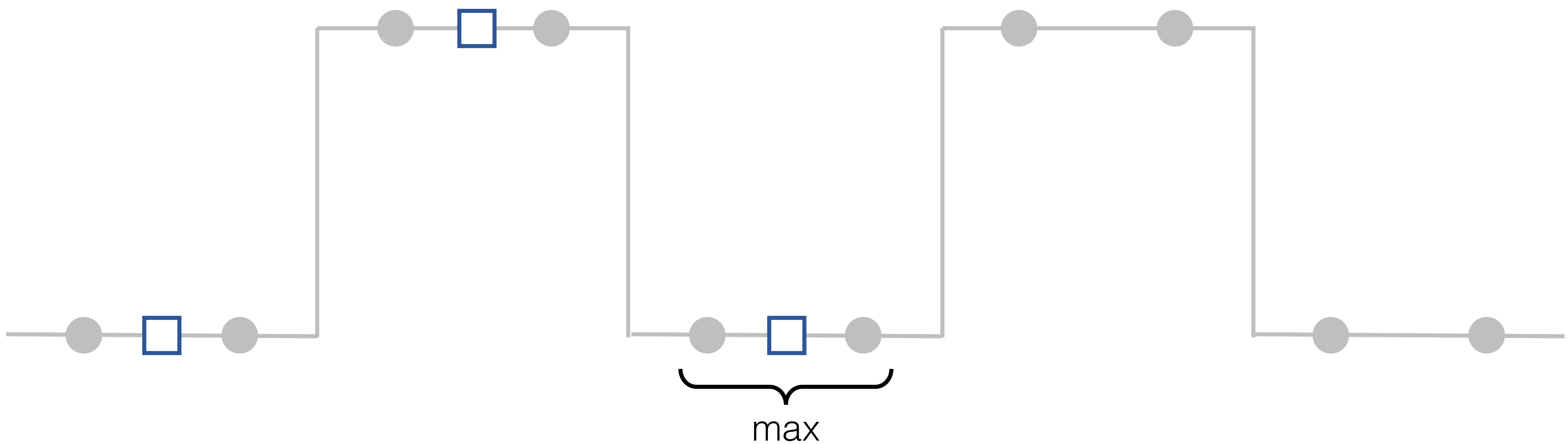

R. Zhang, Making Convolutional Networks Shift-Invariant Again, in International Conference on Machine Learning, 2019.

A. Azulay and Y. Weiss, Why do deep convolutional networks generalize so poorly to small image transformations?, Journal of Machine Learning Research, 2019.

Invariance studies in CNN

- These results do not fully extend to the ***discrete framework***
- **Strided** convolution and pooling operators may greatly diverge from shift invariance, due to **aliasing** when subsampling high-frequency signals

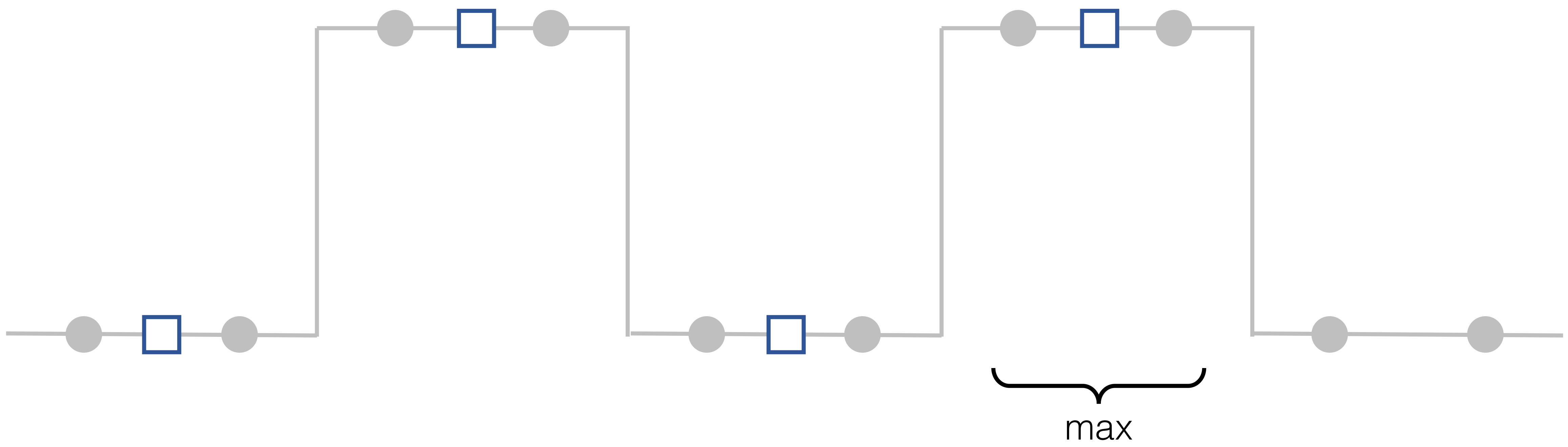

R. Zhang, Making Convolutional Networks Shift-Invariant Again, in International Conference on Machine Learning, 2019.

A. Azulay and Y. Weiss, Why do deep convolutional networks generalize so poorly to small image transformations?, Journal of Machine Learning Research, 2019.

Invariance studies in CNN

- These results do not fully extend to the ***discrete framework***
- **Strided** convolution and pooling operators may greatly diverge from shift invariance, due to **aliasing** when subsampling high-frequency signals

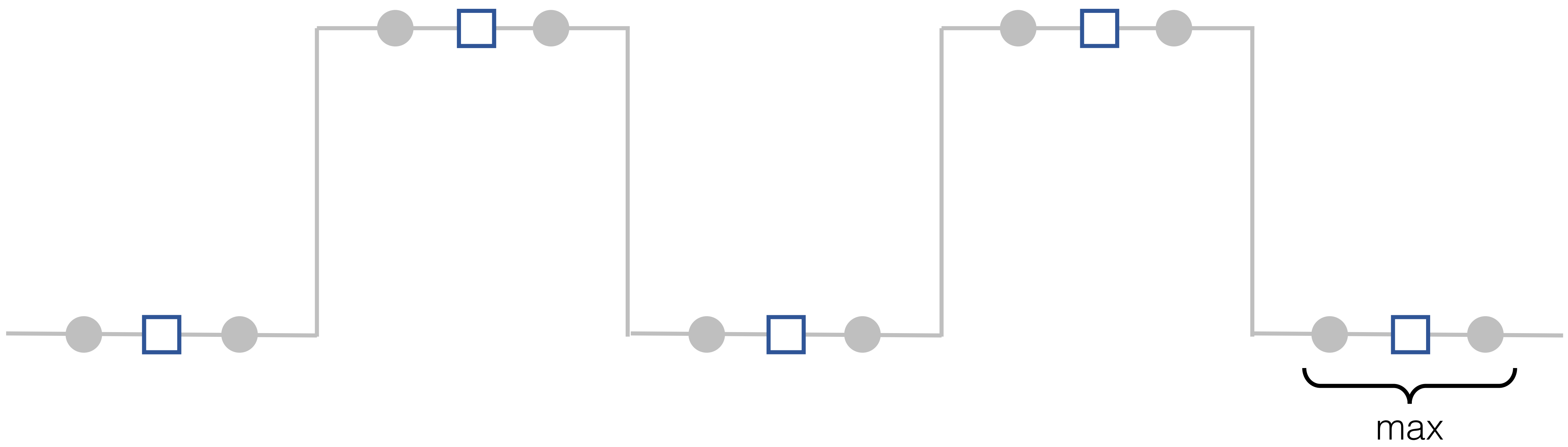

R. Zhang, Making Convolutional Networks Shift-Invariant Again, in International Conference on Machine Learning, 2019.

A. Azulay and Y. Weiss, Why do deep convolutional networks generalize so poorly to small image transformations?, Journal of Machine Learning Research, 2019.

Invariance studies in CNN

- These results do not fully extend to the ***discrete framework***
- **Strided** convolution and pooling operators may greatly diverge from shift invariance, due to **aliasing** when subsampling high-frequency signals

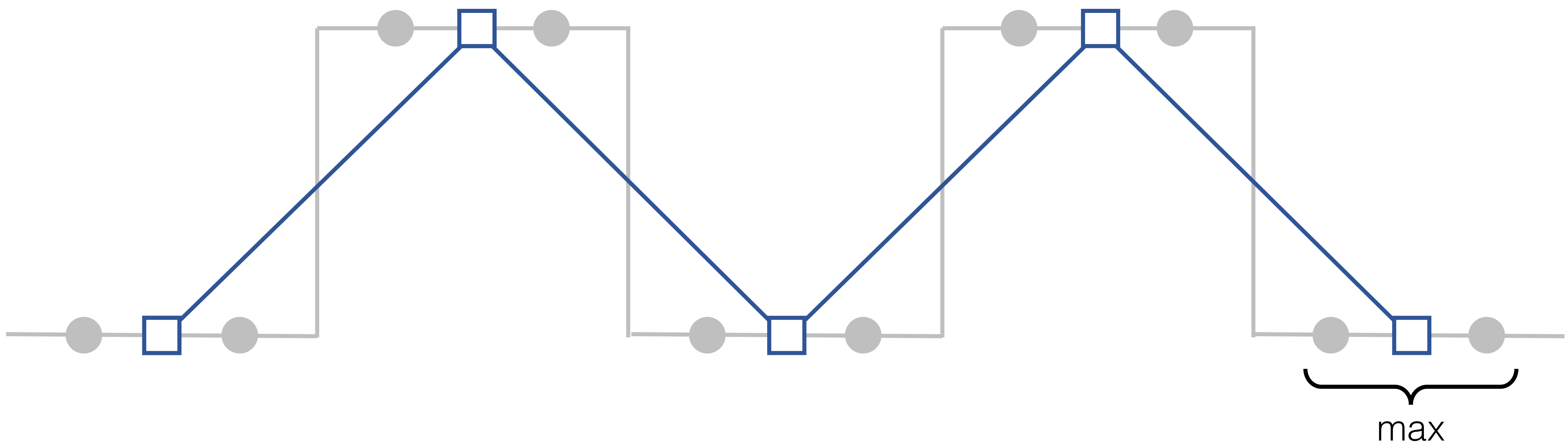

R. Zhang, Making Convolutional Networks Shift-Invariant Again, in International Conference on Machine Learning, 2019.

A. Azulay and Y. Weiss, Why do deep convolutional networks generalize so poorly to small image transformations?, Journal of Machine Learning Research, 2019.

Invariance studies in CNN

- These results do not fully extend to the ***discrete framework***
- **Strided** convolution and pooling operators may greatly diverge from shift invariance, due to **aliasing** when subsampling high-frequency signals

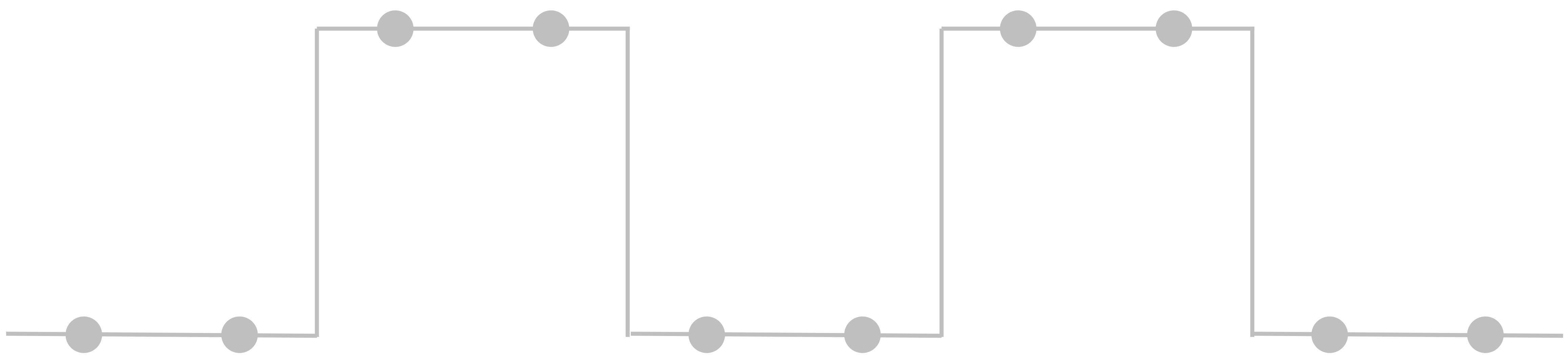

R. Zhang, Making Convolutional Networks Shift-Invariant Again, in International Conference on Machine Learning, 2019.

A. Azulay and Y. Weiss, Why do deep convolutional networks generalize so poorly to small image transformations?, Journal of Machine Learning Research, 2019.

Invariance studies in CNN

- These results do not fully extend to the ***discrete framework***
- **Strided** convolution and pooling operators may greatly diverge from shift invariance, due to **aliasing** when subsampling high-frequency signals

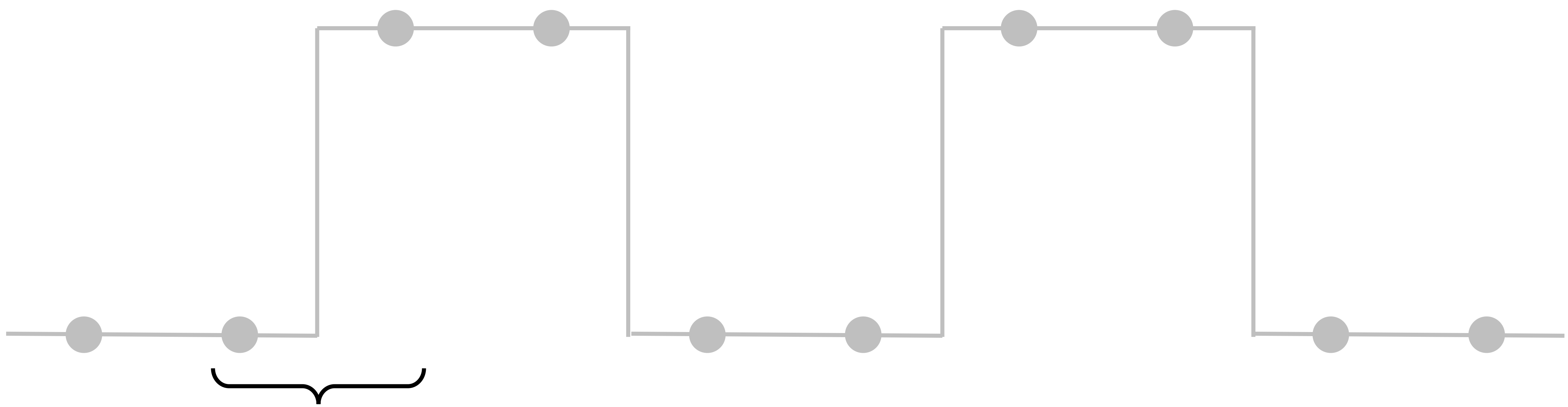

R. Zhang, Making Convolutional Networks Shift-Invariant Again, in International Conference on Machine Learning, 2019.

A. Azulay and Y. Weiss, Why do deep convolutional networks generalize so poorly to small image transformations?, Journal of Machine Learning Research, 2019.

Invariance studies in CNN

- These results do not fully extend to the ***discrete framework***
- **Strided** convolution and pooling operators may greatly diverge from shift invariance, due to **aliasing** when subsampling high-frequency signals

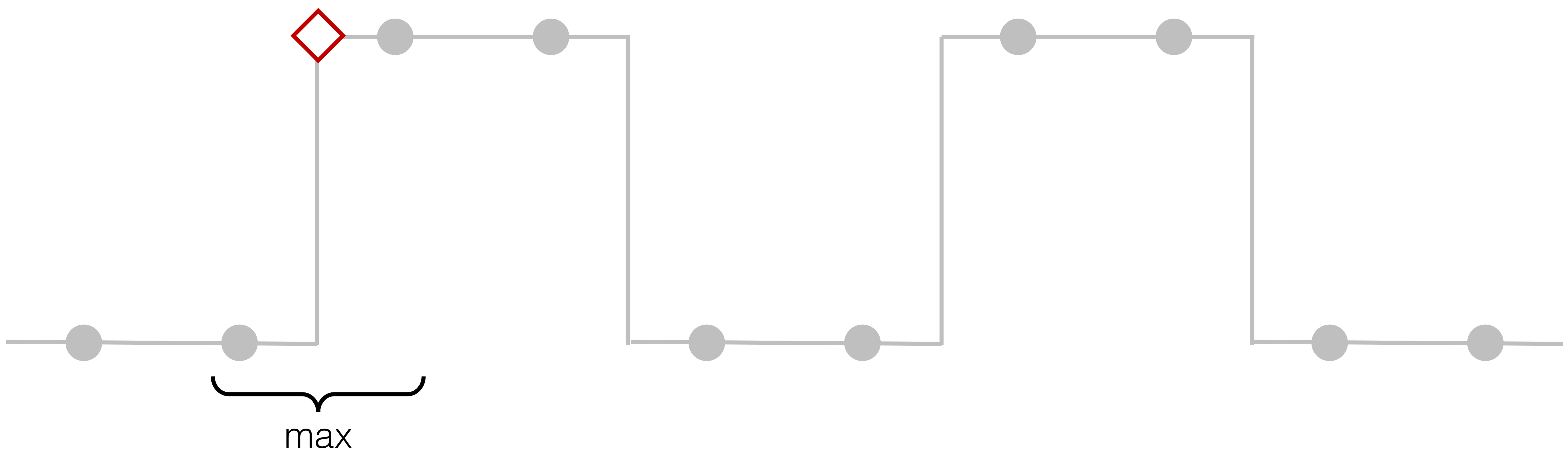

R. Zhang, Making Convolutional Networks Shift-Invariant Again, in International Conference on Machine Learning, 2019.

A. Azulay and Y. Weiss, Why do deep convolutional networks generalize so poorly to small image transformations?, Journal of Machine Learning Research, 2019.

Invariance studies in CNN

- These results do not fully extend to the ***discrete framework***
- **Strided** convolution and pooling operators may greatly diverge from shift invariance, due to **aliasing** when subsampling high-frequency signals

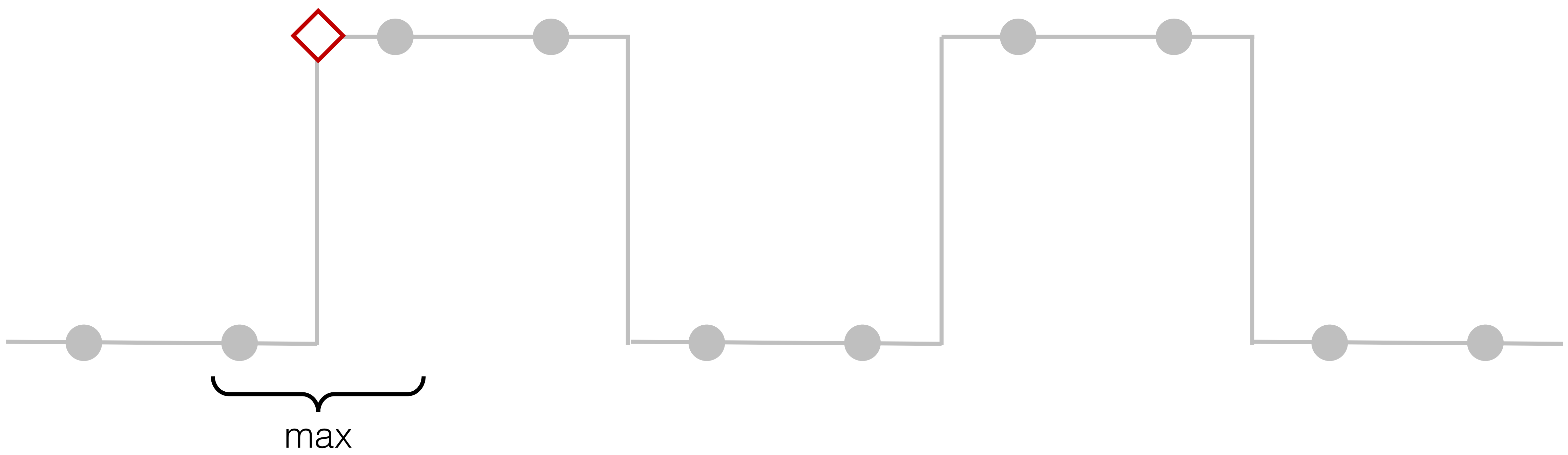

R. Zhang, Making Convolutional Networks Shift-Invariant Again, in International Conference on Machine Learning, 2019.

A. Azulay and Y. Weiss, Why do deep convolutional networks generalize so poorly to small image transformations?, Journal of Machine Learning Research, 2019.

Invariance studies in CNN

- These results do not fully extend to the ***discrete framework***
- **Strided** convolution and pooling operators may greatly diverge from shift invariance, due to **aliasing** when subsampling high-frequency signals

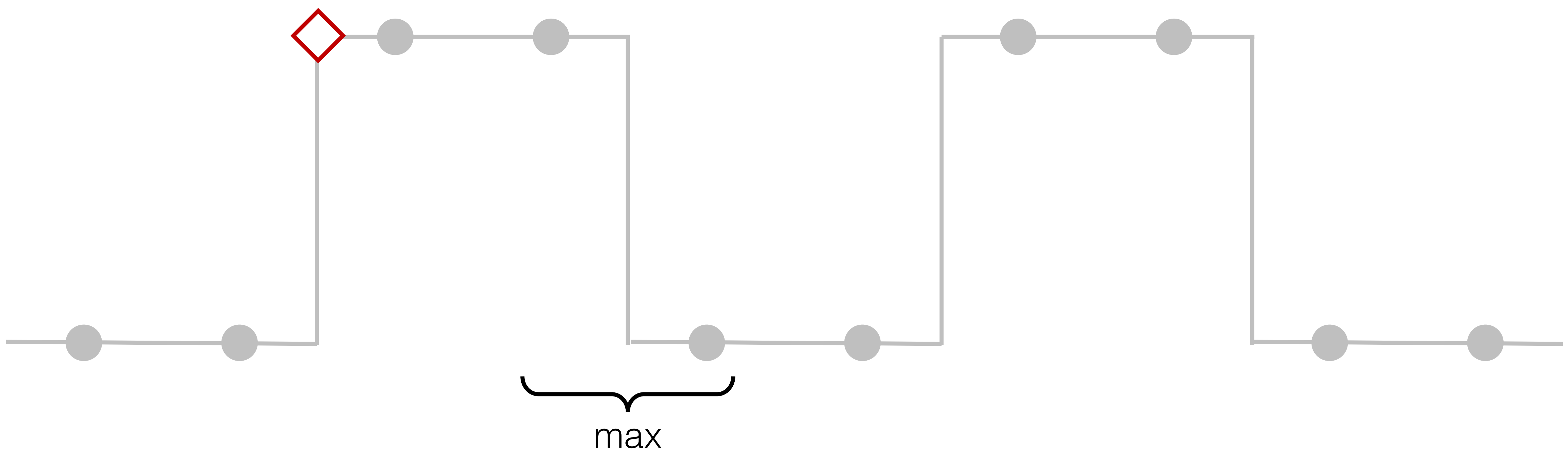

R. Zhang, Making Convolutional Networks Shift-Invariant Again, in International Conference on Machine Learning, 2019.

A. Azulay and Y. Weiss, Why do deep convolutional networks generalize so poorly to small image transformations?, Journal of Machine Learning Research, 2019.

Invariance studies in CNN

- These results do not fully extend to the ***discrete framework***
- **Strided** convolution and pooling operators may greatly diverge from shift invariance, due to **aliasing** when subsampling high-frequency signals

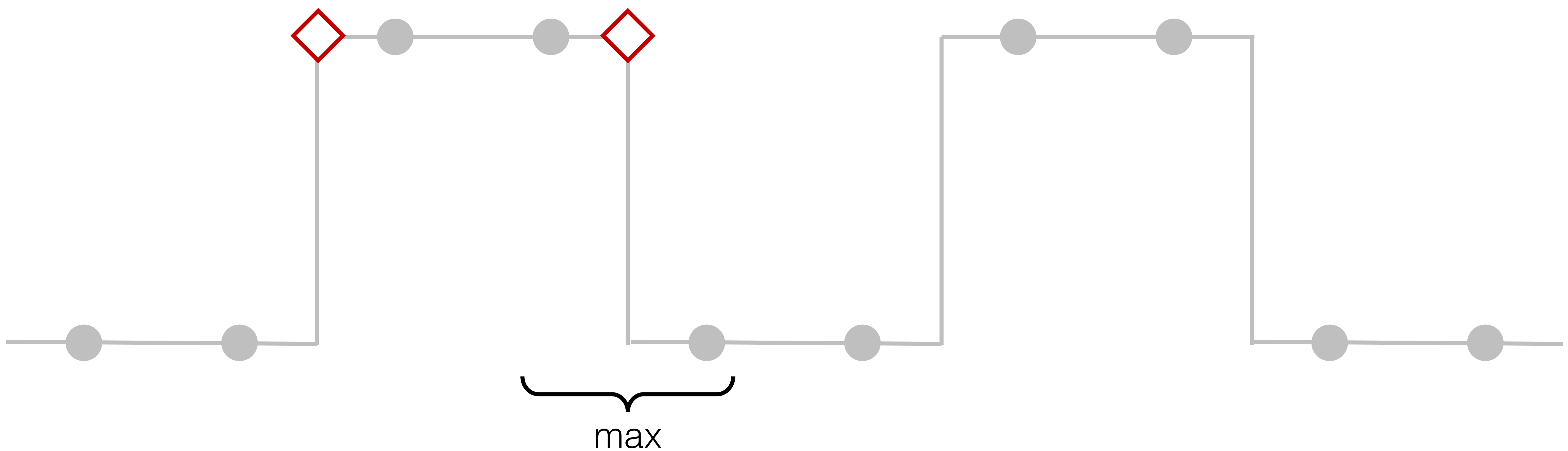

R. Zhang, Making Convolutional Networks Shift-Invariant Again, in International Conference on Machine Learning, 2019.

A. Azulay and Y. Weiss, Why do deep convolutional networks generalize so poorly to small image transformations?, Journal of Machine Learning Research, 2019.

Invariance studies in CNN

- These results do not fully extend to the ***discrete framework***
- **Strided** convolution and pooling operators may greatly diverge from shift invariance, due to **aliasing** when subsampling high-frequency signals

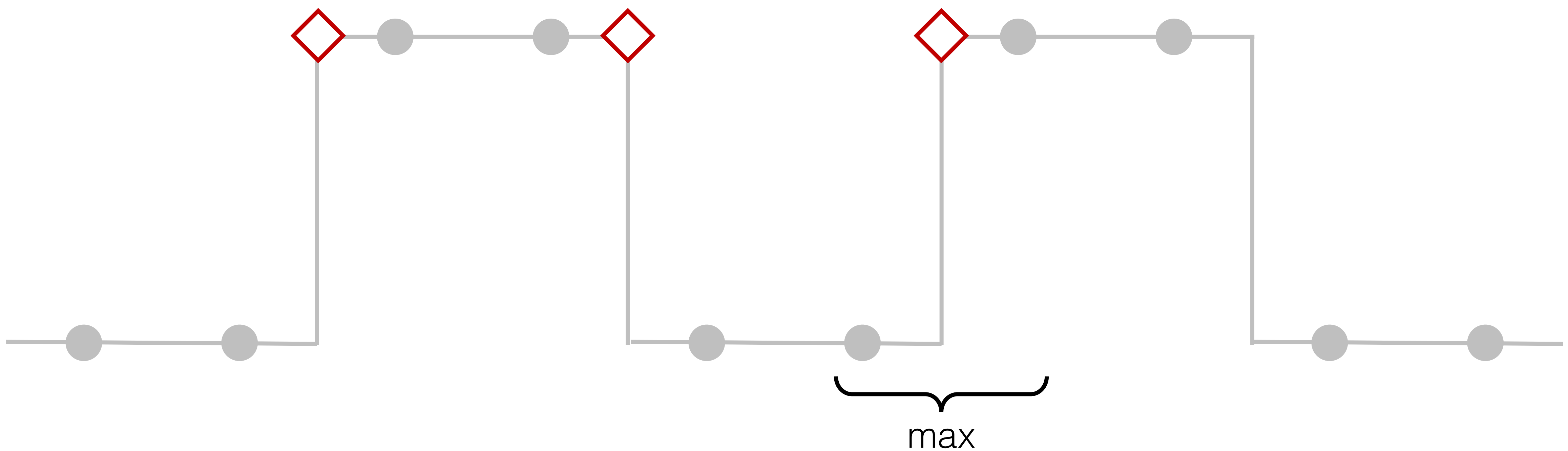

R. Zhang, Making Convolutional Networks Shift-Invariant Again, in International Conference on Machine Learning, 2019.

A. Azulay and Y. Weiss, Why do deep convolutional networks generalize so poorly to small image transformations?, Journal of Machine Learning Research, 2019.

Invariance studies in CNN

- These results do not fully extend to the ***discrete framework***
- **Strided** convolution and pooling operators may greatly diverge from shift invariance, due to **aliasing** when subsampling high-frequency signals

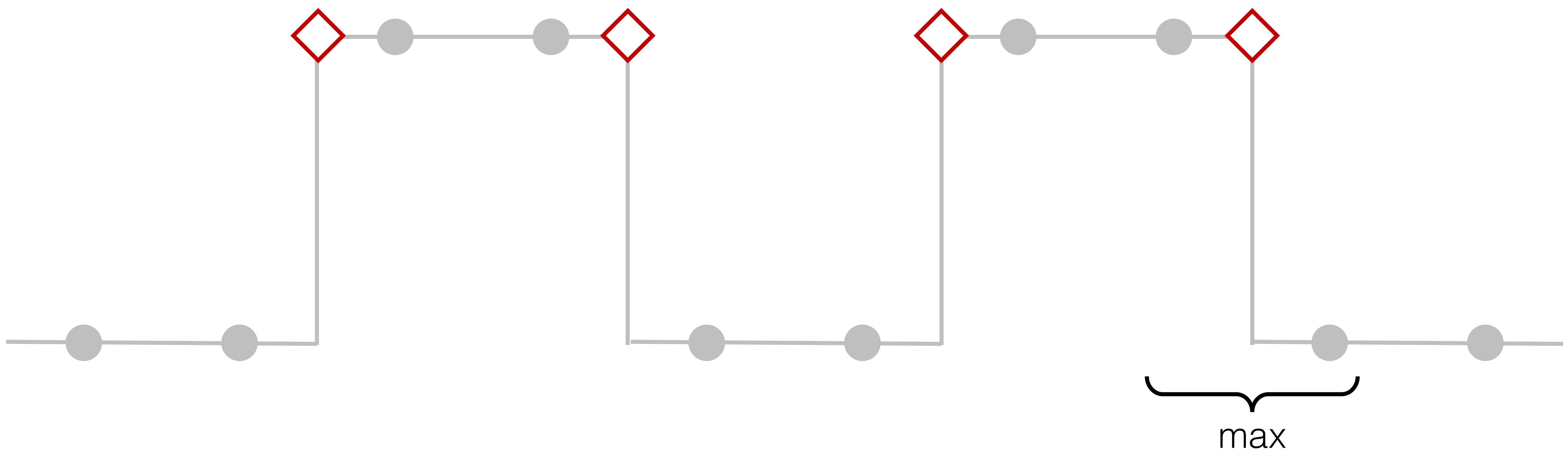

R. Zhang, Making Convolutional Networks Shift-Invariant Again, in International Conference on Machine Learning, 2019.

A. Azulay and Y. Weiss, Why do deep convolutional networks generalize so poorly to small image transformations?, Journal of Machine Learning Research, 2019.

Invariance studies in CNN

- These results do not fully extend to the ***discrete framework***
- **Strided** convolution and pooling operators may greatly diverge from shift invariance, due to **aliasing** when subsampling high-frequency signals

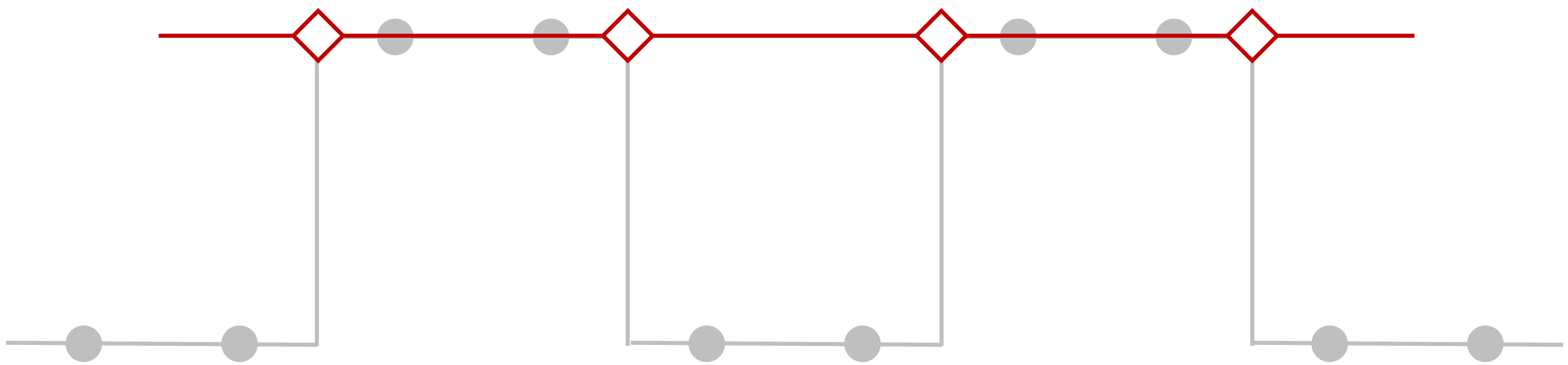

R. Zhang, Making Convolutional Networks Shift-Invariant Again, in International Conference on Machine Learning, 2019.

A. Azulay and Y. Weiss, Why do deep convolutional networks generalize so poorly to small image transformations?, Journal of Machine Learning Research, 2019.

Invariance studies in CNN

- These results do not fully extend to the ***discrete framework***
- **Strided** convolution and pooling operators may greatly diverge from shift invariance, due to **aliasing** when subsampling high-frequency signals

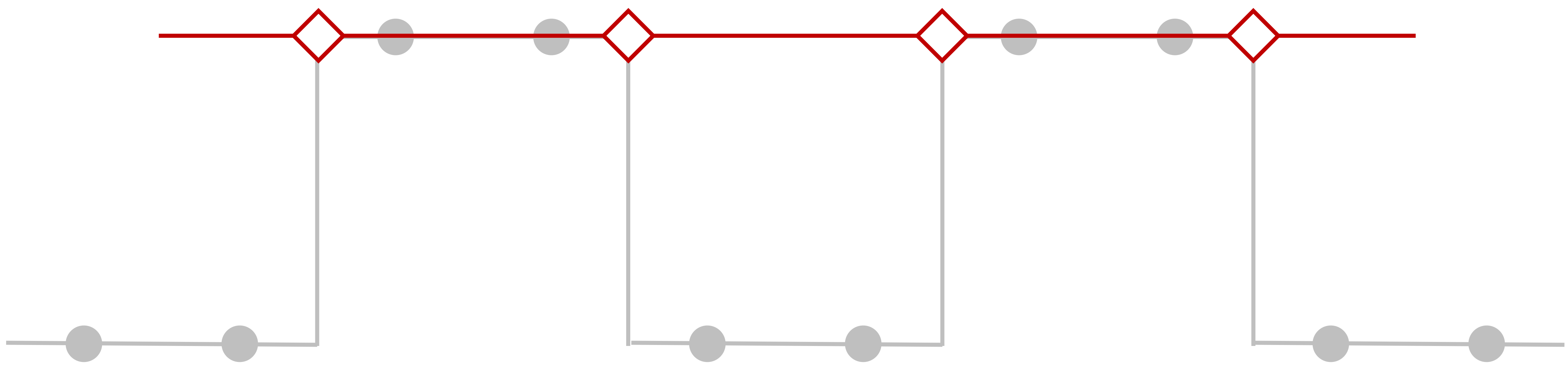

R. Zhang, Making Convolutional Networks Shift-Invariant Again, in International Conference on Machine Learning, 2019.

A. Azulay and Y. Weiss, Why do deep convolutional networks generalize so poorly to small image transformations?, Journal of Machine Learning Research, 2019.

Invariance studies in CNN

- These results do not fully extend to the ***discrete framework***
- **Strided** convolution and pooling operators may greatly diverge from shift invariance, due to **aliasing** when subsampling high-frequency signals

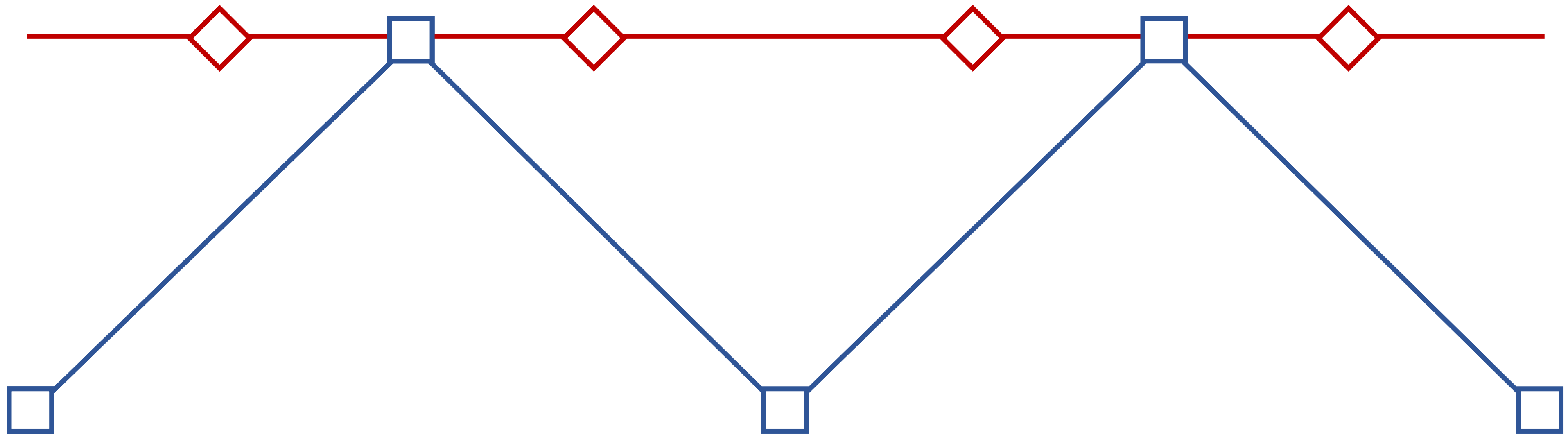

R. Zhang, Making Convolutional Networks Shift-Invariant Again, in International Conference on Machine Learning, 2019.

A. Azulay and Y. Weiss, Why do deep convolutional networks generalize so poorly to small image transformations?, Journal of Machine Learning Research, 2019.

Aliasing breaks shift-invariance

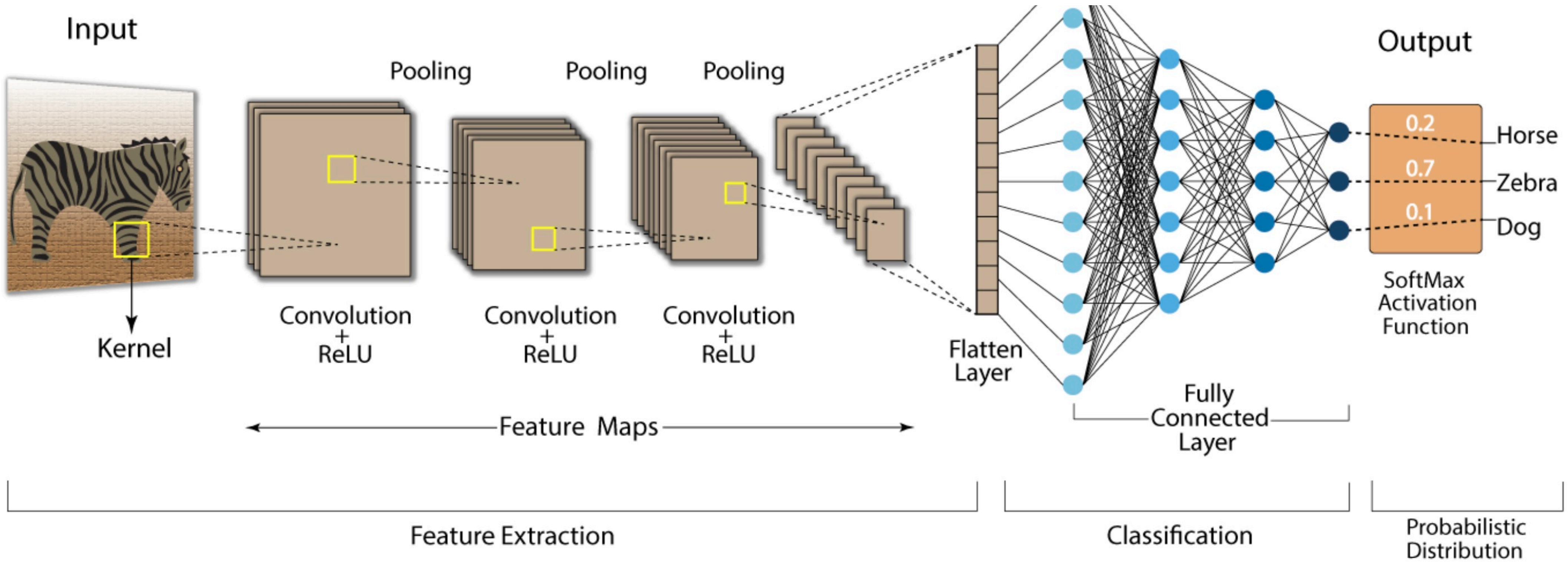

Source : https://developersbreach.com/convolution-neural-network-deep-learning/

Aliasing breaks shift-invariance

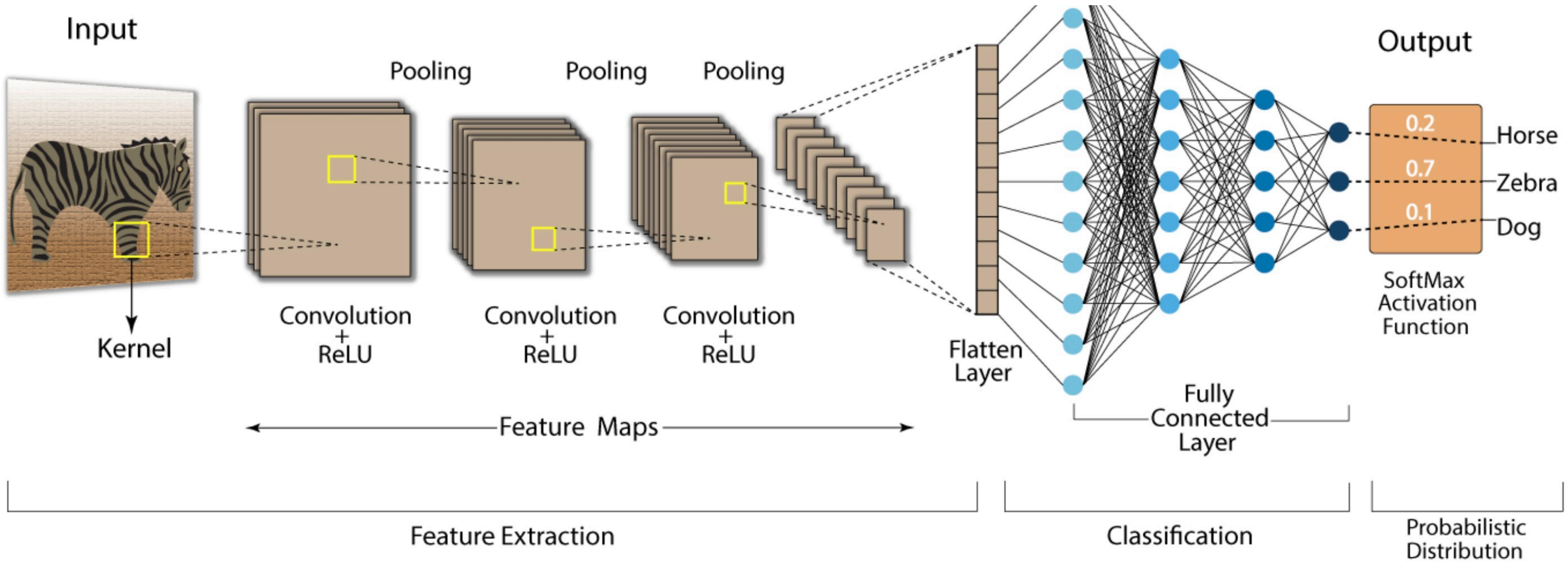

Source : https://developersbreach.com/convolution-neural-network-deep-learning/

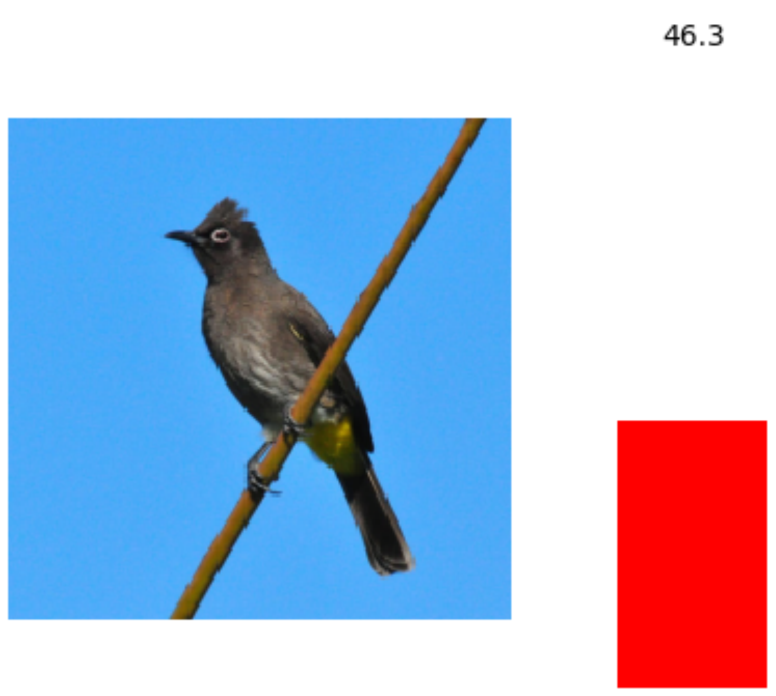

Blind spots in the shift-invariance studies

Blind spots in the shift-invariance studies

- The **effect of the max pooling operator on network stability** under small input shifts has not been investigated, particularly when used in combination with Gabor-like convolutions.

Blind spots in the shift-invariance studies

- The **effect of the max pooling operator on network stability** under small input shifts has not been investigated, particularly when used in combination with Gabor-like convolutions.

- In the discrete case, the presence of subsampled convolutions with oriented band-pass filters can lead to aliasing artifacts. To our knowledge, **the literature lacks theoretical studies that take these aliasing effects into account**.

Blind spots in the shift-invariance studies

- The **effect of the max pooling operator on network stability** under small input shifts has not been investigated, particularly when used in combination with Gabor-like convolutions.

- In the discrete case, the presence of subsampled convolutions with oriented band-pass filters can lead to aliasing artifacts. To our knowledge, **the literature lacks theoretical studies that take these aliasing effects into account**.

- Although extensive studies have been conducted on complex-valued convolutions followed by modulus, **a link is missing to extend these results to standard CNNs**, which implement real-valued convolutions and spatial pooling operators.

Focus on the first layer

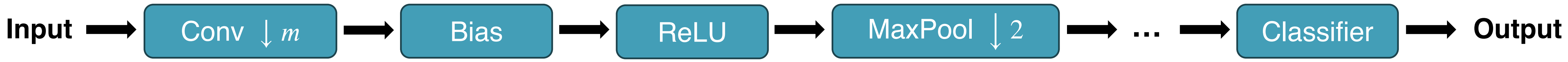

Focus on the first layer

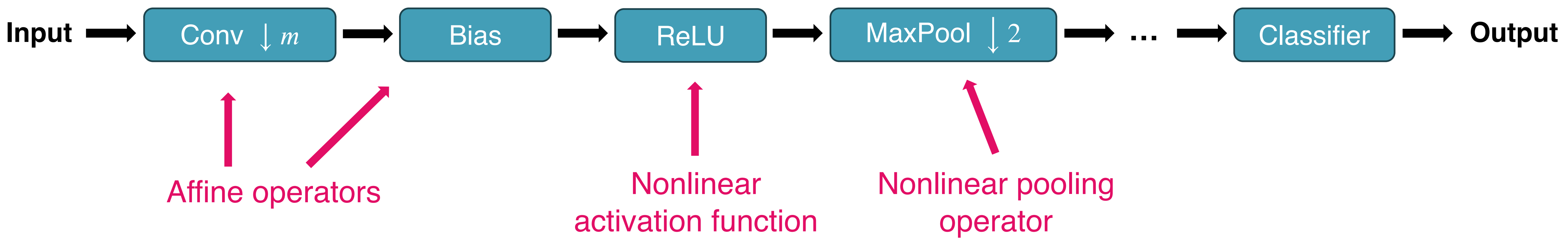

Focus on the first layer

Focus on the first layer

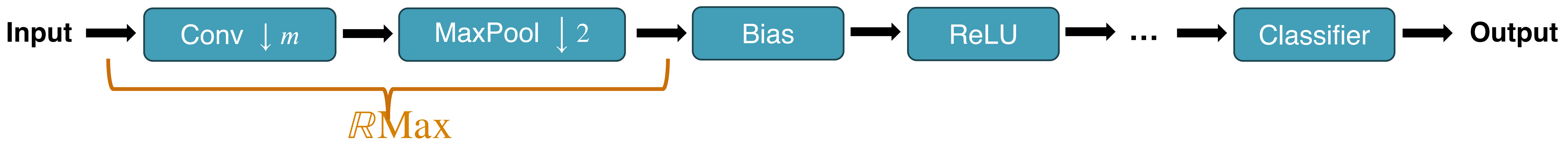

Focus on the first layer

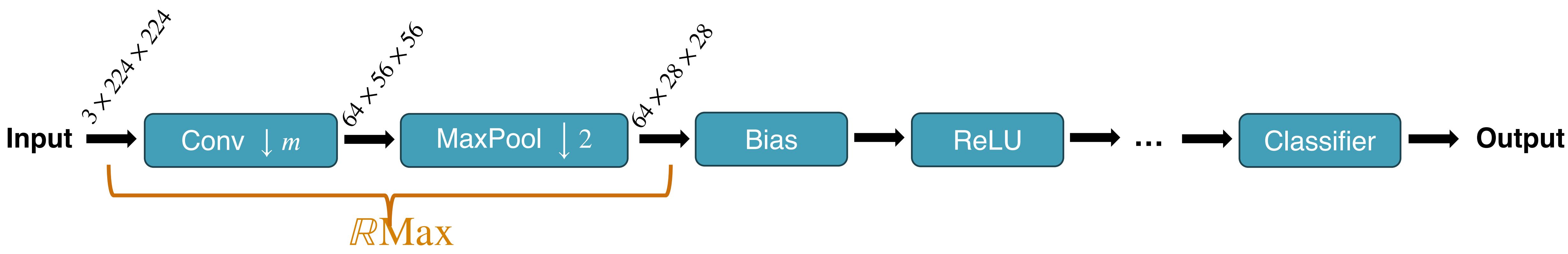

Example: AlexNet (2012)

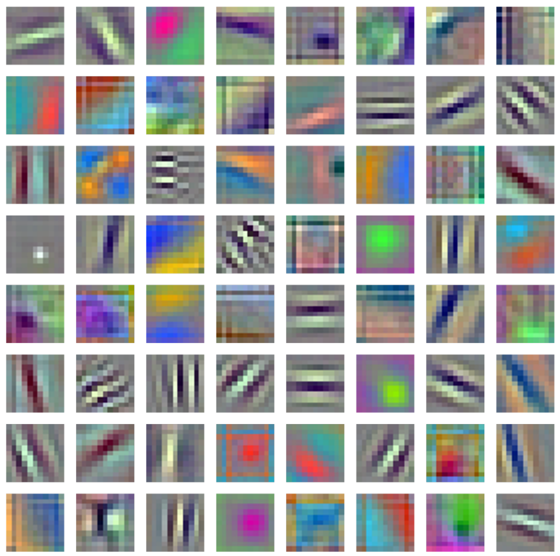

Focus on the first layer

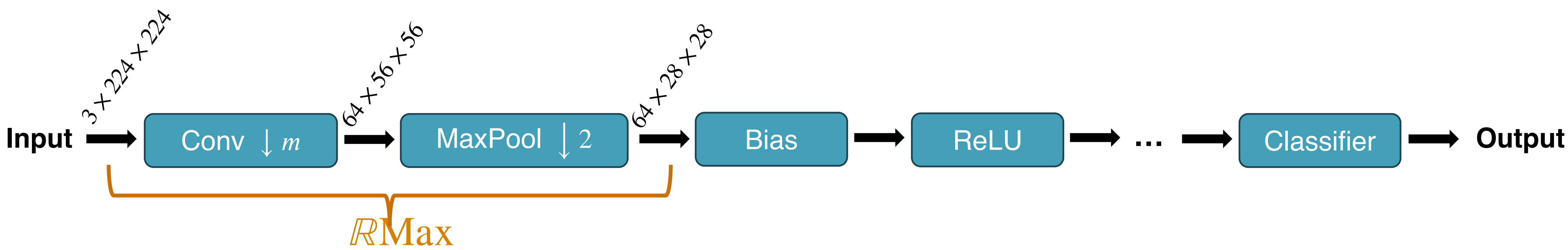

Band-pass "**Gabor-like**" filters

Example: AlexNet (2012)

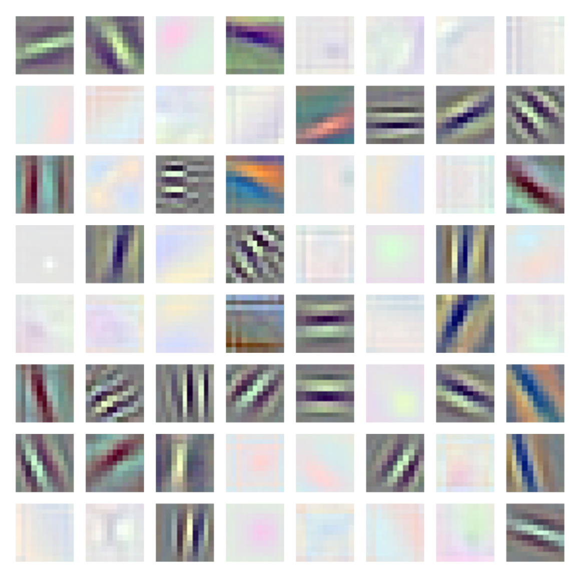

Focus on the first layer

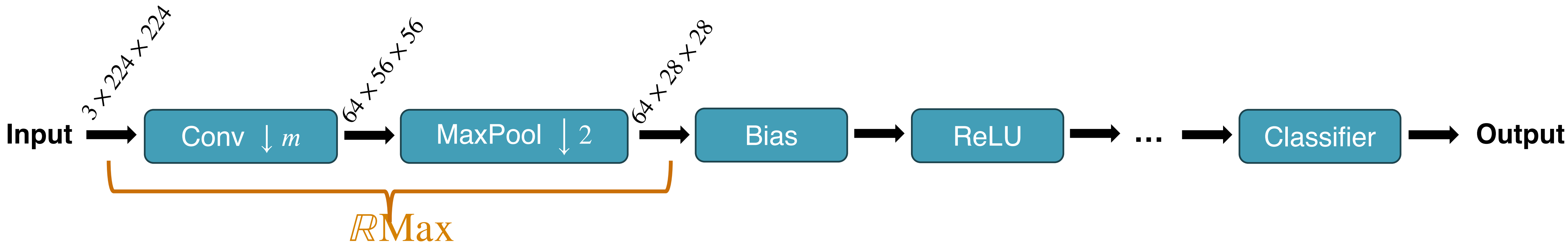

Band-pass **"Gabor-like"** filters

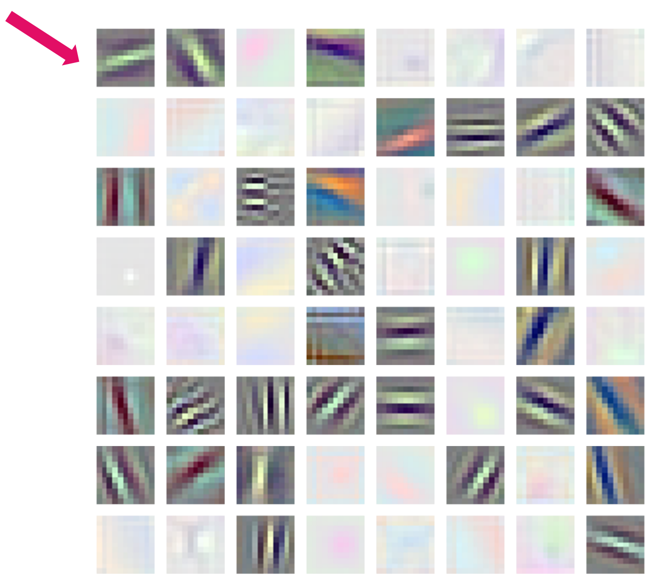

Example: AlexNet
(2012)

Rai, Mehang, and Pablo Rivas. "A review of convolutional neural networks and Gabor filters in object recognition." *2020 International Conference on Computational Science and Computational Intelligence (CSCI)*. IEEE, 2020.

Yosinski J, Clune J, Bengio Y, and Lipson H. How transferable are features in deep neural networks? In Advances in Neural Information Processing Systems 27 (NIPS '14), NIPS Foundation, 2014.

Subsampled convolutions, a real problem!

Subsampled convolution
(retains one value out of two)

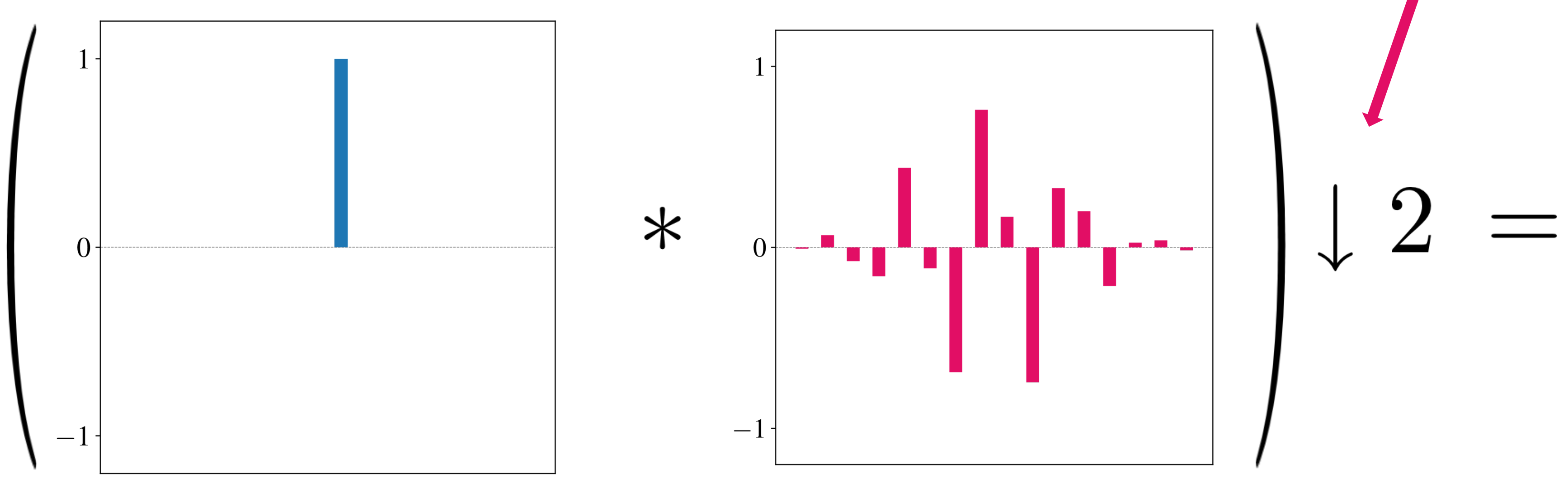

Input signal

Band-pass
convolution kernel

Output signal

Subsampled convolutions, a real problem!

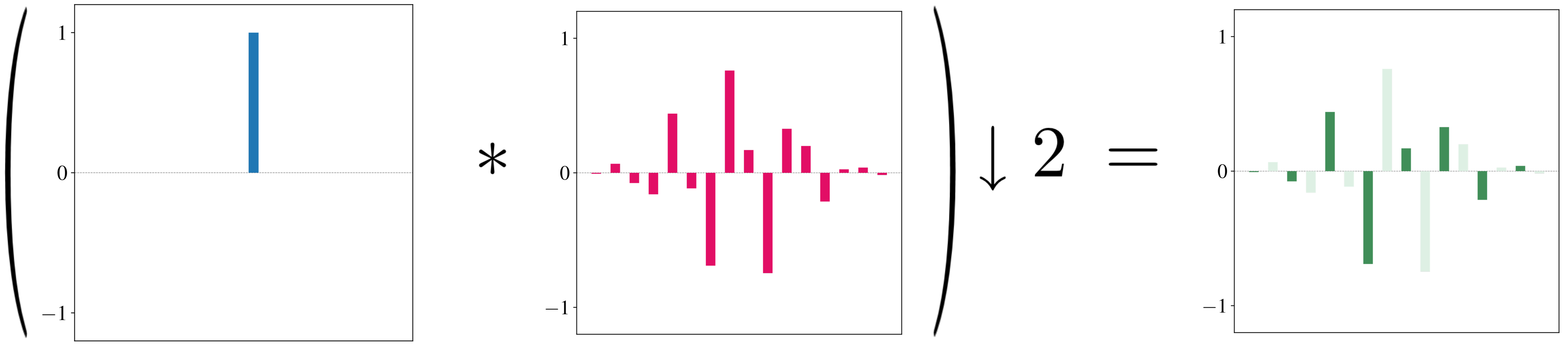

Input signal

Band-pass convolution kernel

Output signal

Subsampled convolutions, a real problem!

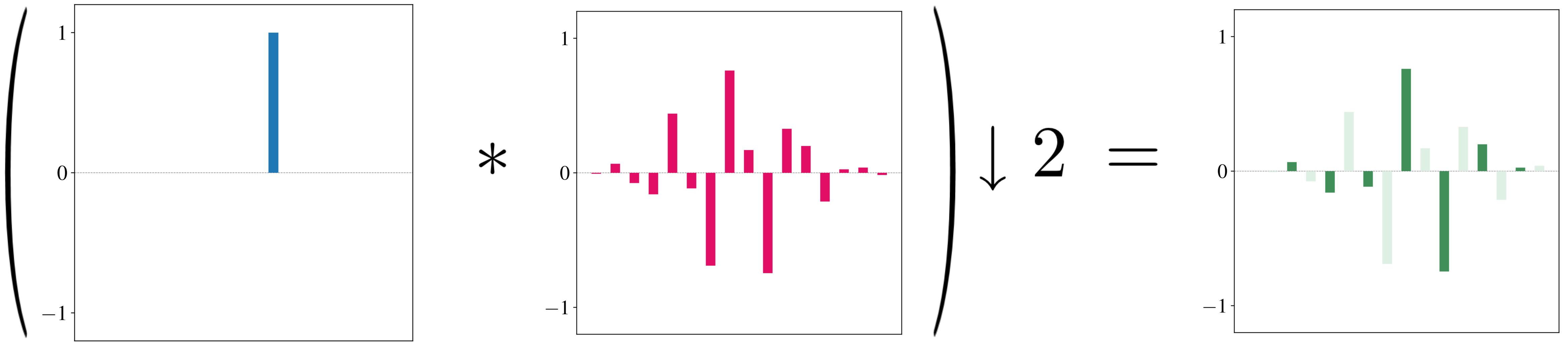

Input signal

Band-pass
convolution kernel

Output signal

Subsampled convolutions, a real problem!

Subsampling a high-frequency signal
→ **Aliasing effect**
→ **Instability to small input shifts**

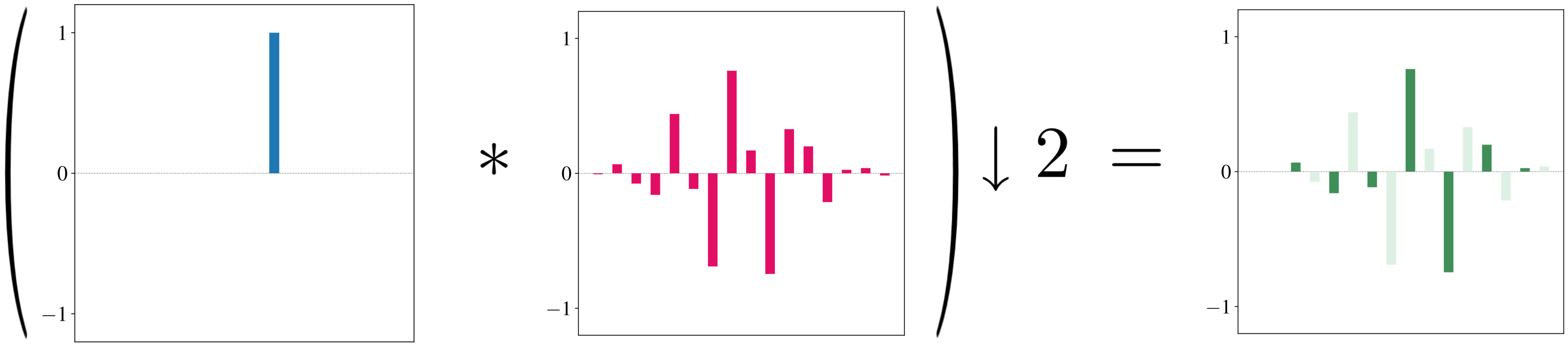

Input signal

Band-pass
convolution kernel

Output signal

Subsampled convolutions, a real problem!

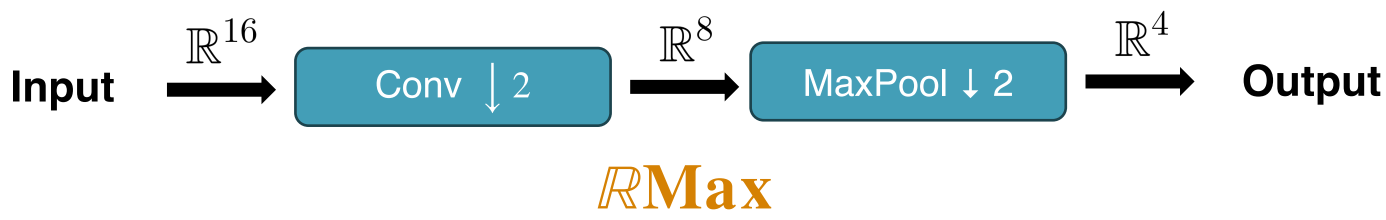

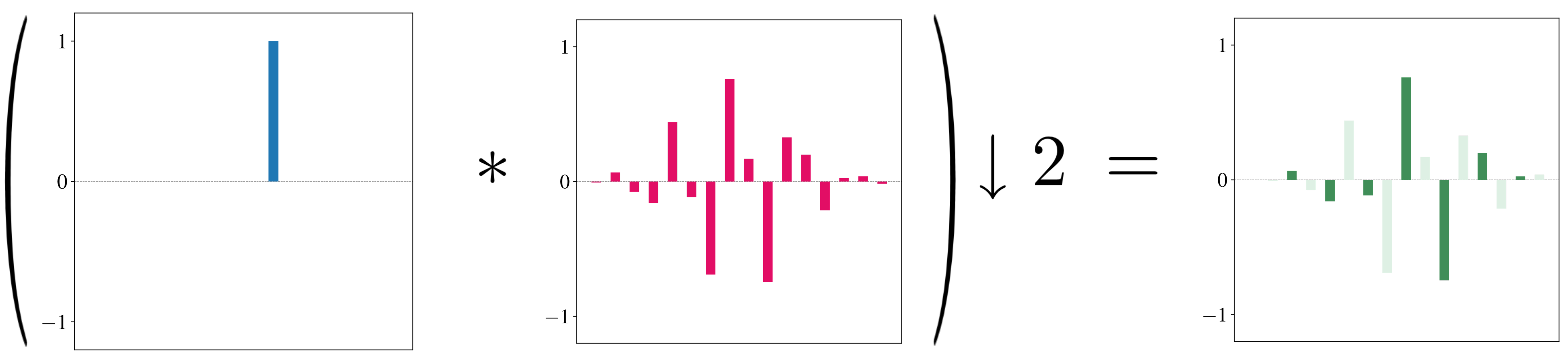

Input signal

Band-pass
convolution kernel

Output signal

Subsampled convolutions, a real problem!

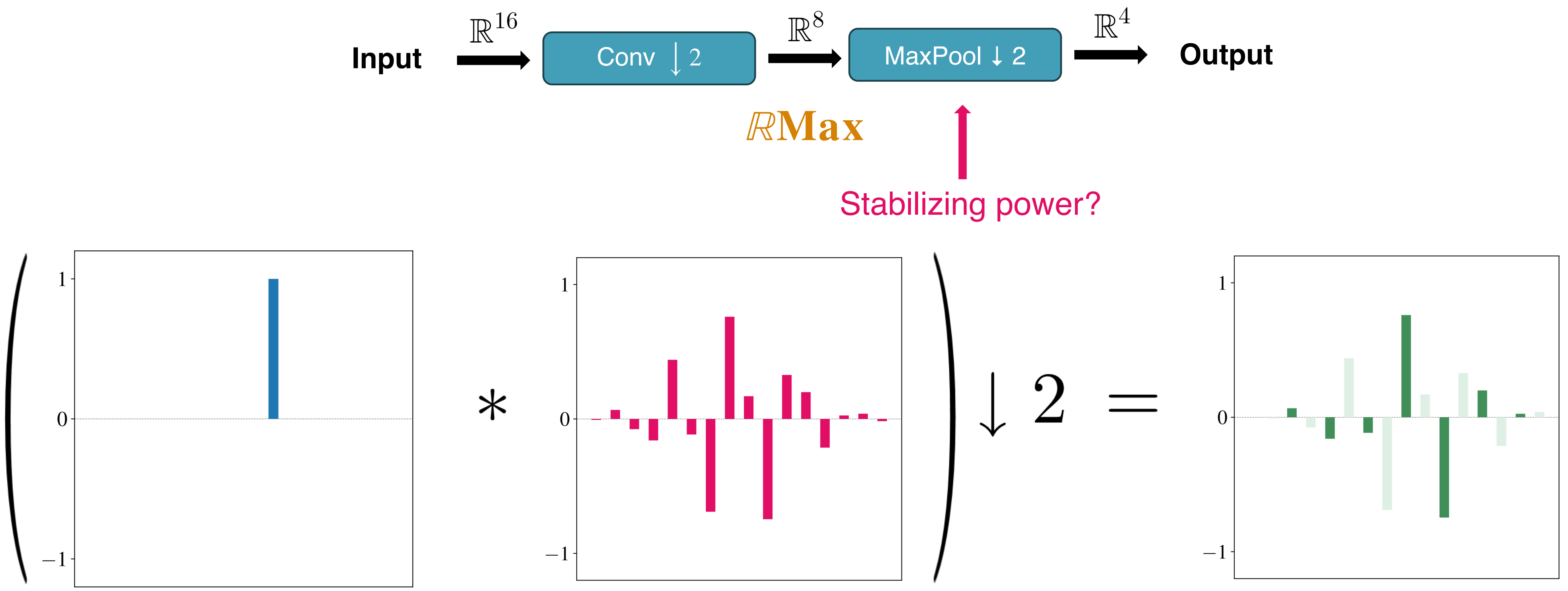

Input signal

Band-pass
convolution kernel

Output signal

Complex-valued convolutions at rescue

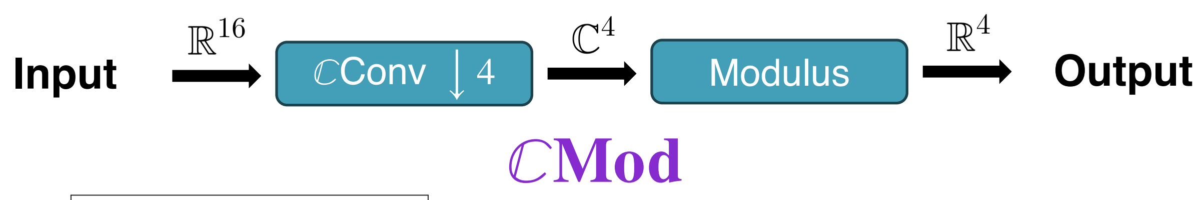

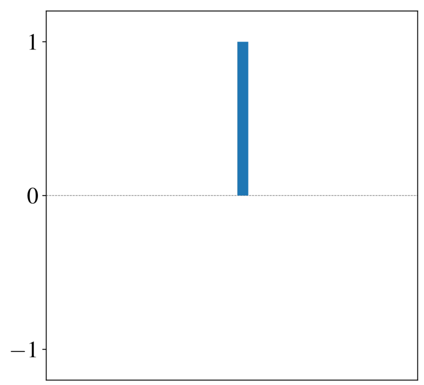

Input signal

$*$

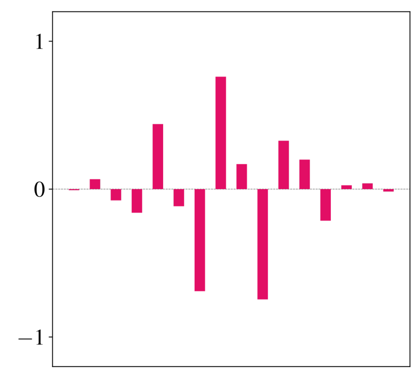

Complex-valued convolutions at rescue

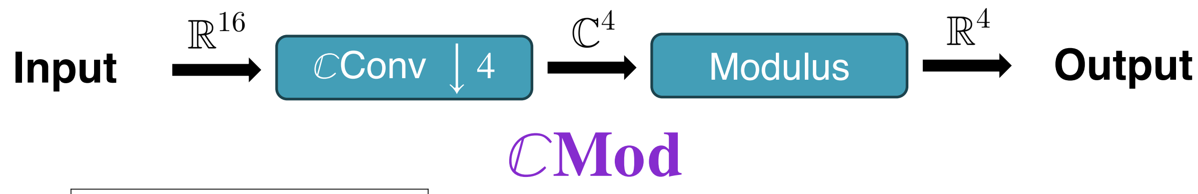

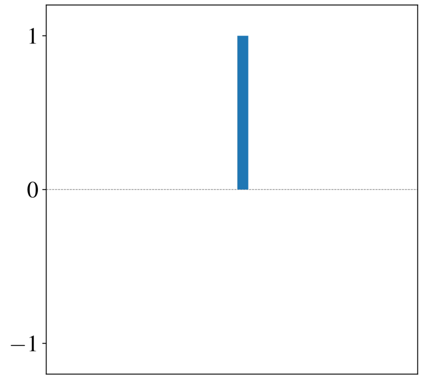

Input signal

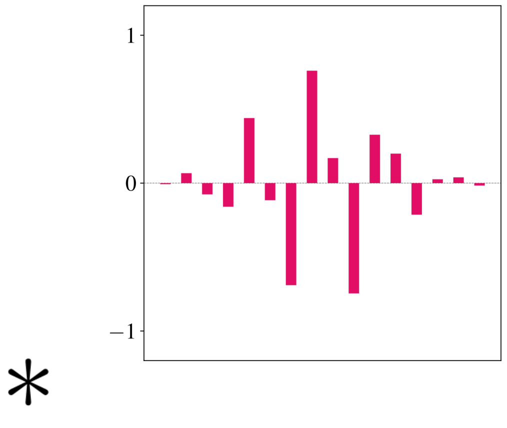

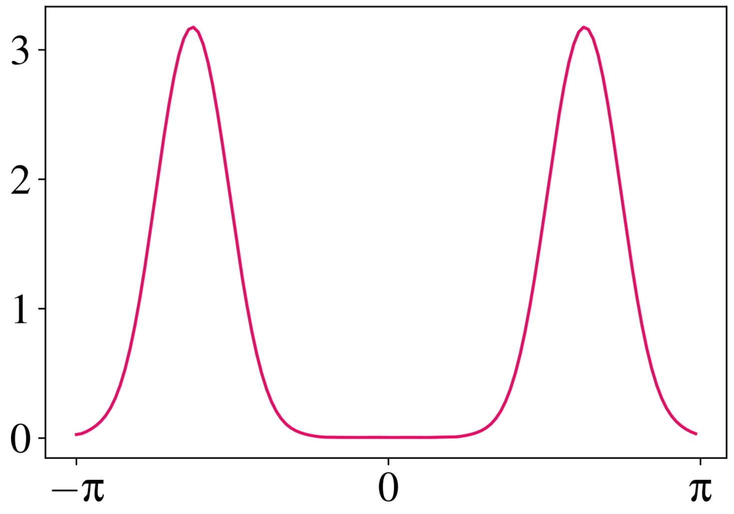

Fourier transform modulus

Complex-valued convolutions at rescue

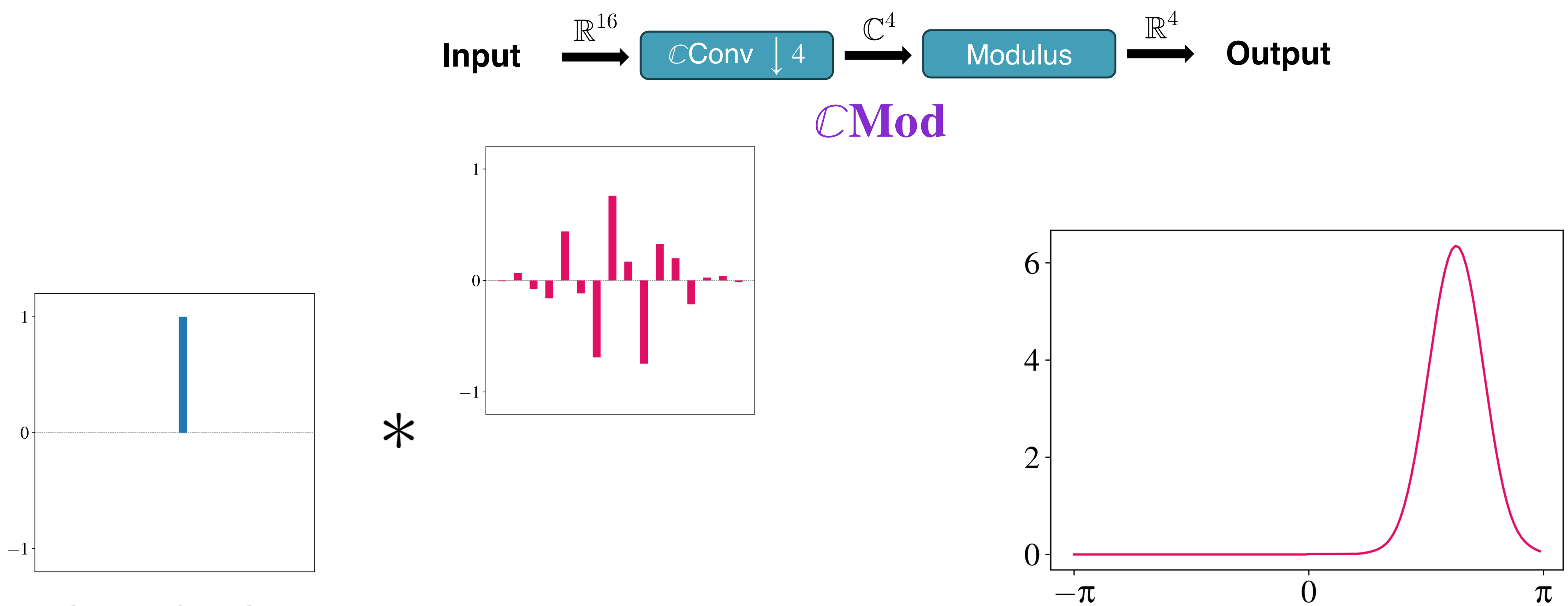

Input signal

Fourier transform modulus

Complex-valued convolutions at rescue

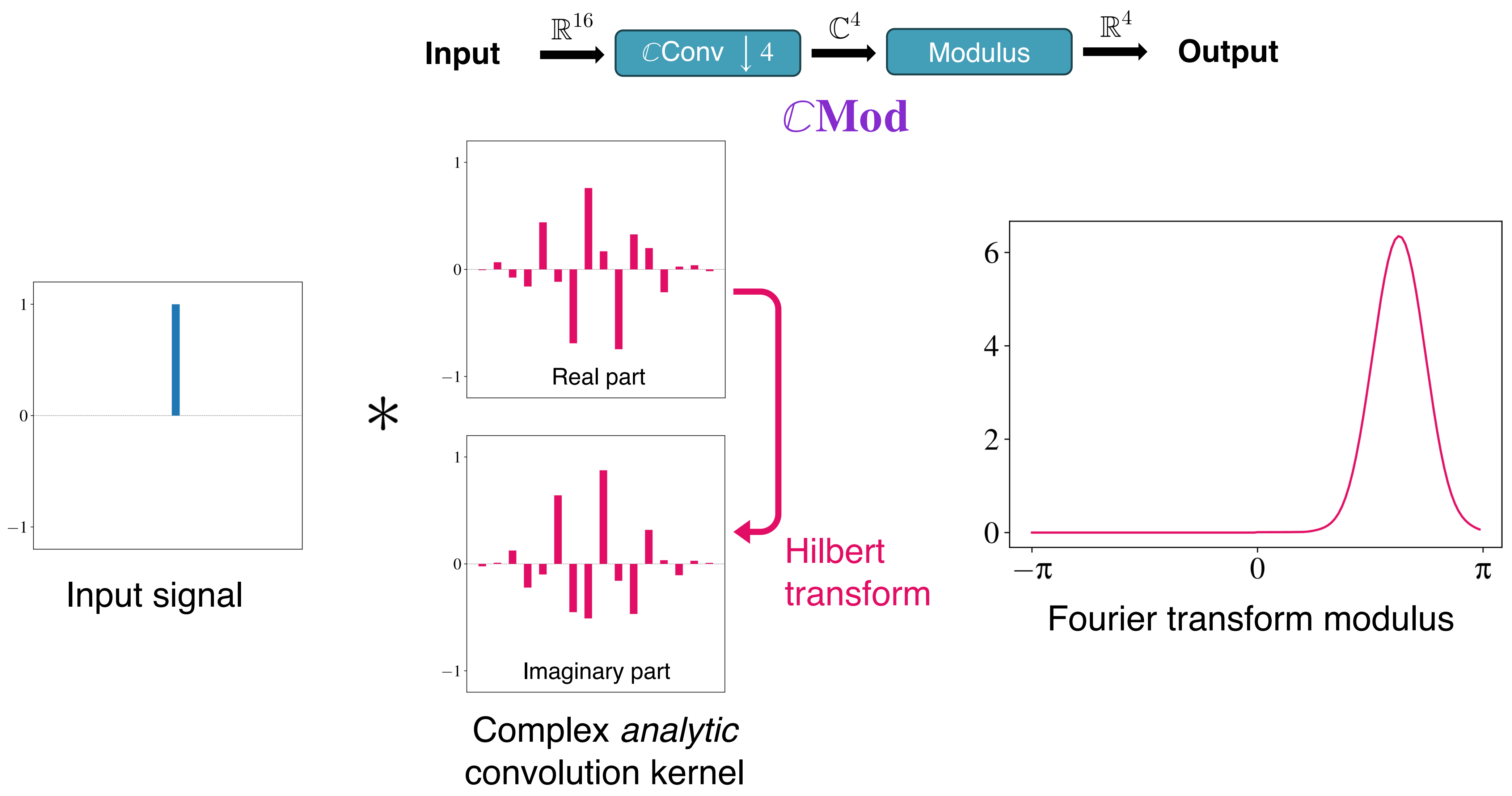

Complex-valued convolutions at rescue

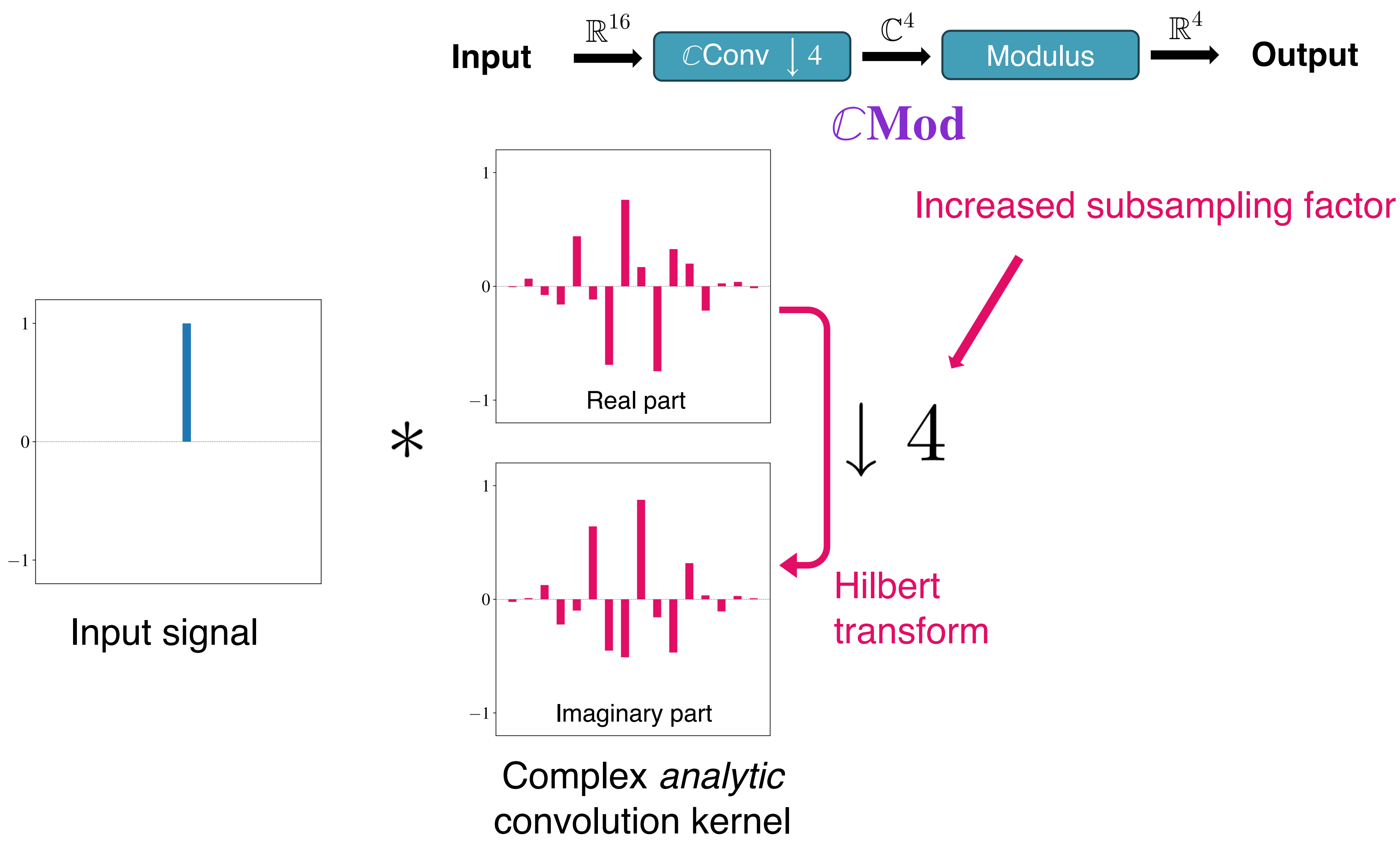

Complex-valued convolutions at rescue

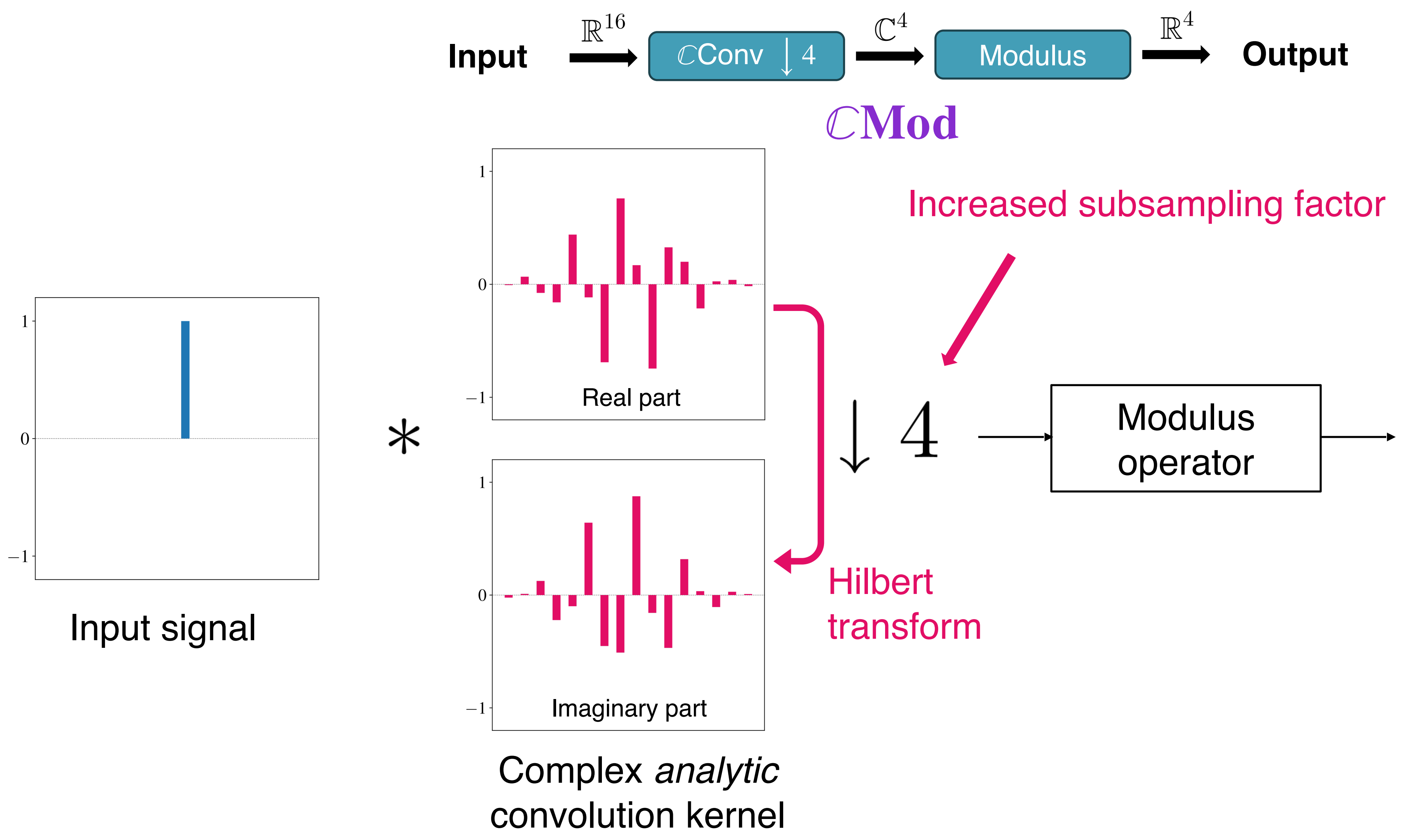

Complex-valued convolutions at rescue

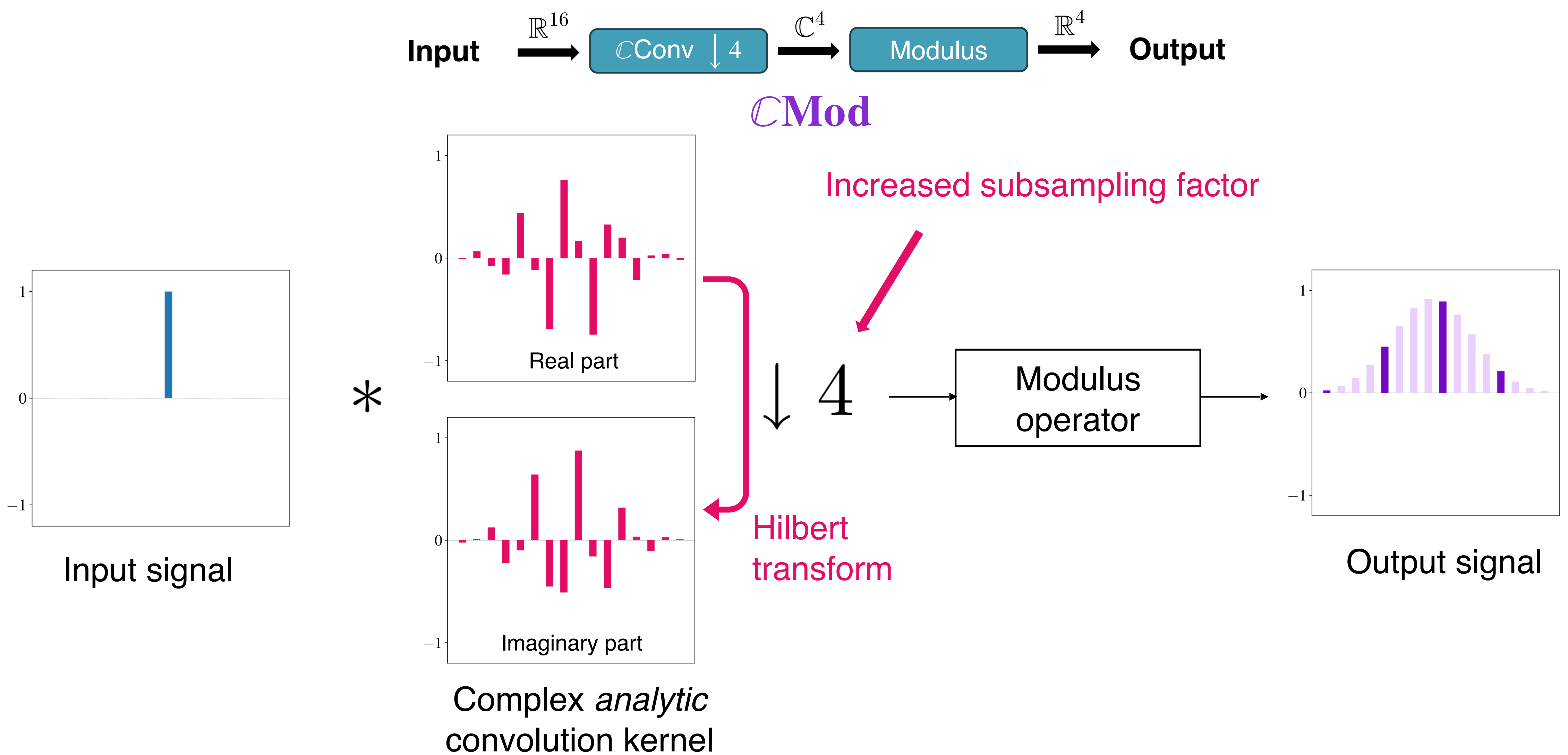

Complex-valued convolutions at rescue

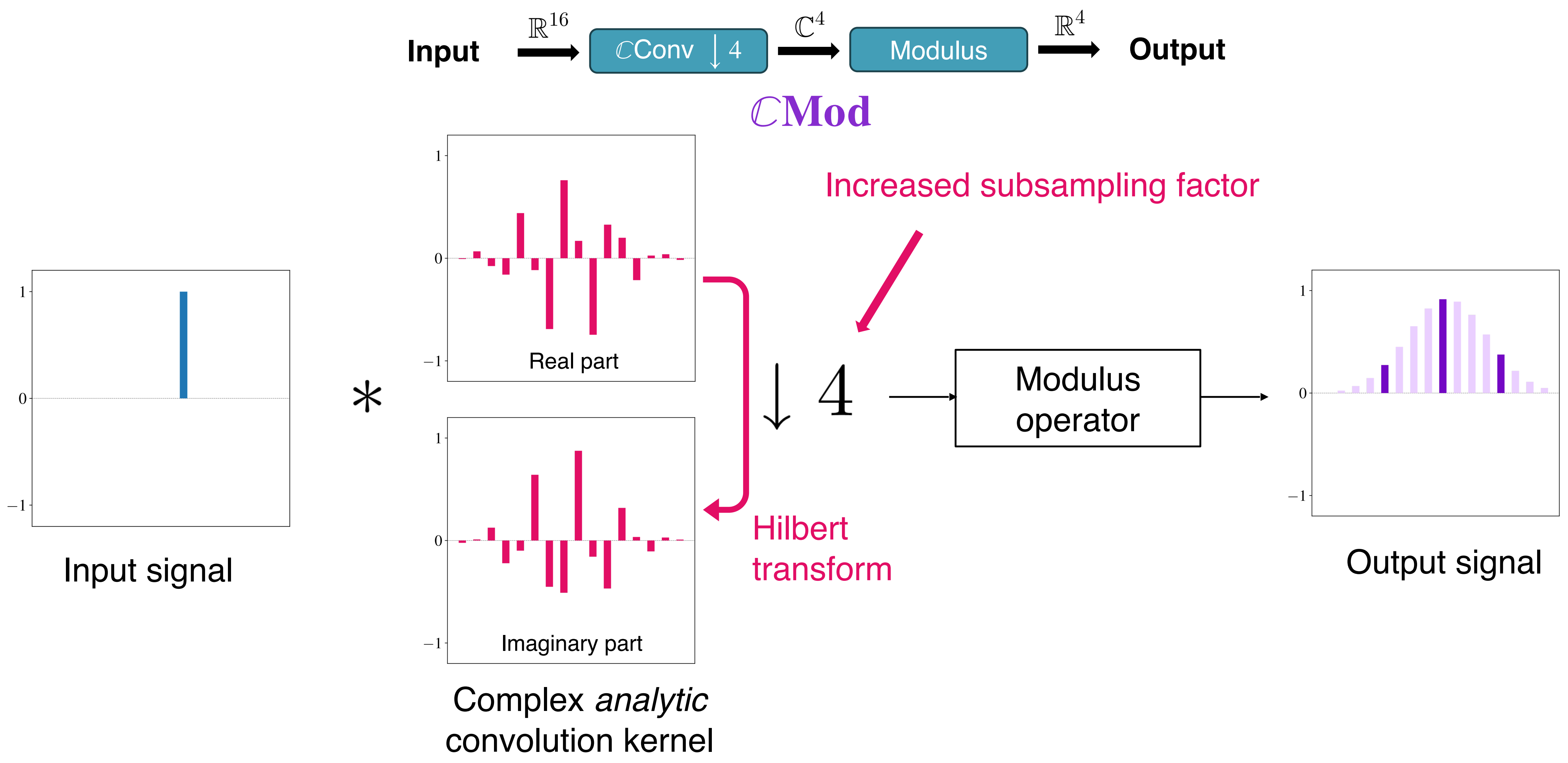

Complex-valued convolutions at rescue

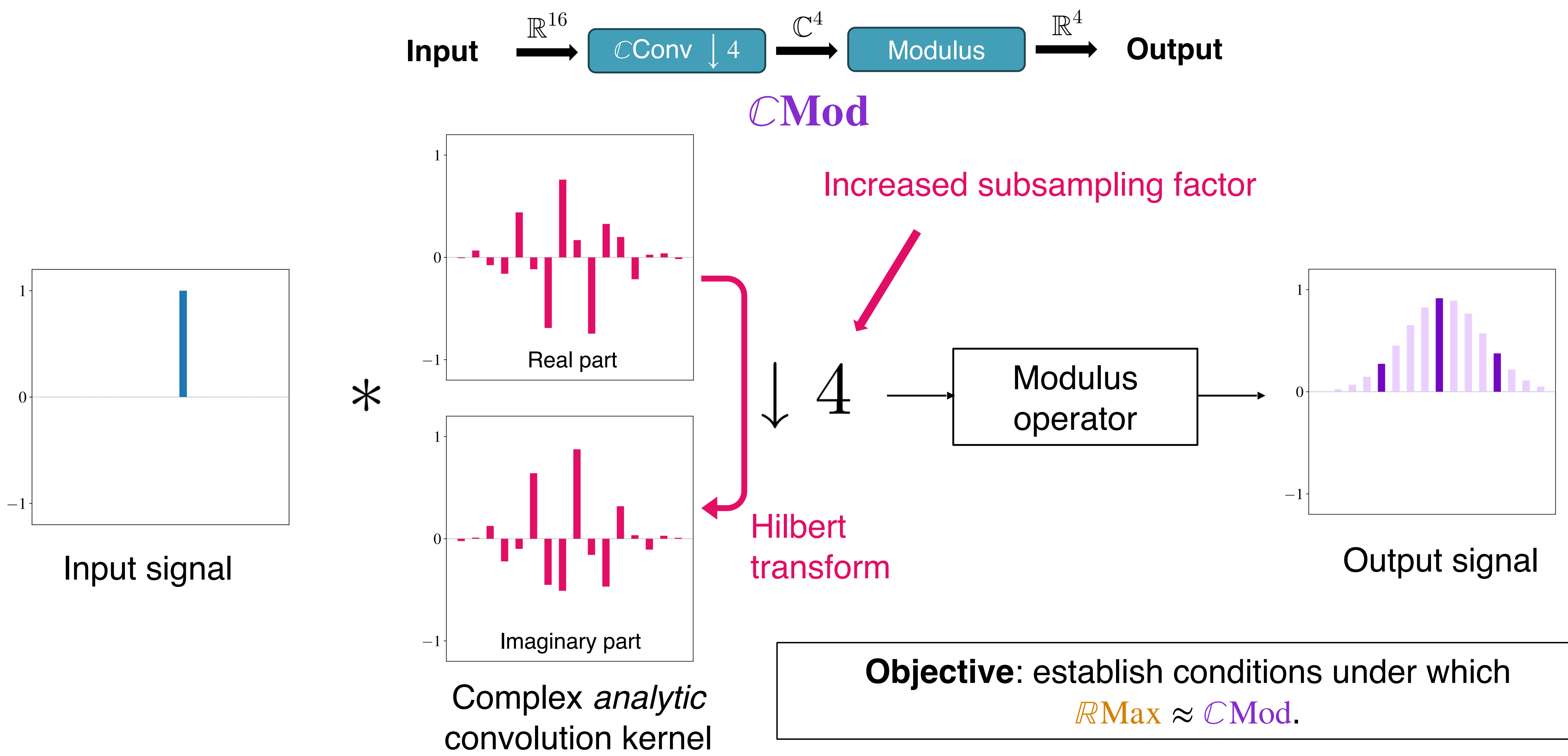

Objective: establish conditions under which $\mathbb{R}$Max $\approx$ $\mathbb{C}$Mod.

Fundamental hypothesis on filter

- Band-pass, oriented and **analytic** *Gabor-like* filters W

Fundamental hypothesis on filter

- Band-pass, oriented and **analytic** *Gabor-like* filters W

$\mathrm{V} =$ 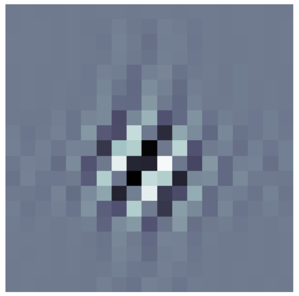

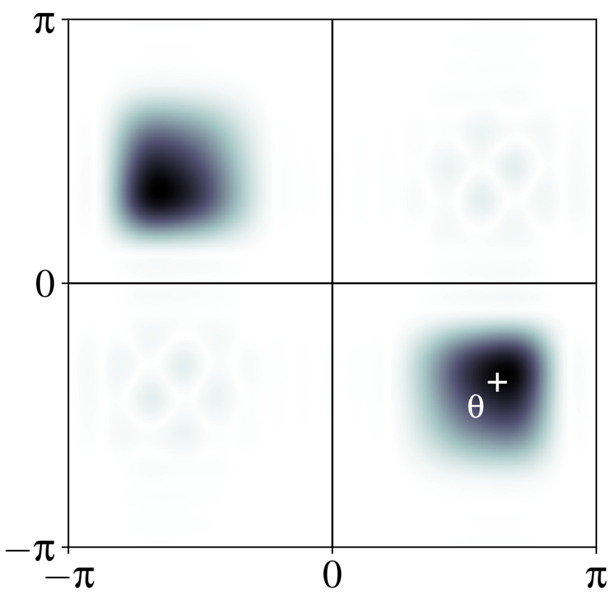

Fundamental hypothesis on filter

- Band-pass, oriented and **analytic** *Gabor-like* filters W

$\mathrm{V} =$ 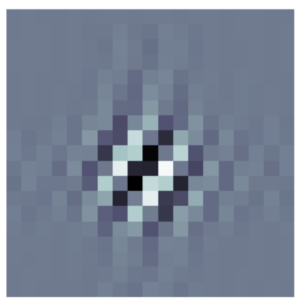

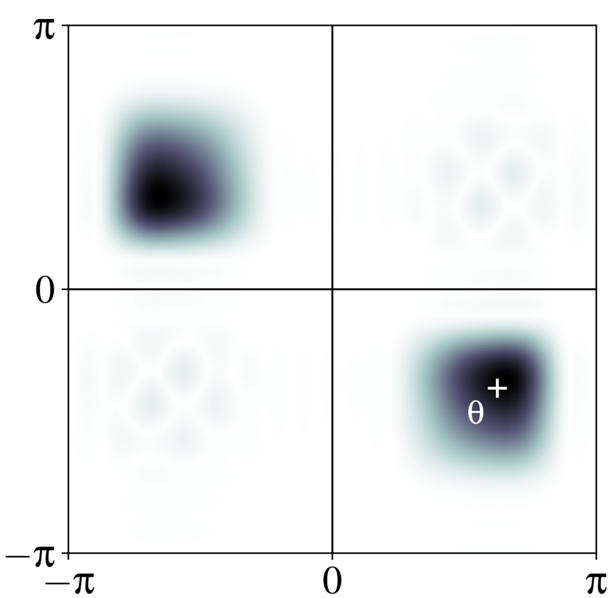

$\mathrm{W} =$ 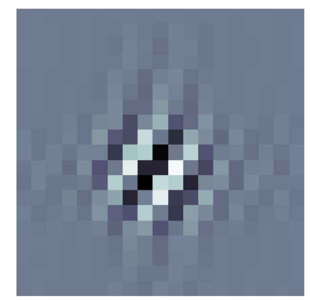 $+\, i$ 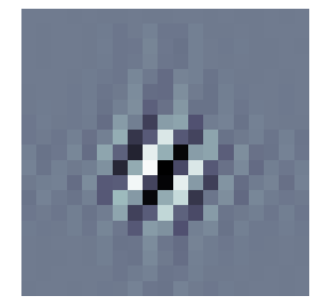

V $\qquad$ $\mathcal{H}(\mathrm{V})$

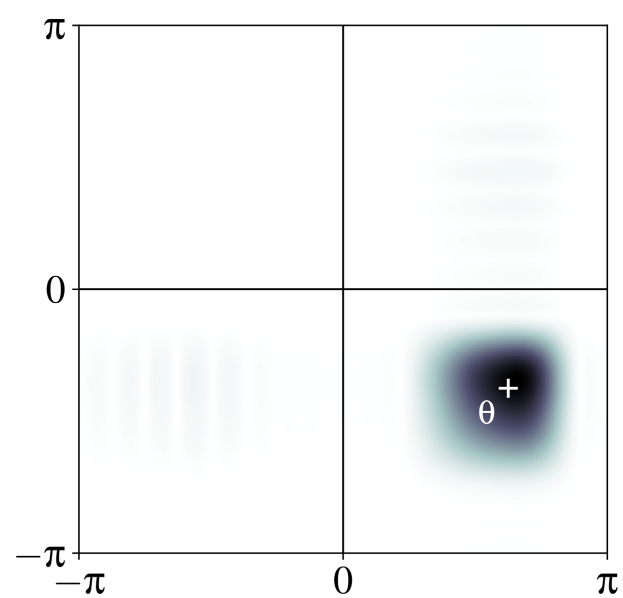

Fundamental hypothesis on filter

- Band-pass, oriented and **analytic** *Gabor-like* filters W

$\mathrm{V} =$ 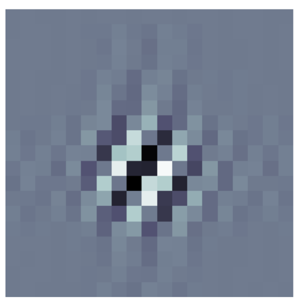

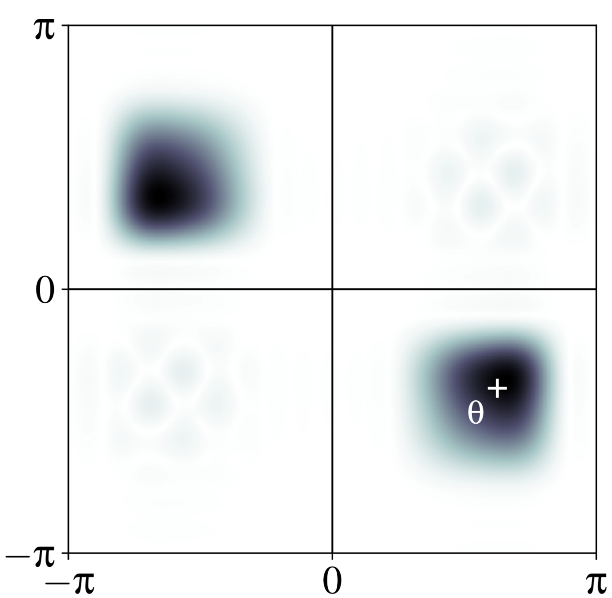

$\mathrm{W} =$ 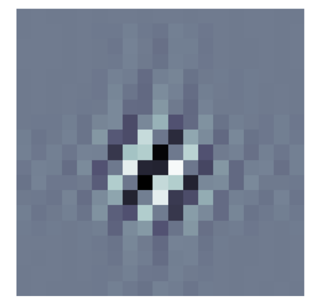 $+\, i$ 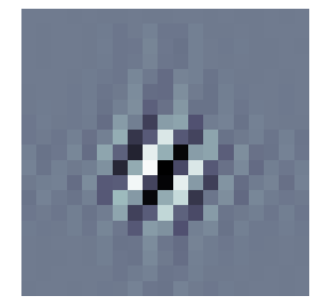

V $\qquad$ $\mathcal{H}(\mathrm{V})$

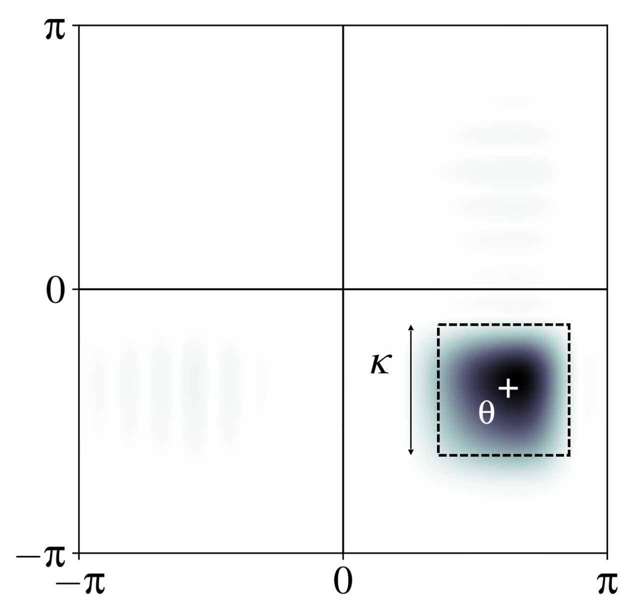

Fundamental hypothesis on filter

- Band-pass, oriented and **analytic** *Gabor-like* filters W

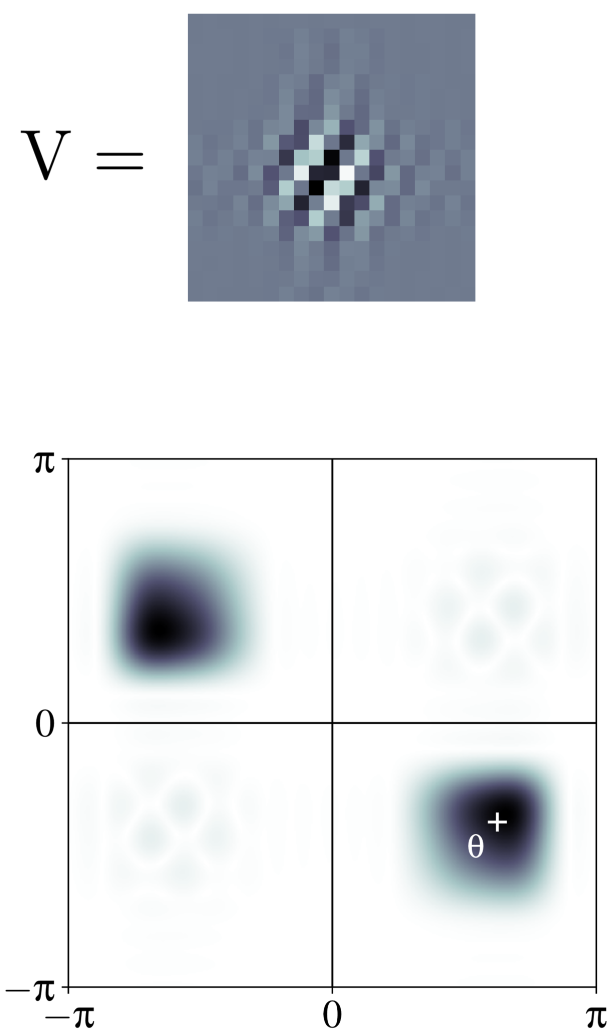

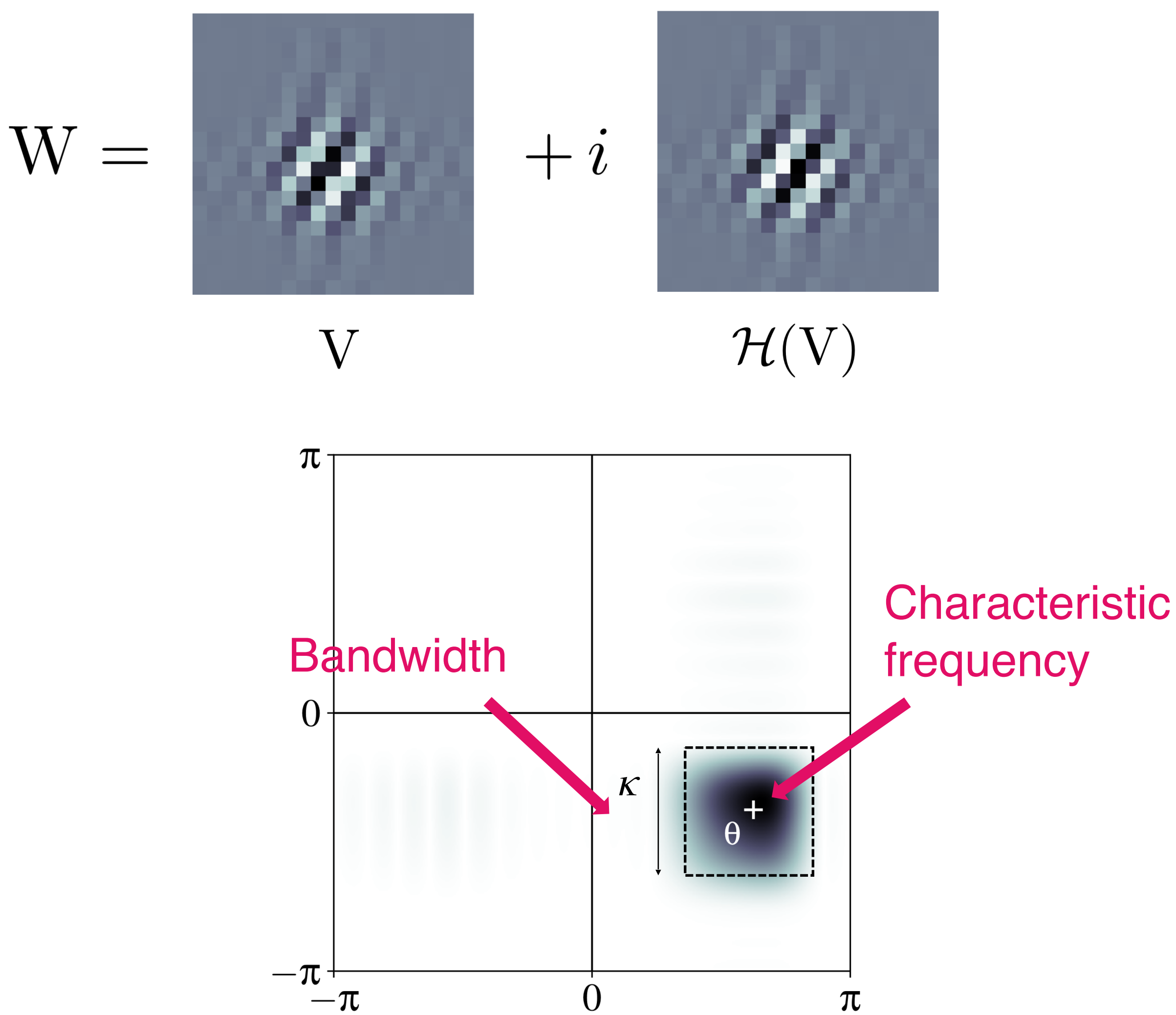

Fundamental hypothesis on filter

- Band-pass, oriented and **analytic** *Gabor-like* filters W

$\mathrm{V} =$ 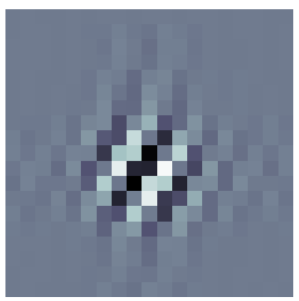

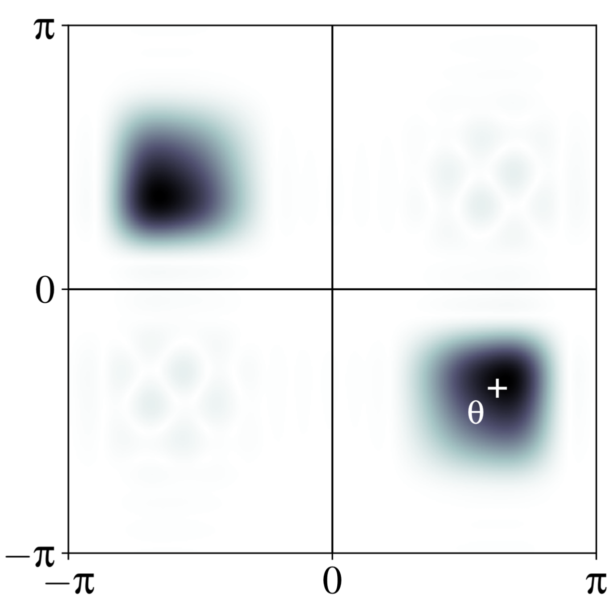

$\mathrm{W} = \mathrm{V} + i\,\mathcal{H}(\mathrm{V})$

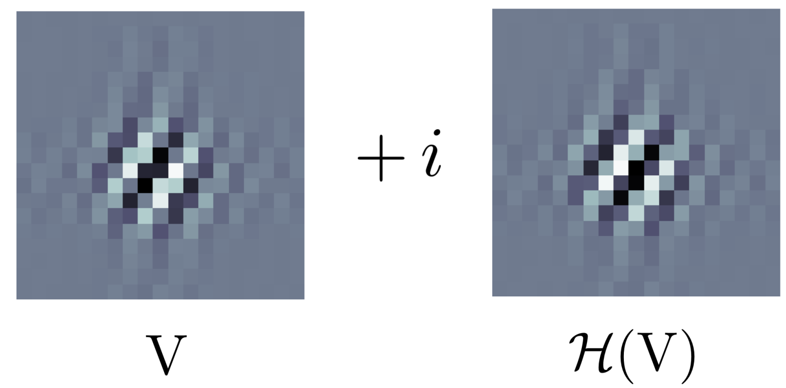

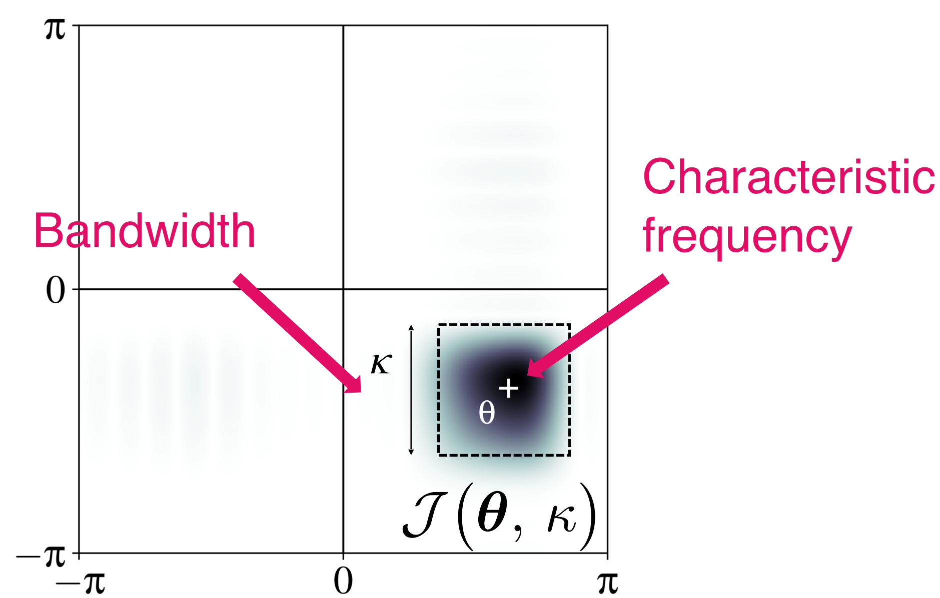

Two operators to compare

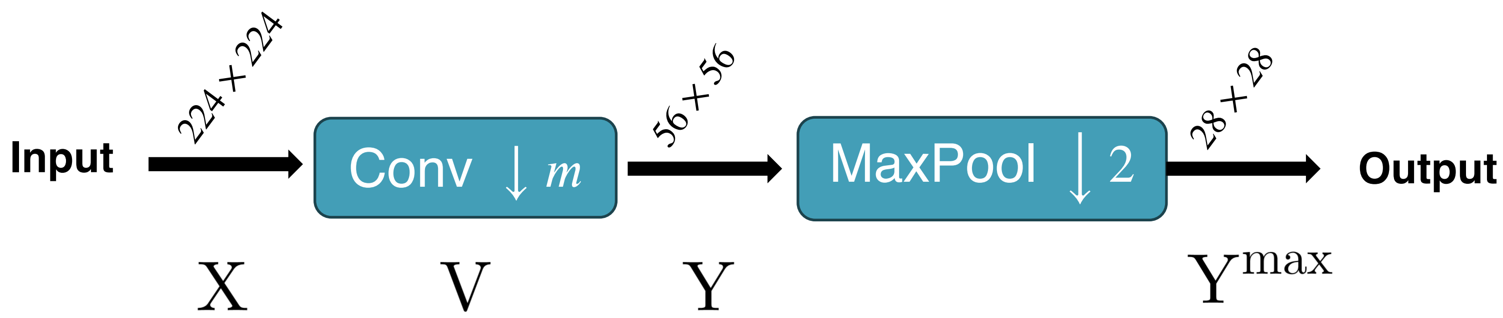

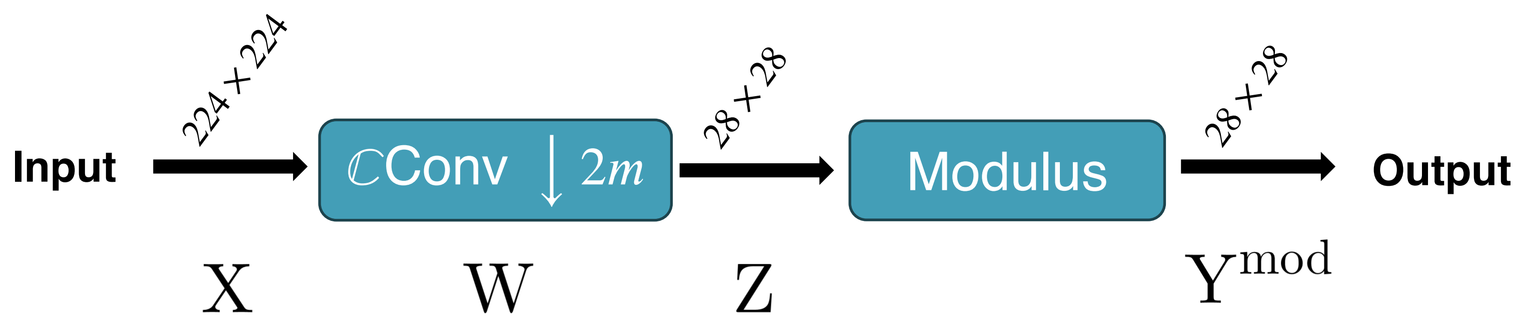

Two operators to compare

$\mathbb{R}$**Max**

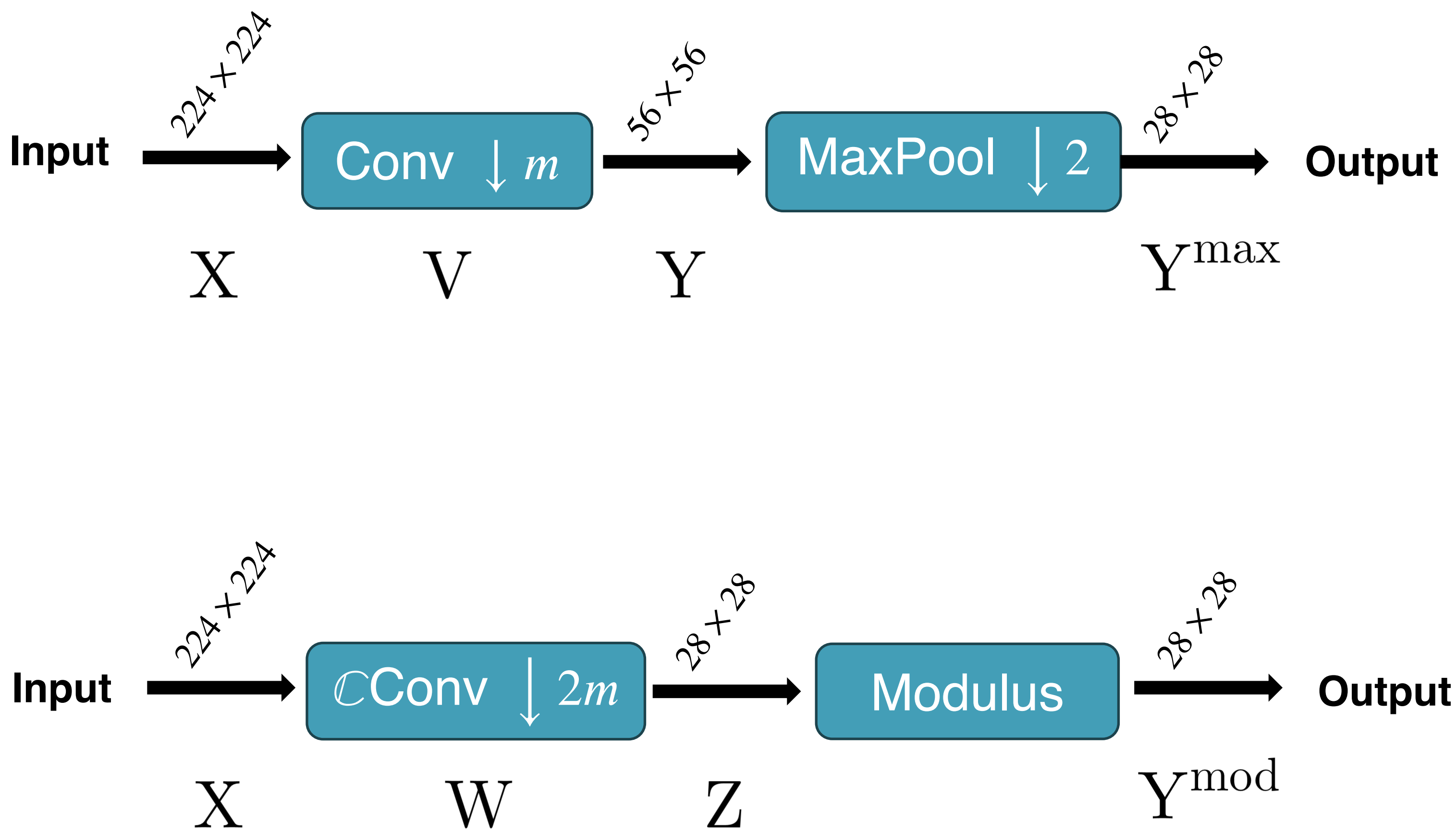

Two operators to compare

$\mathbb{R}$**Max**

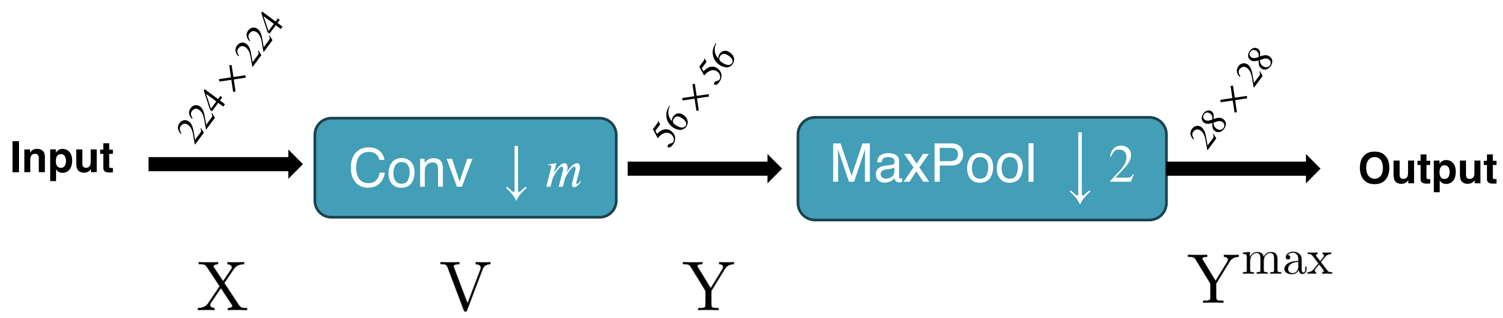

$\mathbb{C}$**Mod**

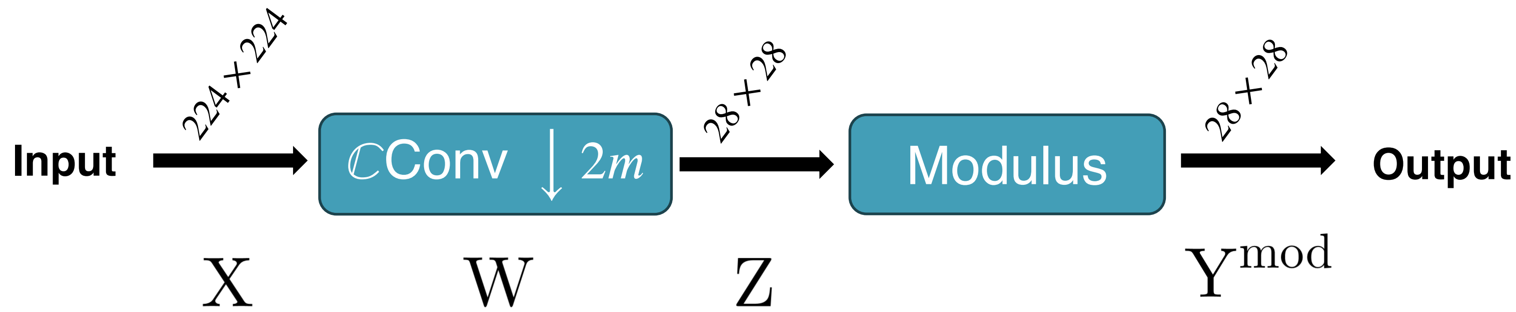

Two operators to compare

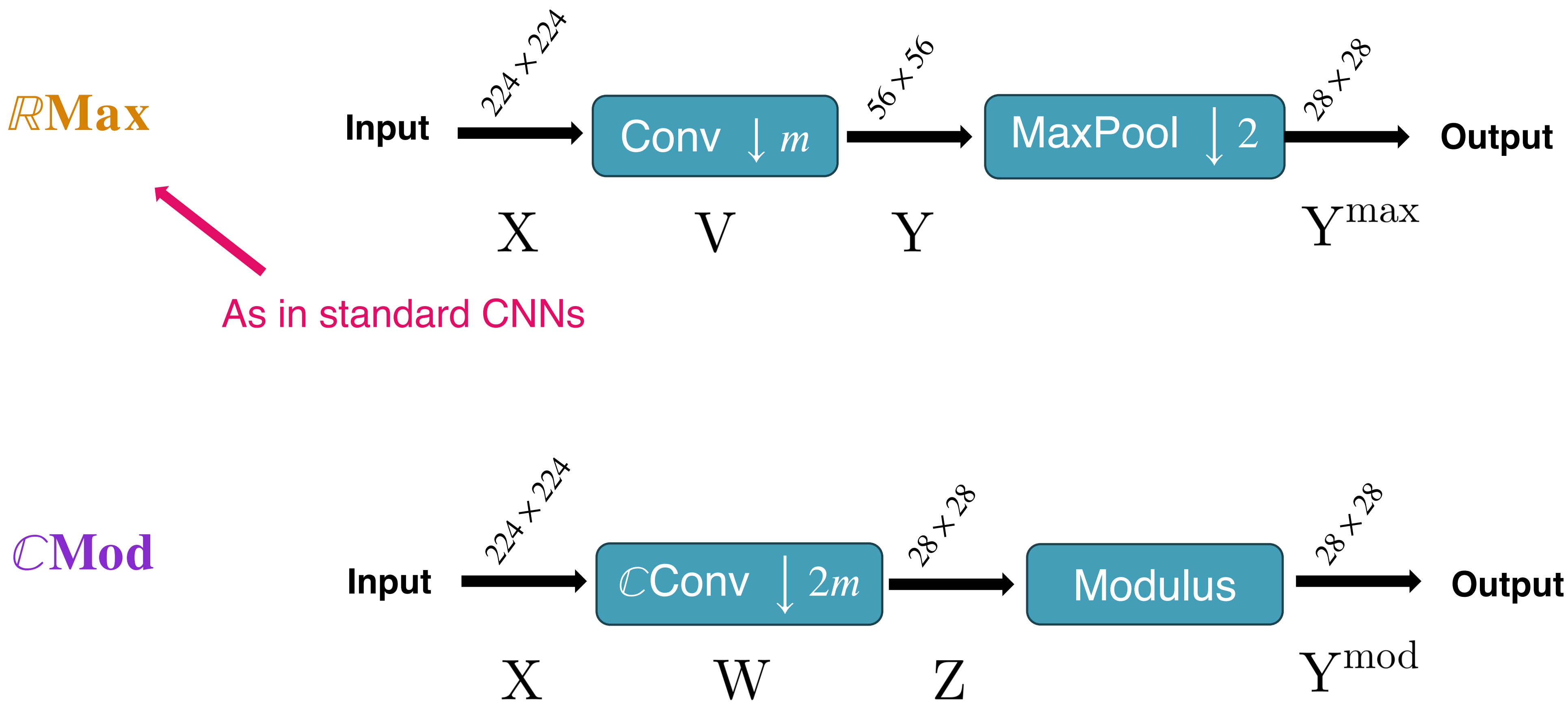

Two operators to compare

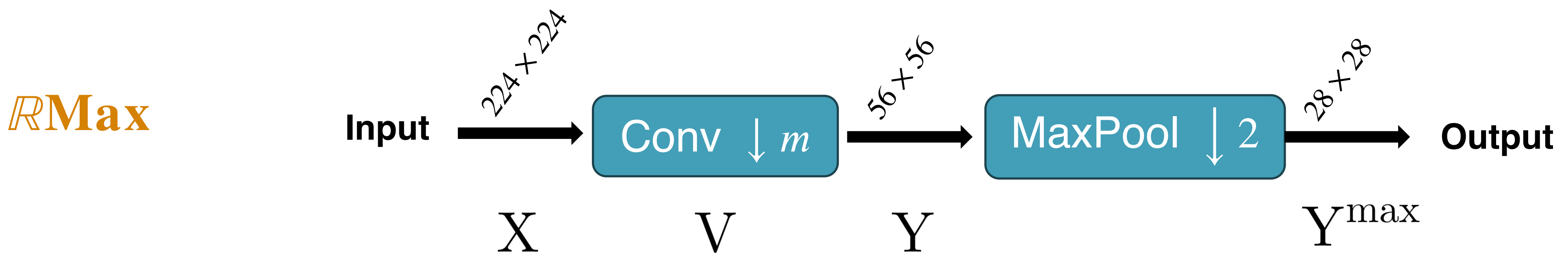

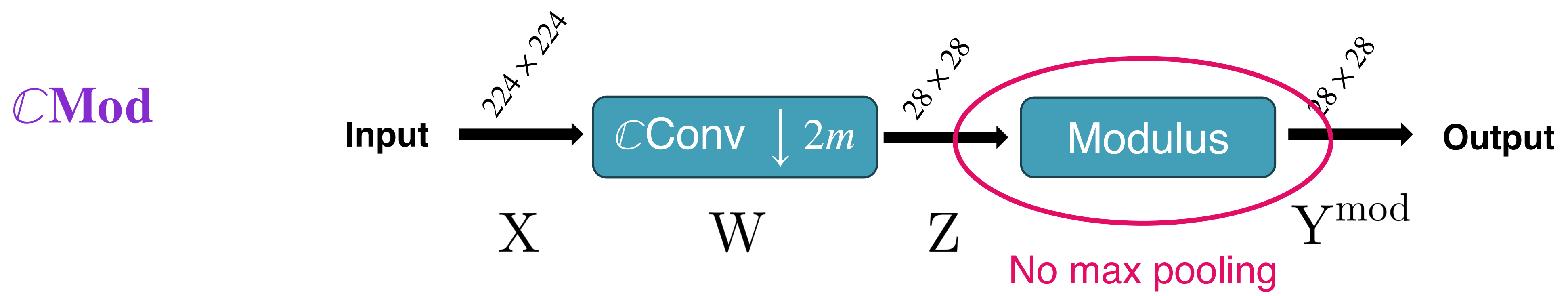

Two operators to compare

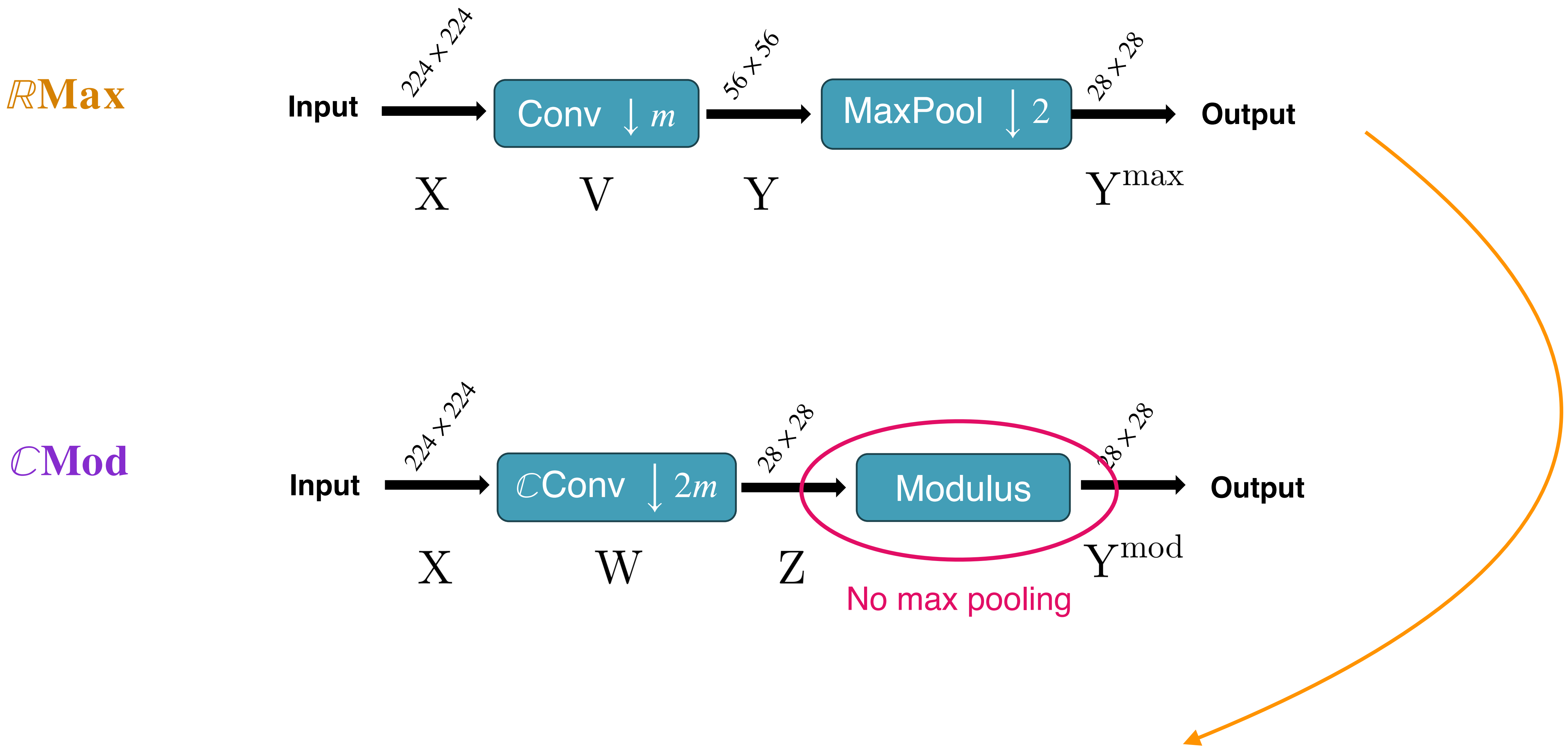

Two operators to compare

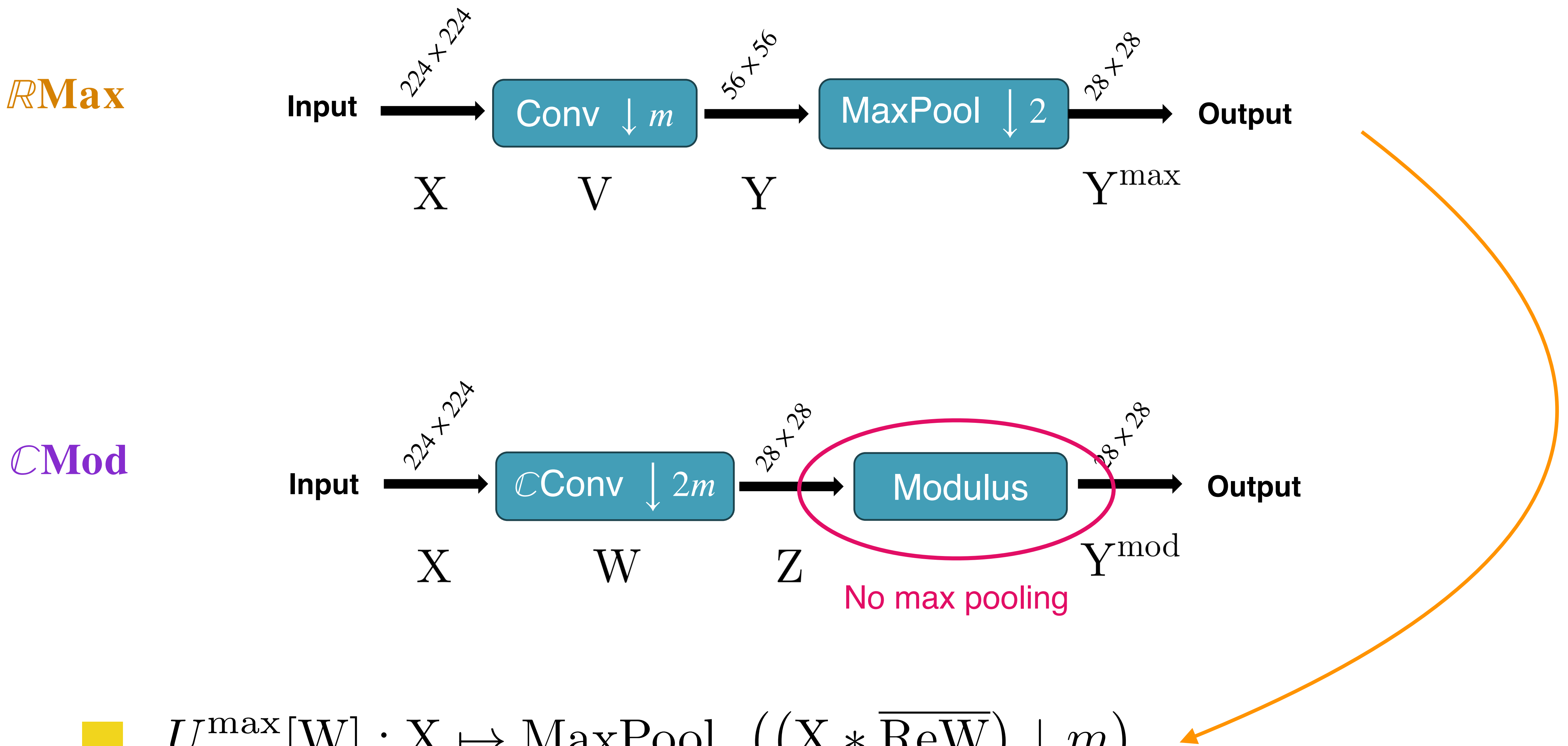

- $U^{max}_{m,q}[W] : X \mapsto \mathrm{MaxPool}_q \left(\left(X * \overline{\mathrm{Re} W} \right) \downarrow m \right)$

Two operators to compare

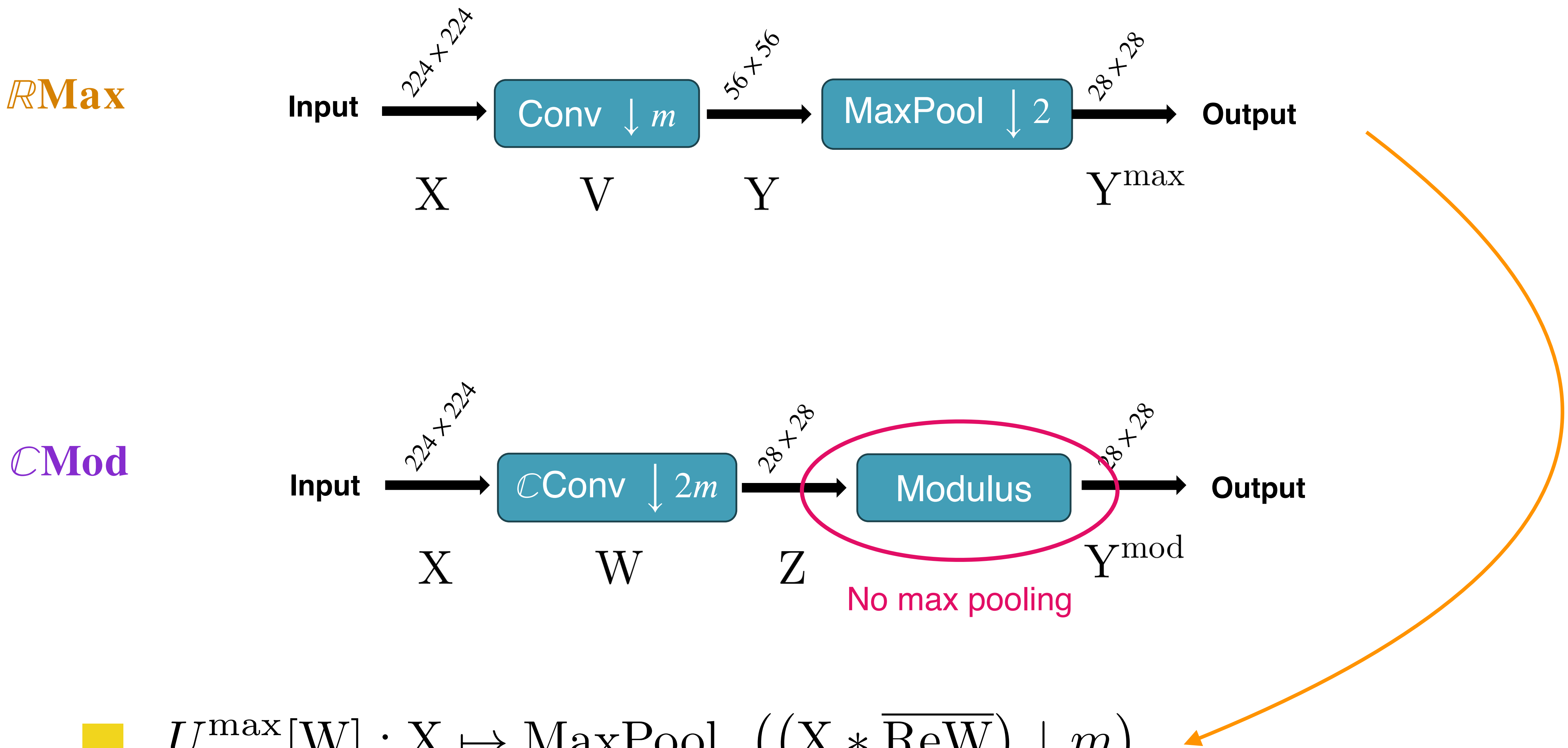

- $U^{\max}_{m,q}[\mathrm{W}] : \mathrm{X} \mapsto \mathrm{MaxPool}_q\left(\left(\mathrm{X} * \overline{\mathrm{Re}\mathrm{W}}\right) \downarrow m\right)$

$$(\mathrm{X} * \overline{\mathrm{V}})[\boldsymbol{n}] := \sum_{\boldsymbol{p} \in \mathbb{Z}^2} \mathrm{X}[\boldsymbol{p}]\overline{\mathrm{V}}[\boldsymbol{n} - \boldsymbol{p}] \qquad \overline{\mathrm{V}}[\boldsymbol{n}] := \mathrm{V}[-\boldsymbol{n}]$$

$$\mathrm{MaxPool}_q(\mathrm{Y})[\boldsymbol{n}] := \max_{\|\boldsymbol{p}\|_\infty \leq q} \mathrm{Y}[2\boldsymbol{n} + \boldsymbol{p}] \qquad (\mathrm{Y} \downarrow m)[\boldsymbol{n}] := \mathrm{Y}[m\boldsymbol{n}]$$

Two operators to compare

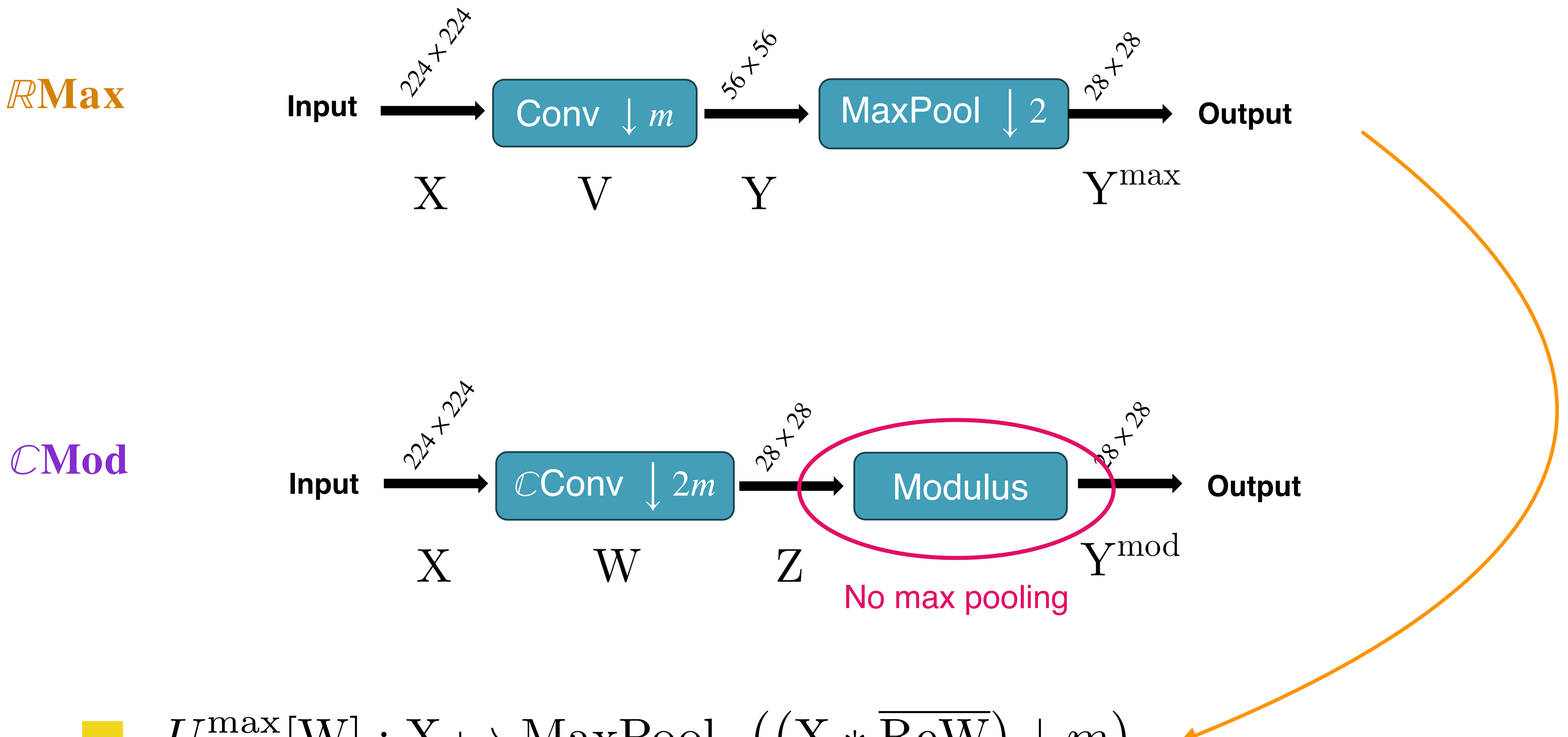

- $U^{\max}_{m,q}[\mathrm{W}] : \mathrm{X} \mapsto \mathrm{MaxPool}_q \left(\left(\mathrm{X} * \overline{\mathrm{Re W}} \right) \downarrow m \right)$

Two operators to compare

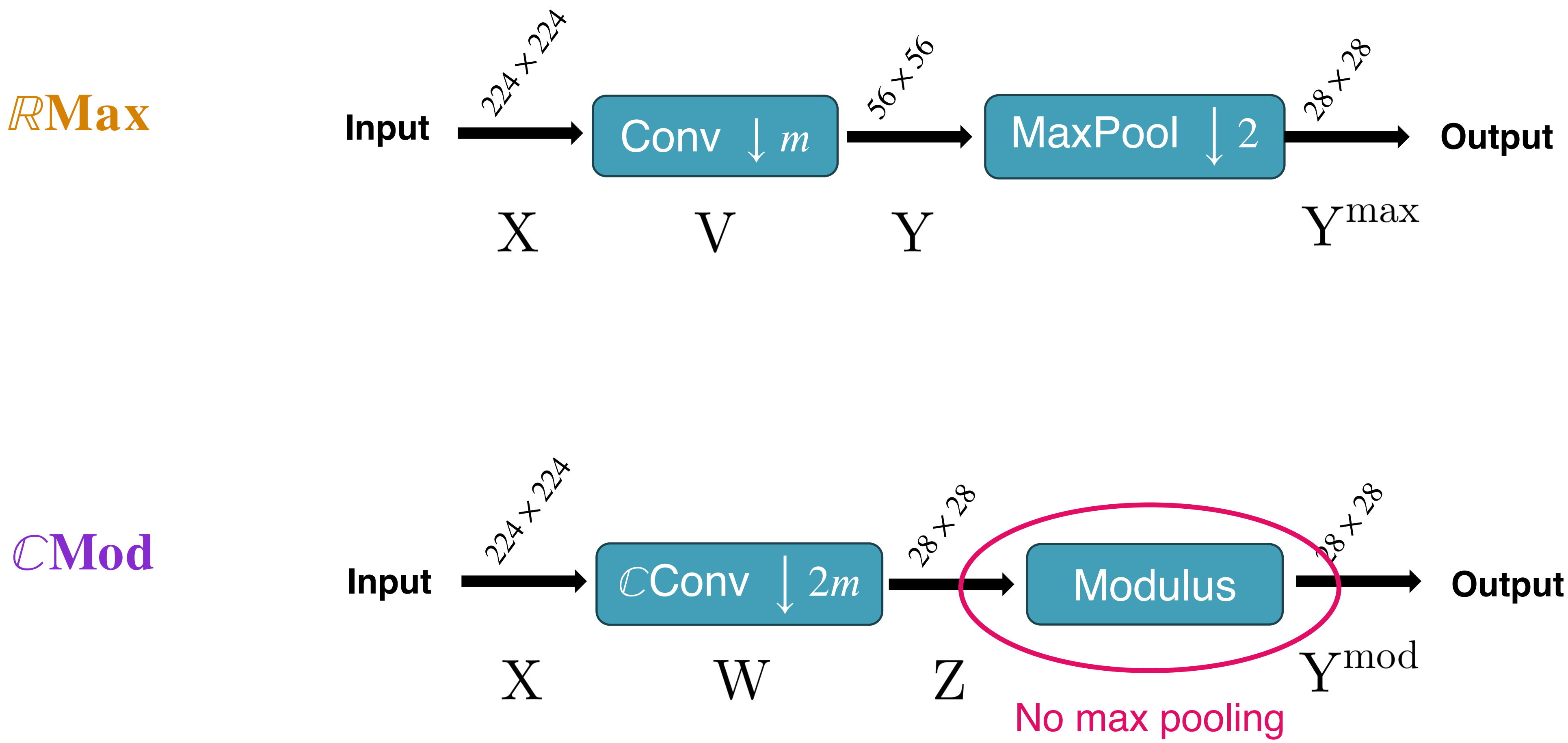

- $U^{\max}_{m,q}[\mathrm{W}] : \mathrm{X} \mapsto \mathrm{MaxPool}_q\left(\left(\mathrm{X} * \overline{\mathrm{Re}\mathrm{W}}\right) \downarrow m\right)$

Two operators to compare

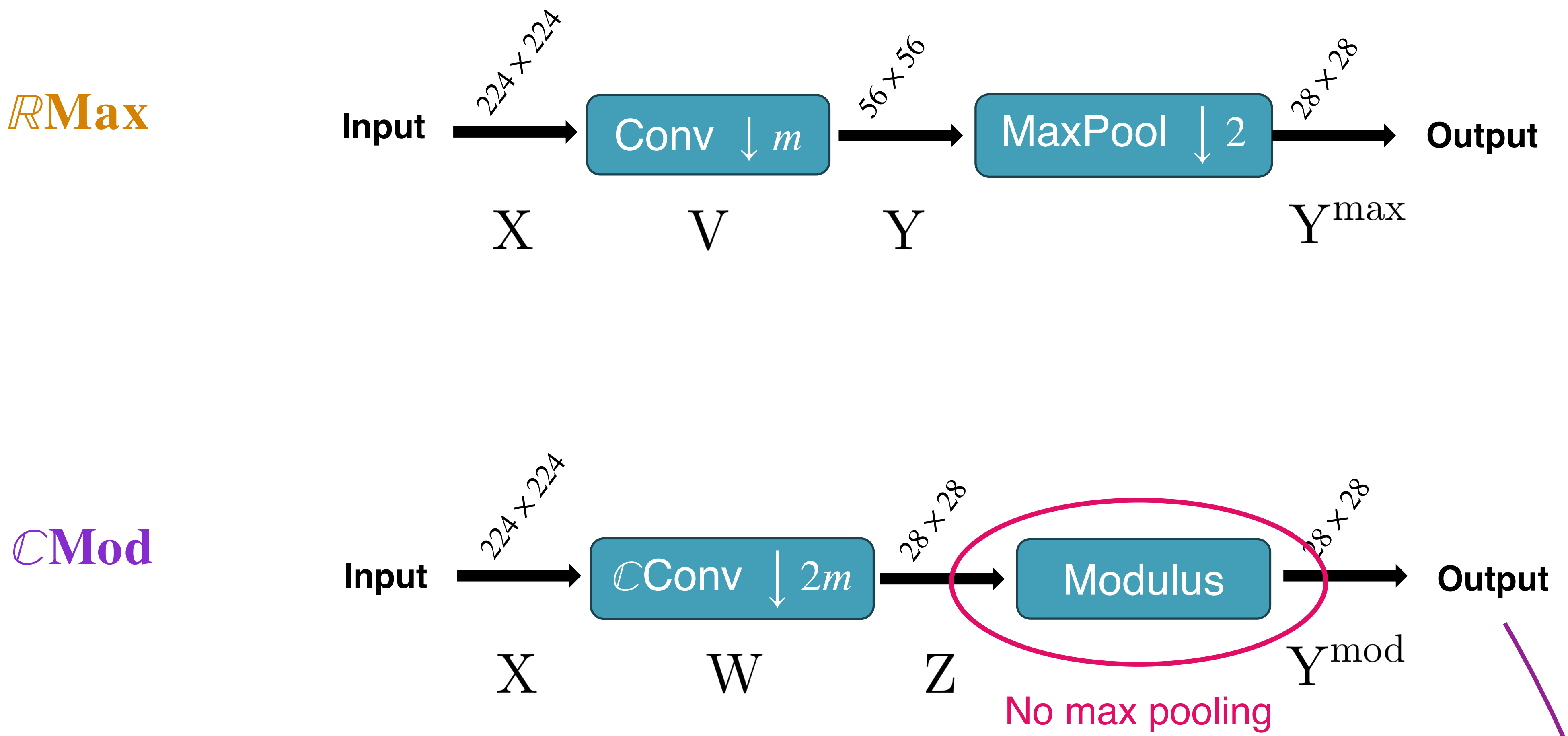

- $U^{\max}_{m,q}[\mathrm{W}] : \mathrm{X} \mapsto \mathrm{MaxPool}_q \left(\left(\mathrm{X} * \overline{\mathrm{Re}\mathrm{W}} \right) \downarrow m \right)$
- $U^{\mathrm{mod}}_{m}[\mathrm{W}] : \mathrm{X} \mapsto \left| \left(\mathrm{X} * \overline{\mathrm{W}} \right) \downarrow (2m) \right|$

Roadmap

Roadmap

- Show that, **under the Gabor hypothesis**, $\mathbb{C}\mathbf{Mod}$ is **stable** with respect to small input shifts

Roadmap

- Show that, **under the Gabor hypothesis**, $\mathbb{C}\mathbf{Mod}$ is **stable** with respect to small input shifts

- **Establish conditions** on the filter's frequency and orientation under which $\mathbb{R}\mathbf{Max}$ and $\mathbb{C}\mathbf{Mod}$ **produce comparable outputs**:

$$U_{m,q}^{\max}[\mathrm{W}](\mathrm{X}) \approx U_{m}^{\mathrm{mod}}[\mathrm{W}](\mathrm{X})$$

Roadmap

- Show that, **under the Gabor hypothesis**, $\mathbb{C}\mathbf{Mod}$ is **stable** with respect to small input shifts

- **Establish conditions** on the filter's frequency and orientation under which $\mathbb{R}\mathbf{Max}$ and $\mathbb{C}\mathbf{Mod}$ **produce comparable outputs**:

$$U_{m,q}^{\max}[\mathrm{W}](\mathrm{X}) \approx U_m^{\mathrm{mod}}[\mathrm{W}](\mathrm{X})$$

- Deduce a **measure of shift invariance** for $\mathbb{R}\mathbf{Max}$ operator, which benefits from the stability of $\mathbb{C}\mathbf{Mod}$

Roadmap

- Show that, **under the Gabor hypothesis**, $\mathbb{C}\mathbf{Mod}$ is **stable** with respect to small input shifts

- **Establish conditions** on the filter's frequency and orientation under which $\mathbb{R}\mathbf{Max}$ and $\mathbb{C}\mathbf{Mod}$ **produce comparable outputs**:

$$U_{m,q}^{\max}[\mathrm{W}](\mathrm{X}) \approx U_{m}^{\mathrm{mod}}[\mathrm{W}](\mathrm{X})$$

- Deduce a **measure of shift invariance** for $\mathbb{R}\mathbf{Max}$ operator, which benefits from the stability of $\mathbb{C}\mathbf{Mod}$

- Extend our results to **multichannel operators** (RGB images), such as implemented in conventional CNN architectures

Roadmap

- Show that, **under the Gabor hypothesis**, $\mathbb{C}$**Mod** is **stable** with respect to small input shifts

- **Establish conditions** on the filter's frequency and orientation under which $\mathbb{R}$**Max** and $\mathbb{C}$**Mod** **produce comparable outputs**:

$$U_{m,q}^{\max}[\mathrm{W}](\mathrm{X}) \approx U_m^{\mathrm{mod}}[\mathrm{W}](\mathrm{X})$$

- Deduce a **measure of shift invariance** for $\mathbb{R}$**Max** operator, which benefits from the stability of $\mathbb{C}$**Mod**

- Extend our results to **multichannel operators** (RGB images), such as implemented in conventional CNN architectures

- Experimental validation on a deterministic setting based on the **dual-tree** complex wavelet packet transform (DT-CWPT)

Detour via the continuous framework

- Using the **Shannon-Whittaker sampling theorem**

ℝ**Max**

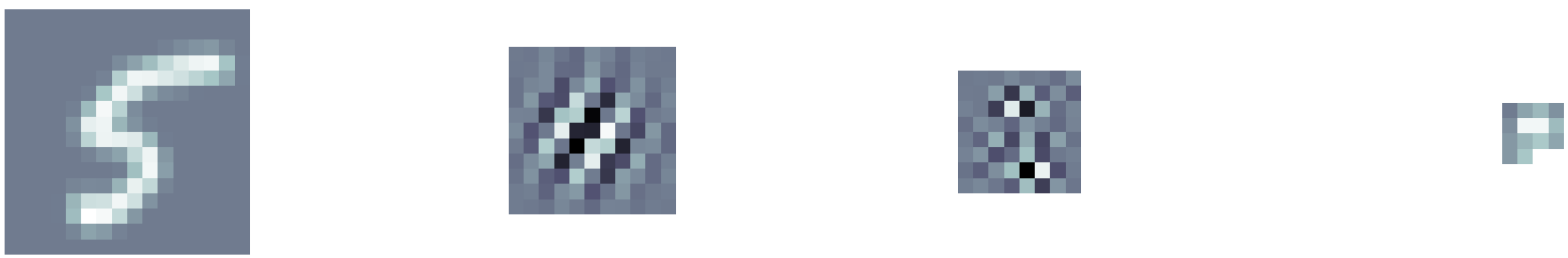

$(\; X \quad \star \quad \mathrm{Re}(W) \;) \downarrow m \quad = \quad Y \qquad\qquad Y^{\mathrm{max}}$

Detour via the continuous framework

- Using the **Shannon-Whittaker sampling theorem**

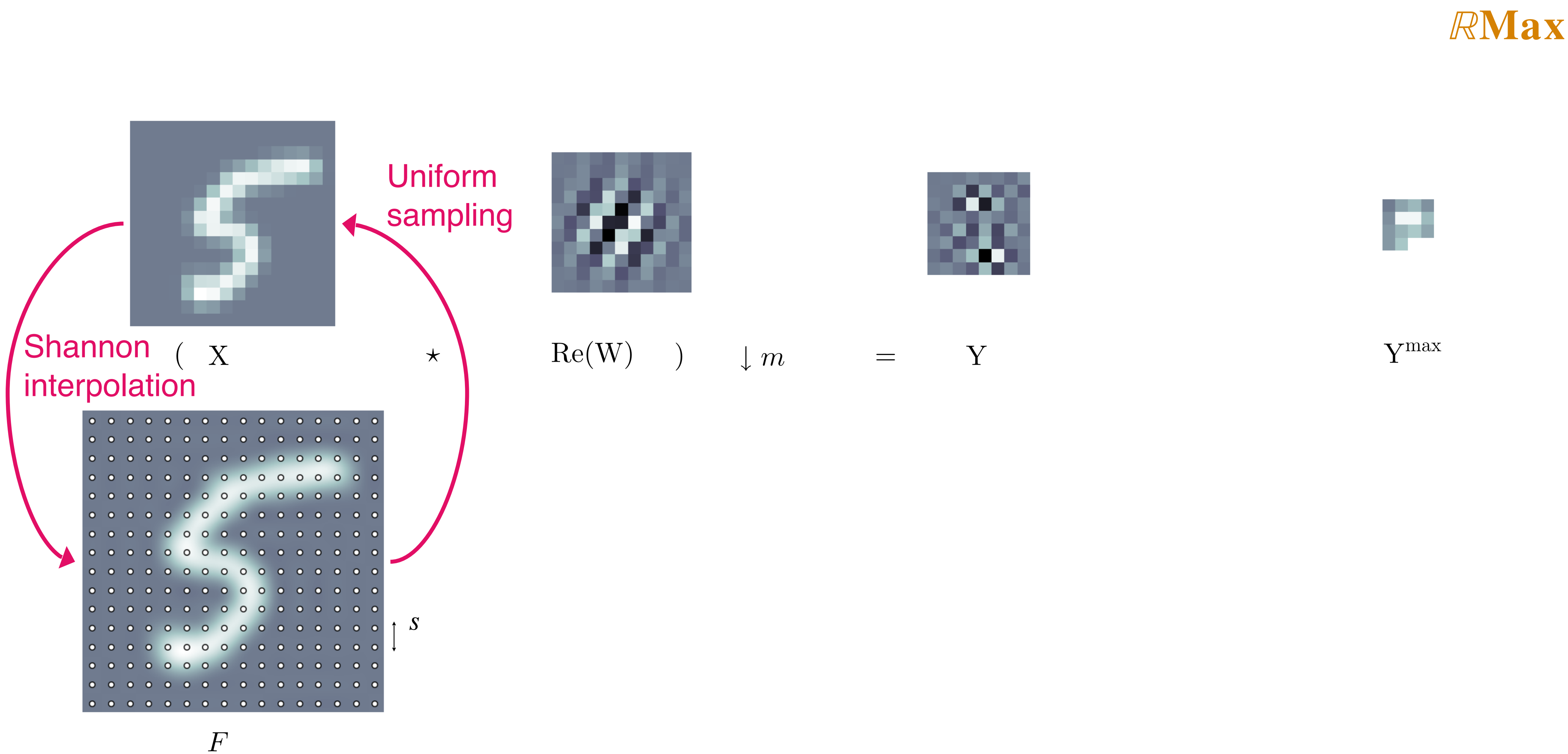

Detour via the continuous framework

- Using the **Shannon-Whittaker sampling theorem**

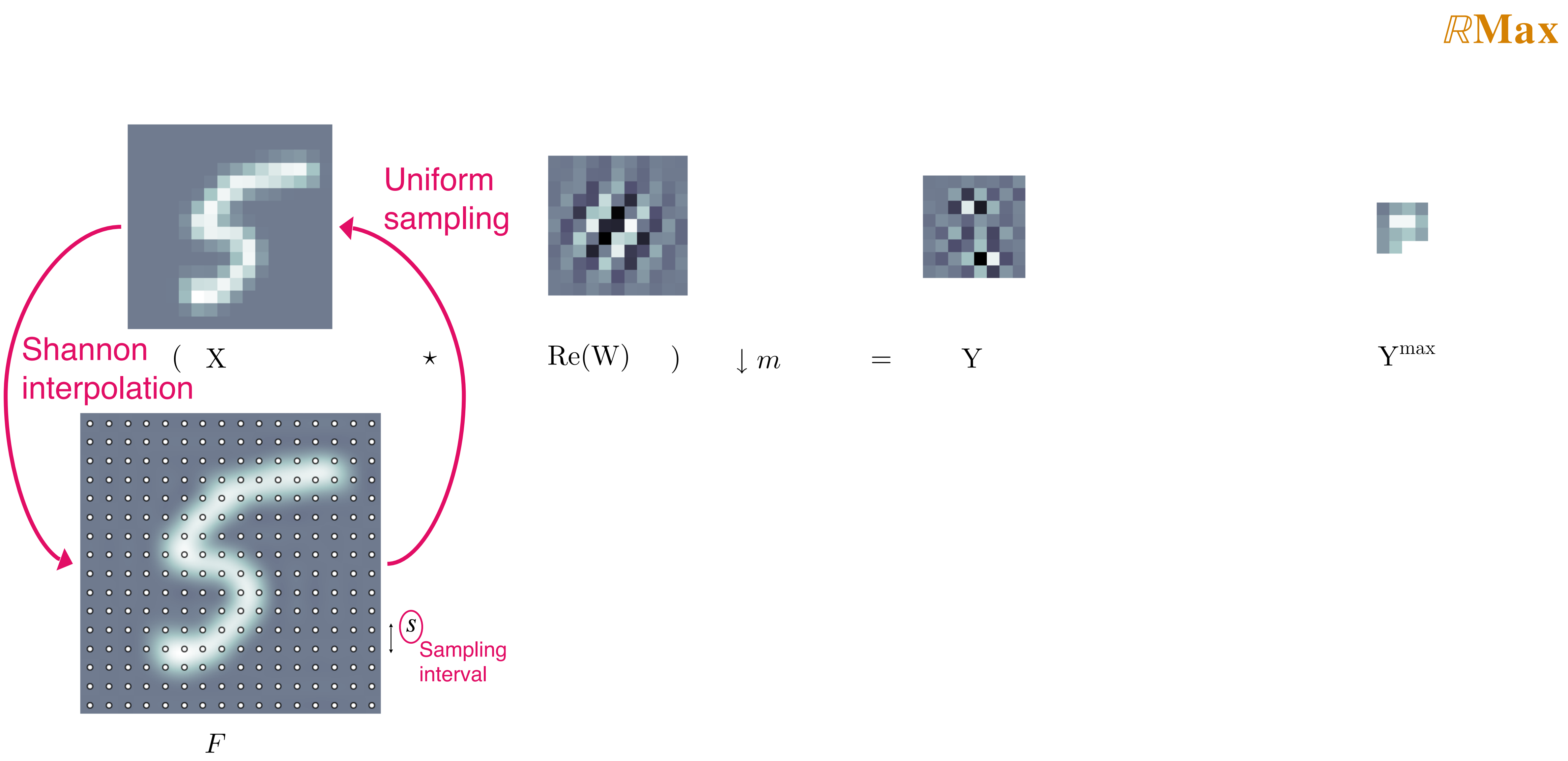

Detour via the continuous framework

- Using the **Shannon-Whittaker sampling theorem**

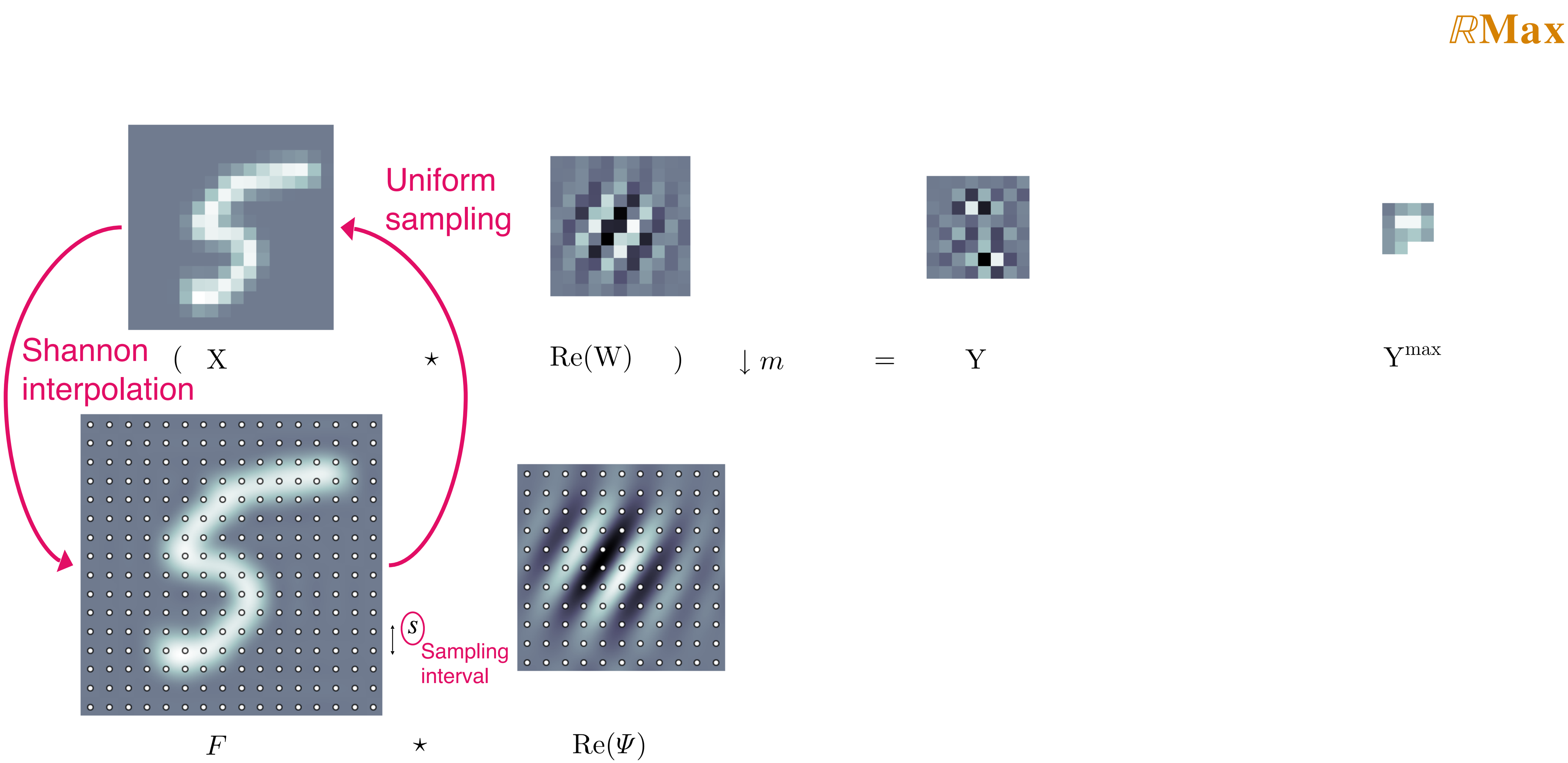

Detour via the continuous framework

- Using the **Shannon-Whittaker sampling theorem**

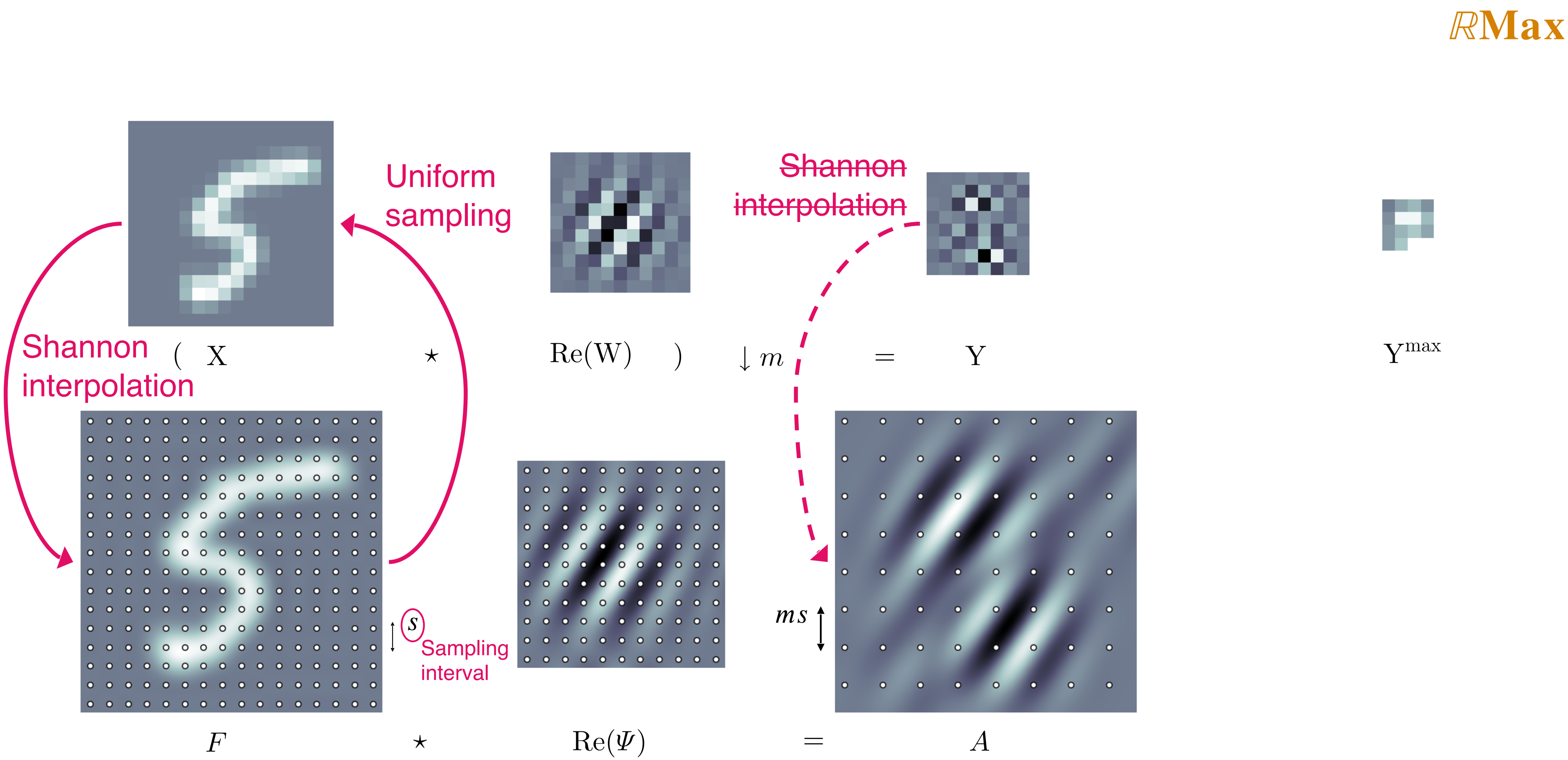

Detour via the continuous framework

- Using the **Shannon-Whittaker sampling theorem**

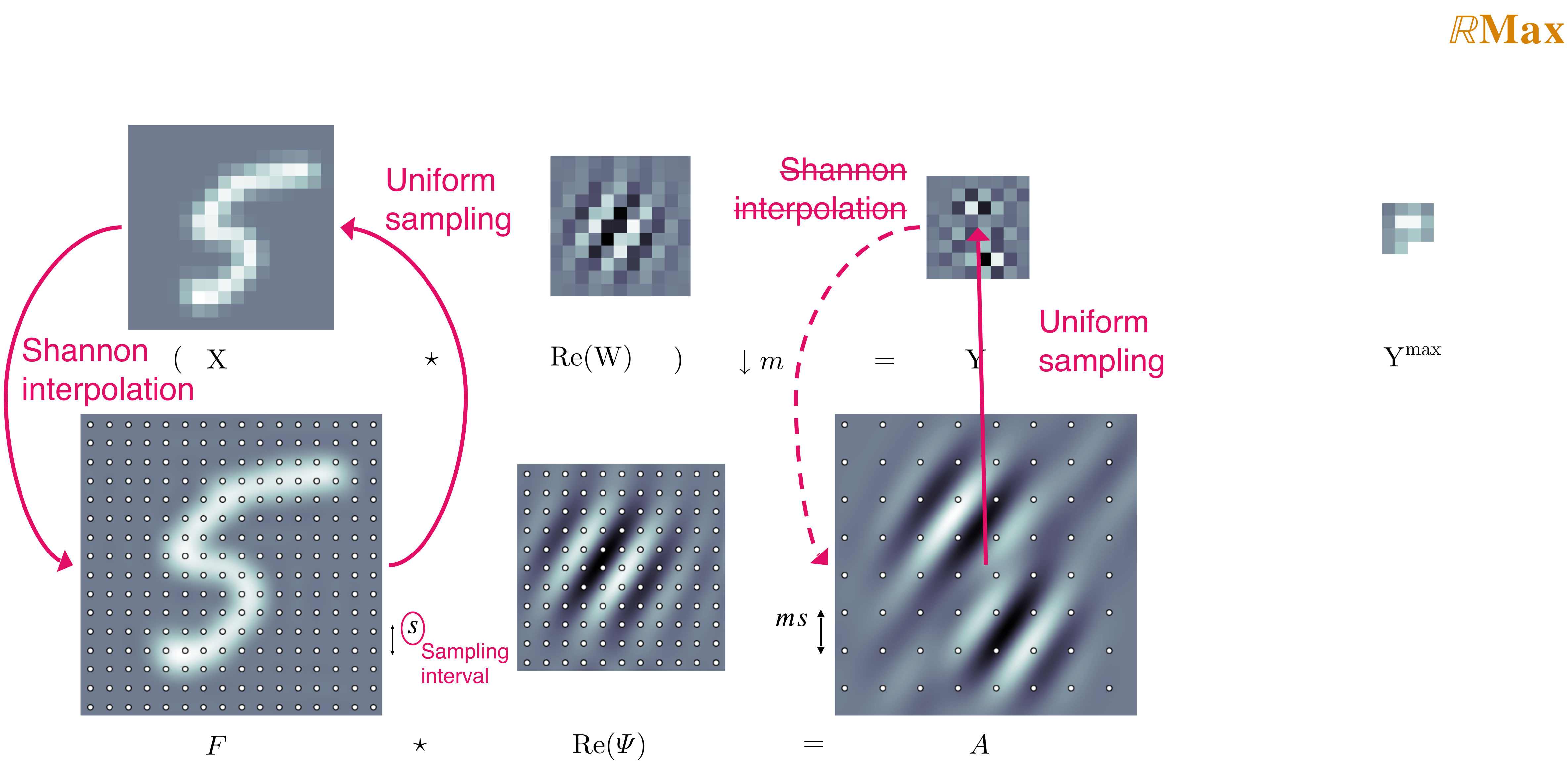

Detour via the continuous framework

- Using the **Shannon-Whittaker sampling theorem**

$$\mathrm{Y}^{\max}[\boldsymbol{n}] = \max_{\|\boldsymbol{p}\|_\infty \leq q} \big(F \star \mathrm{Re}(\Psi)\big)(2ms\boldsymbol{n} + ms\boldsymbol{p})$$

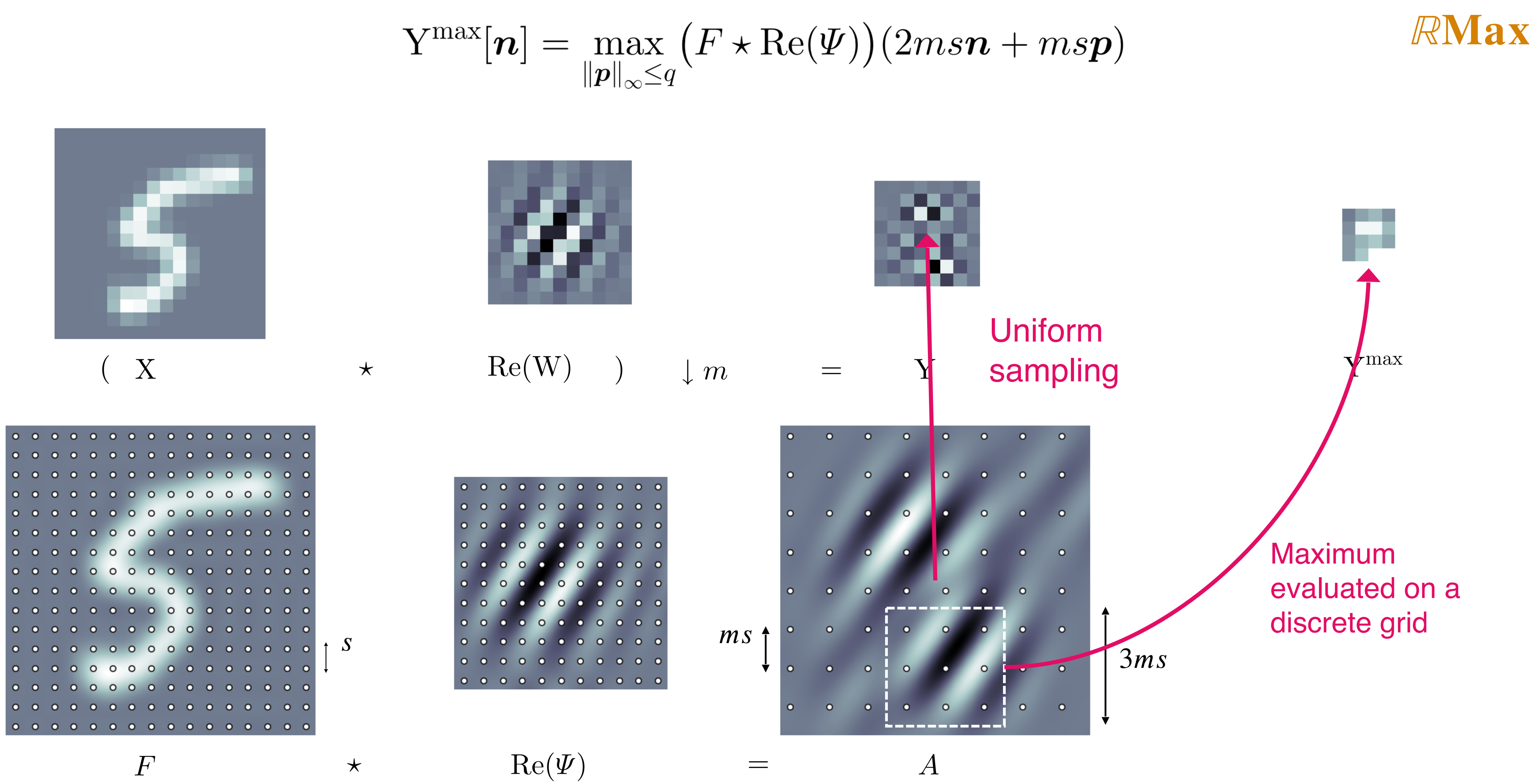

Detour via the continuous framework

- Using the **Shannon-Whittaker sampling theorem**

$$\mathrm{Y}^{\max}[\boldsymbol{n}] = \max_{\|\boldsymbol{p}\|_\infty \leq q} \left(F \star \mathrm{Re}(\Psi)\right)(2ms\boldsymbol{n} + ms\boldsymbol{p})$$

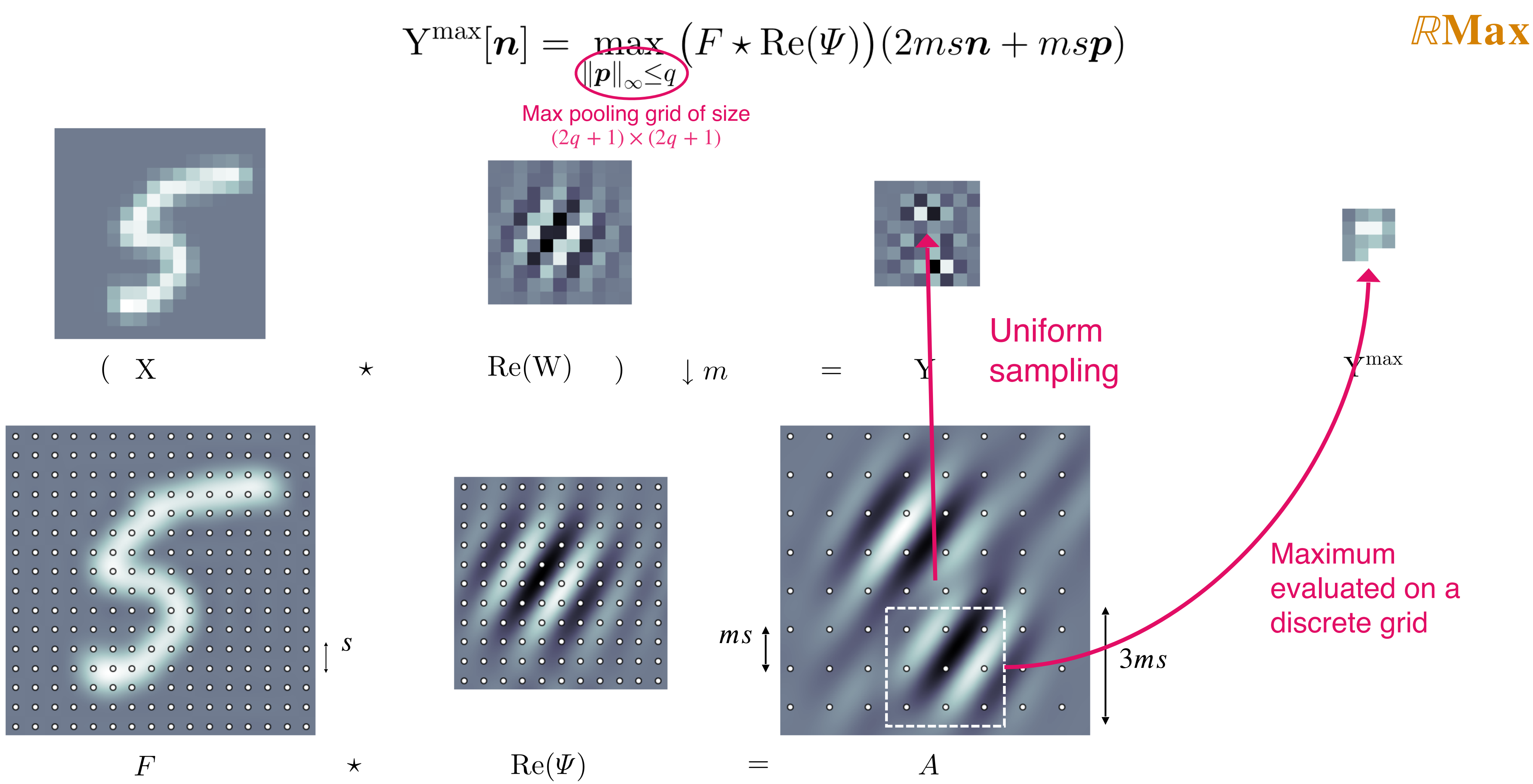

Detour via the continuous framework

- Using the **Shannon-Whittaker sampling theorem**

$$\mathrm{Y}^{\max}[\boldsymbol{n}] = \max_{\|\boldsymbol{p}\|_\infty \leq q} \left(F \star \mathrm{Re}(\Psi)\right)(2ms\boldsymbol{n} + ms\boldsymbol{p})$$

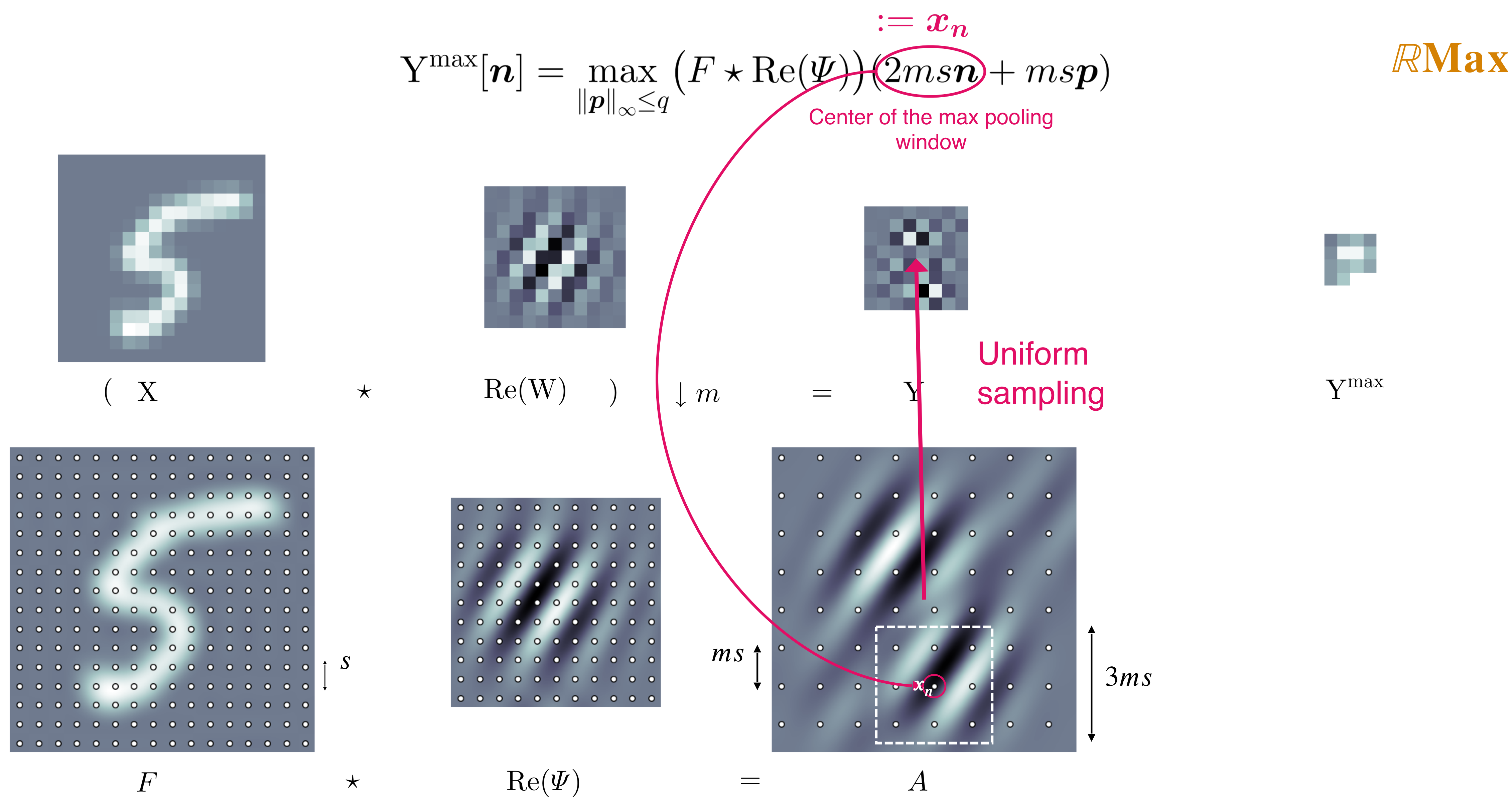

Detour via the continuous framework

- Using the **Shannon-Whittaker sampling theorem**

$$\mathrm{Y}^{\max}[\boldsymbol{n}] = \max_{\|\boldsymbol{p}\|_\infty \leq q} \big(F \star \mathrm{Re}(\Psi)\big)(2ms\boldsymbol{n} + \underbrace{ms\boldsymbol{p}}_{:= h_p})$$

Browsing the max pooling grid

$\mathbb{R}$**Max**

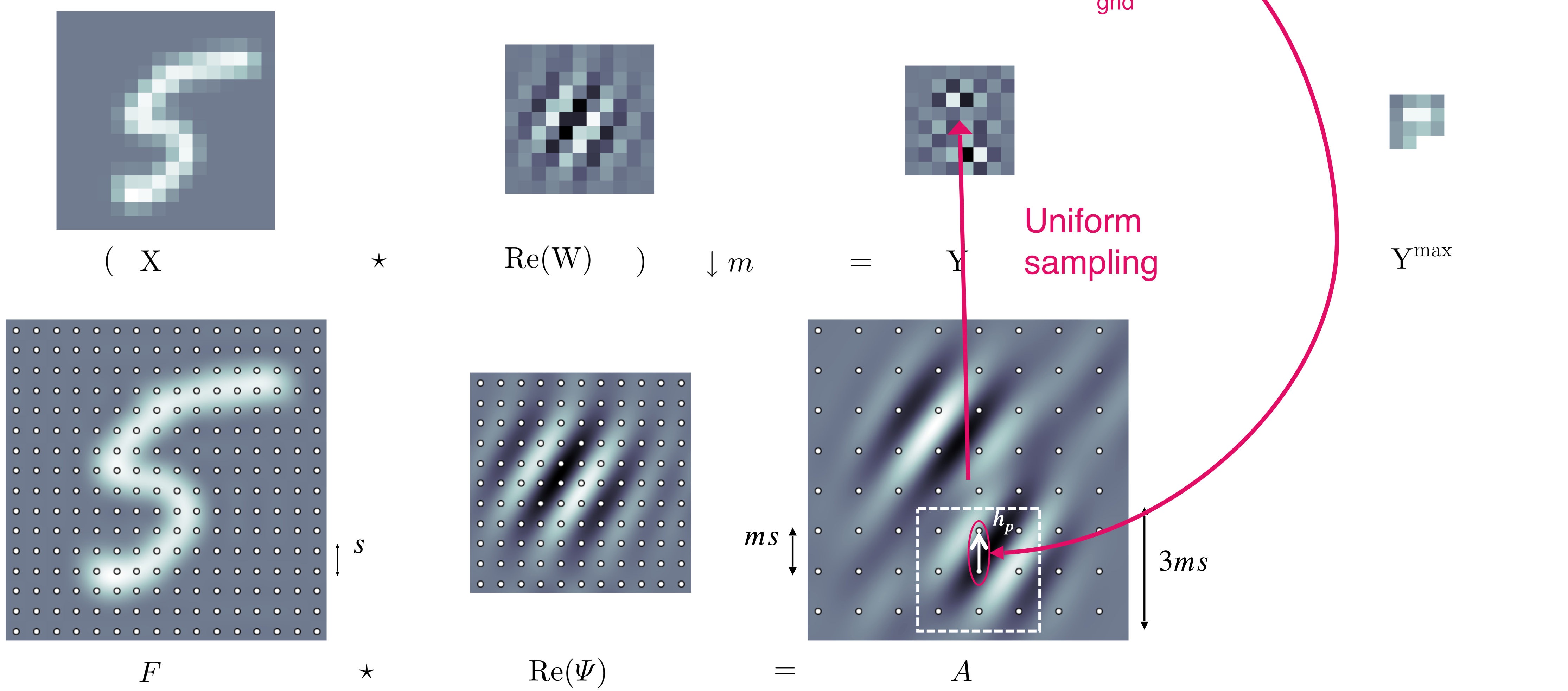

Detour via the continuous framework

- What if we search for the maximum **continuously** in the window?

$$\mathrm{Y}_0^{\max}[\boldsymbol{n}] = \max_{\|\boldsymbol{h}\|_\infty \leq \frac{3ms}{2}} \big(F \star \mathrm{Re}(\Psi)\big)(\boldsymbol{x_n} + \boldsymbol{h}) \approx \mathrm{Y}^{\max}[\boldsymbol{n}]?$$

$\mathbb{R}\mathbf{Max_0}$

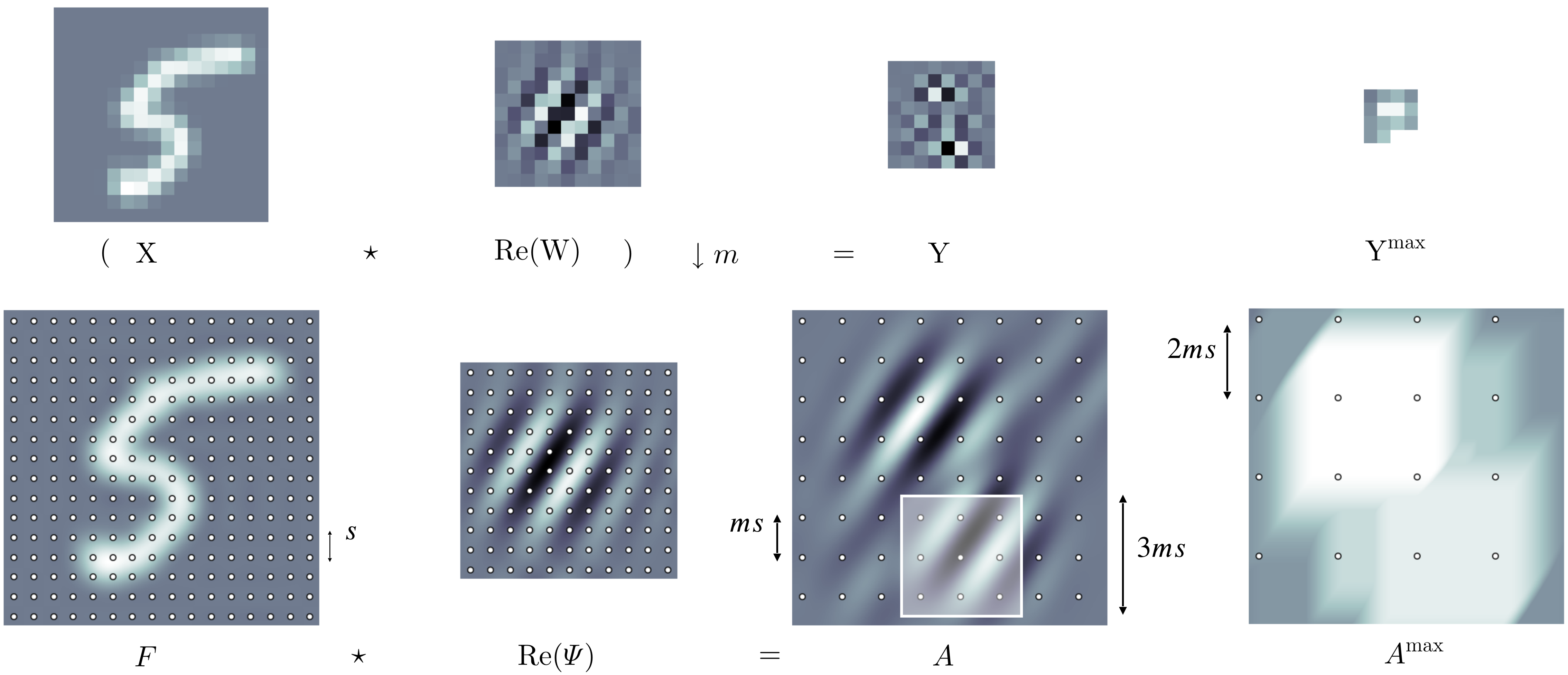

Detour via the continuous framework

- What if we search for the maximum **continuously** in the window?

$$\mathrm{Y}_0^{\max}[\boldsymbol{n}] = \max_{\|\boldsymbol{h}\|_\infty \le \frac{3ms}{2}} \big(F \star \mathrm{Re}(\Psi)\big)(\boldsymbol{x}_{\boldsymbol{n}} + \boldsymbol{h}) \approx \mathrm{Y}^{\max}[\boldsymbol{n}]?$$

$\mathbb{R}\mathbf{Max}_0$

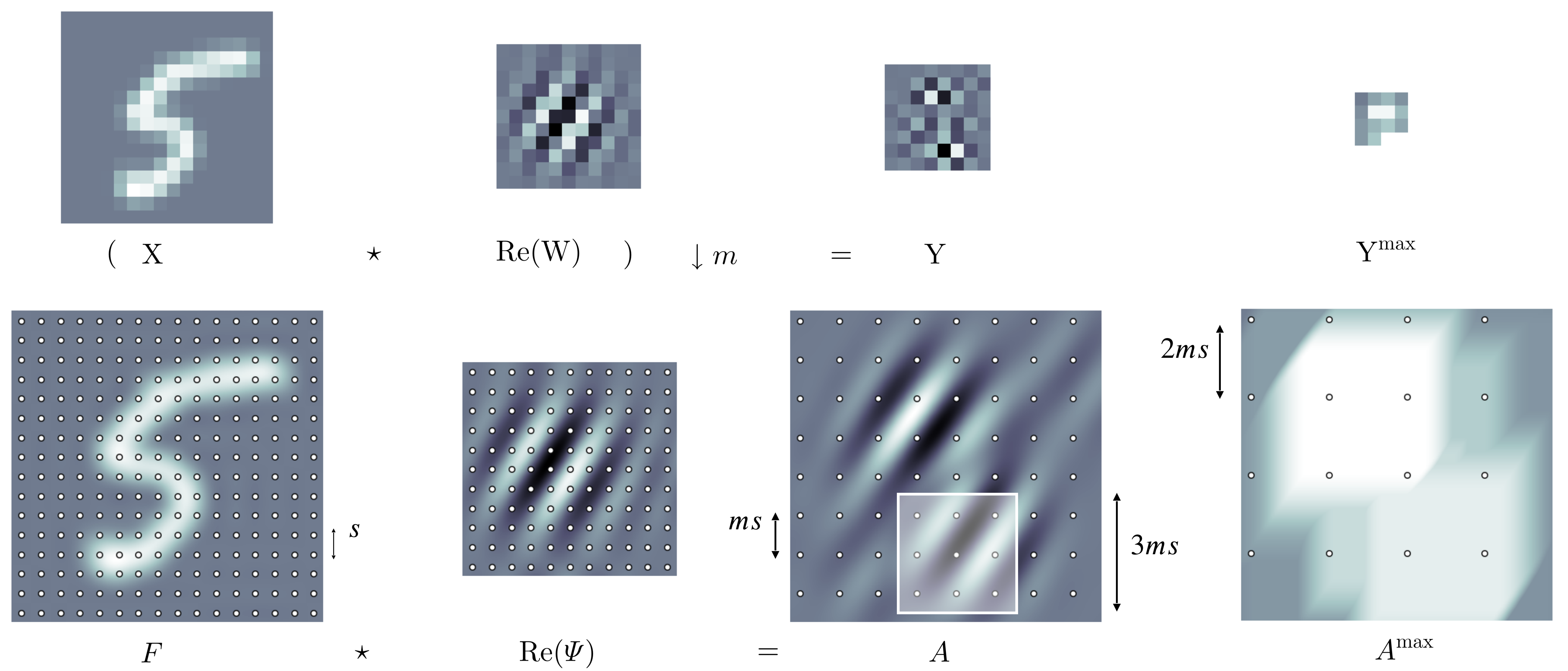

Detour via the continuous framework

- What if we search for the maximum **continuously** in the window?

$\mathbb{R}\mathbf{Max_0}$

$$\mathrm{Y}_0^{\max}[\boldsymbol{n}] = \max_{\|\boldsymbol{h}\|_\infty \leq \frac{3ms}{2}} \big(F \star \mathrm{Re}(\Psi)\big)(\boldsymbol{x_n} + \boldsymbol{h}) \approx \mathrm{Y}^{\max}[\boldsymbol{n}]?$$

Continuous window covering the max pooling grid

Browsing the whole window

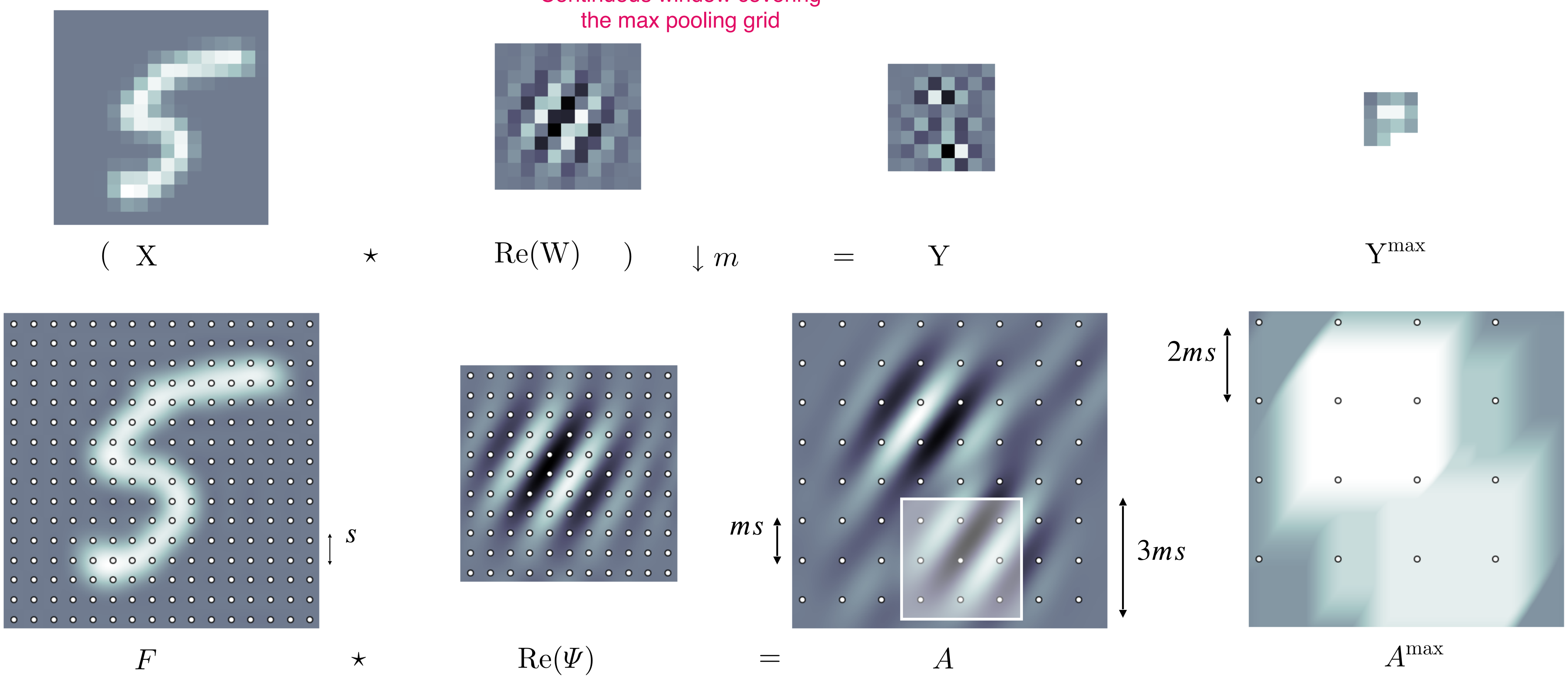

Detour via the continuous framework

- What if we search for the maximum **continuously** in the window?

$$\mathrm{Y}_0^{\max}[\boldsymbol{n}] = \max_{\|\boldsymbol{h}\|_\infty \le \frac{3ms}{2}} \big(F \star \mathrm{Re}(\Psi)\big)(\boldsymbol{x_n} + \boldsymbol{h}) \approx \mathrm{Y}^{\max}[\boldsymbol{n}]?$$

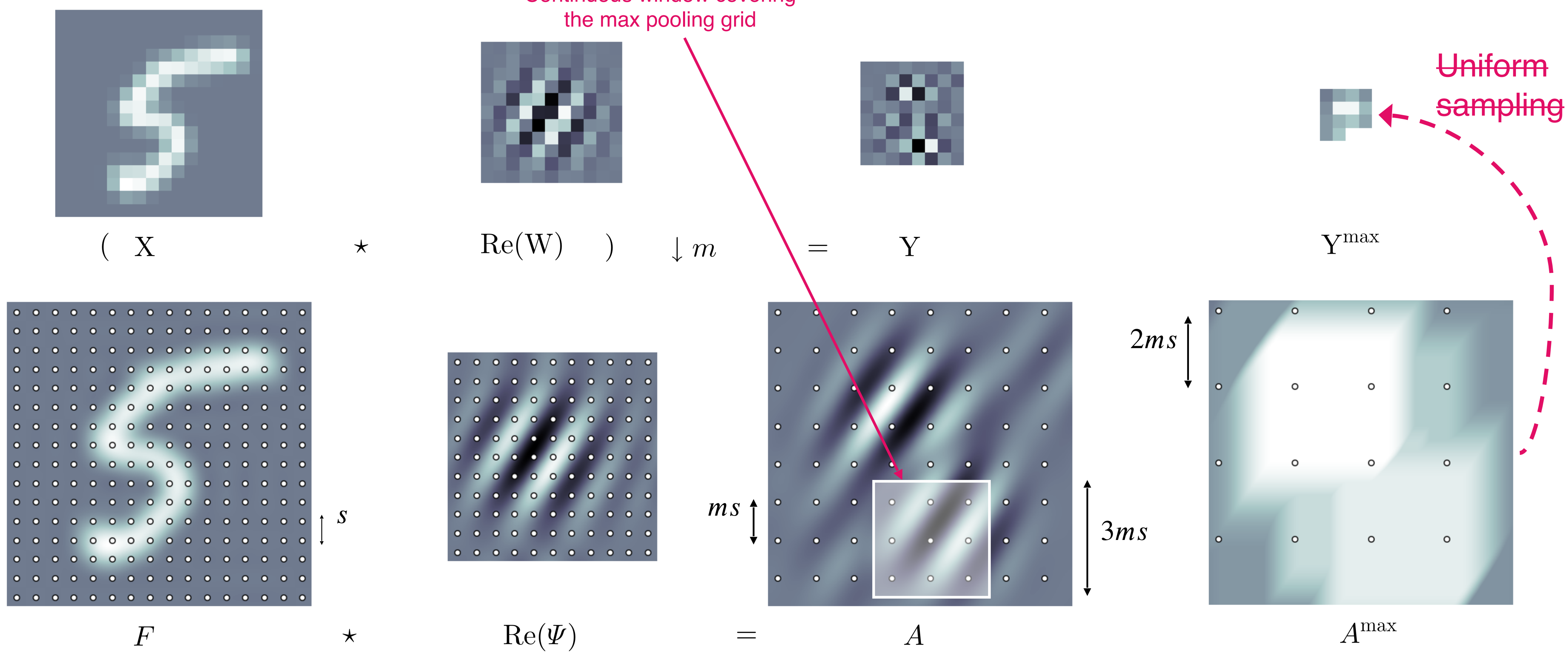

Detour via the continuous framework

- The output $\mathrm{Y}^{\mathrm{mod}}$ can be obtained by a uniform sampling of $|F * \Psi|$

ℂMod

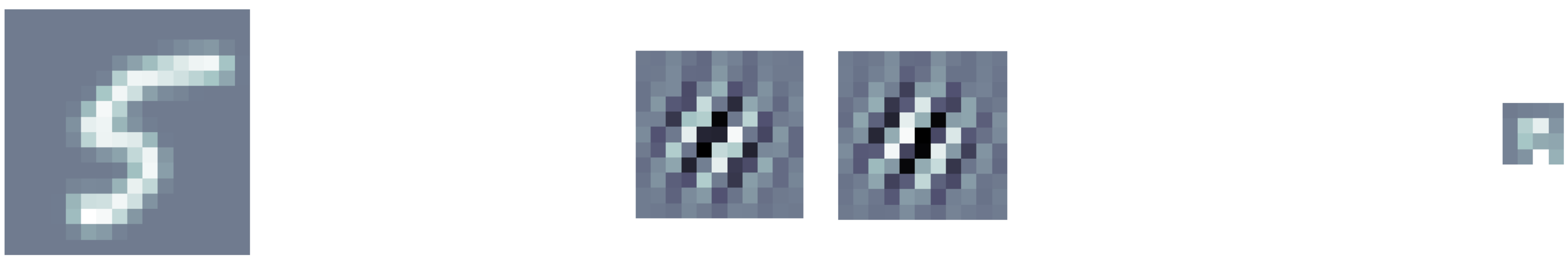

$$\left| \left(\mathrm{X} \star \mathrm{W} \right) \downarrow 2m \right| = \mathrm{Y}^{\mathrm{mod}}$$

Detour via the continuous framework

- The output $\mathrm{Y}^{\mathrm{mod}}$ can be obtained by a uniform sampling of $|F * \Psi|$

$\mathbb{C}$Mod

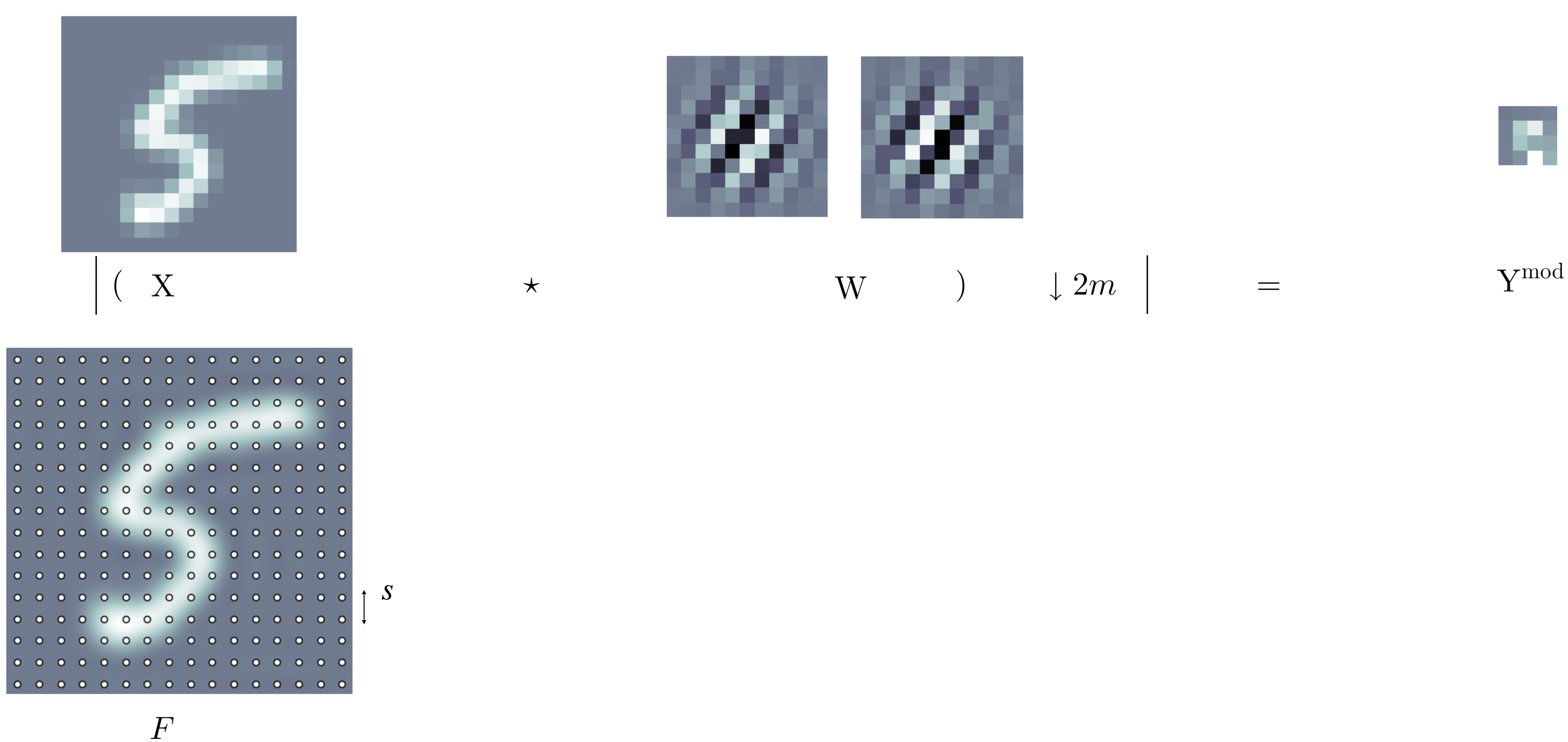

Detour via the continuous framework

- The output $\mathrm{Y}^{\mathrm{mod}}$ can be obtained by a uniform sampling of $|F * \Psi|$

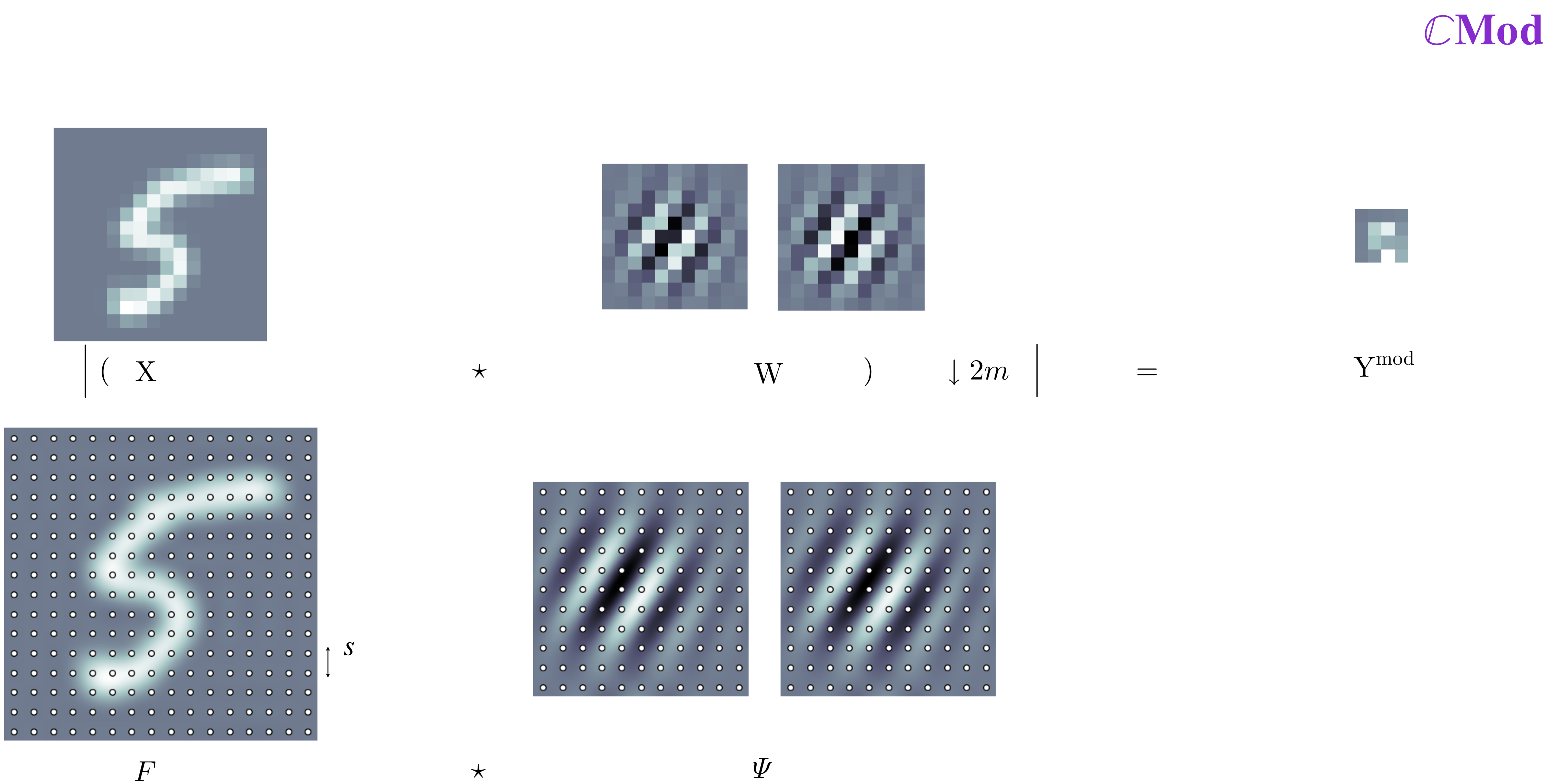

Detour via the continuous framework

- The output $\mathrm{Y}^{\mathrm{mod}}$ can be obtained by a uniform sampling of $|F * \Psi|$

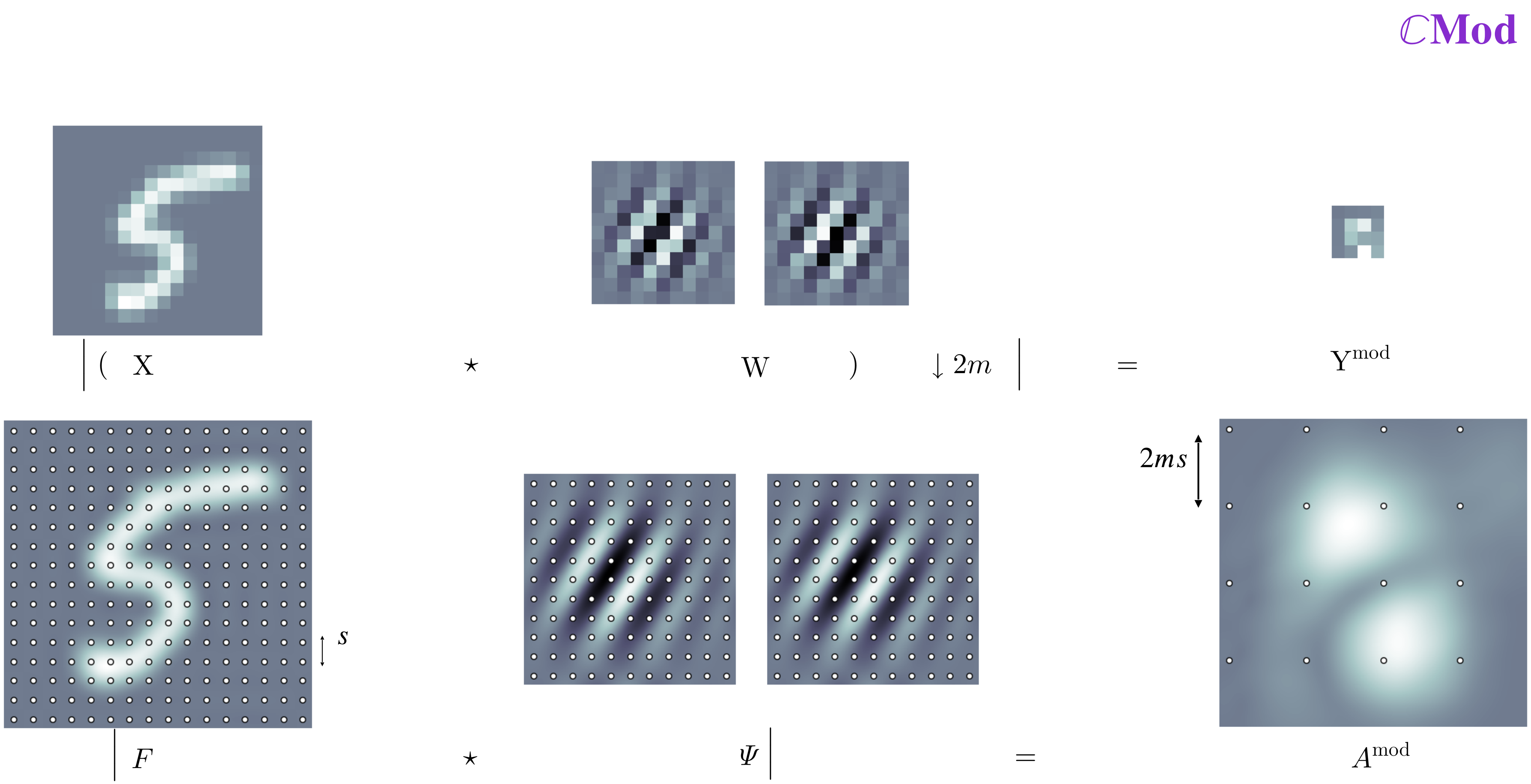

Detour via the continuous framework

- The output $\mathrm{Y}^{\mathrm{mod}}$ can be obtained by a uniform sampling of $|F * \Psi|$

$\mathbb{C}\mathbf{Mod}$

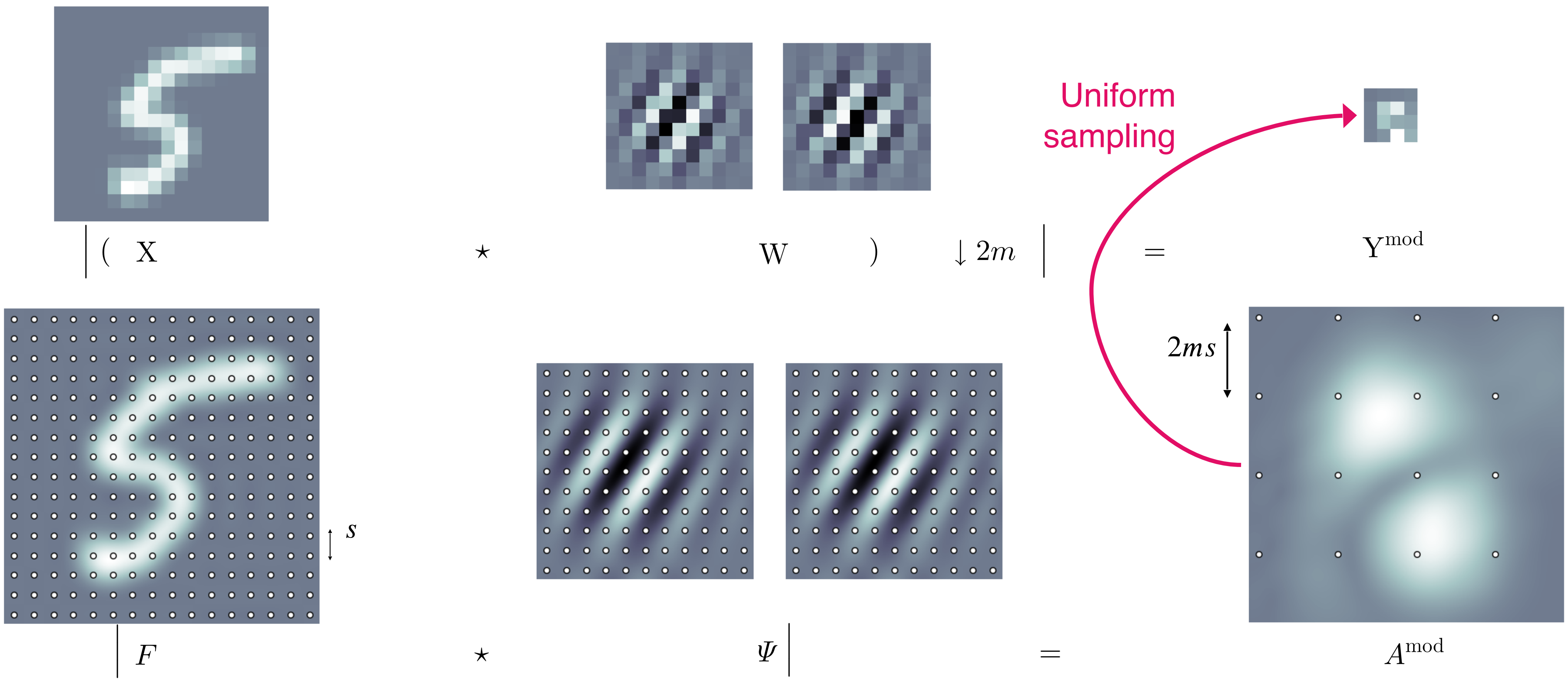

Detour via the continuous framework

- The output $\mathrm{Y}^{\mathrm{mod}}$ can be obtained by a uniform sampling of $|F * \Psi|$

$$\mathrm{Y}^{\mathrm{mod}}[\boldsymbol{n}] = \left|\left(F \star \Psi\right)(2ms\boldsymbol{n})\right|$$

ℂMod

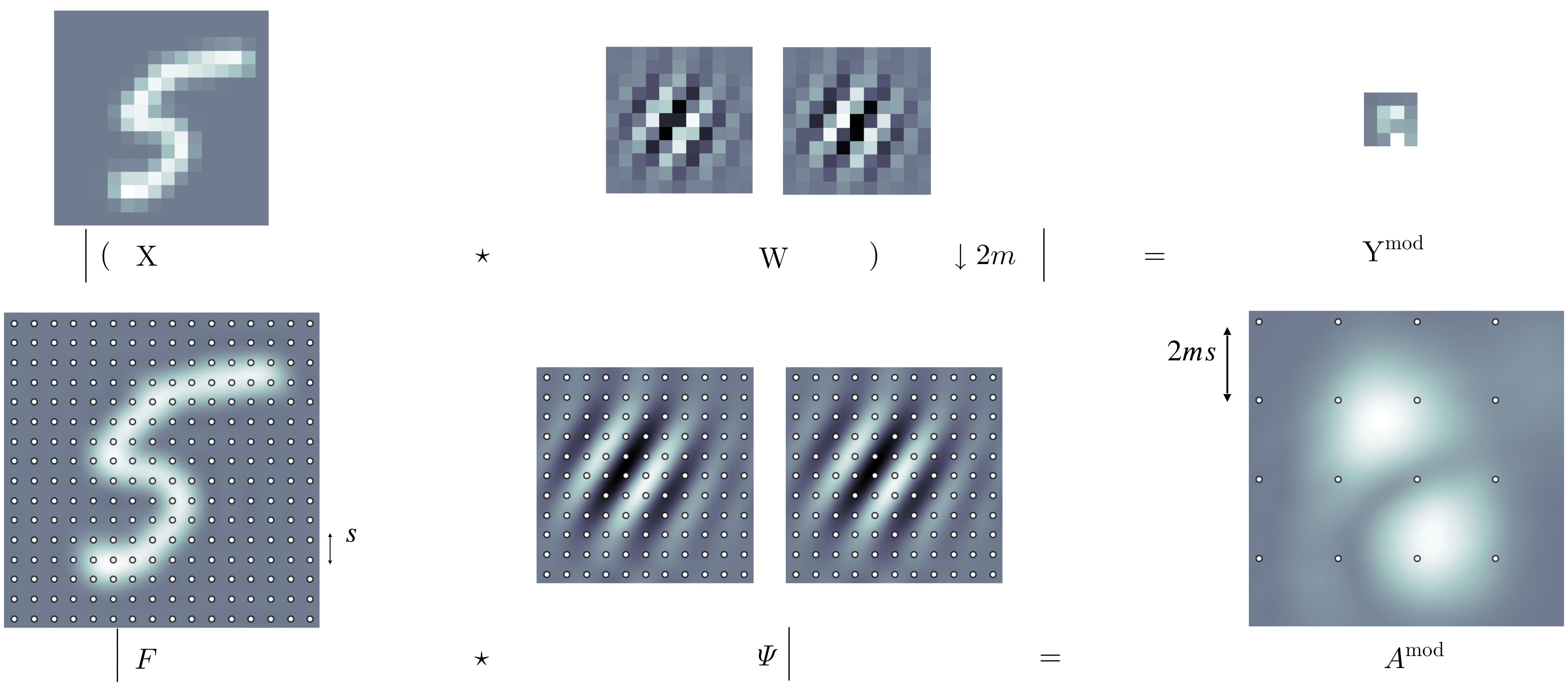

Detour via the continuous framework

- The output $\mathrm{Y}^{\mathrm{mod}}$ can be obtained by a uniform sampling of $|F * \Psi|$

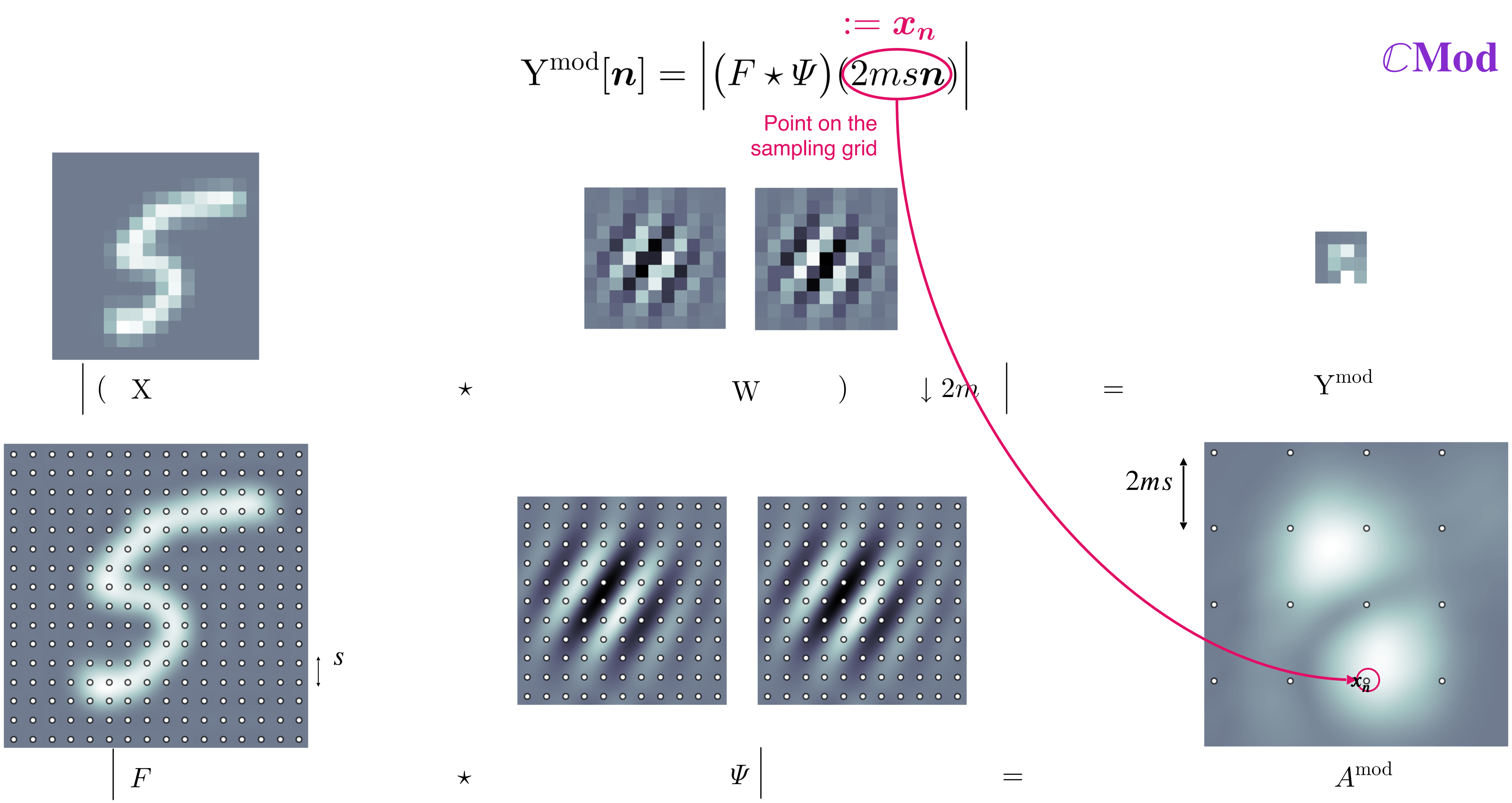

From high to low-frequency

From high to low-frequency

- $\mathcal{V}\big(\boldsymbol{\nu},\,\varepsilon\big) := \Big\{\varPsi \in L^2_{\mathbb{C}}(\mathbb{R}^2) \,\Big|\, \operatorname{supp}\widehat{\varPsi} \subset B_\infty(\boldsymbol{\nu},\,\varepsilon/2)\Big\}.$

From high to low-frequency

- $\mathcal{V}(\boldsymbol{\nu}, \varepsilon) := \left\{ \Psi \in L^2_{\mathbb{C}}(\mathbb{R}^2) \;\middle|\; \operatorname{supp} \widehat{\Psi} \subset B_\infty(\boldsymbol{\nu}, \varepsilon/2) \right\}.$
- $F_0 : \boldsymbol{x} \mapsto (F * \overline{\Psi})(\boldsymbol{x}) e^{i\langle \boldsymbol{\nu}, \boldsymbol{x} \rangle} \xrightarrow{\Psi \in \mathcal{V}(\boldsymbol{\nu}, \varepsilon)} \operatorname{supp} \widehat{F_0} \subset B_\infty(\varepsilon/2)$

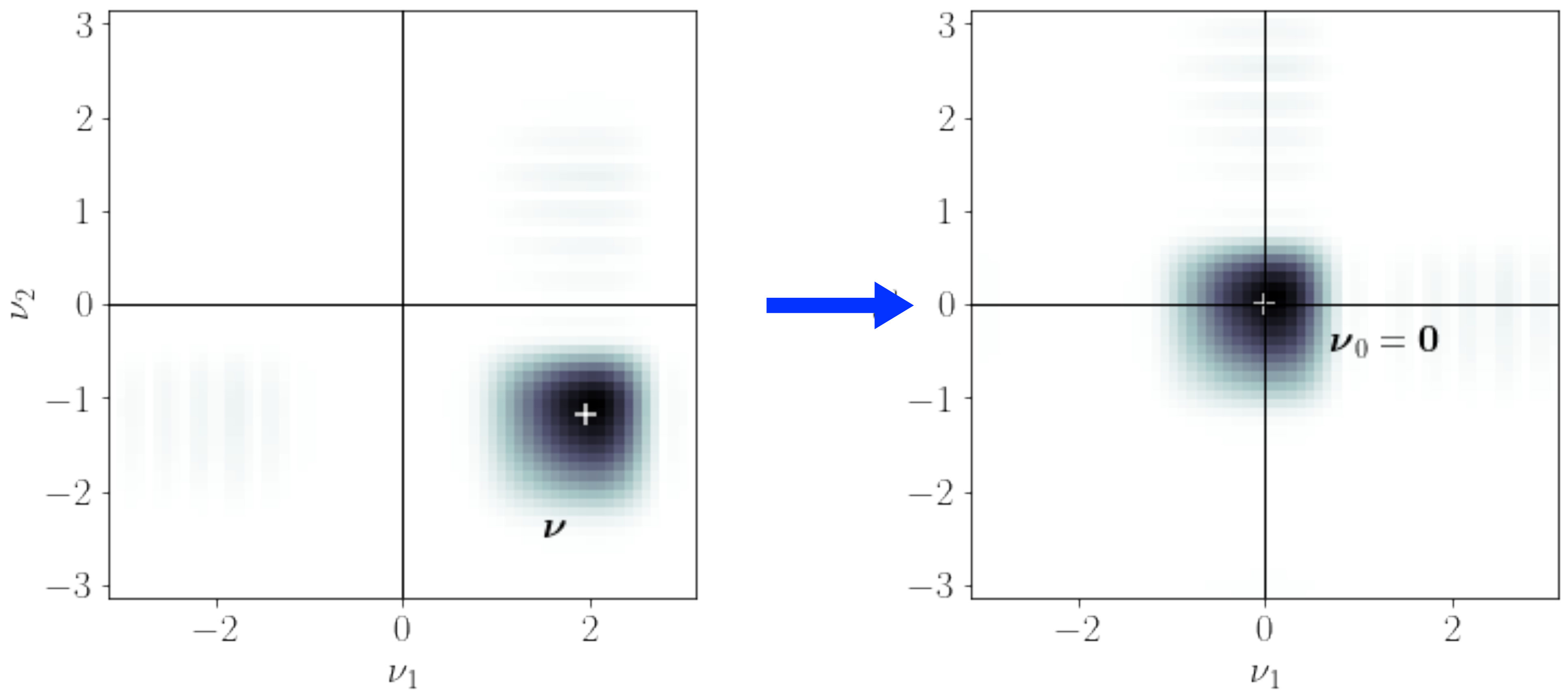

From high to low-frequency

- $\mathcal{V}(\boldsymbol{\nu}, \varepsilon) := \left\{ \Psi \in L^2_{\mathbb{C}}(\mathbb{R}^2) \,\middle|\, \operatorname{supp} \widehat{\Psi} \subset B_\infty(\boldsymbol{\nu}, \varepsilon/2) \right\}.$
- $F_0 : \boldsymbol{x} \mapsto (F * \overline{\Psi})(\boldsymbol{x}) \mathrm{e}^{i\langle \boldsymbol{\nu}, \boldsymbol{x}\rangle} \xrightarrow{\Psi \in \mathcal{V}(\boldsymbol{\nu},\varepsilon)} \operatorname{supp}\widehat{F_0} \subset B_\infty(\varepsilon/2)$

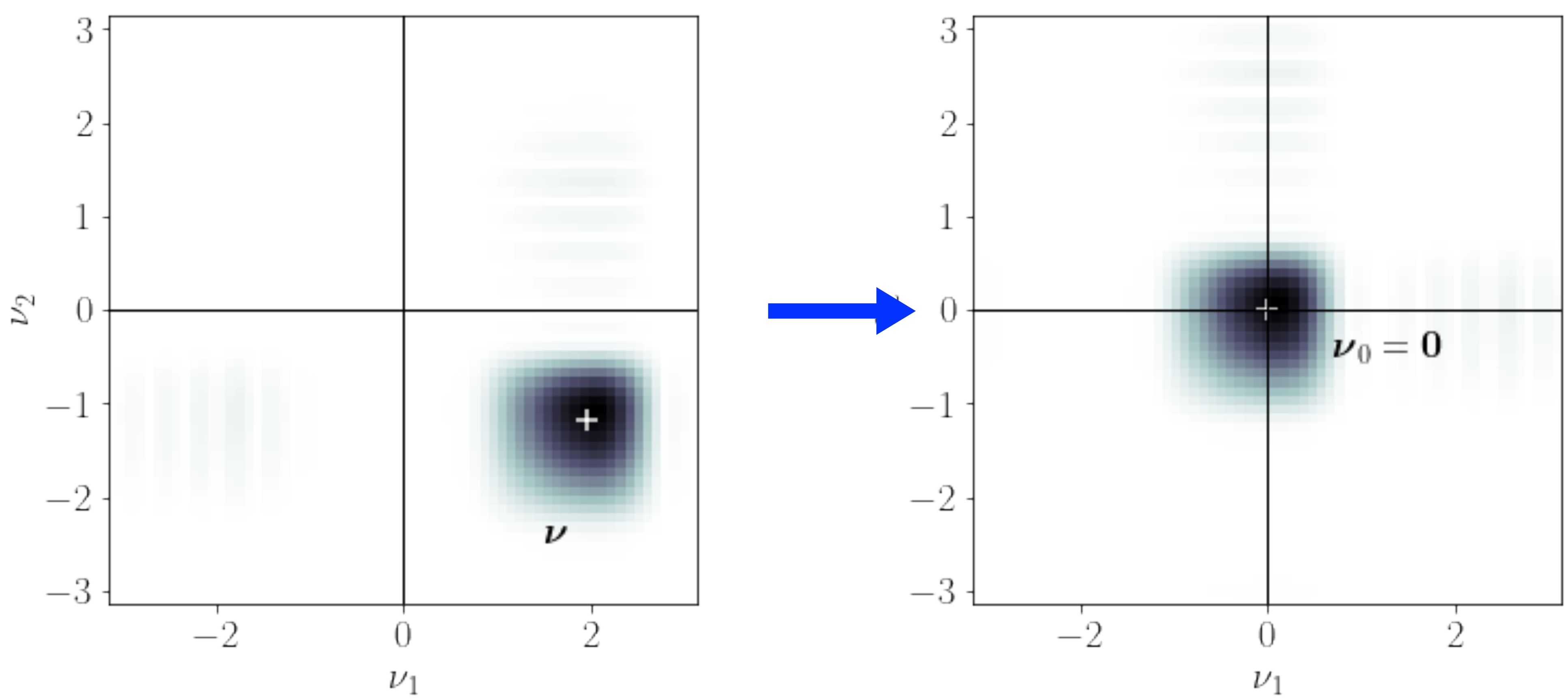

- **Shift-invariance bound** for low-frequency functions:

$$\|\mathcal{T}_{\boldsymbol{h}} F_0 - F_0\|_{L^2} \leq \alpha(\varepsilon \boldsymbol{h}) \|F_0\|_{L^2} \qquad \alpha : \boldsymbol{\tau} \mapsto \frac{\|\boldsymbol{\tau}\|_1}{2}$$

Shift-invariance of CMod in the discrete framework

Shift-invariance of CMod in the discrete framework

Theorem (Shift invariance of $\mathbb{C}\mathbf{Mod}$)

If $\mathrm{W} \in \mathcal{J}\big(\boldsymbol{\theta},\, \kappa\big)$ and $\kappa \leq \pi/m$

then for any input image with finite support $\mathrm{X} \in l^2_{\mathbb{R}}(\mathbb{Z}^2)$

$$\left\| U_m^{\mathrm{mod}}(\mathcal{T}_{\boldsymbol{u}}\mathrm{X}) - U_m^{\mathrm{mod}}\mathrm{X} \right\|_2 \leq \alpha(\kappa \boldsymbol{u}) \left\| U_m^{\mathrm{mod}}\mathrm{X} \right\|_2$$

Shift-invariance of CMod in the discrete framework

Theorem (Shift invariance of $\mathbb{C}\mathbf{Mod}$)

If $\mathrm{W} \in \mathcal{J}(\boldsymbol{\theta}, \kappa)$ and $\kappa \leq \pi/m$

then for any input image with finite support $\mathrm{X} \in l^2_{\mathbb{R}}(\mathbb{Z}^2)$

$$\left\| U_m^{\mathrm{mod}}(\mathcal{T}_{\boldsymbol{u}}\mathrm{X}) - U_m^{\mathrm{mod}}\mathrm{X} \right\|_2 \leq \alpha(\kappa \boldsymbol{u}) \left\| U_m^{\mathrm{mod}}\mathrm{X} \right\|_2$$

$$\alpha : \boldsymbol{\tau} \mapsto \frac{\|\boldsymbol{\tau}\|_1}{2}$$

From CMod to RMax in the continuous framework

- **I. Waldspurger intuition** linking the two operators:

From CMod to RMax in the continuous framework

- **I. Waldspurger intuition** linking the two operators:

$$F_0 : \boldsymbol{x} \mapsto (F * \overline{\Psi})(\boldsymbol{x})\mathrm{e}^{i\langle \boldsymbol{\nu}, \boldsymbol{x}\rangle} \xrightarrow{\Psi \in \mathcal{V}(\boldsymbol{\nu}, \varepsilon)} \mathrm{supp}\widehat{F_0} \subset B_\infty(\varepsilon/2)$$

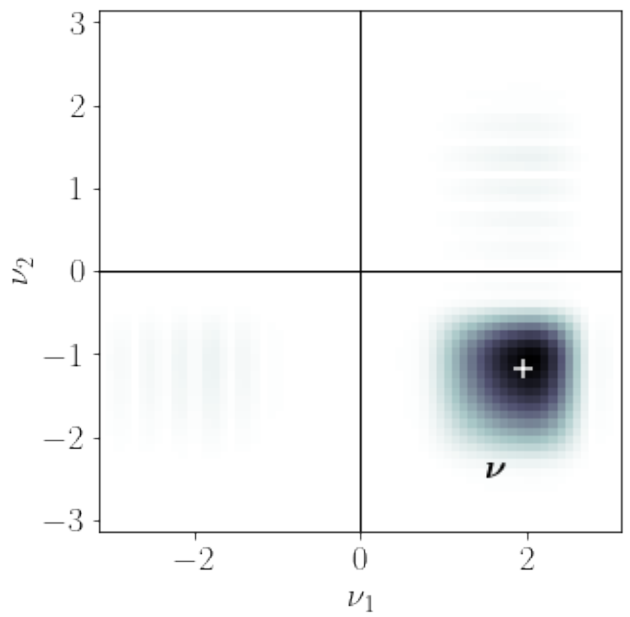

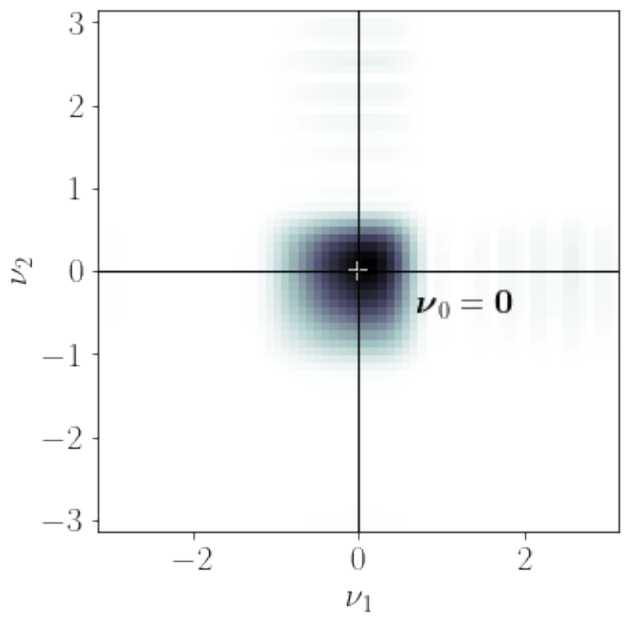

From CMod to RMax in the continuous framework

- **I. Waldspurger intuition** linking the two operators:

$$F_0 : \boldsymbol{x} \mapsto (F * \overline{\Psi})(\boldsymbol{x})\mathrm{e}^{i\langle \boldsymbol{\nu}, \boldsymbol{x}\rangle} \xrightarrow{\Psi \in \mathcal{V}(\boldsymbol{\nu}, \varepsilon)} \mathrm{supp}\widehat{F_0} \subset B_\infty(\varepsilon/2)$$

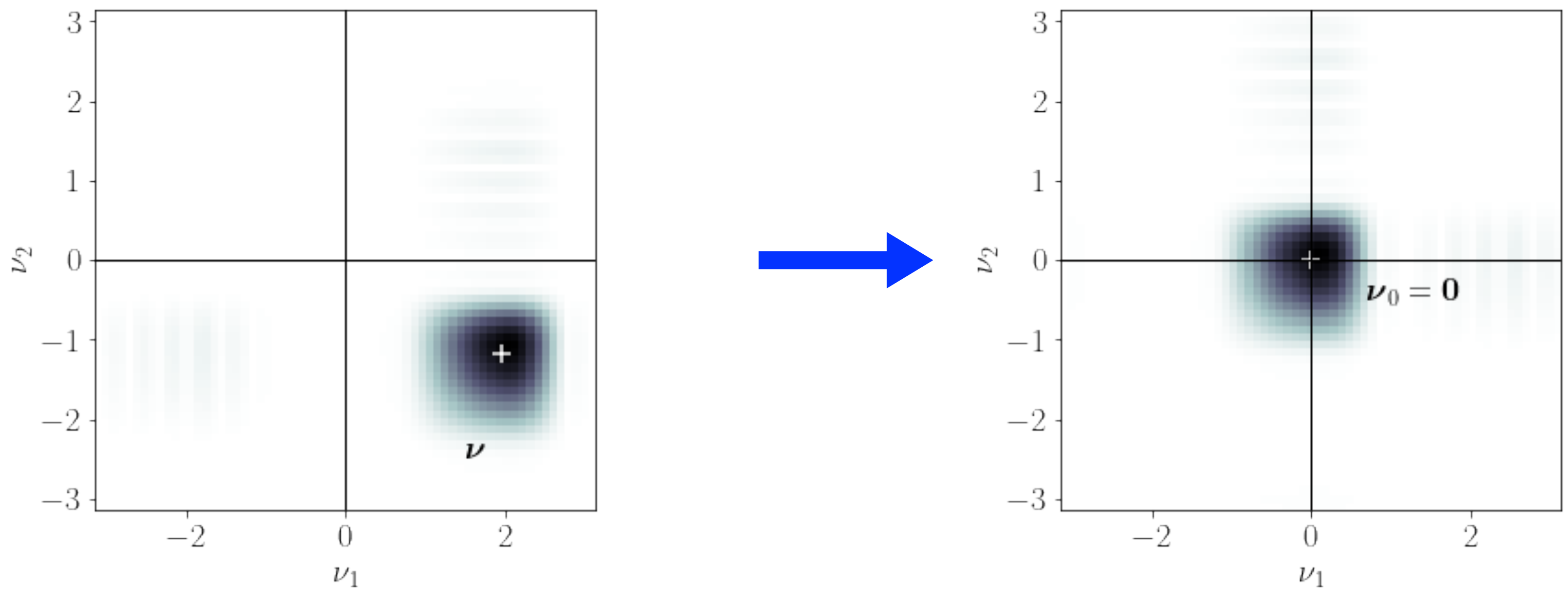

$$(F * \mathrm{Re}\,\overline{\Psi})(\boldsymbol{x}) = \mathrm{Re}((F * \overline{\Psi})(\boldsymbol{x})) = \mathrm{Re}(F_0(\boldsymbol{x})\mathrm{e}^{-i\langle \boldsymbol{\nu}, \boldsymbol{x}\rangle})$$

From CMod to RMax in the continuous framework

- **I. Waldspurger intuition** linking the two operators:

$$F_0 : \boldsymbol{x} \mapsto (F * \overline{\Psi})(\boldsymbol{x})\mathrm{e}^{i\langle \boldsymbol{\nu}, \boldsymbol{x}\rangle} \xrightarrow{\Psi \in \mathcal{V}(\boldsymbol{\nu}, \varepsilon)} \mathrm{supp}\widehat{F_0} \subset B_\infty(\varepsilon/2)$$

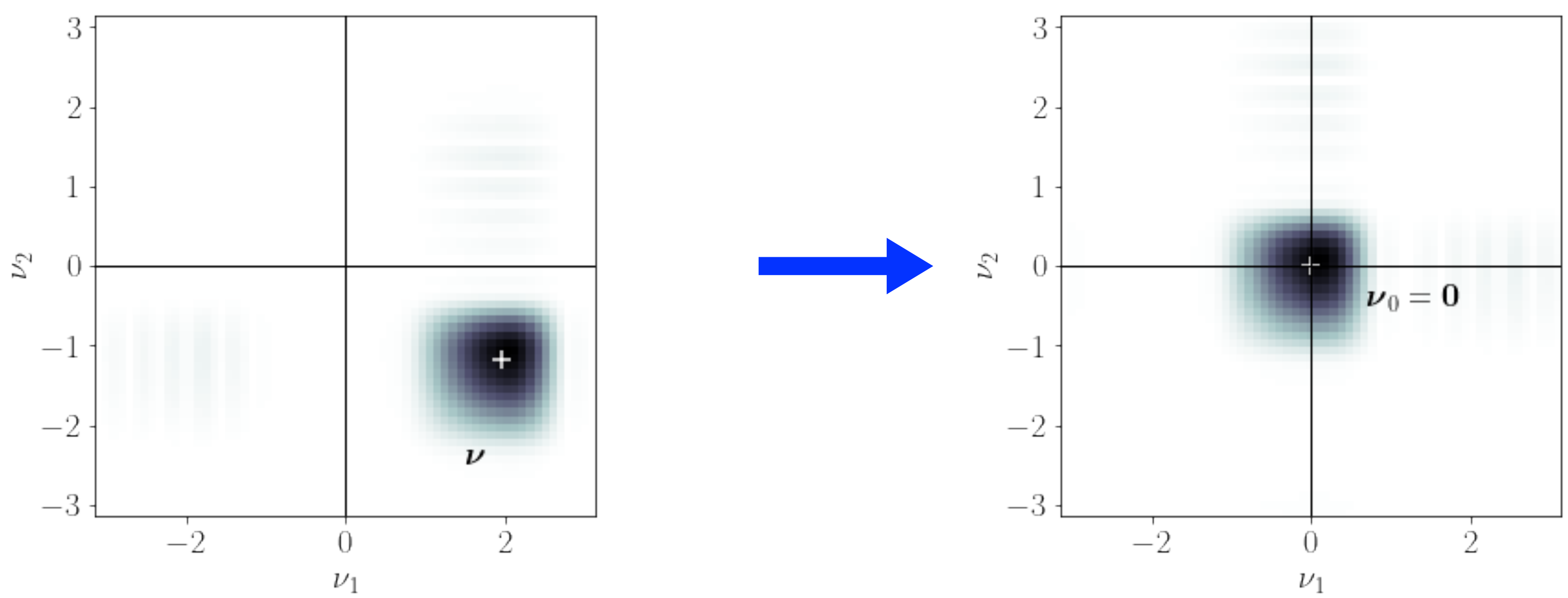

$$(F * \mathrm{Re}\,\overline{\Psi})(\boldsymbol{x}) = \mathrm{Re}((F * \overline{\Psi})(\boldsymbol{x})) = \mathrm{Re}(F_0(\boldsymbol{x})\mathrm{e}^{-i\langle \boldsymbol{\nu},\, \boldsymbol{x}\rangle})$$

$$(F * \mathrm{Re}\,\overline{\Psi})(\boldsymbol{x} + \boldsymbol{h}) \approx \mathrm{Re}(F_0(\boldsymbol{x})\mathrm{e}^{-i\langle \boldsymbol{\nu},\, \boldsymbol{x}+\boldsymbol{h}\rangle}) = \mathrm{Re}((F * \overline{\Psi})(\boldsymbol{x})\mathrm{e}^{-i\langle \boldsymbol{\nu},\, \boldsymbol{h}\rangle})$$

From CMod to RMax in the continuous framework

- **I. Waldspurger intuition** linking the two operators:

$$F_0 : \boldsymbol{x} \mapsto (F * \overline{\Psi})(\boldsymbol{x}) \mathrm{e}^{i\langle \boldsymbol{\nu}, \boldsymbol{x} \rangle} \xrightarrow{\Psi \in \mathcal{V}(\boldsymbol{\nu}, \varepsilon)} \mathrm{supp}\widehat{F_0} \subset B_\infty(\varepsilon/2)$$

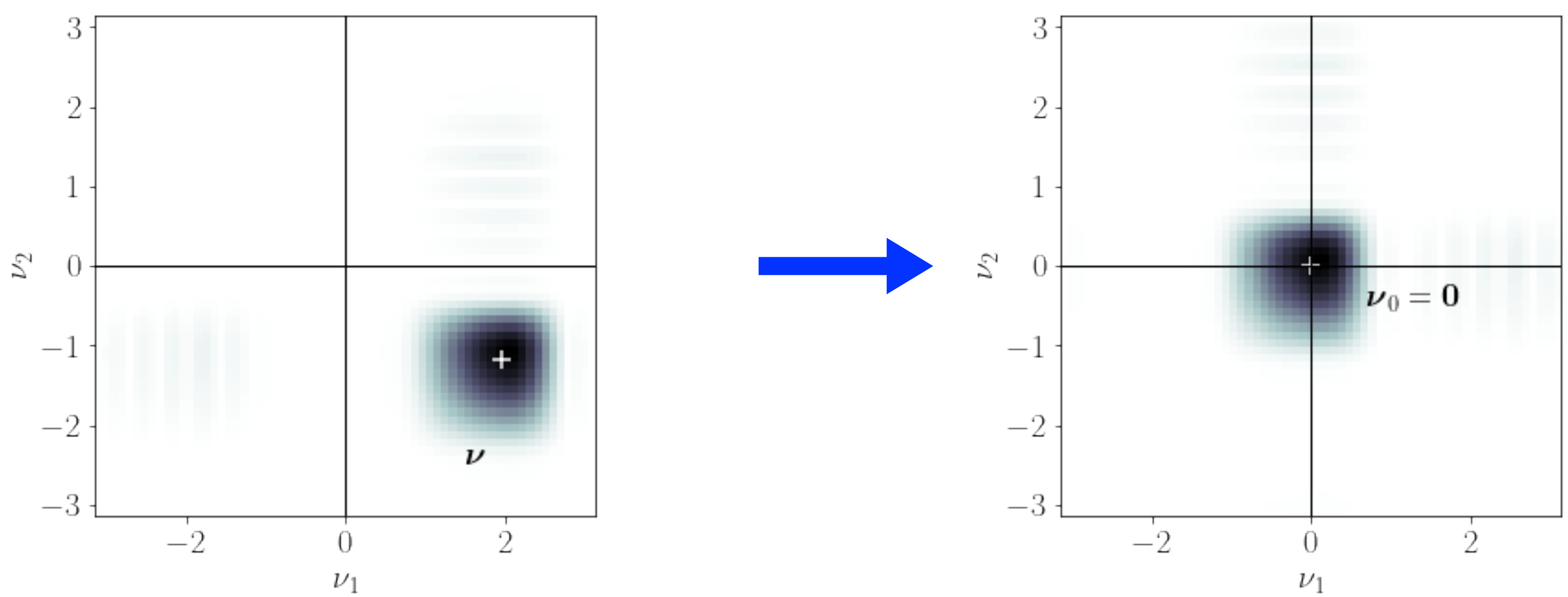

$$\|\boldsymbol{h}\|_2 \ll 2\pi/\varepsilon \implies F_0(\boldsymbol{x} + \boldsymbol{h}) \approx F_0(\boldsymbol{x})$$

$$(F * \mathrm{Re}\,\overline{\Psi})(\boldsymbol{x}) = \mathrm{Re}((F * \overline{\Psi})(\boldsymbol{x})) = \mathrm{Re}(F_0(\boldsymbol{x})\mathrm{e}^{-i\langle \boldsymbol{\nu}, \boldsymbol{x} \rangle})$$

$$(F * \mathrm{Re}\,\overline{\Psi})(\boldsymbol{x} + \boldsymbol{h}) \approx \mathrm{Re}(F_0(\boldsymbol{x})\mathrm{e}^{-i\langle \boldsymbol{\nu}, \boldsymbol{x}+\boldsymbol{h} \rangle}) = \mathrm{Re}((F * \overline{\Psi})(\boldsymbol{x})\mathrm{e}^{-i\langle \boldsymbol{\nu}, \boldsymbol{h} \rangle})$$

From CMod to RMax in the continuous framework

- **I. Waldspurger intuition** linking the two operators:

$$F_0 : \boldsymbol{x} \mapsto (F * \overline{\Psi})(\boldsymbol{x})\mathrm{e}^{i\langle \boldsymbol{\nu}, \boldsymbol{x}\rangle} \xrightarrow{\Psi \in \mathcal{V}(\boldsymbol{\nu}, \varepsilon)} \mathrm{supp}\widehat{F_0} \subset B_\infty(\varepsilon/2)$$

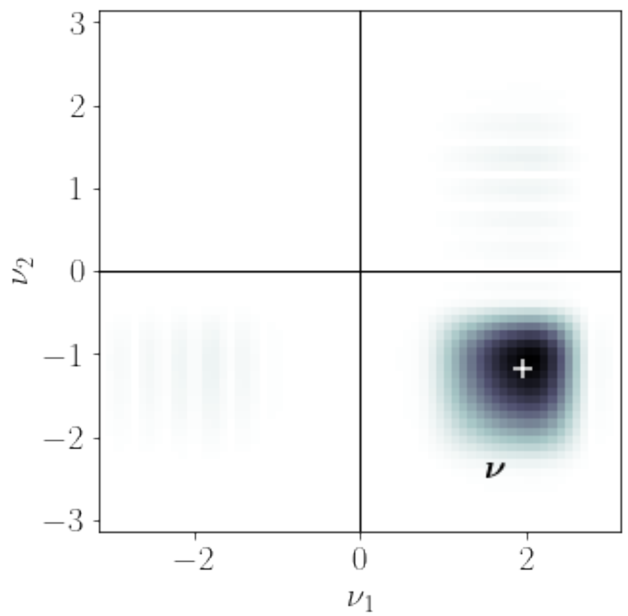

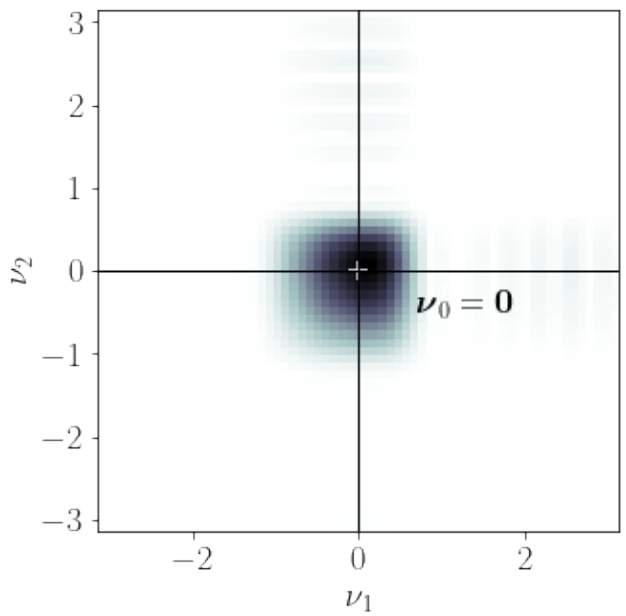

$$(F * \overline{\Psi})(\boldsymbol{x}) = |(F * \overline{\Psi})(\boldsymbol{x})|\mathrm{e}^{-iH(\boldsymbol{x})} \qquad \|\boldsymbol{h}\|_2 \ll 2\pi/\varepsilon \implies F_0(\boldsymbol{x}+\boldsymbol{h}) \approx F_0(\boldsymbol{x})$$

$$(F * \mathrm{Re}\,\overline{\Psi})(\boldsymbol{x}) = \mathrm{Re}((F * \overline{\Psi})(\boldsymbol{x})) = \mathrm{Re}(F_0(\boldsymbol{x})\mathrm{e}^{-i\langle \boldsymbol{\nu},\, \boldsymbol{x}\rangle})$$

$$(F * \mathrm{Re}\,\overline{\Psi})(\boldsymbol{x}+\boldsymbol{h}) \approx \mathrm{Re}(F_0(\boldsymbol{x})\mathrm{e}^{-i\langle \boldsymbol{\nu},\, \boldsymbol{x}+\boldsymbol{h}\rangle}) = \mathrm{Re}((F * \overline{\Psi})(\boldsymbol{x})\mathrm{e}^{-i\langle \boldsymbol{\nu},\, \boldsymbol{h}\rangle})$$

From CMod to RMax in the continuous framework

- **I. Waldspurger intuition** linking the two operators:

$$F_0 : \boldsymbol{x} \mapsto (F * \overline{\Psi})(\boldsymbol{x})\mathrm{e}^{i\langle \boldsymbol{\nu}, \boldsymbol{x}\rangle} \xrightarrow{\Psi \in \mathcal{V}(\boldsymbol{\nu}, \varepsilon)} \mathrm{supp}\widehat{F_0} \subset B_\infty(\varepsilon/2)$$

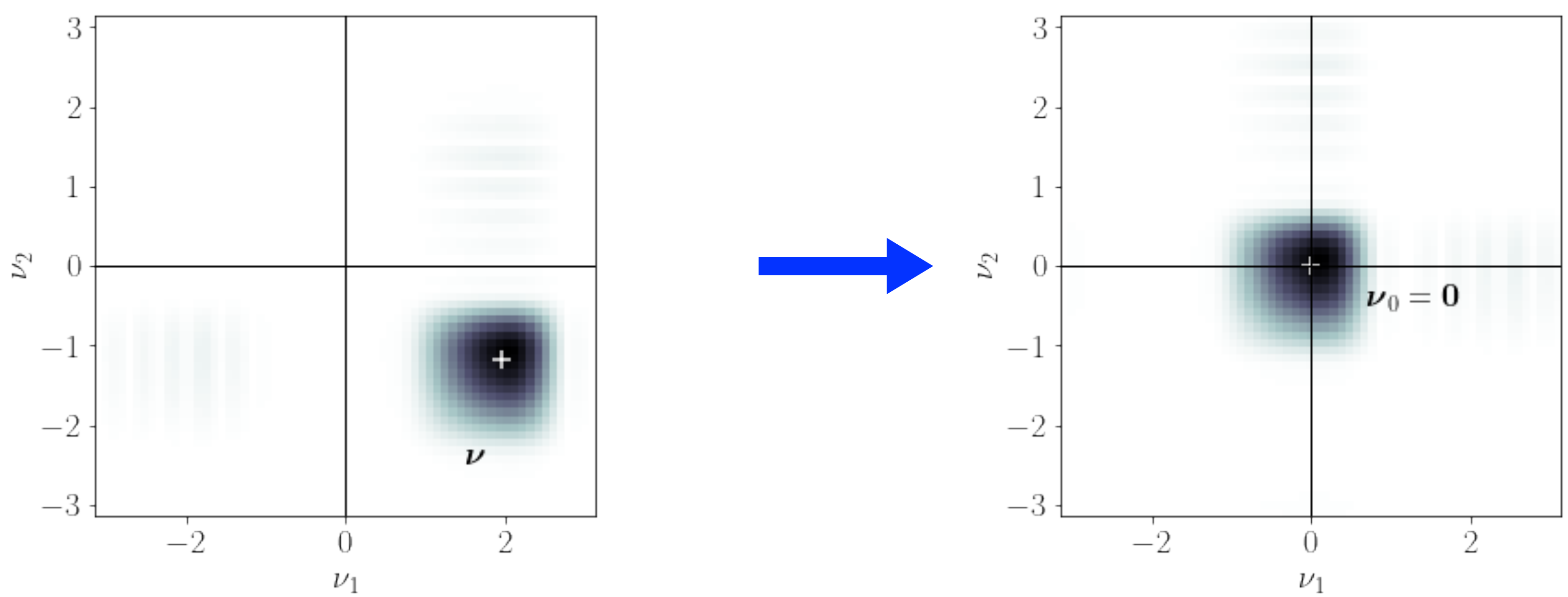

$$(F * \overline{\Psi})(\boldsymbol{x}) = |(F * \overline{\Psi})(\boldsymbol{x})|\mathrm{e}^{-iH(\boldsymbol{x})} \qquad \|\boldsymbol{h}\|_2 \ll 2\pi/\varepsilon \implies F_0(\boldsymbol{x} + \boldsymbol{h}) \approx F_0(\boldsymbol{x})$$

$$(F * \mathrm{Re}\,\overline{\Psi})(\boldsymbol{x}) = \mathrm{Re}((F * \overline{\Psi})(\boldsymbol{x})) = \mathrm{Re}(F_0(\boldsymbol{x})\mathrm{e}^{-i\langle \boldsymbol{\nu},\, \boldsymbol{x}\rangle})$$

$$(F * \mathrm{Re}\,\overline{\Psi})(\boldsymbol{x} + \boldsymbol{h}) \approx \mathrm{Re}(F_0(\boldsymbol{x})\mathrm{e}^{-i\langle \boldsymbol{\nu},\, \boldsymbol{x}+\boldsymbol{h}\rangle}) = \mathrm{Re}((F * \overline{\Psi})(\boldsymbol{x})\mathrm{e}^{-i\langle \boldsymbol{\nu},\, \boldsymbol{h}\rangle})$$

$$(F * \mathrm{Re}\,\overline{\Psi})(\boldsymbol{x} + \boldsymbol{h}) \approx |(F * \overline{\Psi})(\boldsymbol{x})| \cos(\langle \boldsymbol{\nu},\, \boldsymbol{h}\rangle - H(\boldsymbol{x}))$$

From CMod to RMax in the continuous framework

- **I. Waldspurger intuition** linking the two operators:

$$F_0 : \boldsymbol{x} \mapsto (F * \overline{\Psi})(\boldsymbol{x}) \mathrm{e}^{i\langle \boldsymbol{\nu}, \boldsymbol{x}\rangle} \xrightarrow{\Psi \in \mathcal{V}(\boldsymbol{\nu}, \varepsilon)} \mathrm{supp}\widehat{F_0} \subset B_\infty(\varepsilon/2)$$

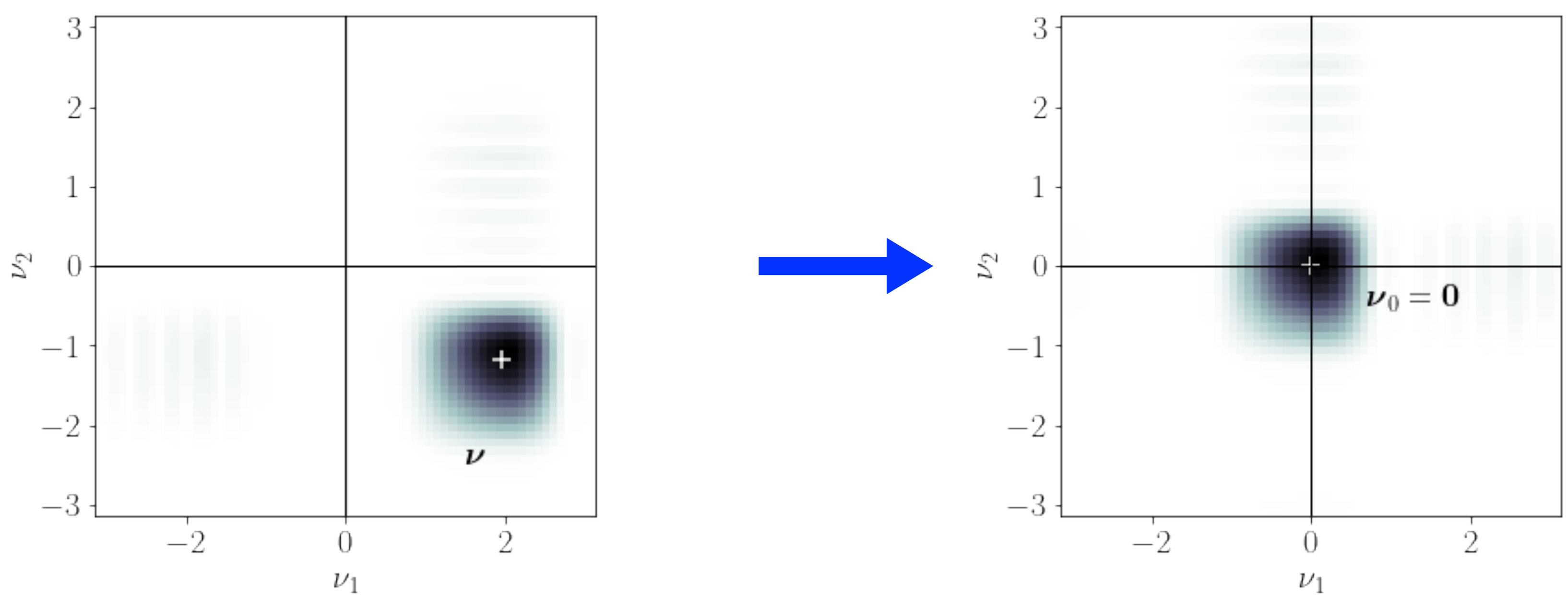

$$(F * \overline{\Psi})(\boldsymbol{x}) = |(F * \overline{\Psi})(\boldsymbol{x})| \mathrm{e}^{-iH(\boldsymbol{x})} \qquad \|\boldsymbol{h}\|_2 \ll 2\pi/\varepsilon \implies F_0(\boldsymbol{x} + \boldsymbol{h}) \approx F_0(\boldsymbol{x})$$

$$(F * \mathrm{Re}\,\overline{\Psi})(\boldsymbol{x}) = \mathrm{Re}((F * \overline{\Psi})(\boldsymbol{x})) = \mathrm{Re}(F_0(\boldsymbol{x}) \mathrm{e}^{-i\langle \boldsymbol{\nu},\, \boldsymbol{x}\rangle})$$

$$(F * \mathrm{Re}\,\overline{\Psi})(\boldsymbol{x} + \boldsymbol{h}) \approx \mathrm{Re}(F_0(\boldsymbol{x}) \mathrm{e}^{-i\langle \boldsymbol{\nu},\, \boldsymbol{x}+\boldsymbol{h}\rangle}) = \mathrm{Re}((F * \overline{\Psi})(\boldsymbol{x}) \mathrm{e}^{-i\langle \boldsymbol{\nu},\, \boldsymbol{h}\rangle})$$

$$(F * \mathrm{Re}\,\overline{\Psi})(\boldsymbol{x} + \boldsymbol{h}) \approx |(F * \overline{\Psi})(\boldsymbol{x})| \cos(\langle \boldsymbol{\nu},\, \boldsymbol{h}\rangle - H(\boldsymbol{x}))$$

$G(\boldsymbol{x},\, \boldsymbol{h})$

From CMod to RMax in the continuous framework

- **I. Waldspurger intuition** linking the two operators:

$$(F * \mathrm{Re}\,\overline{\Psi})(\boldsymbol{x}+\boldsymbol{h}) \approx |(F * \overline{\Psi})(\boldsymbol{x})| \cos(\langle \boldsymbol{\nu}, \boldsymbol{h}\rangle - H(\boldsymbol{x}))$$

From CMod to RMax in the continuous framework

- **I. Waldspurger intuition** linking the two operators:

$$(F * \mathrm{Re}\,\overline{\Psi})(\boldsymbol{x}+\boldsymbol{h}) \approx |(F * \overline{\Psi})(\boldsymbol{x})| \cos(\langle \boldsymbol{\nu}, \boldsymbol{h}\rangle - H(\boldsymbol{x}))$$

- $U^{\mathrm{mod}}[\Psi]\,(F) : \boldsymbol{x} \mapsto \left|(F * \overline{\Psi})(\boldsymbol{x})\right|$
- $U_r^{\max}[\Psi]\,(F) : \boldsymbol{x} \mapsto \max\limits_{\|\boldsymbol{h}\|_\infty \leq r} (F * \mathrm{Re}\overline{\Psi})(\boldsymbol{x}+\boldsymbol{h})$

From CMod to RMax in the continuous framework

- **I. Waldspurger intuition** linking the two operators:

$$(F * \mathrm{Re}\,\overline{\Psi})(\boldsymbol{x}+\boldsymbol{h}) \approx |(F * \overline{\Psi})(\boldsymbol{x})| \cos(\langle \boldsymbol{\nu}, \boldsymbol{h}\rangle - H(\boldsymbol{x}))$$

- $U^{\mathrm{mod}}[\Psi]\,(F) : \boldsymbol{x} \mapsto \left|(F * \overline{\Psi})(\boldsymbol{x})\right|$
- $U_r^{\mathrm{max}}[\Psi]\,(F) : \boldsymbol{x} \mapsto \max\limits_{\|\boldsymbol{h}\|_\infty \leq r} (F * \mathrm{Re}\overline{\Psi})(\boldsymbol{x}+\boldsymbol{h})$

Max

$$r \ll 2\pi/\varepsilon \implies U_r^{\mathrm{max}} F(\boldsymbol{x}) \approx U^{\mathrm{mod}} F(\boldsymbol{x}) \max_{\|\boldsymbol{h}\|_\infty \leq r} G(\boldsymbol{x}, \boldsymbol{h})$$

From CMod to RMax in the continuous framework

- **I. Waldspurger intuition** linking the two operators:

$$(F * \mathrm{Re}\,\overline{\Psi})(\boldsymbol{x}+\boldsymbol{h}) \approx |(F * \overline{\Psi})(\boldsymbol{x})| \cos(\langle \boldsymbol{\nu}, \boldsymbol{h}\rangle - H(\boldsymbol{x}))$$

- $U^{\mathrm{mod}}[\Psi]\,(F) : \boldsymbol{x} \mapsto \left|(F * \overline{\Psi})(\boldsymbol{x})\right|$
- $U_r^{\max}[\Psi]\,(F) : \boldsymbol{x} \mapsto \max\limits_{\|\boldsymbol{h}\|_\infty \leq r} (F * \mathrm{Re}\overline{\Psi})(\boldsymbol{x}+\boldsymbol{h})$

Max

$$r \ll 2\pi/\varepsilon \implies U_r^{\max} F(\boldsymbol{x}) \approx U^{\mathrm{mod}} F(\boldsymbol{x}) \max_{\|\boldsymbol{h}\|_\infty \leq r} G(\boldsymbol{x}, \boldsymbol{h})$$

- For $r \geq \dfrac{\pi}{\|\boldsymbol{\nu}\|_2}$ the cosine $\boldsymbol{h} \mapsto G(\boldsymbol{x}, \boldsymbol{h})$ reaches 1 on $B_\infty(r)$

From CMod to RMax in the continuous framework

- **I. Waldspurger intuition** linking the two operators:

$$(F * \mathrm{Re}\,\overline{\Psi})(\boldsymbol{x}+\boldsymbol{h}) \approx |(F * \overline{\Psi})(\boldsymbol{x})| \cos(\langle \boldsymbol{\nu}, \boldsymbol{h}\rangle - H(\boldsymbol{x}))$$

- $U^{\mathrm{mod}}[\Psi]\,(F) : \boldsymbol{x} \mapsto \left|(F * \overline{\Psi})(\boldsymbol{x})\right|$
- $U_r^{\max}[\Psi]\,(F) : \boldsymbol{x} \mapsto \max\limits_{\|\boldsymbol{h}\|_\infty \leq r} (F * \mathrm{Re}\overline{\Psi})(\boldsymbol{x}+\boldsymbol{h})$

Max

$$r \ll 2\pi/\varepsilon \implies U_r^{\max} F(\boldsymbol{x}) \approx U^{\mathrm{mod}} F(\boldsymbol{x}) \max_{\|\boldsymbol{h}\|_\infty \leq r} G(\boldsymbol{x}, \boldsymbol{h})$$

- For $r \geq \dfrac{\pi}{\|\boldsymbol{\nu}\|_2}$ the cosine $\boldsymbol{h} \mapsto G(\boldsymbol{x}, \boldsymbol{h})$ reaches 1 on $B_\infty(r)$

$$\frac{\pi}{\|\boldsymbol{\nu}\|_2} \leq r \ll \frac{2\pi}{\varepsilon} \implies U_r^{\max} F(\boldsymbol{x}) \approx U^{\mathrm{mod}} F(\boldsymbol{x})$$

From CMod to RMax in the continuous framework

- **I. Waldspurger intuition** linking the two operators:

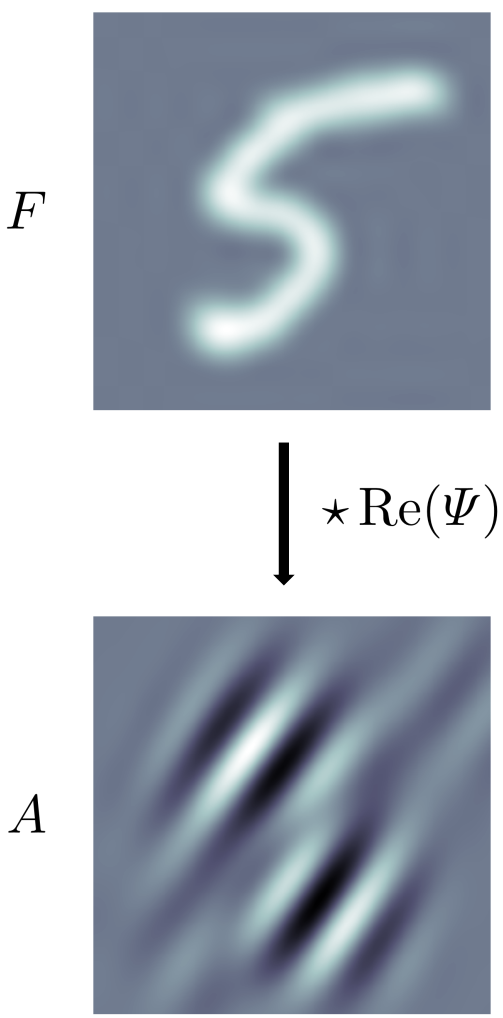

From CMod to RMax in the continuous framework

- **I. Waldspurger intuition** linking the two operators:

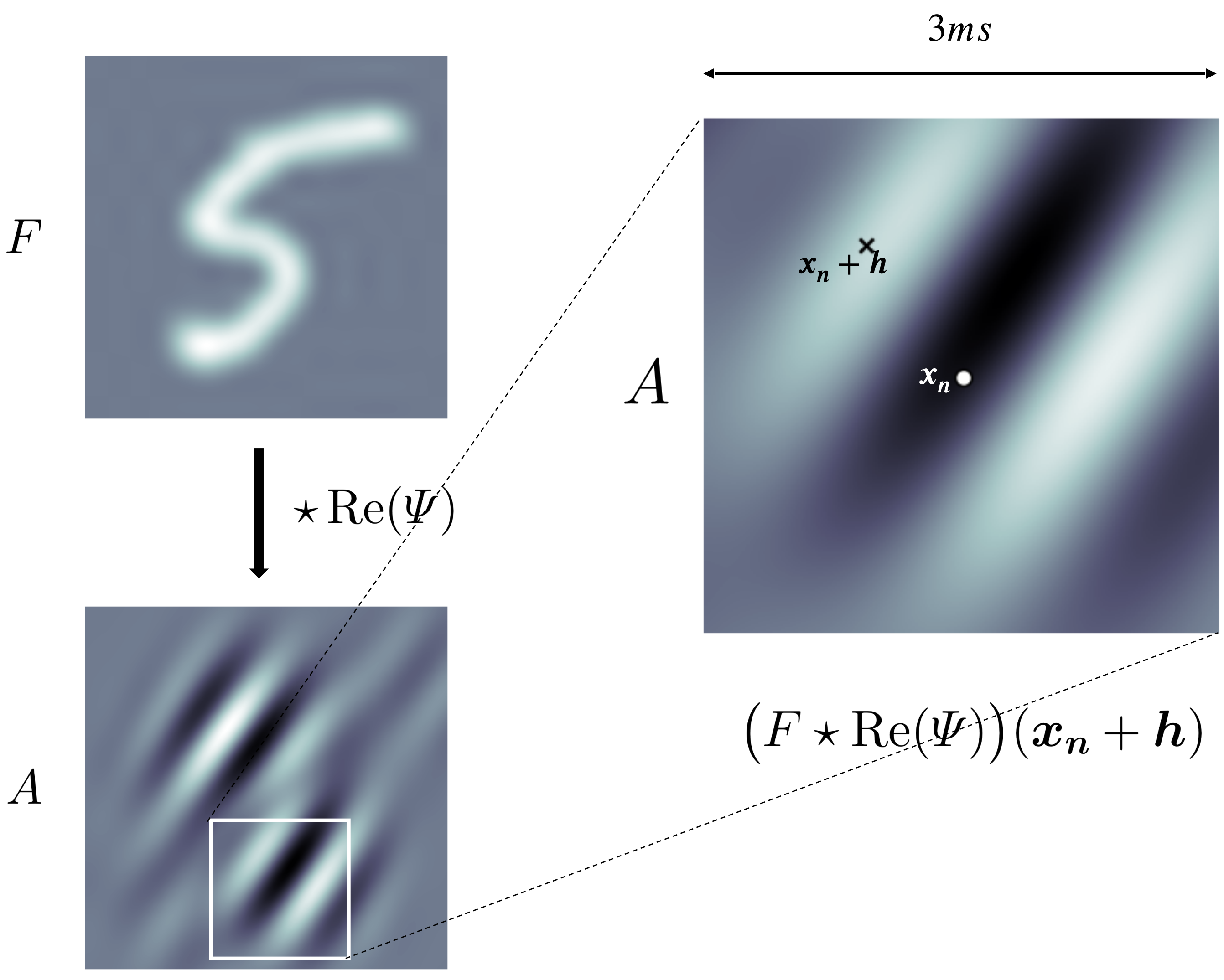

From CMod to RMax in the continuous framework

- **I. Waldspurger intuition** linking the two operators:

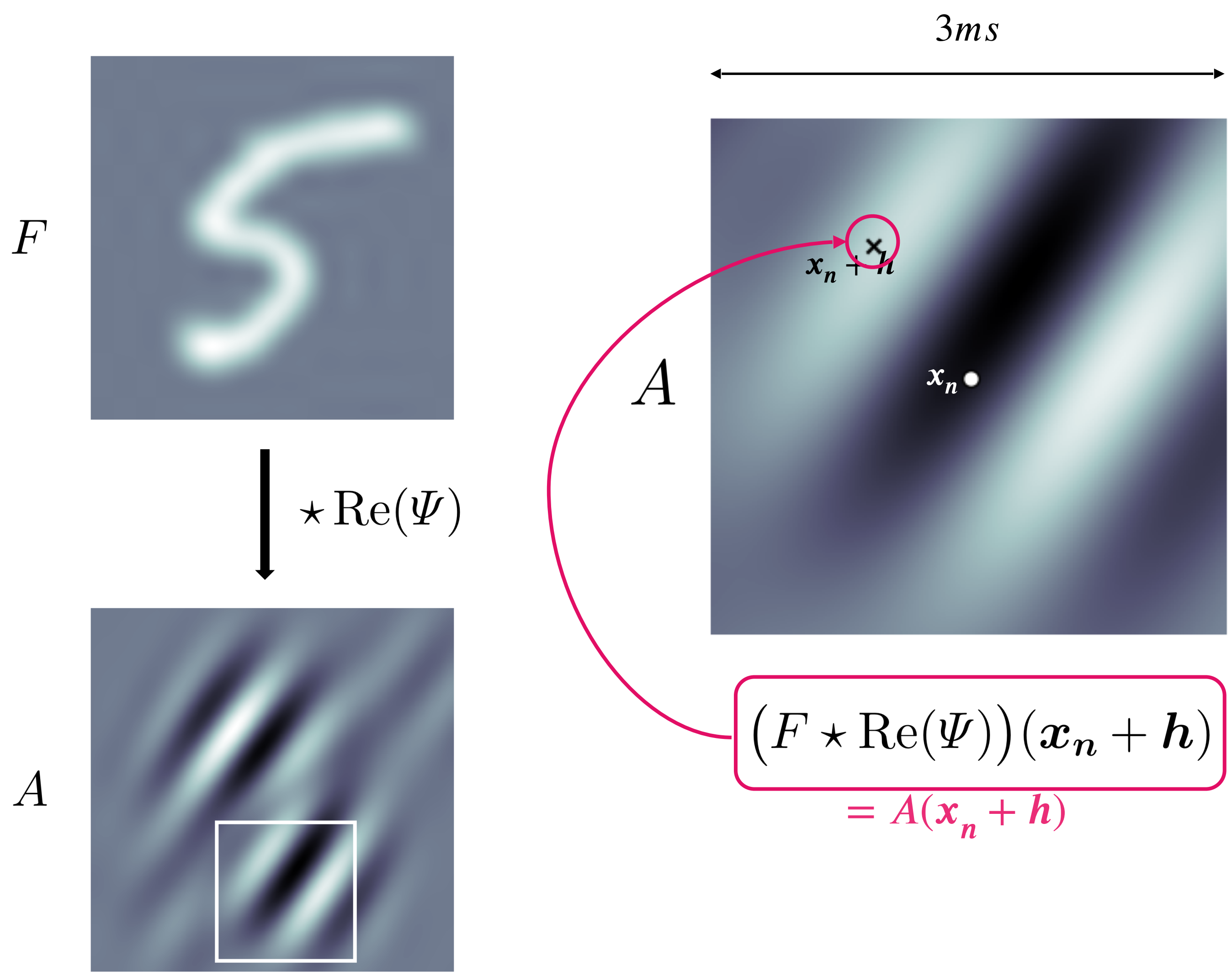

From CMod to RMax in the continuous framework

- **I. Waldspurger intuition** linking the two operators:

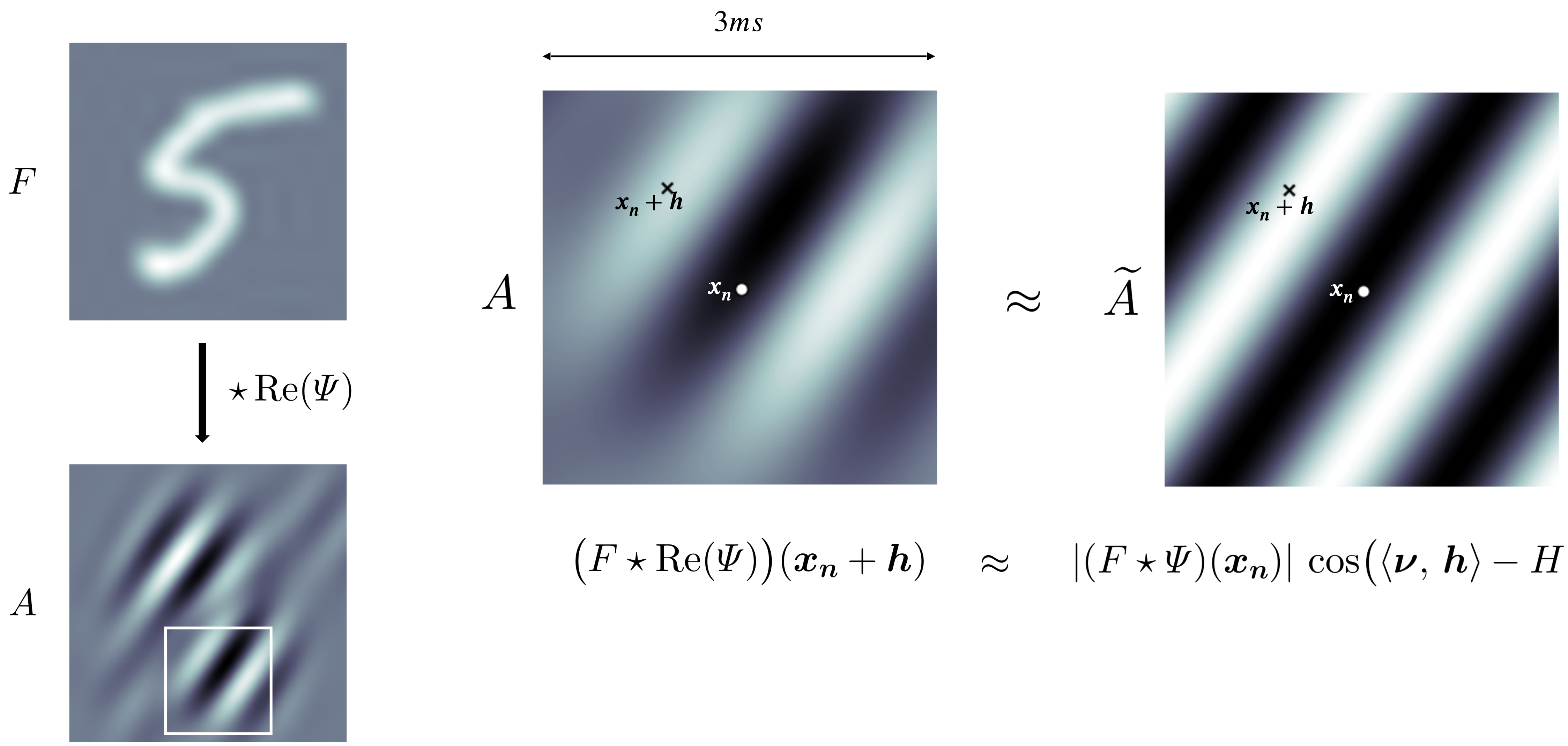

$$\big(F \star \mathrm{Re}(\Psi)\big)(\boldsymbol{x_n} + \boldsymbol{h}) \quad \approx \quad |(F \star \Psi)(\boldsymbol{x_n})| \, \cos\big(\langle \boldsymbol{\nu},\, \boldsymbol{h} \rangle - H(\boldsymbol{x_n})\big)$$

From CMod to RMax in the continuous framework

- **I. Waldspurger intuition** linking the two operators:

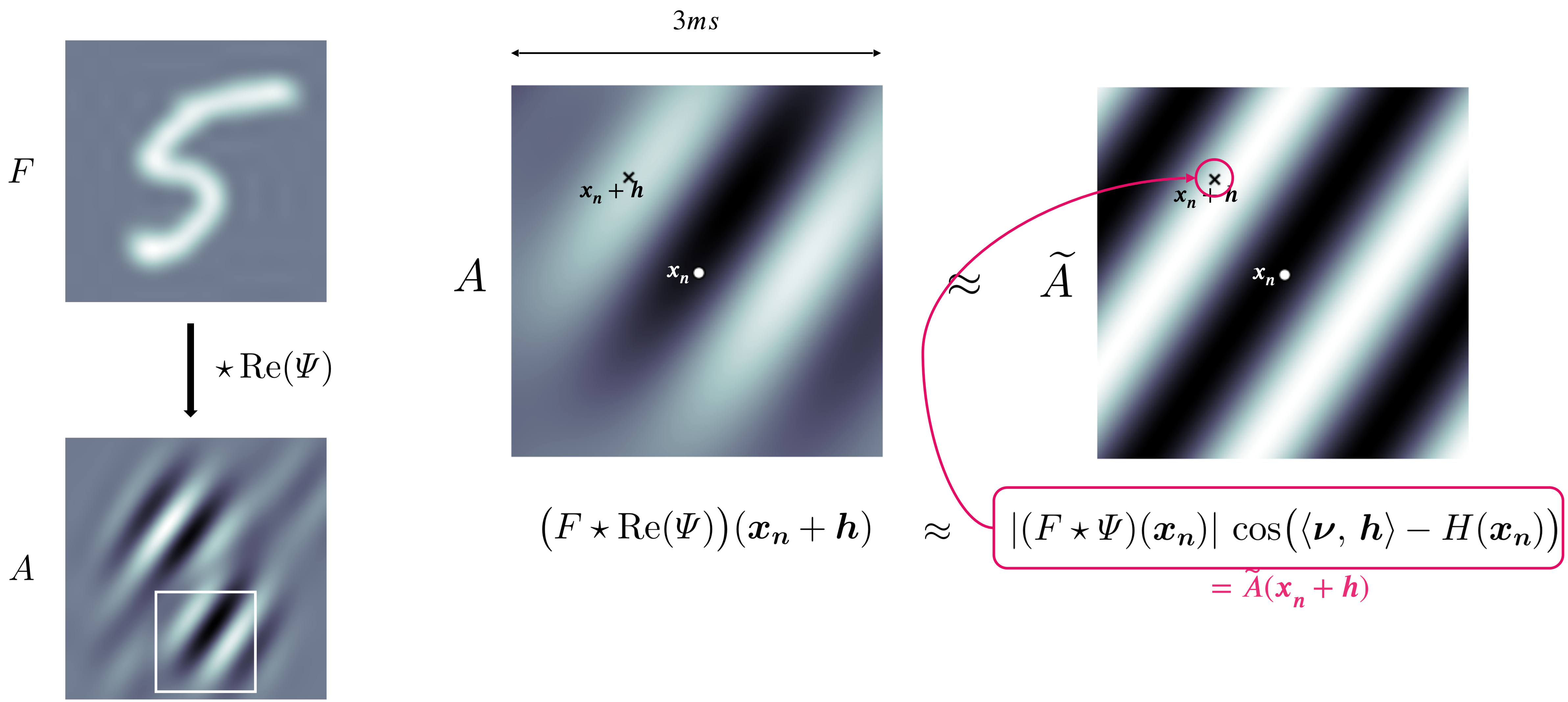

$$\big(F \star \mathrm{Re}(\Psi)\big)(\boldsymbol{x}_n + \boldsymbol{h}) \approx |(F \star \Psi)(\boldsymbol{x}_n)| \cos\big(\langle \boldsymbol{\nu}, \boldsymbol{h}\rangle - H(\boldsymbol{x}_n)\big)$$

$= \widetilde{A}(\boldsymbol{x}_n + \boldsymbol{h})$

From CMod to RMax in the continuous framework

- **I. Waldspurger intuition** linking the two operators:

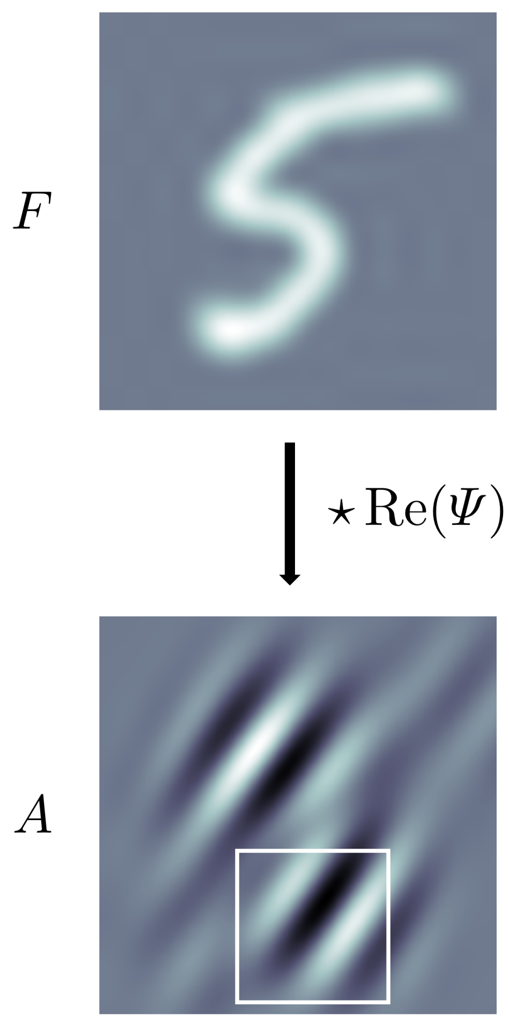

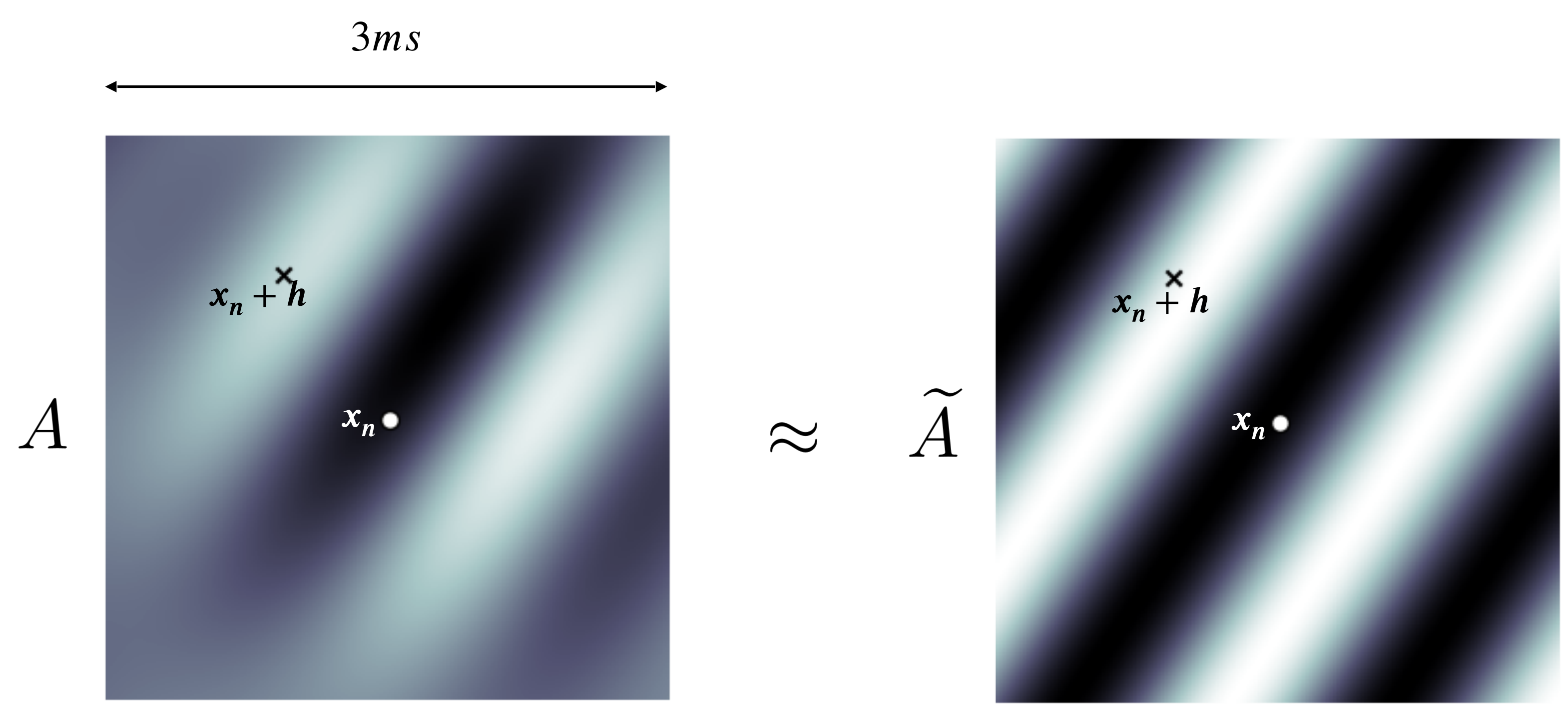

$$\big(F \star \mathrm{Re}(\Psi)\big)(\boldsymbol{x}_n + \boldsymbol{h}) \approx |(F \star \Psi)(\boldsymbol{x}_n)| \cos\big(\langle \boldsymbol{\nu}, \boldsymbol{h}\rangle - H(\boldsymbol{x}_n)\big)$$

$\mathrm{Y}^{\mathrm{mod}}[\boldsymbol{n}]$

From CMod to RMax in the continuous framework

- **I. Waldspurger intuition** linking the two operators:

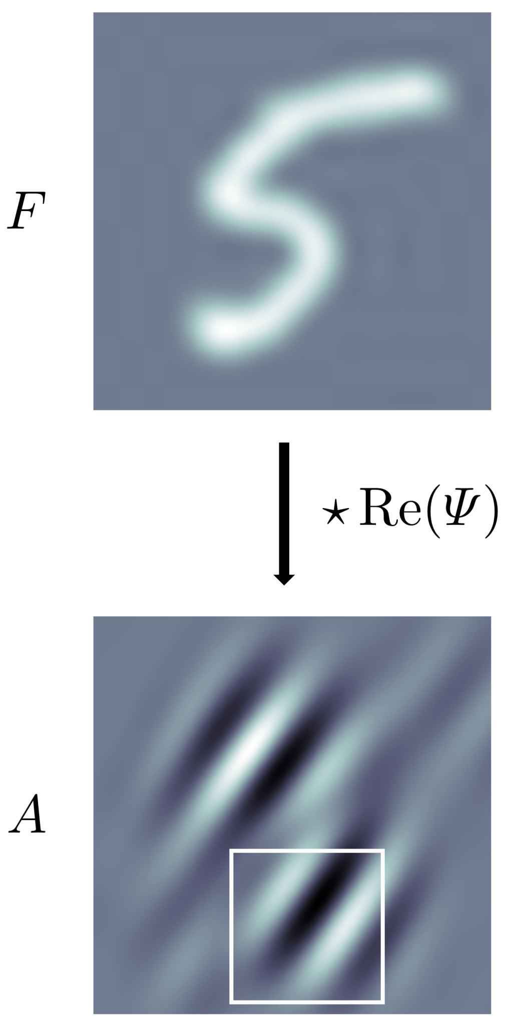

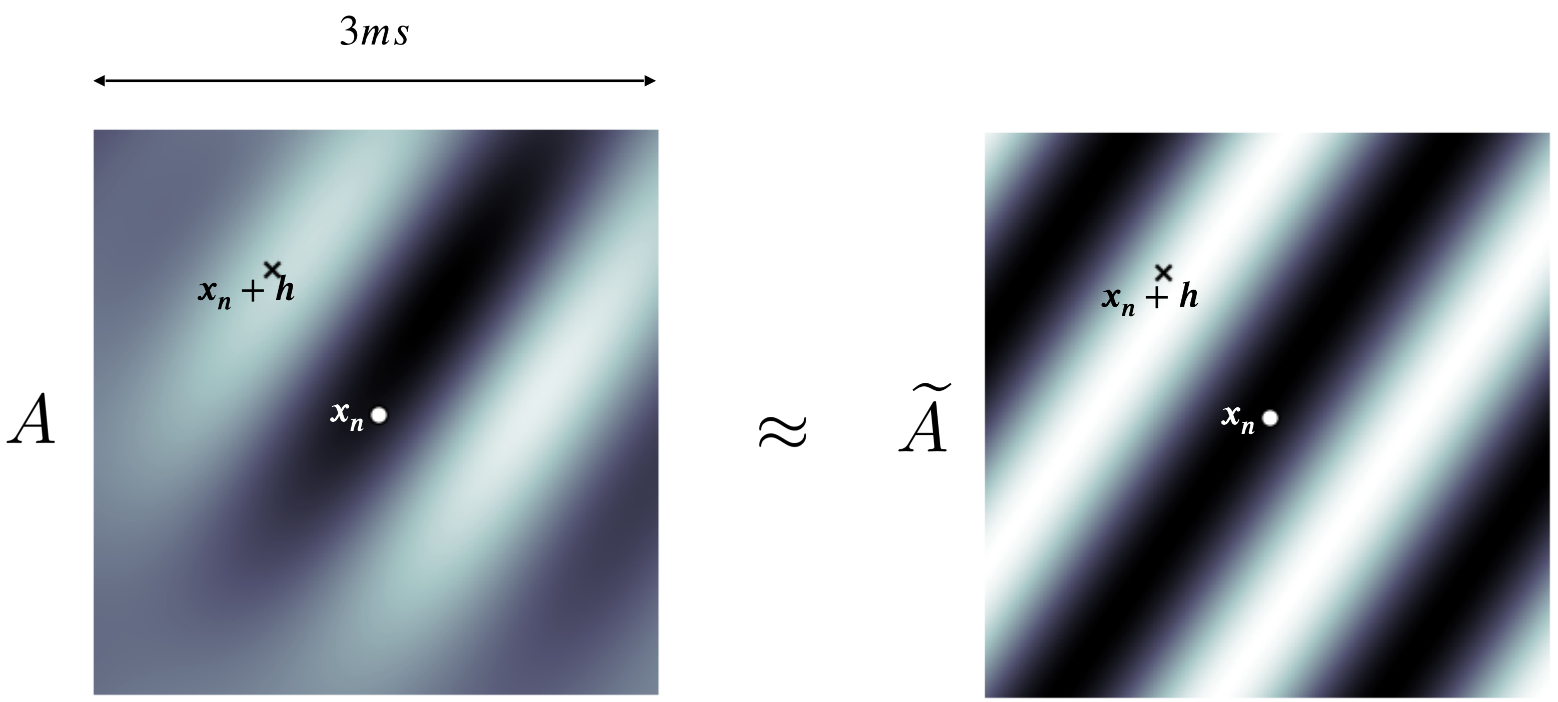

$$\underbrace{\big(F \star \mathrm{Re}(\Psi)\big)(\boldsymbol{x}_n + \boldsymbol{h})}_{\max\limits_{\|\boldsymbol{h}\|_\infty \leq \frac{3ms}{2}}} \approx \underbrace{\big|(F \star \Psi)(\boldsymbol{x}_n)\big|}_{\mathrm{Y}^{\mathrm{mod}}[\boldsymbol{n}]} \underbrace{\cos\big(\langle \boldsymbol{\nu},\, \boldsymbol{h}\rangle - H(\boldsymbol{x}_n)\big)}_{\max\limits_{\|\boldsymbol{h}\|_\infty \leq \frac{3ms}{2}}}$$

From CMod to RMax in the continuous framework

- **I. Waldspurger intuition** linking the two operators:

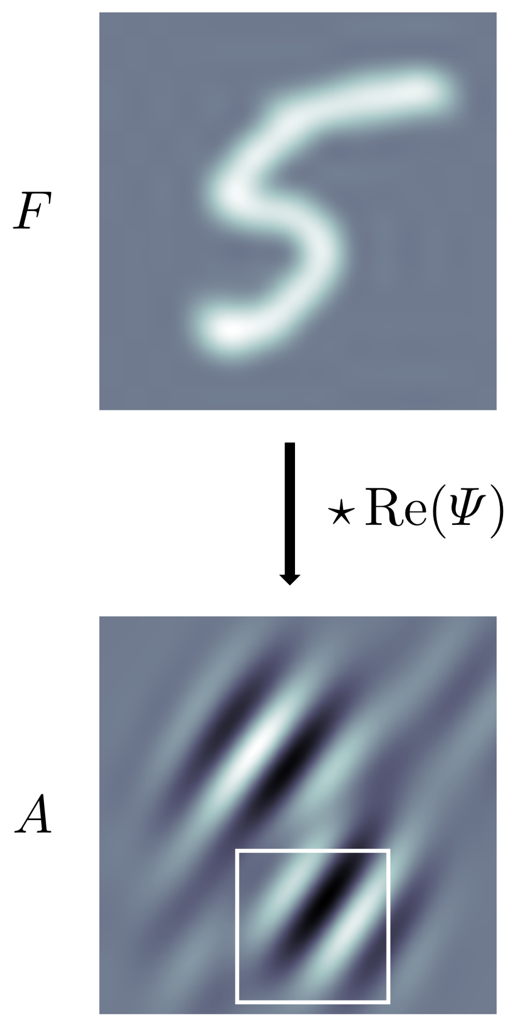

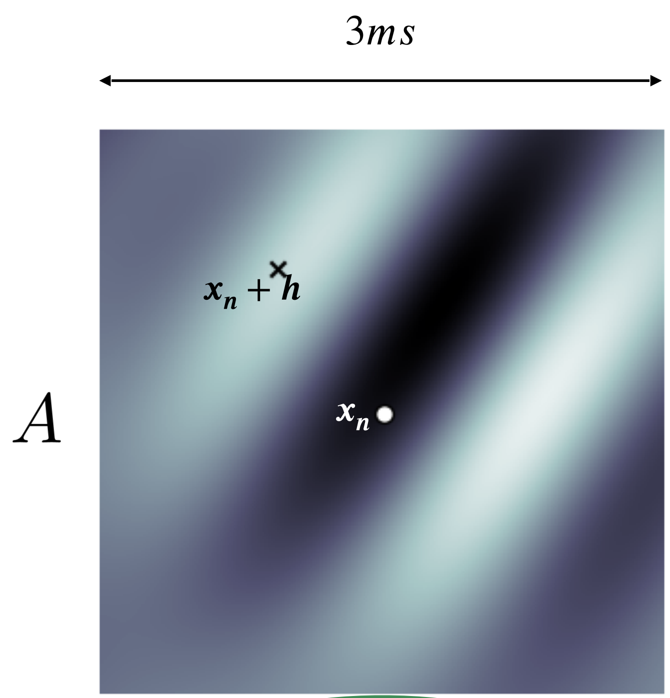

$\approx$

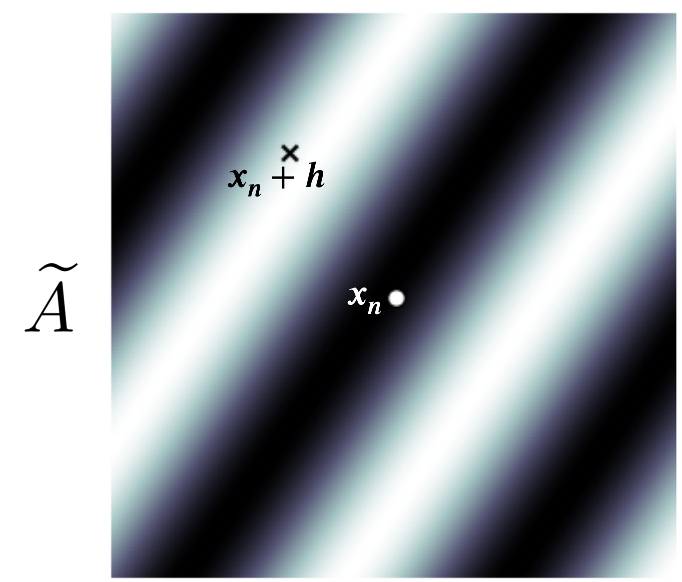

$$\underbrace{\max_{\|\boldsymbol{h}\|_\infty \leq \frac{3ms}{2}}}\big(F \star \mathrm{Re}(\Psi)\big)(\boldsymbol{x_n} + \boldsymbol{h}) \approx \big|(F \star \Psi)(\boldsymbol{x_n})\big| \underbrace{\max_{\|\boldsymbol{h}\|_\infty \leq \frac{3ms}{2}}} \cos\big(\langle \boldsymbol{\nu},\, \boldsymbol{h}\rangle - H(\boldsymbol{x_n})\big)$$

$\mathrm{Y}_0^{\max}[\boldsymbol{n}]$ $\qquad$ $\mathrm{Y}^{\mathrm{mod}}[\boldsymbol{n}]$

From CMod to RMax in the continuous framework

- **I. Waldspurger intuition** linking the two operators:

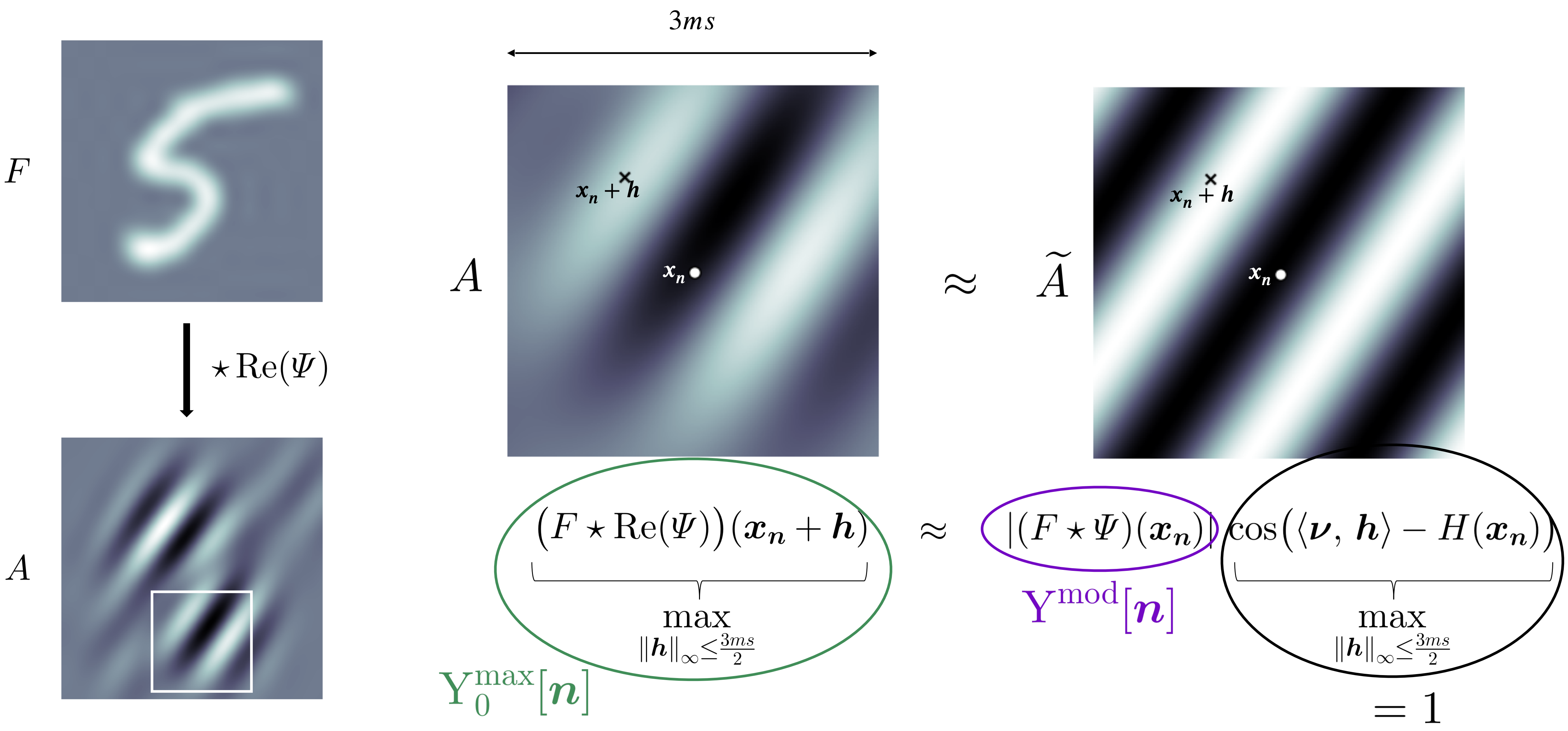

Adaptation to the discrete case

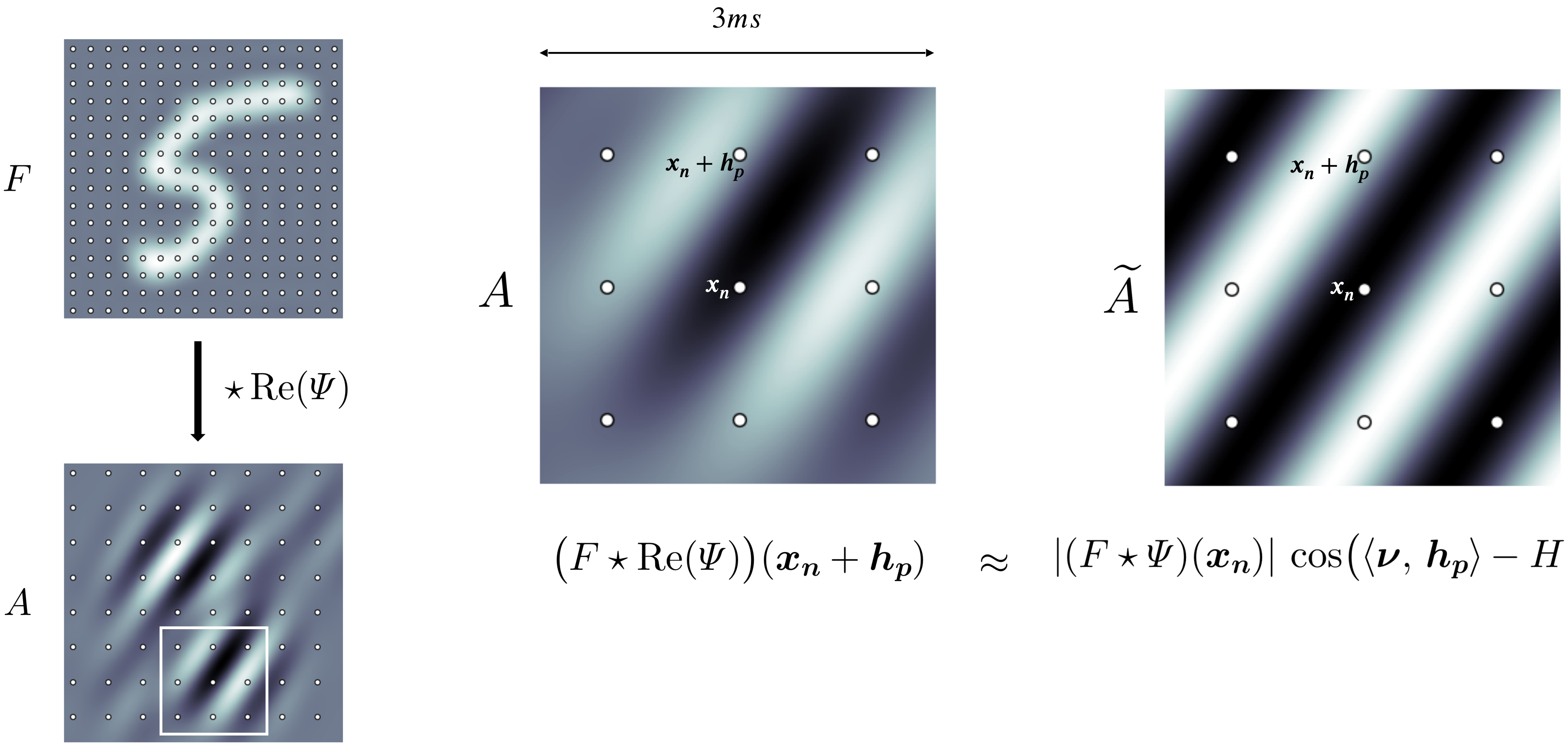

$$\big(F \star \mathrm{Re}(\Psi)\big)(\boldsymbol{x}_n + \boldsymbol{h}_p) \quad \approx \quad |(F \star \Psi)(\boldsymbol{x}_n)| \, \cos\big(\langle \boldsymbol{\nu},\, \boldsymbol{h}_p \rangle - H(\boldsymbol{x}_n)\big)$$

Adaptation to the discrete case

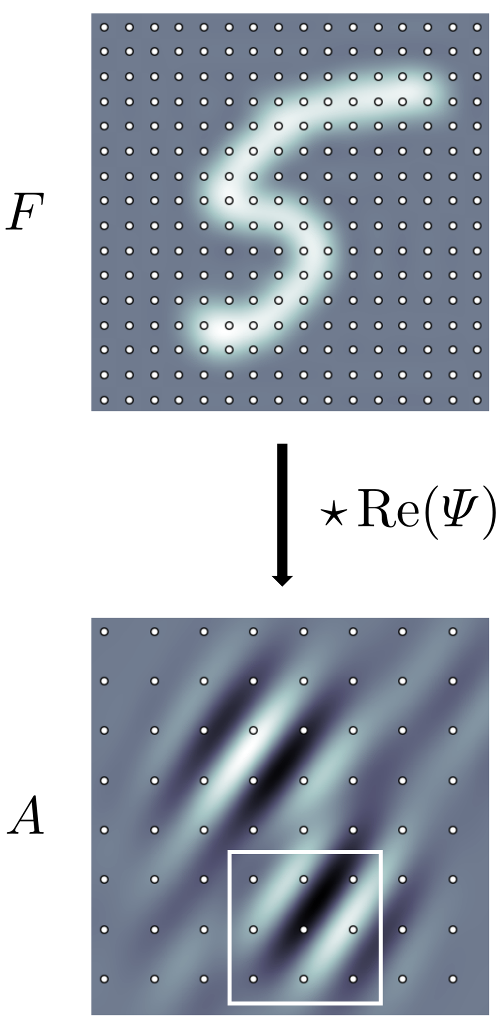

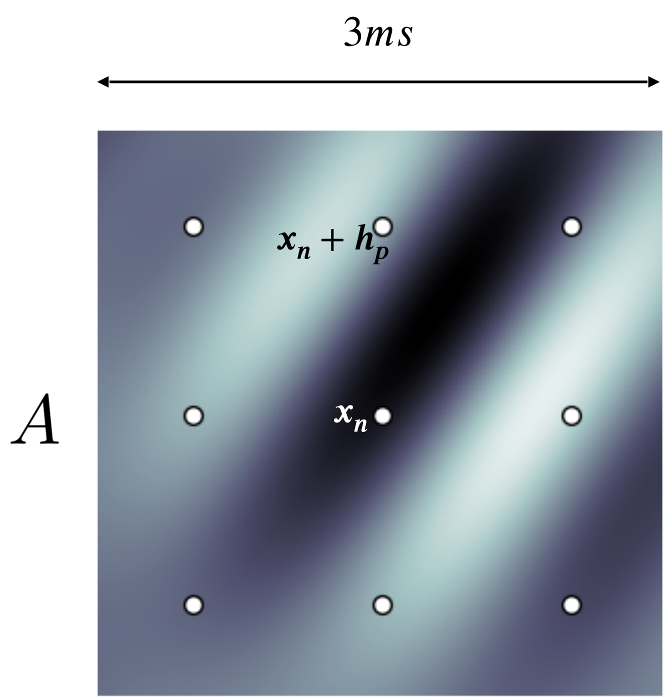

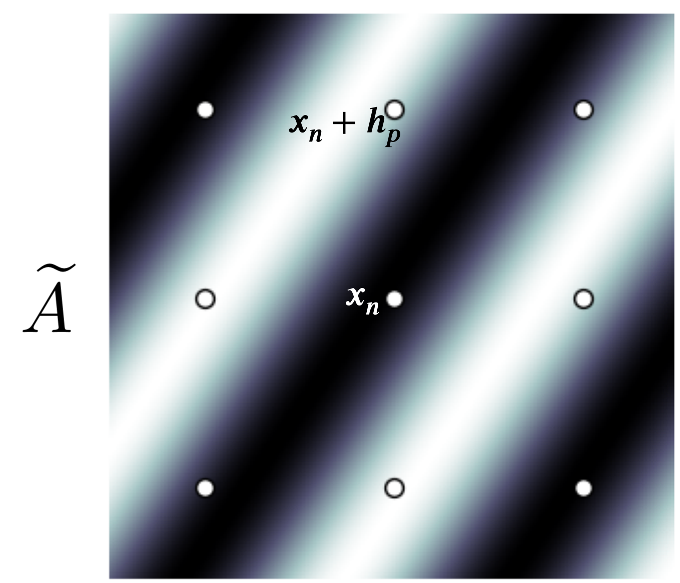

$$\big(F \star \mathrm{Re}(\Psi)\big)(\boldsymbol{x_n} + \boldsymbol{h_p}) \approx |(F \star \Psi)(\boldsymbol{x_n})| \cos\big(\langle \boldsymbol{\nu}, \boldsymbol{h_p} \rangle - H(\boldsymbol{x_n})\big)$$

$\mathrm{Y}^{\mathrm{mod}}[\boldsymbol{n}]$

Adaptation to the discrete case

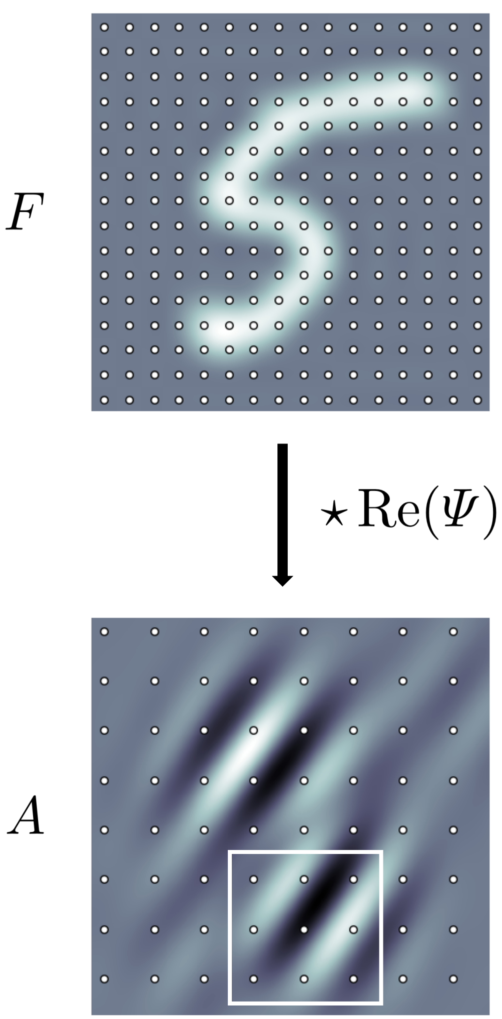

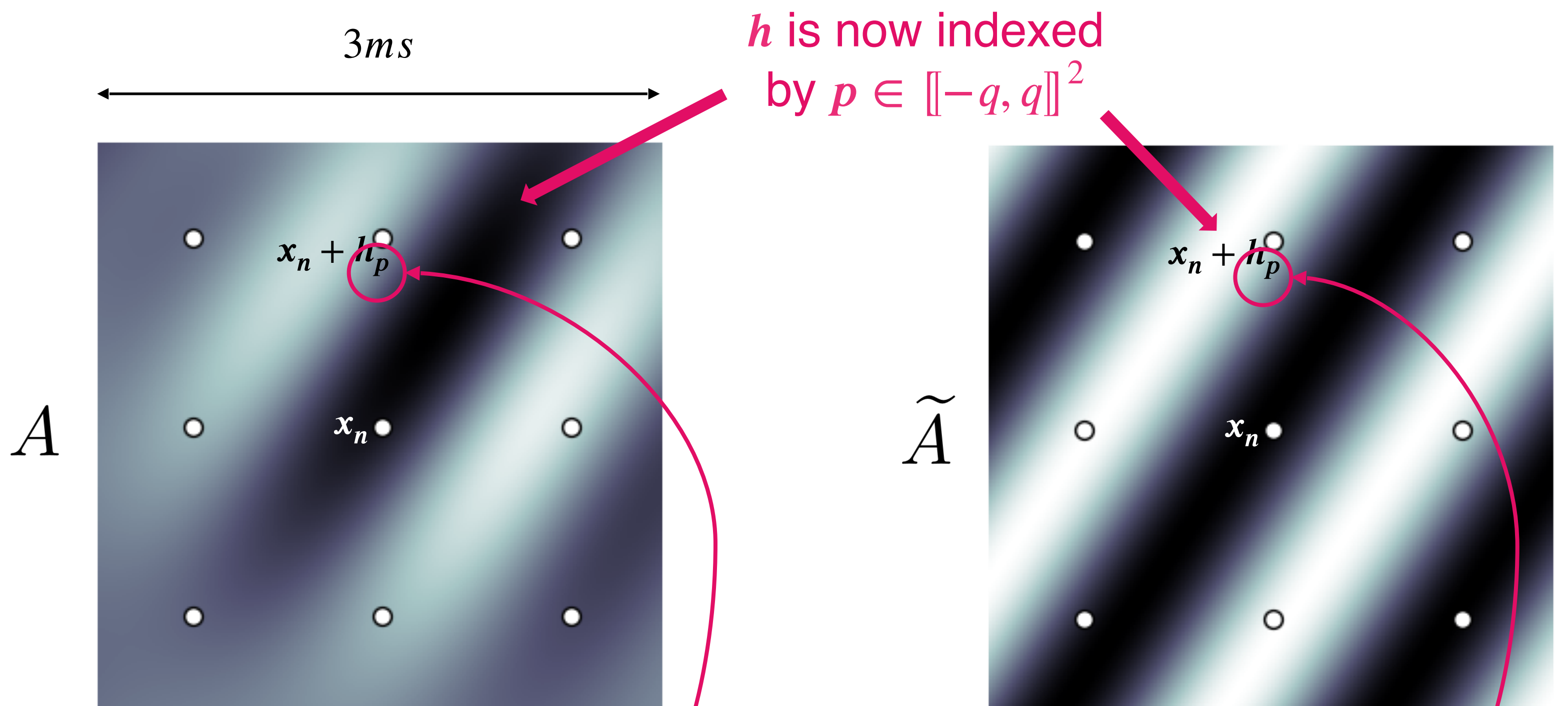

$$\big(F \star \mathrm{Re}(\Psi)\big)(\boldsymbol{x_n} + \boldsymbol{h_p}) \approx \underbrace{|(F\star\Psi)(\boldsymbol{x_n})|}_{\mathrm{Y}^{\mathrm{mod}}[\boldsymbol{n}]} \cos\big(\langle \boldsymbol{\nu}, \boldsymbol{h_p}\rangle - H(\boldsymbol{x_n})\big)$$

Adaptation to the discrete case

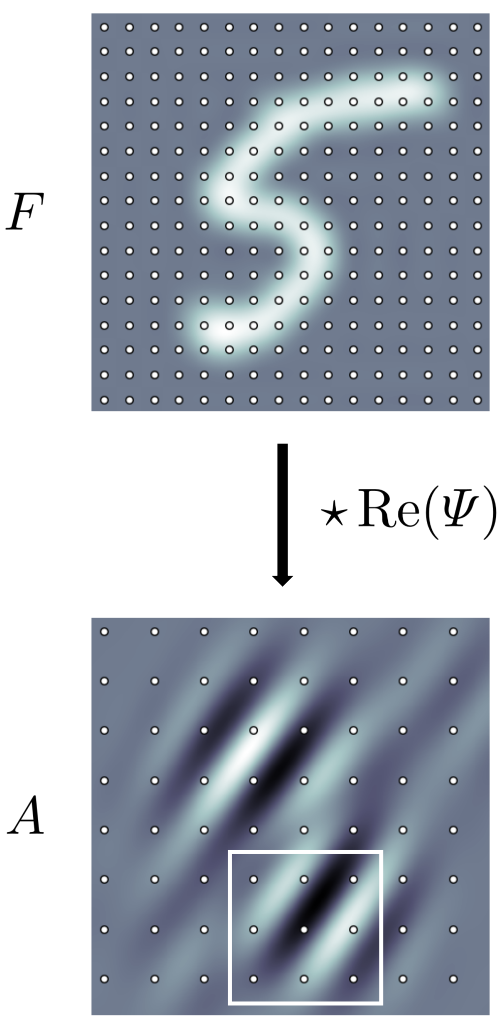

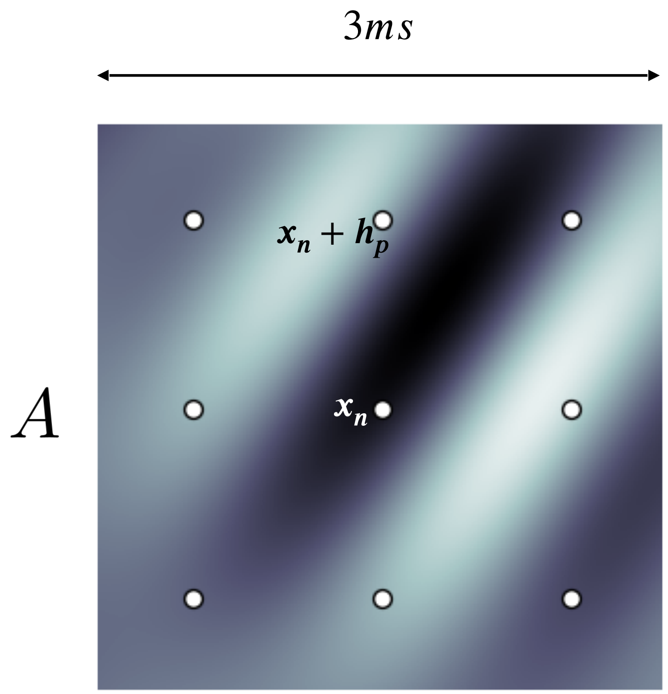

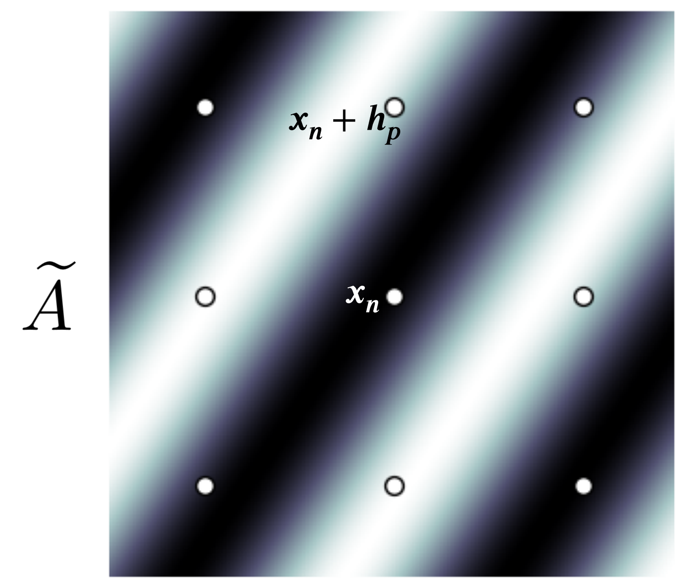

$$\underbrace{\big(F \star \mathrm{Re}(\Psi)\big)(\boldsymbol{x_n} + \boldsymbol{h_p})}_{\max\limits_{\|\boldsymbol{p}\| \leq q}} \approx \underbrace{\big|(F \star \Psi)(\boldsymbol{x_n})\big|}_{\Upsilon^{\mathrm{mod}}[\boldsymbol{n}]} \underbrace{\cos\big(\langle \boldsymbol{\nu},\, \boldsymbol{h_p} \rangle - H(\boldsymbol{x_n})\big)}_{\max\limits_{\|\boldsymbol{p}\| \leq q}}$$

Adaptation to the discrete case

F

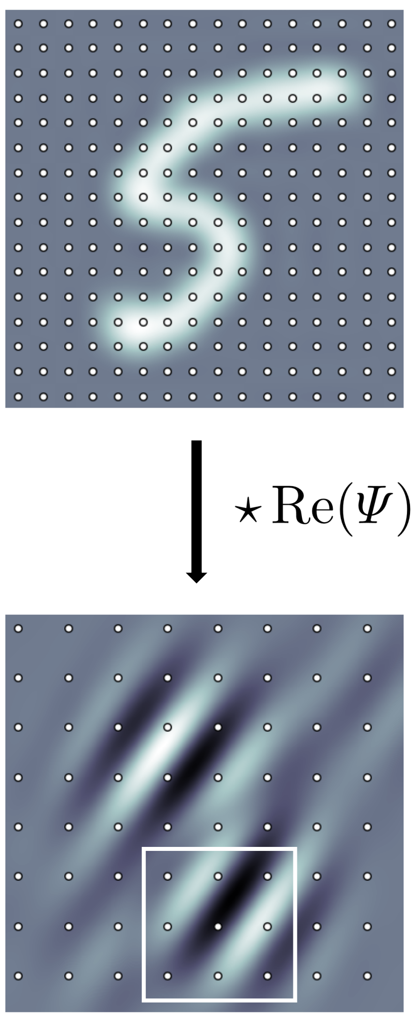

A

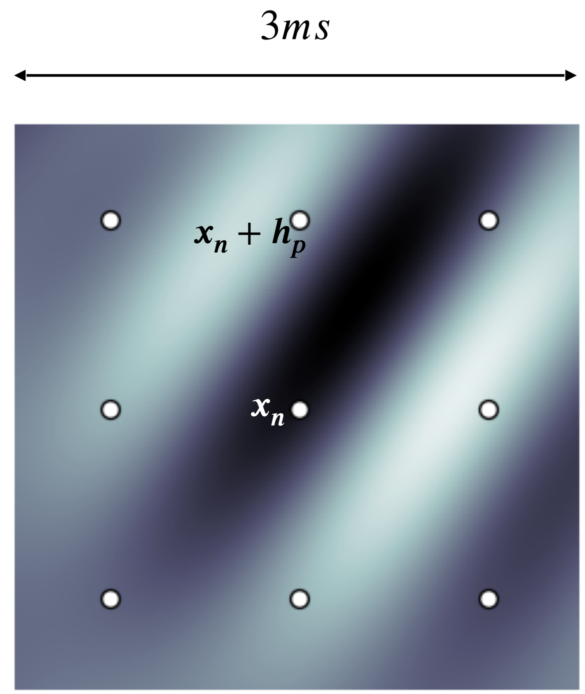

A

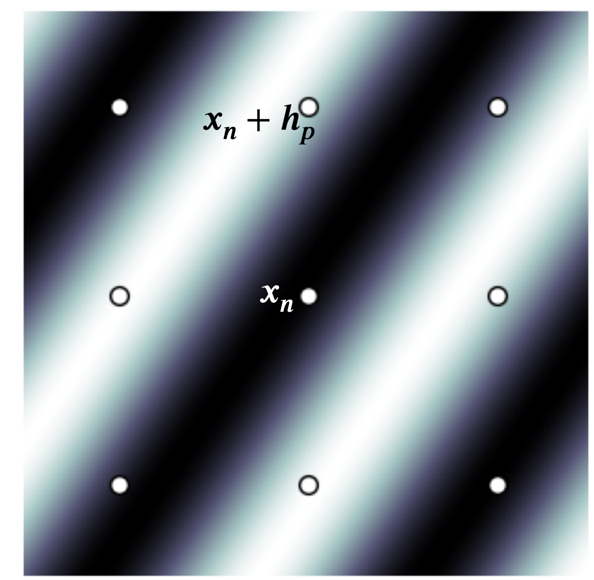

$\widetilde{A}$

$$\underbrace{\big(F \star \mathrm{Re}(\Psi)\big)(\boldsymbol{x}_n + \boldsymbol{h}_p)}_{\max\limits_{\|\boldsymbol{p}\| \leq q}} \approx \underbrace{\big|(F \star \Psi)(\boldsymbol{x}_n)\big|}_{\mathrm{Y}^{\mathrm{mod}}[\boldsymbol{n}]} \underbrace{\cos\big(\langle \boldsymbol{\nu},\, \boldsymbol{h}_p \rangle - H(\boldsymbol{x}_n)\big)}_{\max\limits_{\|\boldsymbol{p}\| \leq q}}$$

Maximum value
over a discrete grid
($q = 1$ in general)

Adaptation to the discrete case

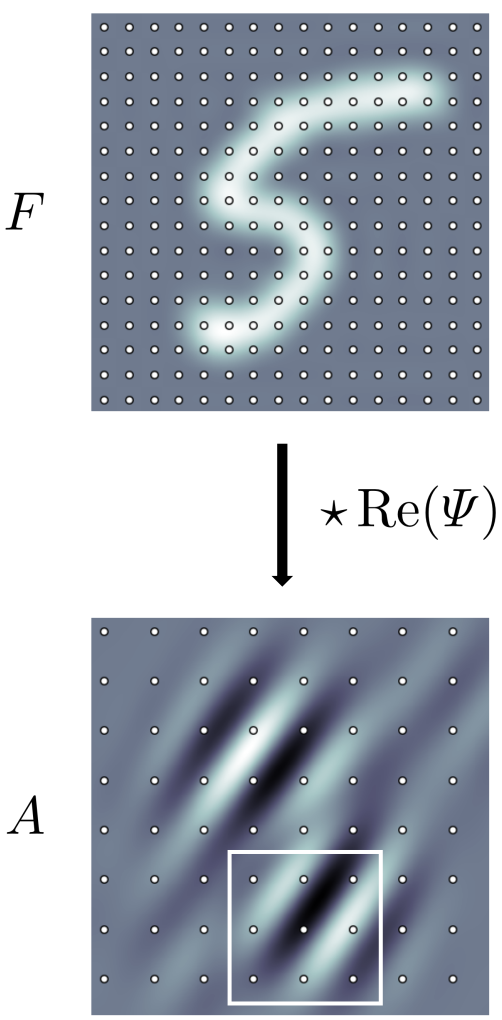

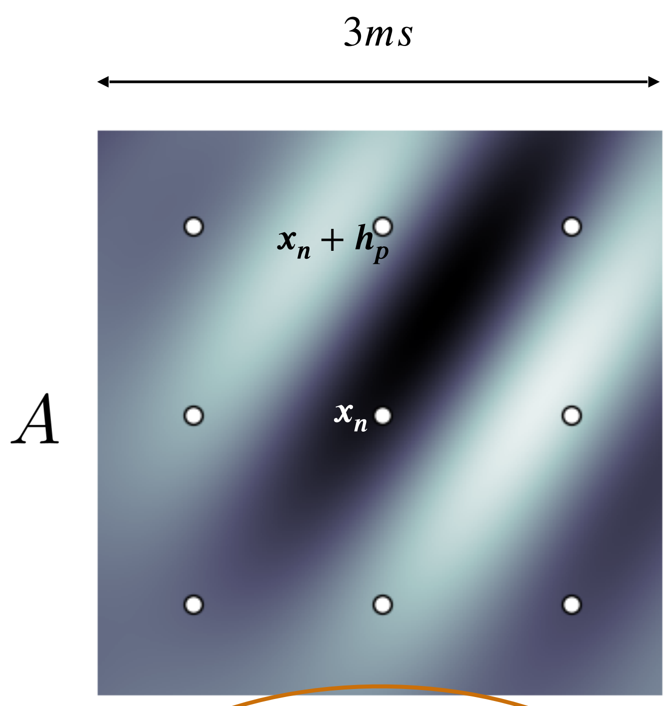

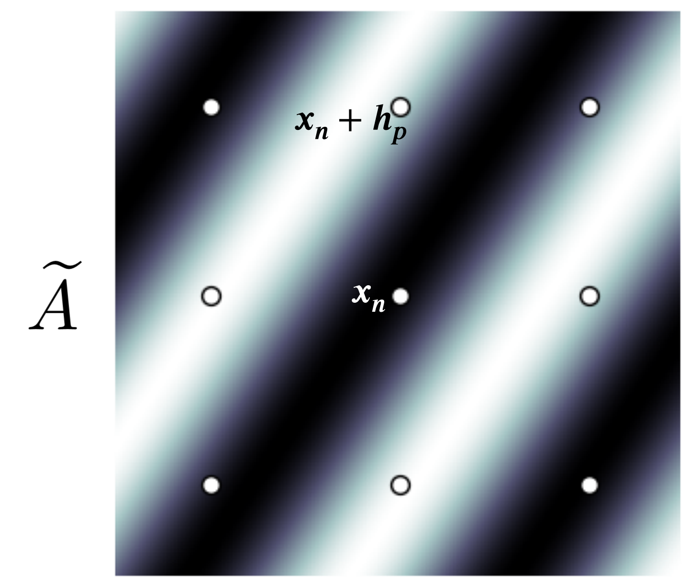

$$\underbrace{\big(F \star \mathrm{Re}(\Psi)\big)(\boldsymbol{x_n} + \boldsymbol{h_p})}_{\max_{\|\boldsymbol{p}\| \leq q}} \approx \big|(F \star \Psi)(\boldsymbol{x_n})\big| \underbrace{\cos\big(\langle \boldsymbol{\nu}, \boldsymbol{h_p} \rangle - H(\boldsymbol{x_n})\big)}_{\max_{\|\boldsymbol{p}\| \leq q}}$$

$\mathrm{Y}^{\max}[\boldsymbol{n}]$ $\qquad$ $\mathrm{Y}^{\mathrm{mod}}[\boldsymbol{n}]$

Maximum value over a discrete grid ($q = 1$ in general)

Adaptation to the discrete case

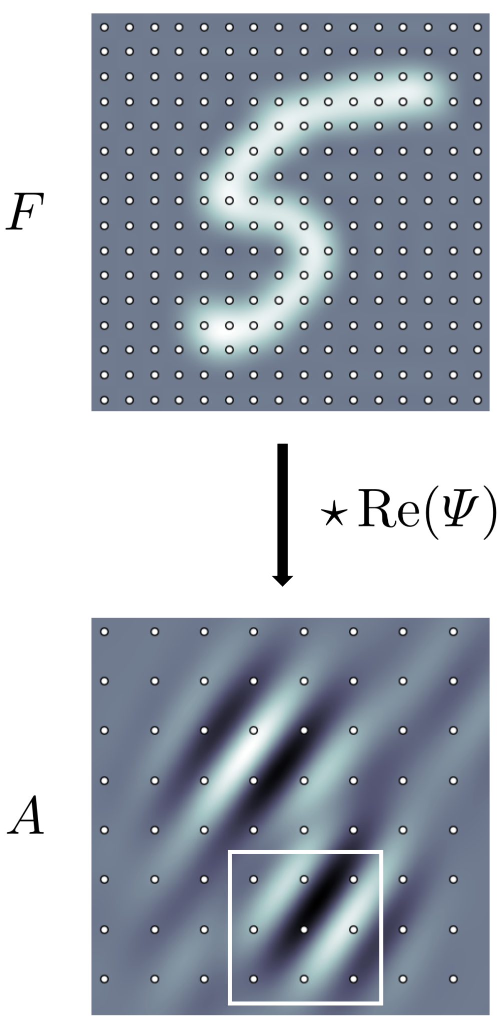

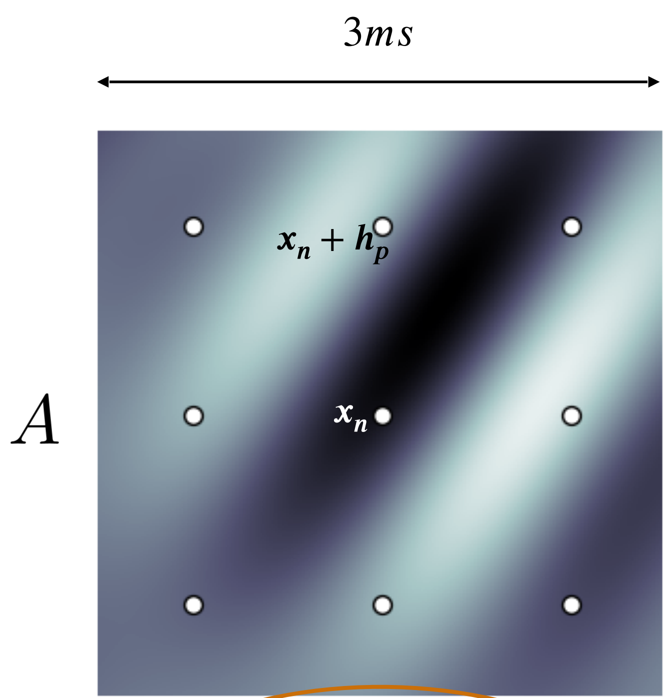

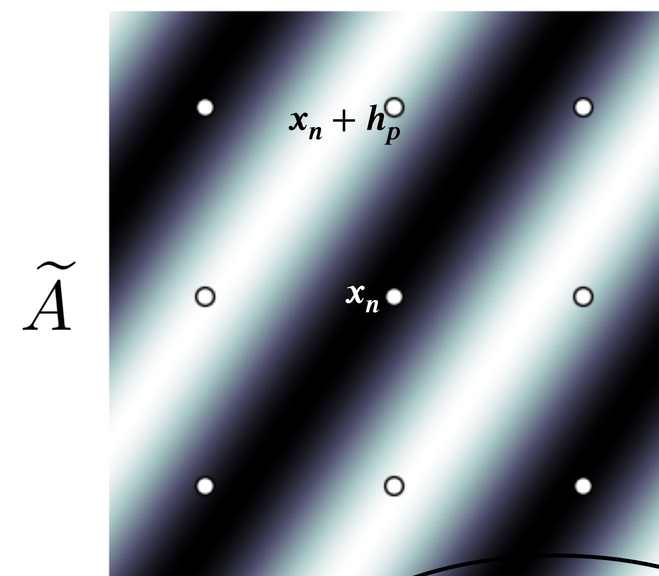

$$\underbrace{\big(F \star \mathrm{Re}(\Psi)\big)(\boldsymbol{x_n} + \boldsymbol{h_p})}_{\max_{\|\boldsymbol{p}\| \leq q}} \approx |(F \star \Psi)(\boldsymbol{x_n})| \underbrace{\cos\big(\langle \boldsymbol{\nu}, \boldsymbol{h_p} \rangle - H(\boldsymbol{x_n})\big)}_{\max_{\|\boldsymbol{p}\| \leq q}}$$

$\mathrm{Y}^{\max}[\boldsymbol{n}]$

$\mathrm{Y}^{\mathrm{mod}}[\boldsymbol{n}]$

$G^{\max}(\boldsymbol{x_n}) \leq 1$

Maximum value over a discrete grid ($q = 1$ in general)

Adaptation to the discrete case

$$q \ll 2\pi/(m\kappa) \quad \Longrightarrow \quad U^{\max}_{m,\,q}\mathrm{X}[\boldsymbol{n}] \approx U^{\mathrm{mod}}_{2m}\mathrm{X}[\boldsymbol{n}] \max_{\|\boldsymbol{p}\|_\infty \leq q} G_{\mathrm{X}}\big(\boldsymbol{x}_{\boldsymbol{n}},\, \boldsymbol{h}_{\boldsymbol{p}}\big),$$

Adaptation to the discrete case

$$q \ll 2\pi/(m\kappa) \quad \Longrightarrow \quad U^{\max}_{m,\,q}\mathrm{X}[\boldsymbol{n}] \approx U^{\mathrm{mod}}_{2m}\mathrm{X}[\boldsymbol{n}] \max_{\|\boldsymbol{p}\|_\infty \leq q} G_{\mathrm{X}}\big(\boldsymbol{x_n},\, \boldsymbol{h_p}\big),$$

Not necessarily reaches 1

Adaptation to the discrete case

$$q \ll 2\pi/(m\kappa) \quad \Longrightarrow \quad U^{\max}_{m,\,q}\mathrm{X}[\boldsymbol{n}] \approx U^{\mathrm{mod}}_{2m}\mathrm{X}[\boldsymbol{n}] \max_{\|\boldsymbol{p}\|_\infty \leq q} G_{\mathrm{X}}\big(\boldsymbol{x_n},\, \boldsymbol{h_p}\big),$$

Not necessarily reaches 1

$$q \ll 2\pi/(m\kappa) \implies \big\|U^{\mathrm{mod}}_{2m}\mathrm{X} - U^{\max}_{m,\,q}\mathrm{X}\big\|_2 \approx \|\delta_{m,\,q}\mathrm{X}\|_2$$

Adaptation to the discrete case

$$q \ll 2\pi/(m\kappa) \quad \Longrightarrow \quad U^{\max}_{m,\,q}\mathrm{X}[\boldsymbol{n}] \approx U^{\mathrm{mod}}_{2m}\mathrm{X}[\boldsymbol{n}] \max_{\|\boldsymbol{p}\|_\infty \leq q} G_{\mathrm{X}}\big(\boldsymbol{x_n},\, \boldsymbol{h_p}\big),$$

Not necessarily reaches 1

$$q \ll 2\pi/(m\kappa) \Longrightarrow \left\|U^{\mathrm{mod}}_{2m}\mathrm{X} - U^{\max}_{m,\,q}\mathrm{X}\right\|_2 \approx \|\delta_{m,\,q}\mathrm{X}\|_2$$

$$\delta_{m,\,q}\mathrm{X}[\boldsymbol{n}] := U^{\mathrm{mod}}_{2m}\mathrm{X}[\boldsymbol{n}] \left(1 - \max_{\|\boldsymbol{p}\|_\infty \leq q} G_{\mathrm{X}}\big(\boldsymbol{x_n},\, \boldsymbol{h_p}\big)\right)$$

Adaptation to the discrete case

$$q \ll 2\pi/(m\kappa) \quad \Longrightarrow \quad U^{\max}_{m,\,q}\mathrm{X}[\boldsymbol{n}] \approx U^{\mathrm{mod}}_{2m}\mathrm{X}[\boldsymbol{n}] \max_{\|\boldsymbol{p}\|_\infty \le q} G_{\mathrm{X}}\big(\boldsymbol{x}_{\boldsymbol{n}},\, \boldsymbol{h}_{\boldsymbol{p}}\big),$$

Not necessarily reaches 1

$$q \ll 2\pi/(m\kappa) \Longrightarrow \left\|U^{\mathrm{mod}}_{2m}\mathrm{X} - U^{\max}_{m,\,q}\mathrm{X}\right\|_2 \approx \left\|\delta_{m,\,q}\mathrm{X}\right\|_2$$

$$\delta_{m,\,q}\mathrm{X}[\boldsymbol{n}] := U^{\mathrm{mod}}_{2m}\mathrm{X}[\boldsymbol{n}]\left(1 - \max_{\|\boldsymbol{p}\|_\infty \le q} G_{\mathrm{X}}\big(\boldsymbol{x}_{\boldsymbol{n}},\, \boldsymbol{h}_{\boldsymbol{p}}\big)\right)$$

Theorem (Bound on the difference of $\mathbb{C}$**Mod** and $\mathbb{R}$**Max**)

If $\kappa \le \pi/m$ and under another reasonable hypothesis

$$\left\|U^{\mathrm{mod}}_{2m}\mathrm{X} - U^{\max}_{m,\,q}\mathrm{X}\right\|_2 \le \left\|\delta_{m,\,q}\mathrm{X}\right\|_2 + \beta_q(m\kappa)\left\|U^{\mathrm{mod}}_{2m}\mathrm{X}\right\|_2$$

Adaptation to the discrete case

$$q \ll 2\pi/(m\kappa) \quad \Longrightarrow \quad U^{\max}_{m,\,q}\mathrm{X}[\boldsymbol{n}] \approx U^{\mathrm{mod}}_{2m}\mathrm{X}[\boldsymbol{n}] \max_{\|\boldsymbol{p}\|_\infty \leq q} G_{\mathrm{X}}\left(\boldsymbol{x}_{\boldsymbol{n}},\, \boldsymbol{h}_{\boldsymbol{p}}\right),$$

Not necessarily reaches 1

$$q \ll 2\pi/(m\kappa) \Longrightarrow \left\|U^{\mathrm{mod}}_{2m}\mathrm{X} - U^{\max}_{m,\,q}\mathrm{X}\right\|_2 \approx \|\delta_{m,\,q}\mathrm{X}\|_2$$

$$\delta_{m,\,q}\mathrm{X}[\boldsymbol{n}] := U^{\mathrm{mod}}_{2m}\mathrm{X}[\boldsymbol{n}] \left(1 - \max_{\|\boldsymbol{p}\|_\infty \leq q} G_{\mathrm{X}}\left(\boldsymbol{x}_{\boldsymbol{n}},\, \boldsymbol{h}_{\boldsymbol{p}}\right)\right) \qquad \beta_q : \kappa' \mapsto q\kappa'.$$

Theorem (Bound on the difference of $\mathbb{C}$**Mod** and $\mathbb{R}$**Max**)

If $\kappa \leq \pi/m$ and under another reasonable hypothesis

$$\left\|U^{\mathrm{mod}}_{2m}\mathrm{X} - U^{\max}_{m,\,q}\mathrm{X}\right\|_2 \leq \left\|\delta_{m,\,q}\mathrm{X}\right\|_2 + \beta_q(m\kappa)\left\|U^{\mathrm{mod}}_{2m}\mathrm{X}\right\|_2$$

Pathological frequencies

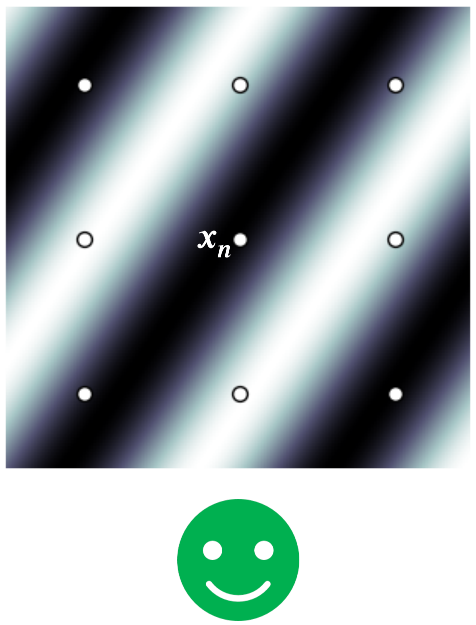

Pathological frequencies

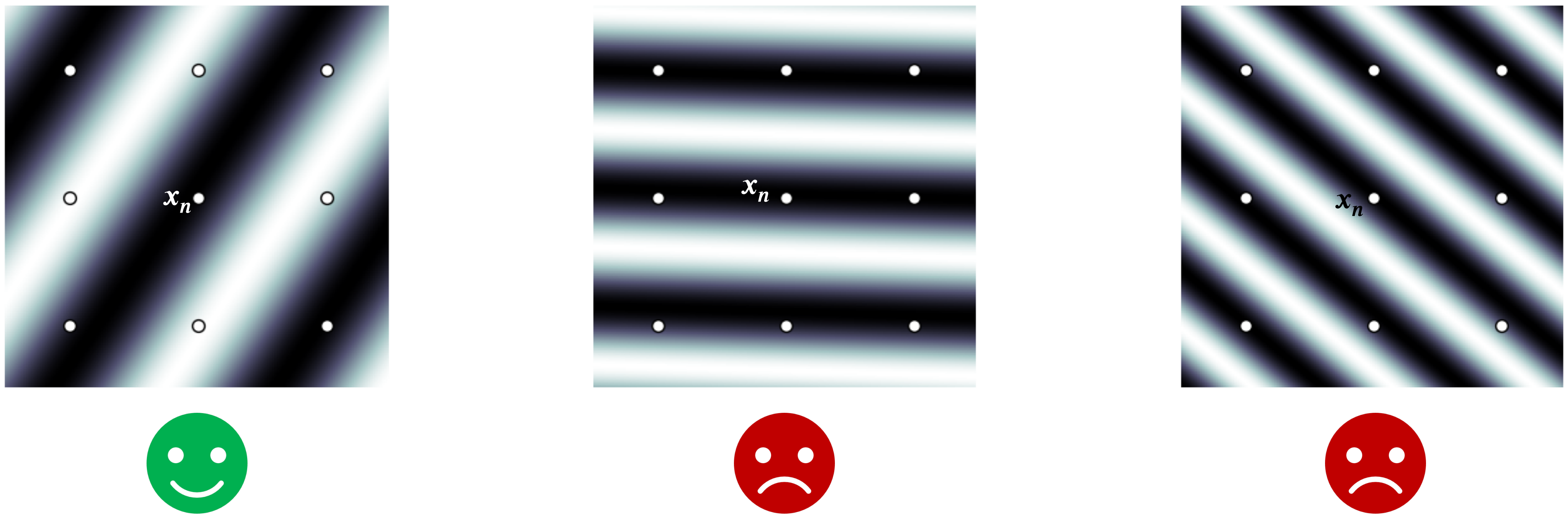

Pathological frequencies

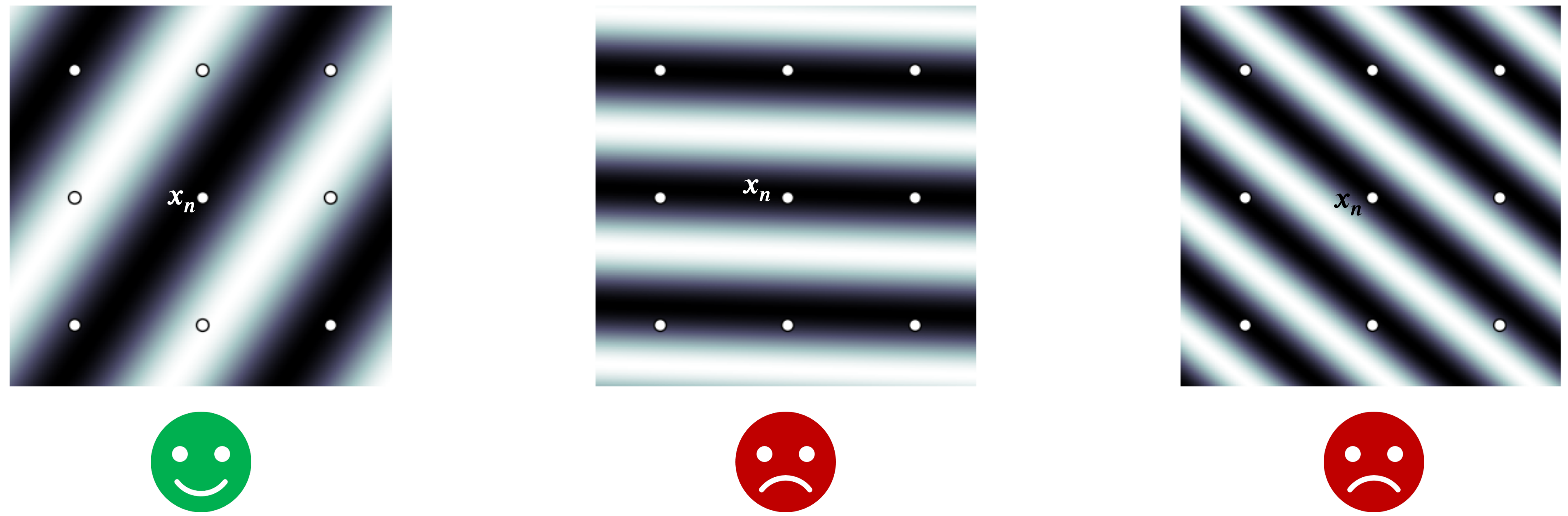

- Need for a probabilistic framework where X (resp. F) is seen as a discrete (resp. continuous) stochastic process on $\mathbb{Z}^2$ (resp. $\mathbb{R}^2$)

Pathological frequencies

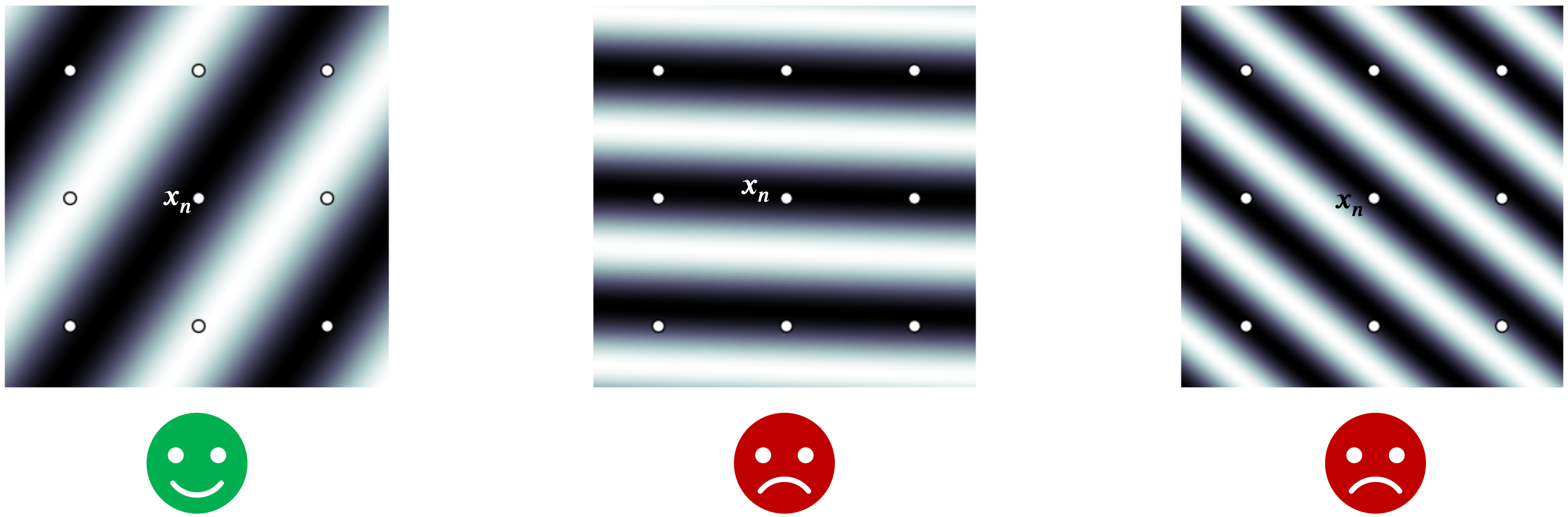

- Need for a probabilistic framework where X (resp. F) is seen as a discrete (resp. continuous) stochastic process on $\mathbb{Z}^2$ (resp. $\mathbb{R}^2$)

- Quantity of interest: $\mathbb{E}\left[\left(1 - G^{\max}(\boldsymbol{x_n})\right)^2\right]$

Pathological frequencies

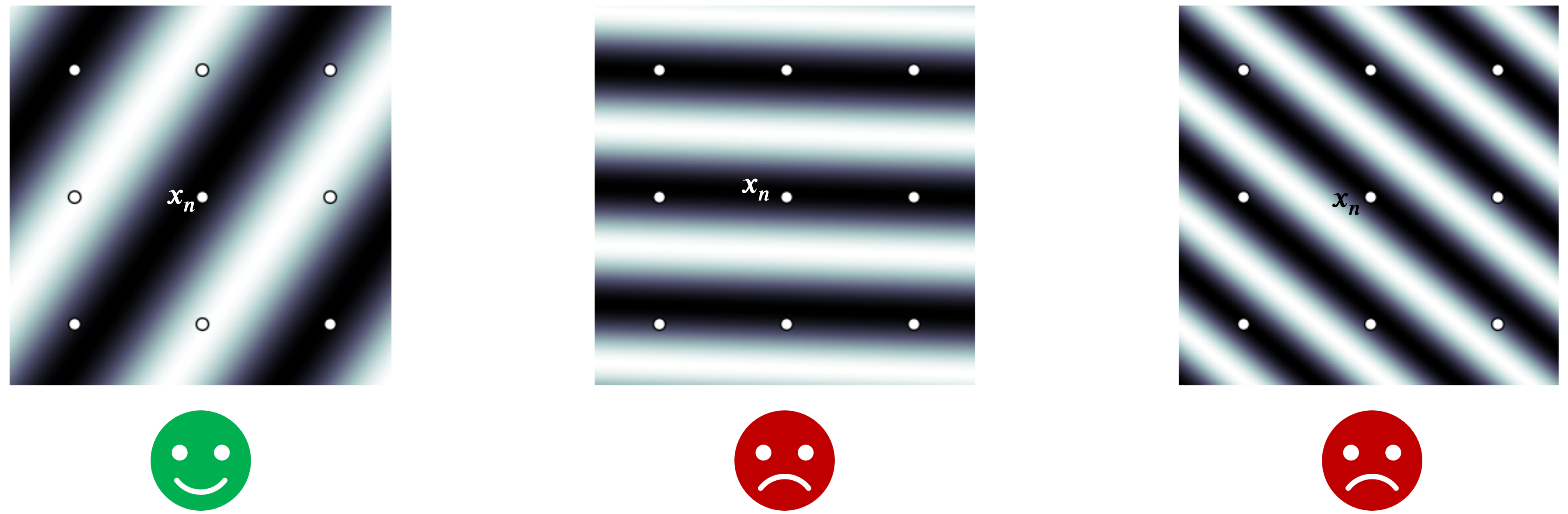

- Need for a probabilistic framework where X (resp. F) is seen as a discrete (resp. continuous) stochastic process on $\mathbb{Z}^2$ (resp. $\mathbb{R}^2$)

- Quantity of interest: $\mathbb{E}\Big[\big(1 - G^{\max}(\boldsymbol{x_n})\big)^2\Big]$

with $G^{\max}(\boldsymbol{x_n}) = \max_{\|\boldsymbol{p}\|_\infty \leq 1} \cos\big(\langle \boldsymbol{\nu}, \boldsymbol{h_p}\rangle - H(\boldsymbol{x_n})\big)$

Pathological frequencies

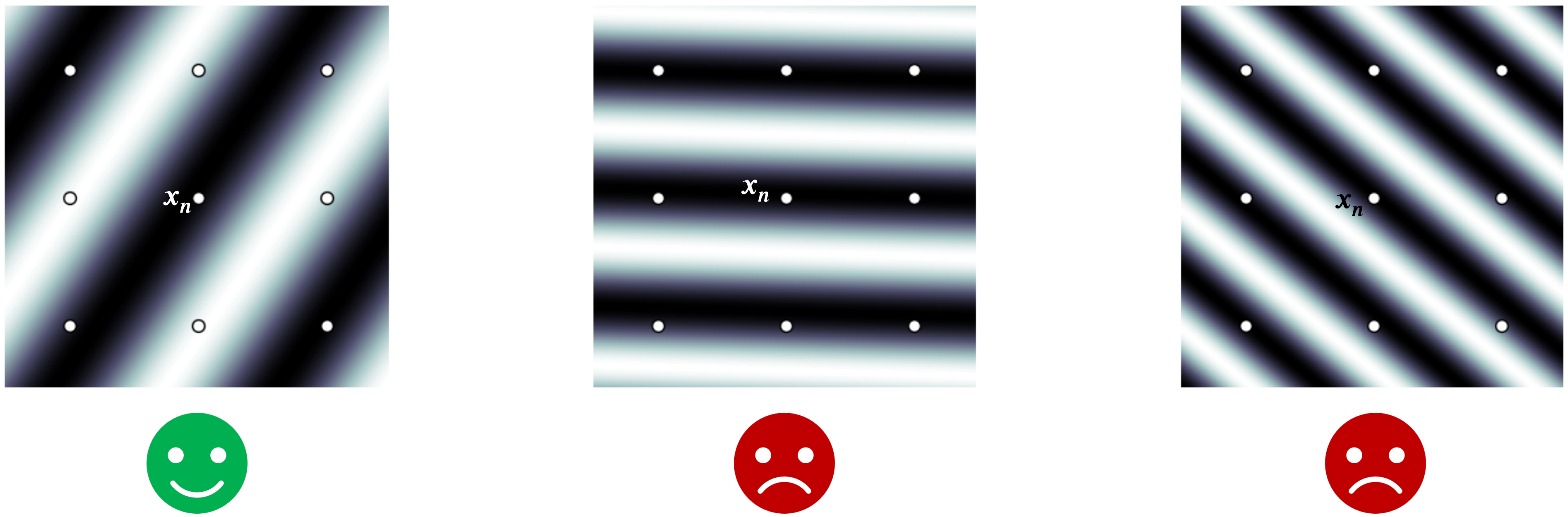

- Need for a probabilistic framework where X (resp. F) is seen as a discrete (resp. continuous) stochastic process on $\mathbb{Z}^2$ (resp. $\mathbb{R}^2$)

- Quantity of interest: $\mathbb{E}\left[\left(1 - G^{\max}(\boldsymbol{x_n})\right)^2\right]$

Hypothesis: uniformly distributed

with $$G^{\max}(\boldsymbol{x_n}) = \max_{\|\boldsymbol{p}\|_\infty \leq 1} \cos\left(\langle \boldsymbol{\nu}, \boldsymbol{h_p} \rangle - H(\boldsymbol{x_n})\right)$$

Main result

- MSE between $\mathbb{C}$**Mod** and $\mathbb{R}$**Max** output

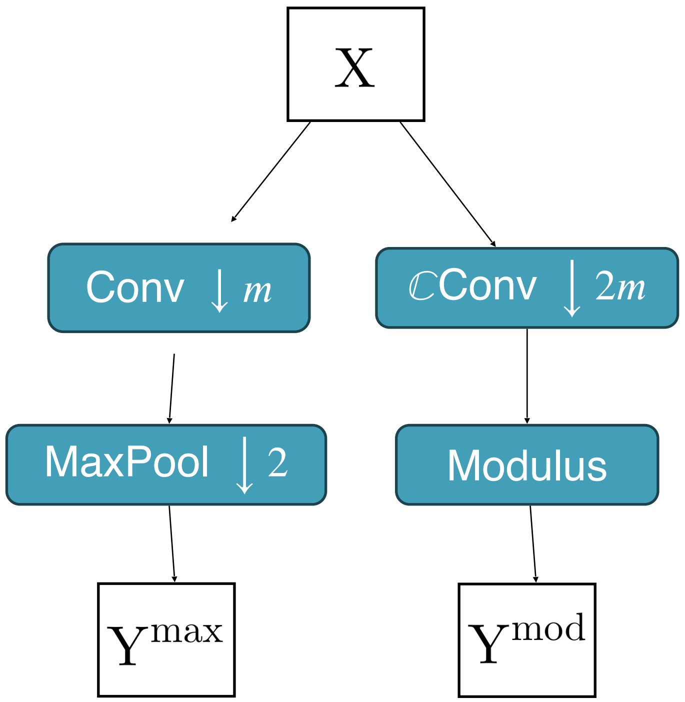

$$\mathbb{E}\left[\frac{\left\|\mathrm{Y}^{\max} - \mathrm{Y}^{\mathrm{mod}}\right\|_2^2}{\left\|\mathrm{Y}^{\mathrm{mod}}\right\|_2^2}\right] \leq \left(\beta_q(m\kappa) + \gamma_q(m\boldsymbol{\theta})\right)^2$$

$$\boldsymbol{\theta} \mapsto \gamma_q(m\boldsymbol{\theta})^2$$
$$q = 1$$

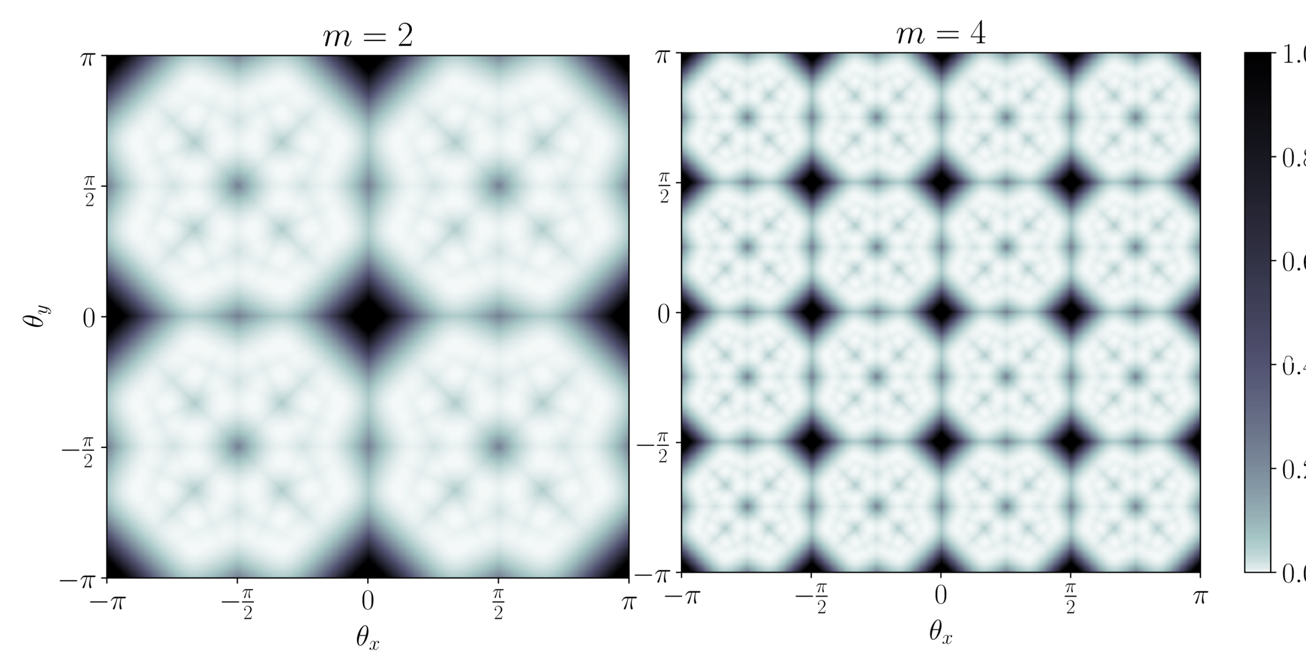

Main result

- MSE between $\mathbb{C}$**Mod** and $\mathbb{R}$**Max** output

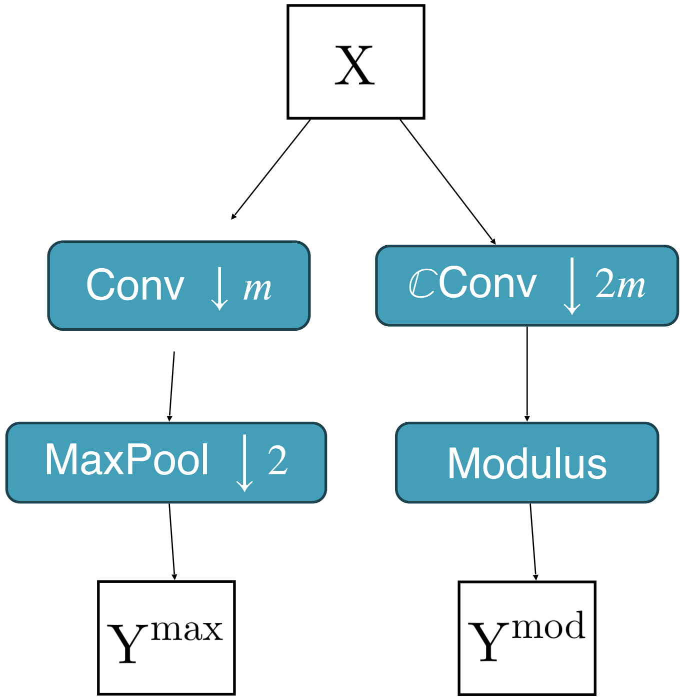

$$\mathbb{E}\left[\frac{\left\|Y^{\max} - Y^{\mathrm{mod}}\right\|_2^2}{\left\|Y^{\mathrm{mod}}\right\|_2^2}\right] \leq \left(\beta_q(m\kappa) + \gamma_q(m\boldsymbol{\theta})\right)^2$$

Upper bound under hypothesis $G^{\max} = 1$

$$\boldsymbol{\theta} \mapsto \gamma_q(m\boldsymbol{\theta})^2$$
$$q = 1$$

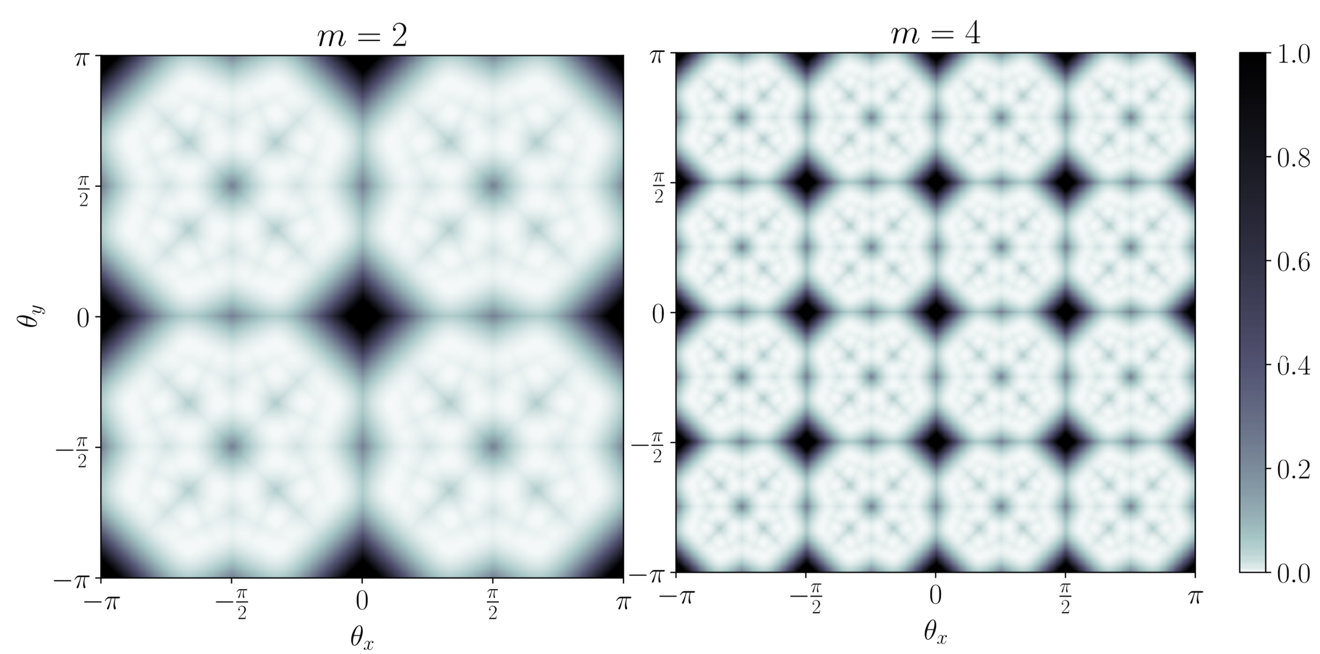

Main result

- MSE between $\mathbb{C}$**Mod** and $\mathbb{R}$**Max** output

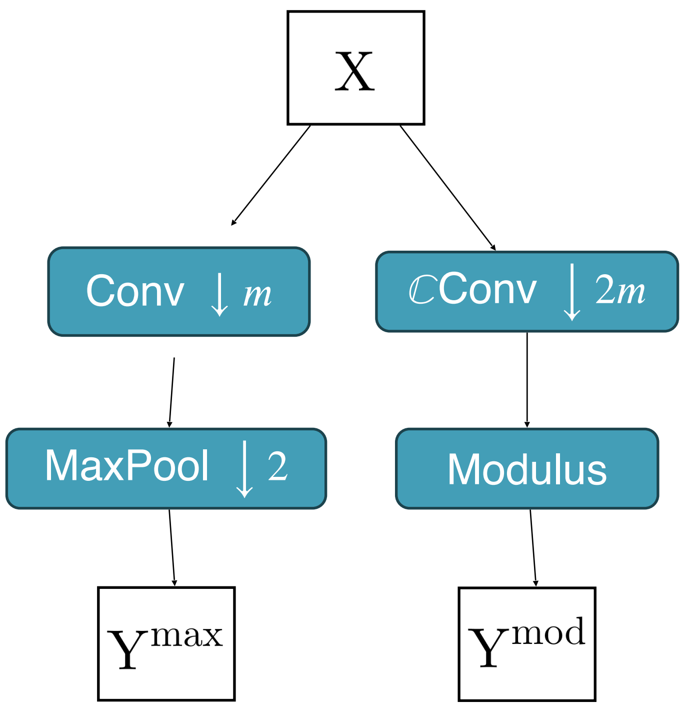

$$\mathbb{E}\left[\frac{\left\|Y^{\max}-Y^{\mathrm{mod}}\right\|_2^2}{\left\|Y^{\mathrm{mod}}\right\|_2^2}\right] \leq \left(\beta_q(m\kappa)+\gamma_q(m\boldsymbol{\theta})\right)^2$$

Discrete nature of the max pooling grid

$$\mathbb{E}\left[\left(1-G^{\max}(\boldsymbol{x_n})\right)^2\right] \rightarrow \quad \boldsymbol{\theta} \mapsto \gamma_q(m\boldsymbol{\theta})^2, \quad q=1$$

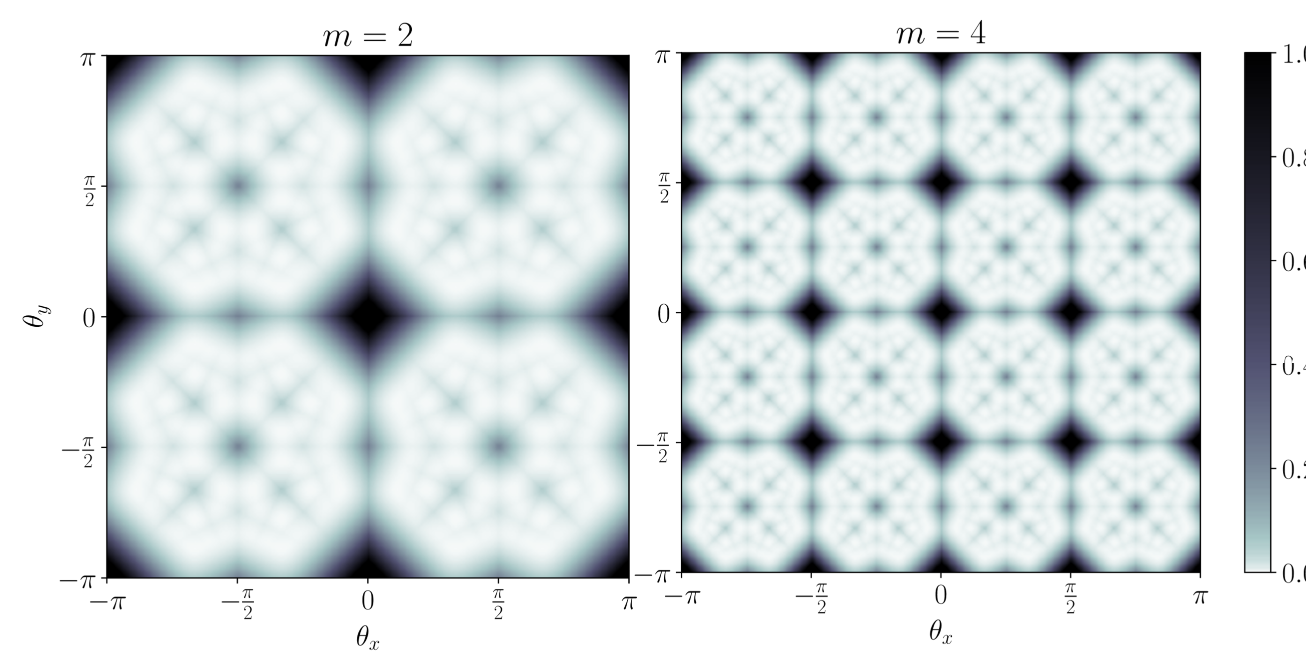

Main result

- MSE between $\mathbb{C}$**Mod** and $\mathbb{R}$**Max** output

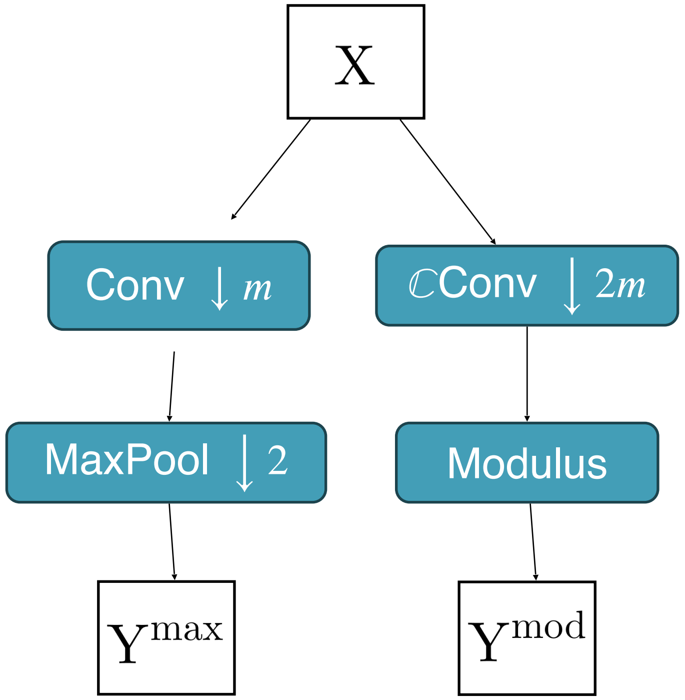

$$\mathbb{E}\left[\frac{\left\|\mathrm{Y}^{\max}-\mathrm{Y}^{\mathrm{mod}}\right\|_2^2}{\left\|\mathrm{Y}^{\mathrm{mod}}\right\|_2^2}\right] \leq \left(\beta_q(m\kappa)+\gamma_q(m\boldsymbol{\theta})\right)^2$$

Discrete nature of the max pooling grid

$$\mathbb{E}\left[\left(1-G^{\max}(\boldsymbol{x_n})\right)^2\right] \rightarrow \boldsymbol{\theta} \mapsto \gamma_q(m\boldsymbol{\theta})^2, \quad q=1$$

$$\gamma_q(\boldsymbol{\omega})=\sqrt{\frac{3}{2}+\frac{1}{4\pi}\sum_{i=0}^{n_q-1}\left(\sin\delta H_i^{(q)}(\boldsymbol{\omega})-8\sin\frac{\delta H_i^{(q)}(\boldsymbol{\omega})}{2}\right)}$$

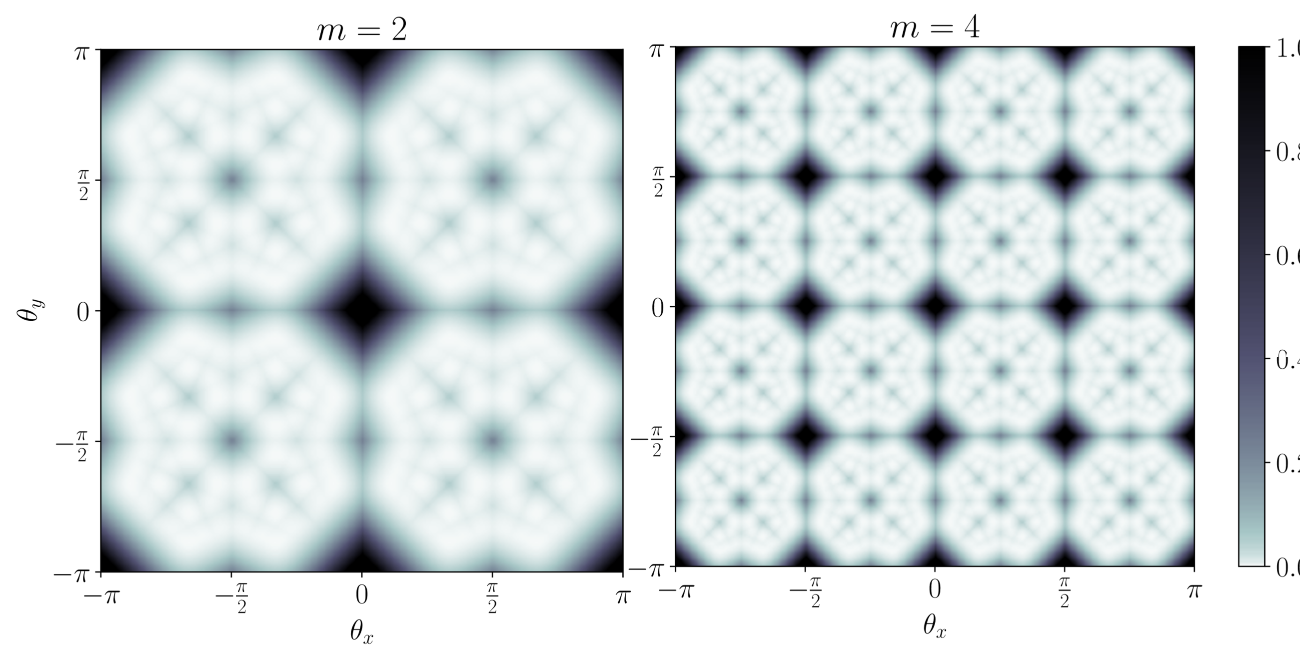

Sketch of the proof

- **Reformulation** of the problem on the unit circle $\mathbb{S}^1 \subset \mathbb{C}$

Sketch of the proof

- **Reformulation** of the problem on the unit circle $\mathbb{S}^1 \subset \mathbb{C}$

  $[z,\, z']_{\mathbb{S}^1} \subset \mathbb{S}^1$ arc on the unit circle going from z to z’

Sketch of the proof

- **Reformulation** of the problem on the unit circle $\mathbb{S}^1 \subset \mathbb{C}$

$[z,\, z']_{\mathbb{S}^1} \subset \mathbb{S}^1$ arc on the unit circle going from z to z'

$$Z_{\mathrm{X}} : \boldsymbol{x} \mapsto \mathrm{e}^{i\, H_{\mathrm{X}}(\boldsymbol{x})} \qquad \text{and} \qquad Z_{\boldsymbol{p}} : \boldsymbol{\omega} \mapsto = \mathrm{e}^{i\langle \boldsymbol{\omega},\, \boldsymbol{p}\rangle}$$

Sketch of the proof

- **Reformulation** of the problem on the unit circle $\mathbb{S}^1 \subset \mathbb{C}$

  $[z,\, z']_{\mathbb{S}^1} \subset \mathbb{S}^1$ arc on the unit circle going from z to z'

  $Z_{\mathrm{X}} : \boldsymbol{x} \mapsto \mathrm{e}^{i\, H_{\mathrm{X}}(\boldsymbol{x})}$ and $Z_{\boldsymbol{p}} : \boldsymbol{\omega} \mapsto = \mathrm{e}^{i \langle \boldsymbol{\omega},\, \boldsymbol{p} \rangle}$

- $G_{\mathrm{X}}(\boldsymbol{x_n},\, \boldsymbol{h_p}) = \mathrm{Re}\big(Z^*_{\mathrm{X}}(\boldsymbol{x_n})\, Z_{\boldsymbol{p}}(m\boldsymbol{\theta})\big)$ ⟶ $\cos\big(\langle \boldsymbol{\nu},\, \boldsymbol{h_p} \rangle - H(\boldsymbol{x_n})\big)$

Sketch of the proof

- **Reformulation** of the problem on the unit circle $\mathbb{S}^1 \subset \mathbb{C}$

  $[z,\, z']_{\mathbb{S}^1} \subset \mathbb{S}^1$ arc on the unit circle going from z to z' $\boldsymbol{h_p} = ms\boldsymbol{p}$

  $Z_{\mathrm{X}} : \boldsymbol{x} \mapsto \mathrm{e}^{i\, H_{\mathrm{X}}(\boldsymbol{x})}$ and $Z_{\boldsymbol{p}} : \boldsymbol{\omega} \mapsto = \mathrm{e}^{i\langle \boldsymbol{\omega},\, \boldsymbol{p}\rangle}$

- $G_{\mathrm{X}}\big(\boldsymbol{x_n},\, \boldsymbol{h_p}\big) = \mathrm{Re}\big(Z_{\mathrm{X}}^*(\boldsymbol{x_n})\, Z_{\boldsymbol{p}}(m\boldsymbol{\theta})\big)$ ⟶ $\cos\big(\langle \boldsymbol{\nu},\, \boldsymbol{h_p}\rangle - H(\boldsymbol{x_n})\big)$

Sketch of the proof

- **Reformulation** of the problem on the unit circle $\mathbb{S}^1 \subset \mathbb{C}$

$[z,\, z']_{\mathbb{S}^1} \subset \mathbb{S}^1$ arc on the unit circle going from z to z'

$\boldsymbol{h_p} = ms\boldsymbol{p}$

$Z_{\mathrm{X}} : \boldsymbol{x} \mapsto \mathrm{e}^{i\, H_{\mathrm{X}}(\boldsymbol{x})}$ and $Z_{\boldsymbol{p}} : \boldsymbol{\omega} \mapsto = \mathrm{e}^{i \langle \boldsymbol{\omega},\, \boldsymbol{p} \rangle}$

$\boldsymbol{\nu} = \boldsymbol{\theta}/s$

- $G_{\mathrm{X}}\big(\boldsymbol{x_n},\, \boldsymbol{h_p}\big) = \mathrm{Re}\big(Z^*_{\mathrm{X}}(\boldsymbol{x_n})\, Z_{\boldsymbol{p}}(m\boldsymbol{\theta})\big)$ ⟶ $\cos\big(\langle \boldsymbol{\nu},\, \boldsymbol{h_p} \rangle - H(\boldsymbol{x_n})\big)$

Sketch of the proof

- **Reformulation** of the problem on the unit circle $\mathbb{S}^1 \subset \mathbb{C}$

$[z,\, z']_{\mathbb{S}^1} \subset \mathbb{S}^1$ arc on the unit circle going from z to z'

$$\boldsymbol{h_p} = ms\boldsymbol{p}$$

$$Z_{\mathrm{X}} : \boldsymbol{x} \mapsto \mathrm{e}^{i\, H_{\mathrm{X}}(\boldsymbol{x})} \quad \text{and} \quad Z_{\boldsymbol{p}} : \boldsymbol{\omega} \mapsto = \mathrm{e}^{i\langle \boldsymbol{\omega},\, \boldsymbol{p}\rangle}$$

$$\boldsymbol{\nu} = \boldsymbol{\theta}/s$$

- $G_{\mathrm{X}}\big(\boldsymbol{x_n},\, \boldsymbol{h_p}\big) = \mathrm{Re}\big(Z_{\mathrm{X}}^*(\boldsymbol{x_n})\, Z_{\boldsymbol{p}}(m\boldsymbol{\theta})\big)$ ⟶ $\cos\big(\langle \boldsymbol{\nu},\, \boldsymbol{h_p}\rangle - H(\boldsymbol{x_n})\big)$
- Sort $\{Z_{\boldsymbol{p}}(\boldsymbol{\omega})\}_{\boldsymbol{p}\in\{-q..q\}^2}$ ⟶ $\big(Z_i^{(q)}(\boldsymbol{\omega})\big)_{i\in\{0..n_q-1\}}$ $\quad n_q := (2q+1)^2$

Sketch of the proof

- **Reformulation** of the problem on the unit circle $\mathbb{S}^1 \subset \mathbb{C}$

  $[z,\, z']_{\mathbb{S}^1} \subset \mathbb{S}^1$ arc on the unit circle going from z to z'

  $\boldsymbol{h_p} = ms\boldsymbol{p}$

  $Z_{\mathrm{X}} : \boldsymbol{x} \mapsto \mathrm{e}^{i\,H_{\mathrm{X}}(\boldsymbol{x})}$ and $Z_{\boldsymbol{p}} : \boldsymbol{\omega} \mapsto= \mathrm{e}^{i\langle \boldsymbol{\omega},\, \boldsymbol{p}\rangle}$

  $\boldsymbol{\nu} = \boldsymbol{\theta}/s$

- $G_{\mathrm{X}}\big(\boldsymbol{x_n},\, \boldsymbol{h_p}\big) = \mathrm{Re}\big(Z^*_{\mathrm{X}}(\boldsymbol{x_n})\, Z_{\boldsymbol{p}}(m\boldsymbol{\theta})\big)$ ⟶ $\cos\big(\langle \boldsymbol{\nu},\, \boldsymbol{h_p}\rangle - H(\boldsymbol{x_n})\big)$

- Sort $\{Z_{\boldsymbol{p}}(\boldsymbol{\omega})\}_{\boldsymbol{p}\in\{-q..q\}^2}$ ⟶ $\big(Z_i^{(q)}(\boldsymbol{\omega})\big)_{i\in\{0..n_q-1\}}$ $\quad n_q := (2q+1)^2$

  in ascending order of their argument:

$$0 = H_0^{(q)}(\boldsymbol{\omega}) \leq \cdots \leq H_{n_q-1}^{(q)}(\boldsymbol{\omega}) < 2\pi$$

Sketch of the proof

- **Reformulation** of the problem on the unit circle $\mathbb{S}^1 \subset \mathbb{C}$

  $[z,\, z']_{\mathbb{S}^1} \subset \mathbb{S}^1$ arc on the unit circle going from z to z' $\boldsymbol{h_p} = ms\boldsymbol{p}$

  $Z_{\mathrm{X}} : \boldsymbol{x} \mapsto \mathrm{e}^{i\, H_{\mathrm{X}}(\boldsymbol{x})}$ and $Z_{\boldsymbol{p}} : \boldsymbol{\omega} \mapsto = \mathrm{e}^{i\langle \boldsymbol{\omega},\, \boldsymbol{p}\rangle}$ $\boldsymbol{\nu} = \boldsymbol{\theta}/s$

- $G_{\mathrm{X}}\big(\boldsymbol{x_n},\, \boldsymbol{h_p}\big) = \mathrm{Re}\big(Z_{\mathrm{X}}^*(\boldsymbol{x_n})\, Z_{\boldsymbol{p}}(m\boldsymbol{\theta})\big)$ ⟶ $\cos\big(\langle \boldsymbol{\nu},\, \boldsymbol{h_p}\rangle - H(\boldsymbol{x_n})\big)$
- Sort $\{Z_{\boldsymbol{p}}(\boldsymbol{\omega})\}_{\boldsymbol{p}\in\{-q..q\}^2}$ ⟶ $\big(Z_i^{(q)}(\boldsymbol{\omega})\big)_{i\in\{0..n_q-1\}}$ $n_q := (2q+1)^2$

  in ascending order of their argument:

$$0 = H_0^{(q)}(\boldsymbol{\omega}) \leq \cdots \leq H_{n_q-1}^{(q)}(\boldsymbol{\omega}) < 2\pi$$

$$H_{n_q}^{(q)}(\boldsymbol{\omega}) := 2\pi$$

$$Z_{n_q}^{(q)}(\boldsymbol{\omega}) := 1$$

Sketch of the proof

- **Reformulation** of the problem on the unit circle $\mathbb{S}^1 \subset \mathbb{C}$

$[z,\, z']_{\mathbb{S}^1} \subset \mathbb{S}^1$ arc on the unit circle going from z to z'

$\boldsymbol{h_p} = ms\boldsymbol{p}$

$Z_{\mathrm{X}} : \boldsymbol{x} \mapsto \mathrm{e}^{i\, H_{\mathrm{X}}(\boldsymbol{x})}$ and $Z_{\boldsymbol{p}} : \boldsymbol{\omega} \mapsto = \mathrm{e}^{i\langle \boldsymbol{\omega},\, \boldsymbol{p}\rangle}$

$\boldsymbol{\nu} = \boldsymbol{\theta}/s$

- $G_{\mathrm{X}}\big(\boldsymbol{x_n},\, \boldsymbol{h_p}\big) = \mathrm{Re}\big(Z^*_{\mathrm{X}}(\boldsymbol{x_n})\, Z_{\boldsymbol{p}}(m\boldsymbol{\theta})\big)$ ⟶ $\cos\big(\langle \boldsymbol{\nu},\, \boldsymbol{h_p}\rangle - H(\boldsymbol{x_n})\big)$
- Sort $\{Z_{\boldsymbol{p}}(\boldsymbol{\omega})\}_{\boldsymbol{p}\in\{-q..q\}^2}$ ⟶ $\big(Z_i^{(q)}(\boldsymbol{\omega})\big)_{i\in\{0..n_q-1\}}$ $n_q := (2q+1)^2$

  in ascending order of their argument:

$$H_{n_q}^{(q)}(\boldsymbol{\omega}) := 2\pi$$

$$0 = H_0^{(q)}(\boldsymbol{\omega}) \leq \cdots \leq H_{n_q-1}^{(q)}(\boldsymbol{\omega}) < 2\pi$$

$$Z_{n_q}^{(q)}(\boldsymbol{\omega}) := 1$$

- Split $\mathbb{S}^1$ into n_q arcs delimited by the $Z_i^{(q)}(\boldsymbol{\omega})$

$$\mathfrak{A}_i^{(q)}(\boldsymbol{\omega}) := \begin{cases} \Big[Z_i^{(q)}(\boldsymbol{\omega}),\, Z_{i+1}^{(q)}(\boldsymbol{\omega})\Big]_{\mathbb{S}^1} & \text{if } H_{i+1}^{(q)}(\boldsymbol{\omega}) - H_i^{(q)}(\boldsymbol{\omega}) < 2\pi; \\ \mathbb{S}^1 & \text{otherwise.} \end{cases}$$

Sketch of the proof

- **Reformulation** of the problem on the unit circle $\mathbb{S}^1 \subset \mathbb{C}$

$[z,\, z']_{\mathbb{S}^1} \subset \mathbb{S}^1$ arc on the unit circle going from z to z'

$\boldsymbol{h_p} = ms\boldsymbol{p}$

$Z_{\mathrm{X}} : \boldsymbol{x} \mapsto \mathrm{e}^{i\, H_{\mathrm{X}}(\boldsymbol{x})}$ and $Z_{\boldsymbol{p}} : \boldsymbol{\omega} \mapsto= \mathrm{e}^{i\langle \boldsymbol{\omega},\, \boldsymbol{p}\rangle}$

$\boldsymbol{\nu} = \boldsymbol{\theta}/s$

- $G_{\mathrm{X}}\big(\boldsymbol{x_n},\, \boldsymbol{h_p}\big) = \mathrm{Re}\big(Z^*_{\mathrm{X}}(\boldsymbol{x_n})\, Z_{\boldsymbol{p}}(m\boldsymbol{\theta})\big)$ ⟶ $\cos\big(\langle \boldsymbol{\nu},\, \boldsymbol{h_p}\rangle - H(\boldsymbol{x_n})\big)$

- Sort $\{Z_{\boldsymbol{p}}(\boldsymbol{\omega})\}_{\boldsymbol{p}\in\{-q..q\}^2}$ ⟶ $\big(Z_i^{(q)}(\boldsymbol{\omega})\big)_{i\in\{0..n_q-1\}}$ $\quad n_q := (2q+1)^2$

  in ascending order of their argument:

$$0 = H_0^{(q)}(\boldsymbol{\omega}) \leq \cdots \leq H_{n_q-1}^{(q)}(\boldsymbol{\omega}) < 2\pi$$

$H_{n_q}^{(q)}(\boldsymbol{\omega}) := 2\pi$

$Z_{n_q}^{(q)}(\boldsymbol{\omega}) := 1$

- Split $\mathbb{S}^1$ into n_q arcs delimited by the $Z_i^{(q)}(\boldsymbol{\omega})$

$\delta H_i^{(q)}(\boldsymbol{\omega})$

$$\mathfrak{A}_i^{(q)}(\boldsymbol{\omega}) := \begin{cases} \Big[Z_i^{(q)}(\boldsymbol{\omega}),\, Z_{i+1}^{(q)}(\boldsymbol{\omega})\Big]_{\mathbb{S}^1} & \text{if } H_{i+1}^{(q)}(\boldsymbol{\omega}) - H_i^{(q)}(\boldsymbol{\omega}) < 2\pi; \\ \mathbb{S}^1 & \text{otherwise.} \end{cases}$$

Sketch of the proof

- **Reformulation** of the problem on the unit circle $\mathbb{S}^1 \subset \mathbb{C}$

  $[z,\, z']_{\mathbb{S}^1} \subset \mathbb{S}^1$ arc on the unit circle going from z to z'

  $$\boldsymbol{h_p} = ms\boldsymbol{p}$$

  $$Z_{\mathrm{X}} : \boldsymbol{x} \mapsto \mathrm{e}^{i\, H_{\mathrm{X}}(\boldsymbol{x})} \qquad \text{and} \qquad Z_{\boldsymbol{p}} : \boldsymbol{\omega} \mapsto = \mathrm{e}^{i\langle \boldsymbol{\omega},\, \boldsymbol{p}\rangle}$$

  $$\boldsymbol{\nu} = \boldsymbol{\theta}/s$$

- $G_{\mathrm{X}}\big(\boldsymbol{x_n},\, \boldsymbol{h_p}\big) = \mathrm{Re}\big(Z_{\mathrm{X}}^*(\boldsymbol{x_n})\, Z_{\boldsymbol{p}}(m\boldsymbol{\theta})\big)$ ⟶ $\cos\big(\langle \boldsymbol{\nu},\, \boldsymbol{h_p}\rangle - H(\boldsymbol{x_n})\big)$

Sketch of the proof

- **Reformulation** of the problem on the unit circle $\mathbb{S}^1 \subset \mathbb{C}$

  $[z,\, z']_{\mathbb{S}^1} \subset \mathbb{S}^1$ arc on the unit circle going from z to z'

  $$\boldsymbol{h_p} = ms\boldsymbol{p}$$

  $$Z_{\mathrm{X}} : \boldsymbol{x} \mapsto \mathrm{e}^{i\, H_{\mathrm{X}}(\boldsymbol{x})} \qquad \text{and} \qquad Z_{\boldsymbol{p}} : \boldsymbol{\omega} \mapsto = \mathrm{e}^{i\langle \boldsymbol{\omega},\, \boldsymbol{p}\rangle}$$

  $$\boldsymbol{\nu} = \boldsymbol{\theta}/s$$

- $G_{\mathrm{X}}\big(\boldsymbol{x_n},\, \boldsymbol{h_p}\big) = \mathrm{Re}\big(Z_{\mathrm{X}}^*(\boldsymbol{x_n})\, Z_{\boldsymbol{p}}(m\boldsymbol{\theta})\big)$ ➡ $\cos\big(\langle \boldsymbol{\nu},\, \boldsymbol{h_p}\rangle - H(\boldsymbol{x_n})\big)$
- $\mathsf{G}_{\mathrm{X}}^{\max}(\boldsymbol{x}) = g_{\max}(\mathsf{Z}_{\mathrm{X}}(\boldsymbol{x}))$ ➡ $g_{\max} : z \mapsto \max_{\|\boldsymbol{p}\|_\infty \leq q} \mathrm{Re}\big(z^* Z_{\boldsymbol{p}}\big)$

Sketch of the proof

- **Reformulation** of the problem on the unit circle $\mathbb{S}^1 \subset \mathbb{C}$

  $[z,\, z']_{\mathbb{S}^1} \subset \mathbb{S}^1$ arc on the unit circle going from z to z'

  $\boldsymbol{h_p} = ms\boldsymbol{p}$

  $Z_{\mathrm{X}} : \boldsymbol{x} \mapsto \mathrm{e}^{i\, H_{\mathrm{X}}(\boldsymbol{x})}$ and $Z_{\boldsymbol{p}} : \boldsymbol{\omega} \mapsto = \mathrm{e}^{i\langle \boldsymbol{\omega},\, \boldsymbol{p}\rangle}$

  $\boldsymbol{\nu} = \boldsymbol{\theta}/s$

- $G_{\mathrm{X}}\big(\boldsymbol{x_n},\, \boldsymbol{h_p}\big) = \mathrm{Re}\big(Z^*_{\mathrm{X}}(\boldsymbol{x_n})\, Z_{\boldsymbol{p}}(m\boldsymbol{\theta})\big)$ ➡ $\cos\big(\langle \boldsymbol{\nu},\, \boldsymbol{h_p}\rangle - H(\boldsymbol{x_n})\big)$
- $\mathsf{G}^{\max}_{\mathrm{X}}(\boldsymbol{x}) = g_{\max}(\mathsf{Z}_{\mathrm{X}}(\boldsymbol{x}))$ ➡ $g_{\max} : z \mapsto \max_{\|\boldsymbol{p}\|_\infty \leq q} \mathrm{Re}\big(z^* Z_{\boldsymbol{p}}\big)$
- $\mathsf{Z}_{\mathrm{X}}(\boldsymbol{x})$ **uniformly distributed** on the unit circle (Hypothesis)

Sketch of the proof

- **Reformulation** of the problem on the unit circle $\mathbb{S}^1 \subset \mathbb{C}$

  $[z,\, z']_{\mathbb{S}^1} \subset \mathbb{S}^1$ arc on the unit circle going from z to z'

  $\boldsymbol{h}_{\boldsymbol{p}} = ms\boldsymbol{p}$

  $Z_{\mathrm{X}} : \boldsymbol{x} \mapsto \mathrm{e}^{i\, H_{\mathrm{X}}(\boldsymbol{x})}$ and $Z_{\boldsymbol{p}} : \boldsymbol{\omega} \mapsto = \mathrm{e}^{i\langle \boldsymbol{\omega},\, \boldsymbol{p}\rangle}$

  $\boldsymbol{\nu} = \boldsymbol{\theta}/s$

- $G_{\mathrm{X}}\big(\boldsymbol{x_n},\, \boldsymbol{h_p}\big) = \mathrm{Re}\big(Z_{\mathrm{X}}^*(\boldsymbol{x_n})\, Z_{\boldsymbol{p}}(m\boldsymbol{\theta})\big)$ ⟶ $\cos\big(\langle \boldsymbol{\nu},\, \boldsymbol{h_p}\rangle - H(\boldsymbol{x_n})\big)$
- $\mathsf{G}_{\mathrm{X}}^{\max}(\boldsymbol{x}) = g_{\max}(\mathsf{Z}_{\mathrm{X}}(\boldsymbol{x}))$ ⟶ $g_{\max} : z \mapsto \max\limits_{\|\boldsymbol{p}\|_\infty \leq q} \mathrm{Re}\big(z^* Z_{\boldsymbol{p}}\big)$
- $\mathsf{Z}_{\mathrm{X}}(\boldsymbol{x})$ **uniformly distributed** on the unit circle (Hypothesis)
- The p-th moment is given by

$$\mathbb{E}\left[\mathsf{G}_{\mathrm{X}}^{\max}(\boldsymbol{x})^p\right] = \frac{1}{2\pi}\int_{\mathbb{S}^1} g_{\max}(z)^p\, \mathrm{d}\vartheta(z) = \frac{1}{2\pi}\sum_{i=0}^{n_q-1}\int_{\mathfrak{A}_i^{(q)}} g_{\max}(z)^p\, \mathrm{d}\vartheta(z).$$

Sketch of the proof

- **Reformulation** of the problem on the unit circle $\mathbb{S}^1 \subset \mathbb{C}$

  $[z,\, z']_{\mathbb{S}^1} \subset \mathbb{S}^1$ arc on the unit circle going from z to z' $\boldsymbol{h_p} = ms\boldsymbol{p}$

  $Z_{\mathrm{X}} : \boldsymbol{x} \mapsto \mathrm{e}^{i\,H_{\mathrm{X}}(\boldsymbol{x})}$ and $Z_{\boldsymbol{p}} : \boldsymbol{\omega} \mapsto = \mathrm{e}^{i\langle \boldsymbol{\omega},\, \boldsymbol{p}\rangle}$ $\boldsymbol{\nu} = \boldsymbol{\theta}/s$

- $G_{\mathrm{X}}\big(\boldsymbol{x_n},\, \boldsymbol{h_p}\big) = \mathrm{Re}\big(Z_{\mathrm{X}}^*(\boldsymbol{x_n})\, Z_{\boldsymbol{p}}(m\boldsymbol{\theta})\big)$ ⟶ $\cos\big(\langle \boldsymbol{\nu},\, \boldsymbol{h_p}\rangle - H(\boldsymbol{x_n})\big)$
- $\mathsf{G}_{\mathrm{X}}^{\max}(\boldsymbol{x}) = g_{\max}(\mathsf{Z}_{\mathrm{X}}(\boldsymbol{x}))$ ⟶ $g_{\max} : z \mapsto \max\limits_{\|\boldsymbol{p}\|_\infty \leq q} \mathrm{Re}\big(z^* Z_{\boldsymbol{p}}\big)$
- $\mathsf{Z}_{\mathrm{X}}(\boldsymbol{x})$ **uniformly distributed** on the unit circle (Hypothesis)
- The p-th moment is given by

$$\mathbb{E}\left[\mathsf{G}_{\mathrm{X}}^{\max}(\boldsymbol{x})^p\right] = \frac{1}{2\pi}\int_{\mathbb{S}^1} g_{\max}(z)^p \,\mathrm{d}\vartheta(z) = \frac{1}{2\pi}\sum_{i=0}^{n_q-1}\int_{\mathfrak{A}_i^{(q)}} g_{\max}(z)^p \,\mathrm{d}\vartheta(z).$$

- $\forall z \in \mathfrak{A}_i^{(q)},\; g_{\max}(z) = \max\left(\mathrm{Re}\big(z^* Z_i^{(q)}\big),\, \mathrm{Re}\big(z^* Z_{i+1}^{(q)}\big)\right)$

Sketch of the proof

$$g_{\max} : z \mapsto \max_{\|\boldsymbol{p}\|_\infty \leq q} \mathrm{Re}\big(z^* Z_{\boldsymbol{p}}\big)$$

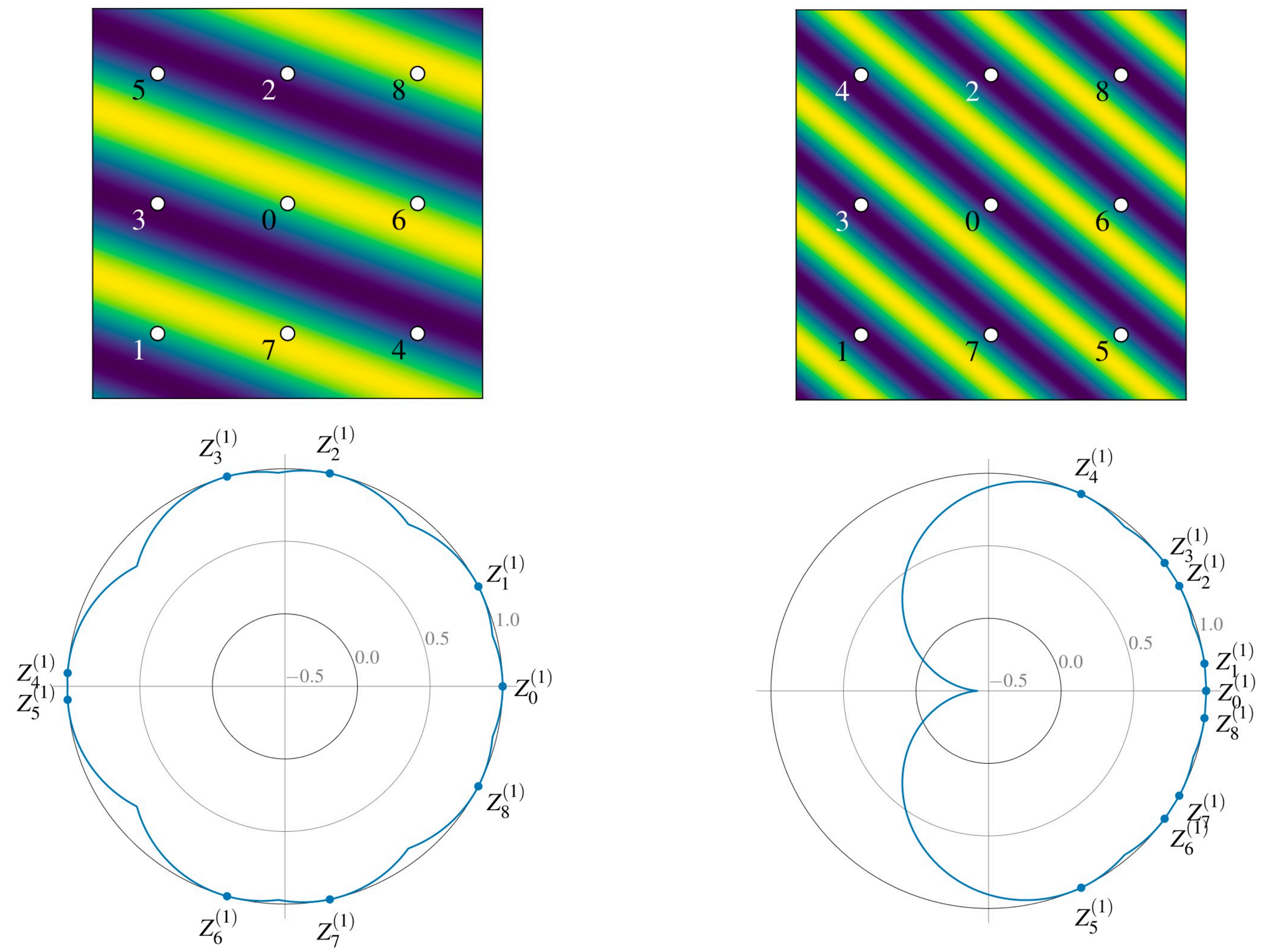

(a) General case

(b) Pathological case

Sketch of the proof

- **Reformulation** of the problem on the unit circle $\mathbb{S}^1 \subset \mathbb{C}$
  - $\forall z \in \mathfrak{A}_i^{(q)},\ g_{\max}(z) = \max\left(\mathrm{Re}\big(z^* Z_i^{(q)}\big),\ \mathrm{Re}\big(z^* Z_{i+1}^{(q)}\big)\right)$

Sketch of the proof

- **Reformulation** of the problem on the unit circle $\mathbb{S}^1 \subset \mathbb{C}$
  - $\forall z \in \mathfrak{A}_i^{(q)},\ g_{\max}(z) = \max\Big(\mathrm{Re}\big(z^* Z_i^{(q)}\big),\ \mathrm{Re}\big(z^* Z_{i+1}^{(q)}\big)\Big)$
  - $\forall z \in \overline{\mathfrak{A}}_i^{(q)},\ g_{\max}(z) = \mathrm{Re}\big(z^* Z_i^{(q)}\big)$

Sketch of the proof

- **Reformulation** of the problem on the unit circle $\mathbb{S}^1 \subset \mathbb{C}$
  - $\forall z \in \mathfrak{A}_i^{(q)},\ g_{\max}(z) = \max\left(\mathrm{Re}\big(z^* Z_i^{(q)}\big),\ \mathrm{Re}\big(z^* Z_{i+1}^{(q)}\big)\right)$
  - $\forall z \in \overline{\mathfrak{A}}_i^{(q)},\ g_{\max}(z) = \mathrm{Re}\big(z^* Z_i^{(q)}\big)$

$$\begin{aligned}
\int_{\mathfrak{A}_i^{(q)}} g_{\max}(z)^p \,\mathrm{d}\vartheta(z) &= 2\int_{\overline{\mathfrak{A}}_i^{(q)}} \mathrm{Re}\big(z^* Z_i^{(q)}\big)^p \,\mathrm{d}\vartheta(z) \\
&= 2\int_{H_i^{(q)}}^{\overline{H}_i^{(q)}} \cos^p\big(\eta - H_i^{(q)}\big)\,\mathrm{d}\eta \\
&= 2\int_0^{\delta H_i^{(q)}/2} \cos^p \eta' \,\mathrm{d}\eta'
\end{aligned}$$

Sketch of the proof

- **Reformulation** of the problem on the unit circle $\mathbb{S}^1 \subset \mathbb{C}$
  - $\forall z \in \mathfrak{A}_i^{(q)},\ g_{\max}(z) = \max\left(\mathrm{Re}\big(z^* Z_i^{(q)}\big),\ \mathrm{Re}\big(z^* Z_{i+1}^{(q)}\big)\right)$
  - $\forall z \in \overline{\mathfrak{A}}_i^{(q)},\ g_{\max}(z) = \mathrm{Re}\big(z^* Z_i^{(q)}\big)$

$$\int_{\mathfrak{A}_i^{(q)}} g_{\max}(z)^p \,\mathrm{d}\vartheta(z) = 2\int_{\overline{\mathfrak{A}}_i^{(q)}} \mathrm{Re}\big(z^* Z_i^{(q)}\big)^p \,\mathrm{d}\vartheta(z) \qquad z \leftarrow \mathrm{e}^{i\eta}$$

$$= 2\int_{H_i^{(q)}}^{\overline{H}_i^{(q)}} \cos^p\big(\eta - H_i^{(q)}\big)\,\mathrm{d}\eta$$

$$= 2\int_0^{\delta H_i^{(q)}/2} \cos^p \eta' \,\mathrm{d}\eta'$$

Sketch of the proof

- **Reformulation** of the problem on the unit circle $\mathbb{S}^1 \subset \mathbb{C}$
  - $\forall z \in \mathfrak{A}_i^{(q)},\ g_{\max}(z) = \max\left(\mathrm{Re}\big(z^* Z_i^{(q)}\big),\ \mathrm{Re}\big(z^* Z_{i+1}^{(q)}\big)\right)$
  - $\forall z \in \overline{\mathfrak{A}}_i^{(q)},\ g_{\max}(z) = \mathrm{Re}\big(z^* Z_i^{(q)}\big)$

$$\int_{\mathfrak{A}_i^{(q)}} g_{\max}(z)^p \,\mathrm{d}\vartheta(z) = 2\int_{\overline{\mathfrak{A}}_i^{(q)}} \mathrm{Re}\big(z^* Z_i^{(q)}\big)^p \,\mathrm{d}\vartheta(z)$$

$$z \leftarrow \mathrm{e}^{i\eta}$$

$$= 2\int_{H_i^{(q)}}^{\overline{H}_i^{(q)}} \cos^p\left(\eta - H_i^{(q)}\right) \mathrm{d}\eta \qquad \overline{H}_i^{(q)} := \big(H_i^{(q)} + H_{i+1}^{(q)}\big)/2$$

$$= 2\int_0^{\delta H_i^{(q)}/2} \cos^p \eta' \,\mathrm{d}\eta'$$

Sketch of the proof

- **Reformulation** of the problem on the unit circle $\mathbb{S}^1 \subset \mathbb{C}$
  - $\forall z \in \mathfrak{A}_i^{(q)},\ g_{\max}(z) = \max\left(\mathrm{Re}\big(z^* Z_i^{(q)}\big),\ \mathrm{Re}\big(z^* Z_{i+1}^{(q)}\big)\right)$
  - $\forall z \in \overline{\mathfrak{A}}_i^{(q)},\ g_{\max}(z) = \mathrm{Re}\big(z^* Z_i^{(q)}\big)$

$$\int_{\mathfrak{A}_i^{(q)}} g_{\max}(z)^p \,\mathrm{d}\vartheta(z) = 2\int_{\overline{\mathfrak{A}}_i^{(q)}} \mathrm{Re}\big(z^* Z_i^{(q)}\big)^p \,\mathrm{d}\vartheta(z) \qquad z \leftarrow \mathrm{e}^{i\eta}$$

$$= 2\int_{H_i^{(q)}}^{\overline{H}_i^{(q)}} \cos^p\left(\eta - H_i^{(q)}\right) \mathrm{d}\eta \qquad \overline{H}_i^{(q)} := \big(H_i^{(q)} + H_{i+1}^{(q)}\big)/2$$

$$= 2\int_0^{\delta H_i^{(q)}/2} \cos^p \eta' \,\mathrm{d}\eta' \qquad \eta' \leftarrow \eta - H_i^{(q)}$$

Sketch of the proof

Sketch of the proof

- $$\mathbb{E}\left[\mathsf{G}_{\mathrm{X}}^{\max}(\boldsymbol{x})\right] = \frac{1}{\pi}\sum_{i=0}^{n_q-1} \sin\frac{\delta H_i^{(q)}}{2};$$
- $$\mathbb{E}\left[\mathsf{G}_{\mathrm{X}}^{\max}(\boldsymbol{x})^2\right] = \frac{1}{2} + \frac{1}{4\pi}\sum_{i=0}^{n_q-1} \sin\delta H_i^{(q)}.$$

Sketch of the proof

- $$\mathbb{E}\left[\mathsf{G}_{\mathrm{X}}^{\max}(\boldsymbol{x})\right] = \frac{1}{\pi}\sum_{i=0}^{n_q-1}\sin\frac{\delta H_i^{(q)}}{2};$$
- $$\mathbb{E}\left[\mathsf{G}_{\mathrm{X}}^{\max}(\boldsymbol{x})^2\right] = \frac{1}{2} + \frac{1}{4\pi}\sum_{i=0}^{n_q-1}\sin\delta H_i^{(q)}.$$
- $\mathsf{Q}_{\mathrm{X}} := 1 - \mathsf{G}_{\mathrm{X}}^{\max}$

Sketch of the proof

- $\mathbb{E}\left[\mathsf{G}_{\mathrm{X}}^{\max}(\boldsymbol{x})\right] = \dfrac{1}{\pi}\displaystyle\sum_{i=0}^{n_q-1} \sin \frac{\delta H_i^{(q)}}{2};$
- $\mathbb{E}\left[\mathsf{G}_{\mathrm{X}}^{\max}(\boldsymbol{x})^2\right] = \dfrac{1}{2} + \dfrac{1}{4\pi}\displaystyle\sum_{i=0}^{n_q-1} \sin \delta H_i^{(q)}.$
- $\mathsf{Q}_{\mathrm{X}} := 1 - \mathsf{G}_{\mathrm{X}}^{\max}$
- By linearity of the expected value

$$\mathbb{E}\left[\mathsf{Q}_{\mathrm{X}}(\boldsymbol{x})^2\right] := \frac{3}{2} + \frac{1}{4\pi}\sum_{i=0}^{n_q-1}\left(\sin \delta H_i^{(q)} - 8 \sin \frac{\delta H_i^{(q)}}{2}\right)$$

Main result

- Shift invariance of ℝ**Max** outputs

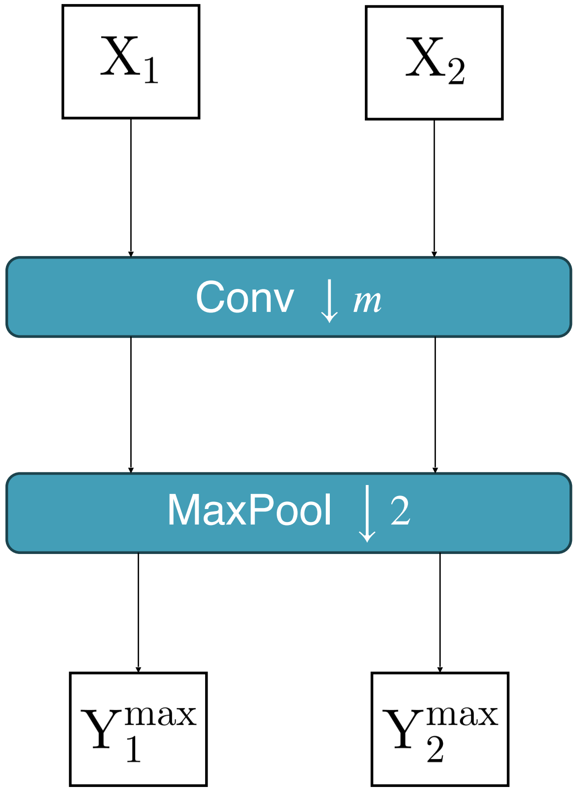

$$\boldsymbol{\theta} \mapsto \gamma_q(m\boldsymbol{\theta})^2$$
$$q = 1$$

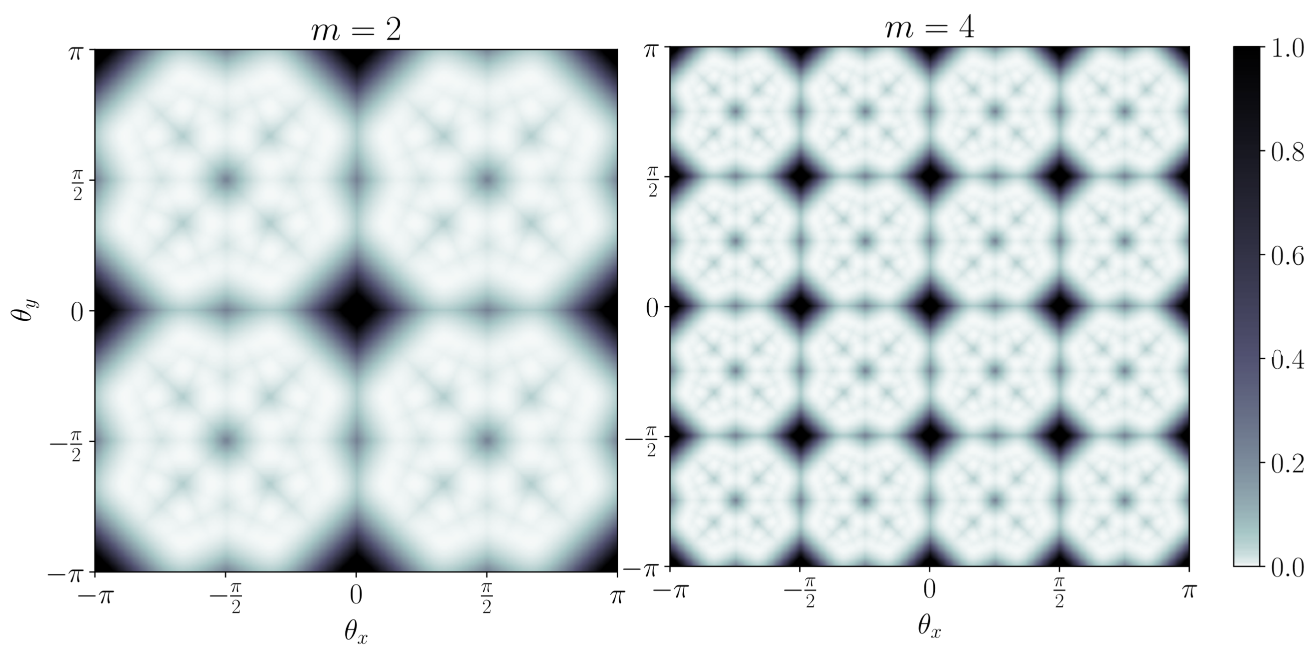

Main result

- Shift invariance of $\mathbb{R}$**Max** outputs

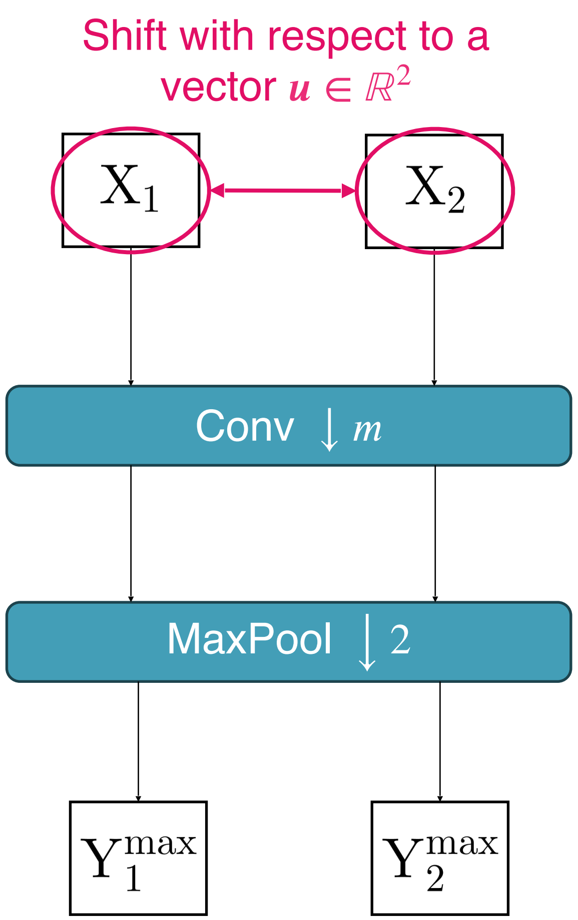

$$\boldsymbol{\theta} \mapsto \gamma_q(m\boldsymbol{\theta})^2$$
$$q = 1$$

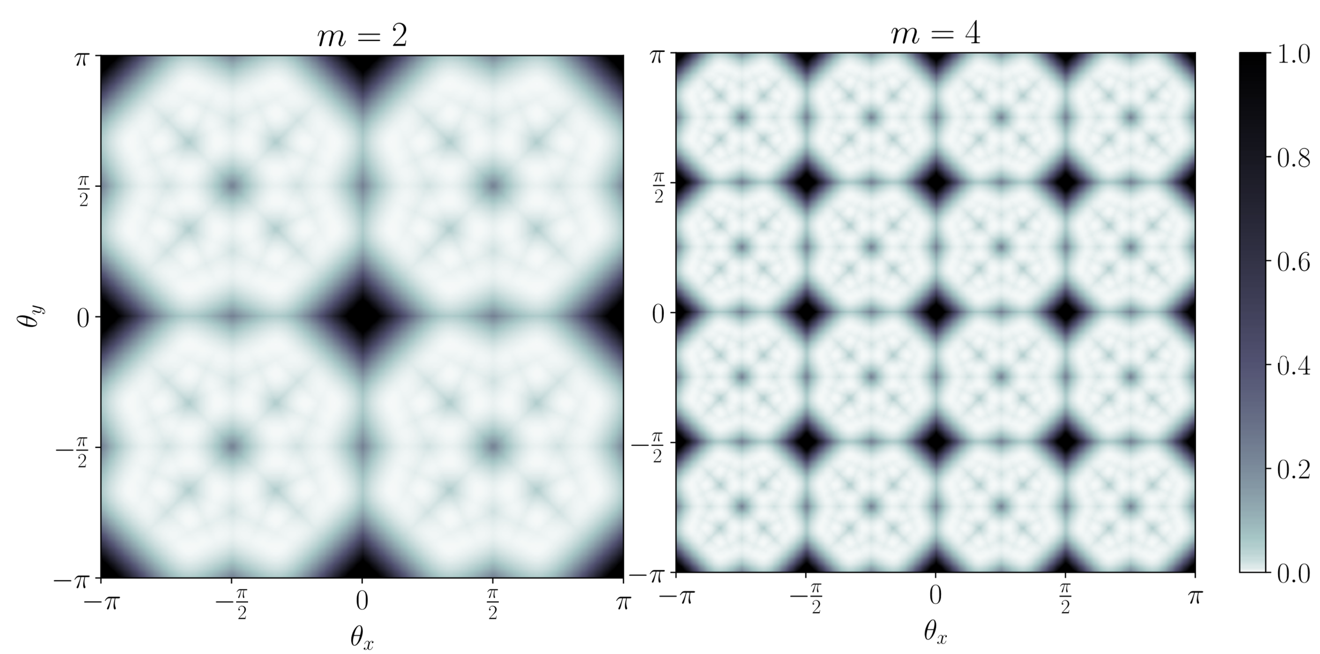

Main result

- Shift invariance of $\mathbb{R}$**Max** outputs

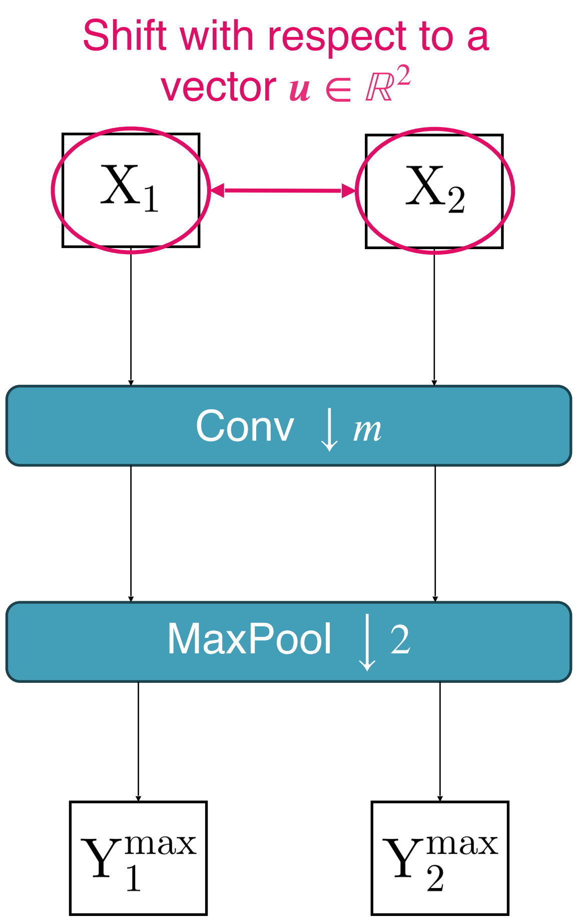

$$\mathbb{E}\left[\frac{\|Y_1^{\max} - Y_2^{\max}\|_2}{\left\|Y_1^{\mathrm{mod}}\right\|_2}\right] \leq 2\big(\beta_q(m\kappa) + \gamma_q(m\boldsymbol{\theta})\big) + \alpha(\kappa\boldsymbol{u})$$

$$\boldsymbol{\theta} \mapsto \gamma_q(m\boldsymbol{\theta})^2$$
$$q = 1$$

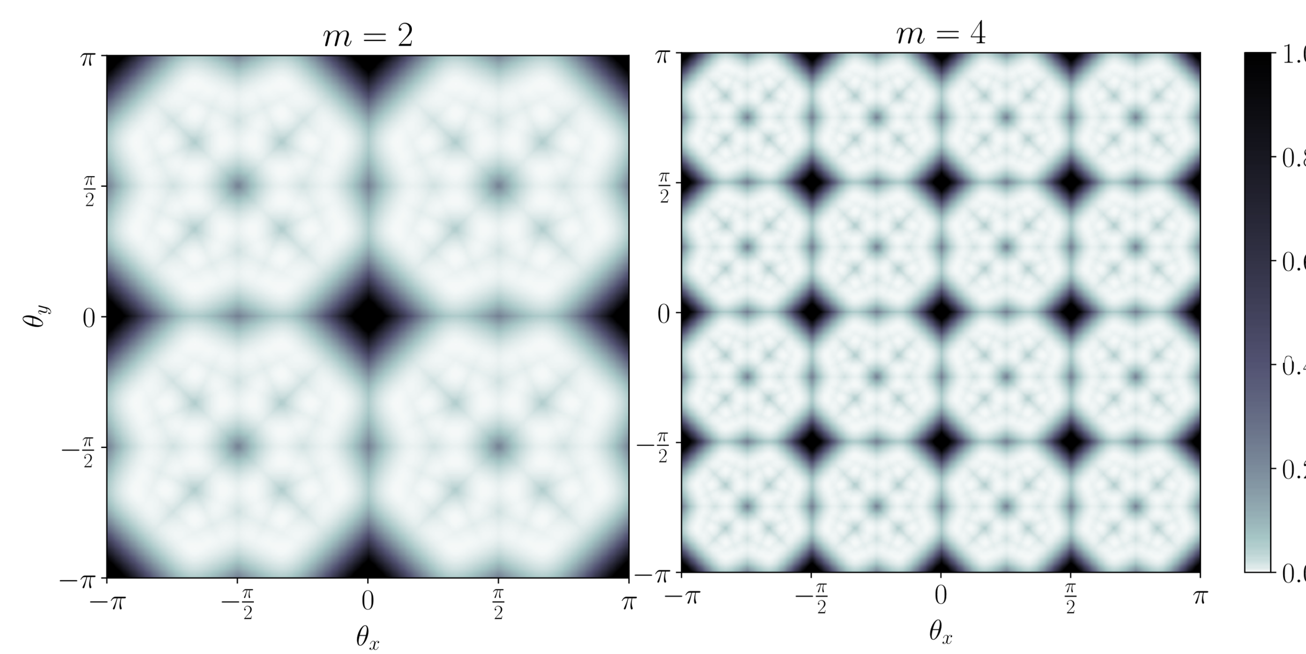

Main result

- Shift invariance of $\mathbb{R}$**Max** outputs

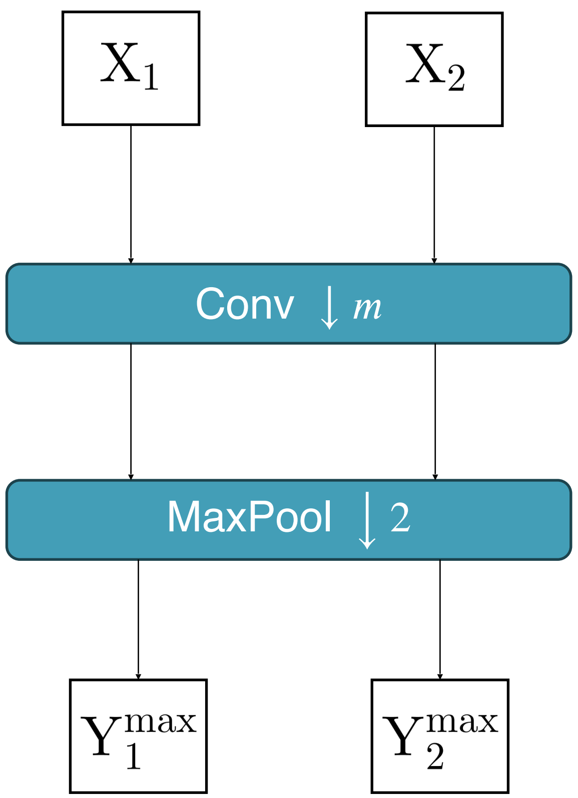

$$\mathbb{E}\left[\frac{\|\mathrm{Y}_1^{\max} - \mathrm{Y}_2^{\max}\|_2}{\left\|\mathrm{Y}_1^{\mathrm{mod}}\right\|_2}\right] \leq 2\big(\beta_q(m\kappa) + \gamma_q(m\boldsymbol{\theta})\big) + \alpha(\kappa\boldsymbol{u})$$

Divergence $\mathbb{R}$Max-$\mathbb{C}$Mod

$$\boldsymbol{\theta} \mapsto \gamma_q(m\boldsymbol{\theta})^2 \quad q = 1$$

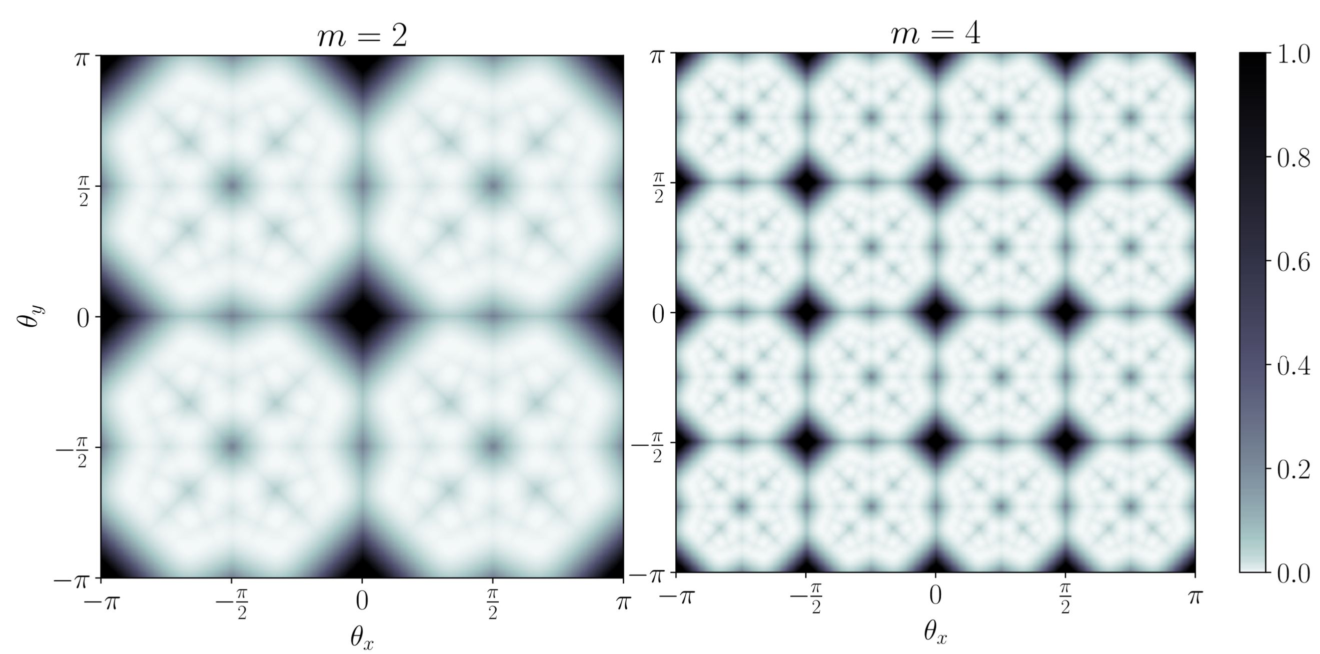

Main result

- Shift invariance of $\mathbb{R}\mathbf{Max}$ outputs

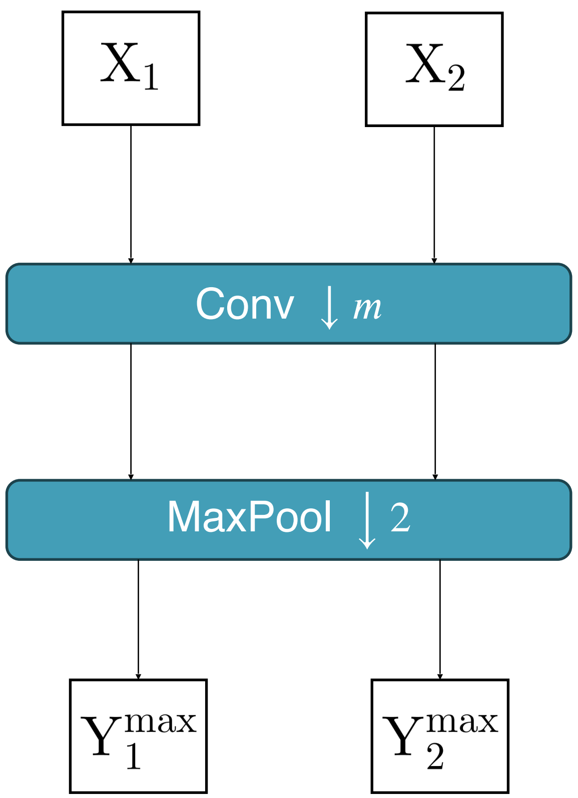

$$\mathbb{E}\left[\frac{\|Y_1^{\max} - Y_2^{\max}\|_2}{\|Y_1^{\mathrm{mod}}\|_2}\right] \leq 2\big(\beta_q(m\kappa) + \gamma_q(m\boldsymbol{\theta})\big) + \alpha(\kappa\boldsymbol{u})$$

Shift invariance of $\mathbb{C}\mathrm{Mod}$ ($O(\kappa\boldsymbol{u})$)

$$\boldsymbol{\theta} \mapsto \gamma_q(m\boldsymbol{\theta})^2$$
$$q = 1$$

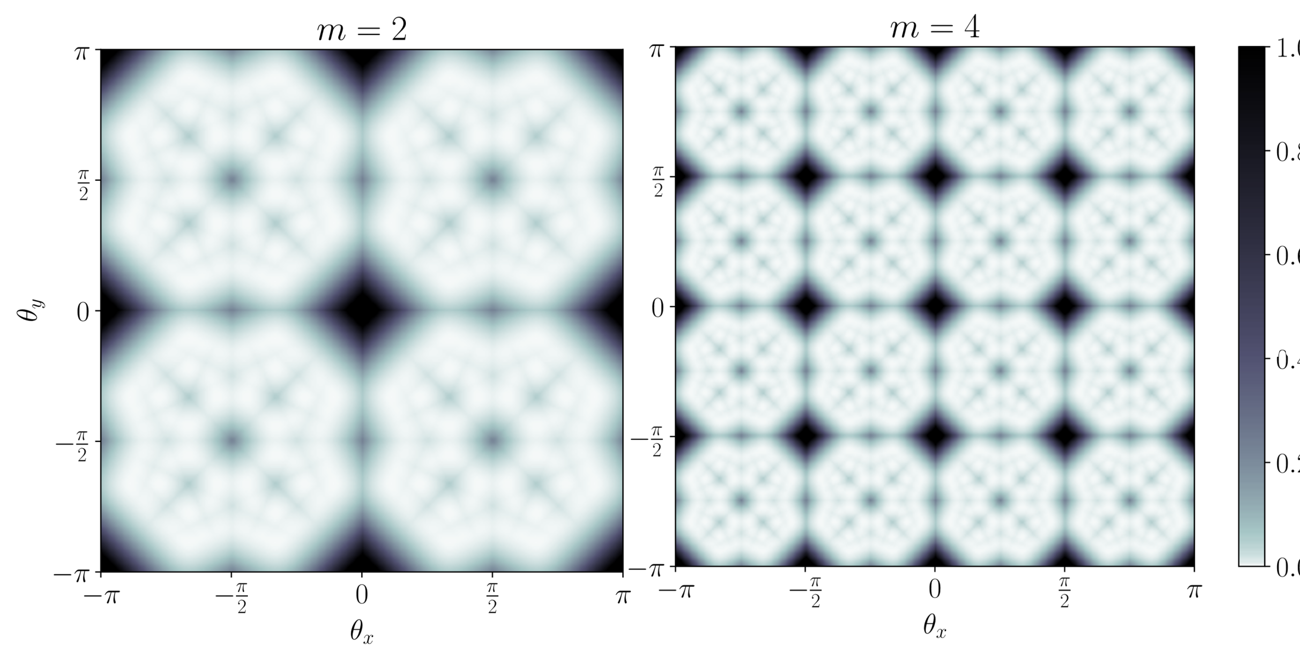

Experimental validation

Experimental validation

- **What we need:**

Experimental validation

- **What we need:**
  - A fully deterministic model with predefined convolution kernels

Experimental validation

- **What we need:**
  - A fully deterministic model with predefined convolution kernels
  - A set of Gabor-like filters tiling the entire frequency plane and a unique bandwidth share across all filters

Experimental validation

- **What we need:**
  - A fully deterministic model with predefined convolution kernels
  - A set of Gabor-like filters tiling the entire frequency plane and a unique bandwidth share across all filters
  - No prediction, only the first layers are implemented

Experimental validation

- **What we need:**
  - A fully deterministic model with predefined convolution kernels
  - A set of Gabor-like filters tiling the entire frequency plane and a unique bandwidth share across all filters
  - No prediction, only the first layers are implemented
  - Dataset: ImageNet-1K, validation set (50 000 images)

Experimental validation

- **What we need:**
  - A fully deterministic model with predefined convolution kernels
  - A set of Gabor-like filters tiling the entire frequency plane and a unique bandwidth share across all filters
  - No prediction, only the first layers are implemented
  - Dataset: ImageNet-1K, validation set (50 000 images)
- **Proposed solution:**

Experimental validation

- **What we need:**
  - A fully deterministic model with predefined convolution kernels
  - A set of Gabor-like filters tiling the entire frequency plane and a unique bandwidth share across all filters
  - No prediction, only the first layers are implemented
  - Dataset: ImageNet-1K, validation set (50 000 images)
- **Proposed solution:**
  - The dual-tree complex wavelet packet transform (DT-CWPT)

Experimental validation

- **What we need:**
  - A fully deterministic model with predefined convolution kernels
  - A set of Gabor-like filters tiling the entire frequency plane and a unique bandwidth share across all filters
  - No prediction, only the first layers are implemented
  - Dataset: ImageNet-1K, validation set (50 000 images)
- **Proposed solution:**
  - The dual-tree complex wavelet packet transform (DT-CWPT)

I. Bayram and I. W. Selesnick, "On the Dual-Tree Complex Wavelet Packet and M-Band Transforms," IEEE TSP, 2008.

Experimental validation

- **What we need:**
  - A fully deterministic model with predefined convolution kernels
  - A set of Gabor-like filters tiling the entire frequency plane and a unique bandwidth share across all filters
  - No prediction, only the first layers are implemented
  - Dataset: ImageNet-1K, validation set (50 000 images)
- **Proposed solution:**
  - The dual-tree complex wavelet packet transform (DT-CWPT)
  - The bandwidth and subsampling are controlled by the depth J

I. Bayram and I. W. Selesnick, "On the Dual-Tree Complex Wavelet Packet and M-Band Transforms," IEEE TSP, 2008.

Experiments

- Filters generated by the DT-CWPT

Case $J = 2$ (two levels of dual-tree decomposition):
$\kappa = \pi/2$;
$m = 2$;
32 filters + complex conjugates.

Experiments

- Filters generated by the DT-CWPT

Case $J = 2$ (two levels of dual-tree decomposition):
$\kappa = \pi/2$;
$m = 2$;
32 filters + complex conjugates.

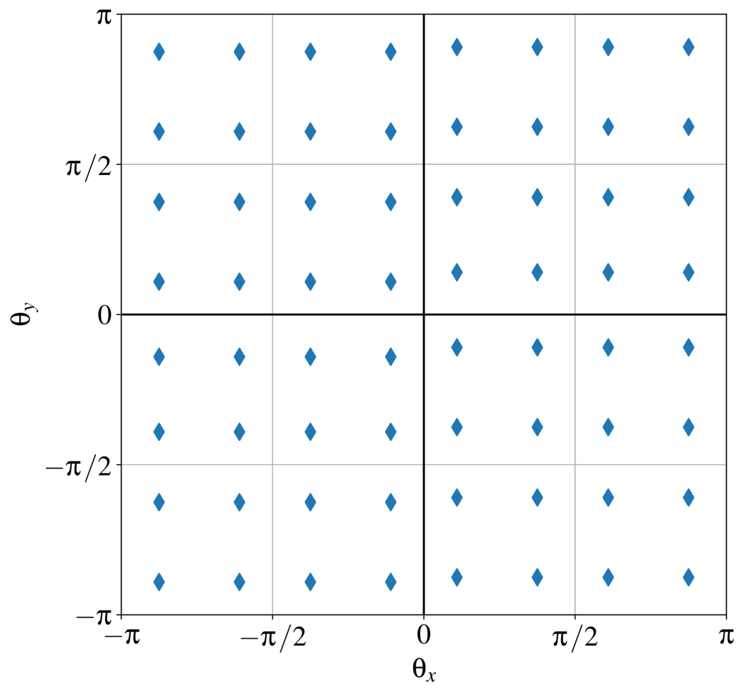

Experiments

- Filters generated by the DT-CWPT

Case $J = 2$ (two levels of dual-tree decomposition):
$\kappa = \pi/2$;
$m = 2$;
32 filters + complex conjugates.

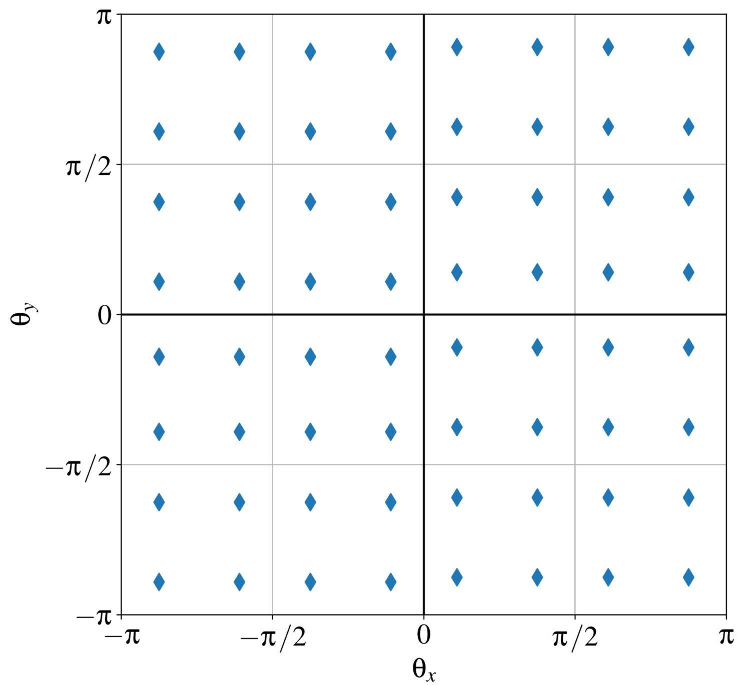

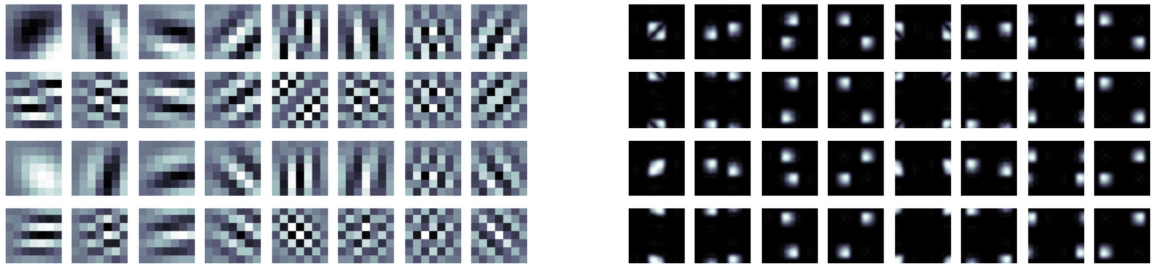

Spatial domain   Fourier domain

DT-ℂWPT
(real part only)

Experiments

- Filters generated by the DT-CWPT

Case $J = 2$ (two levels of dual-tree decomposition):
$\kappa = \pi/2$;
$m = 2$;
32 filters + complex conjugates.

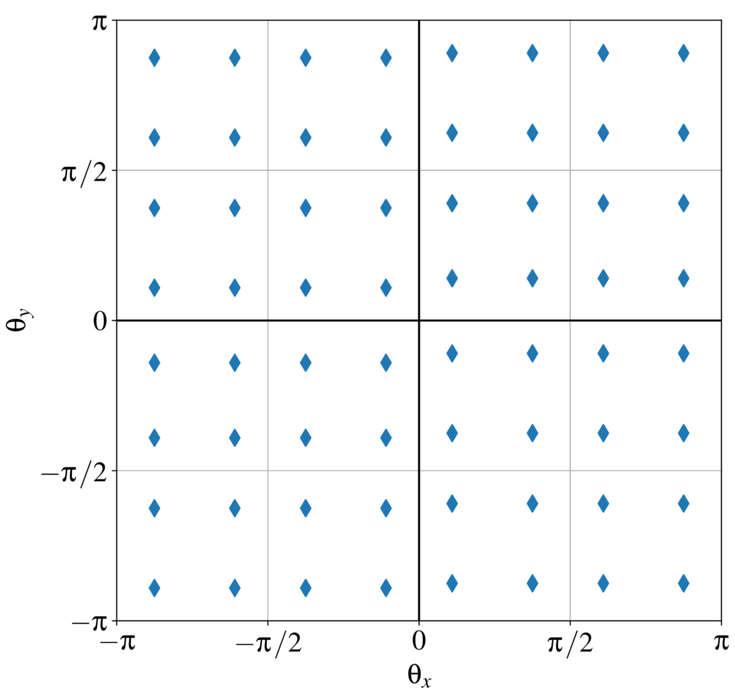

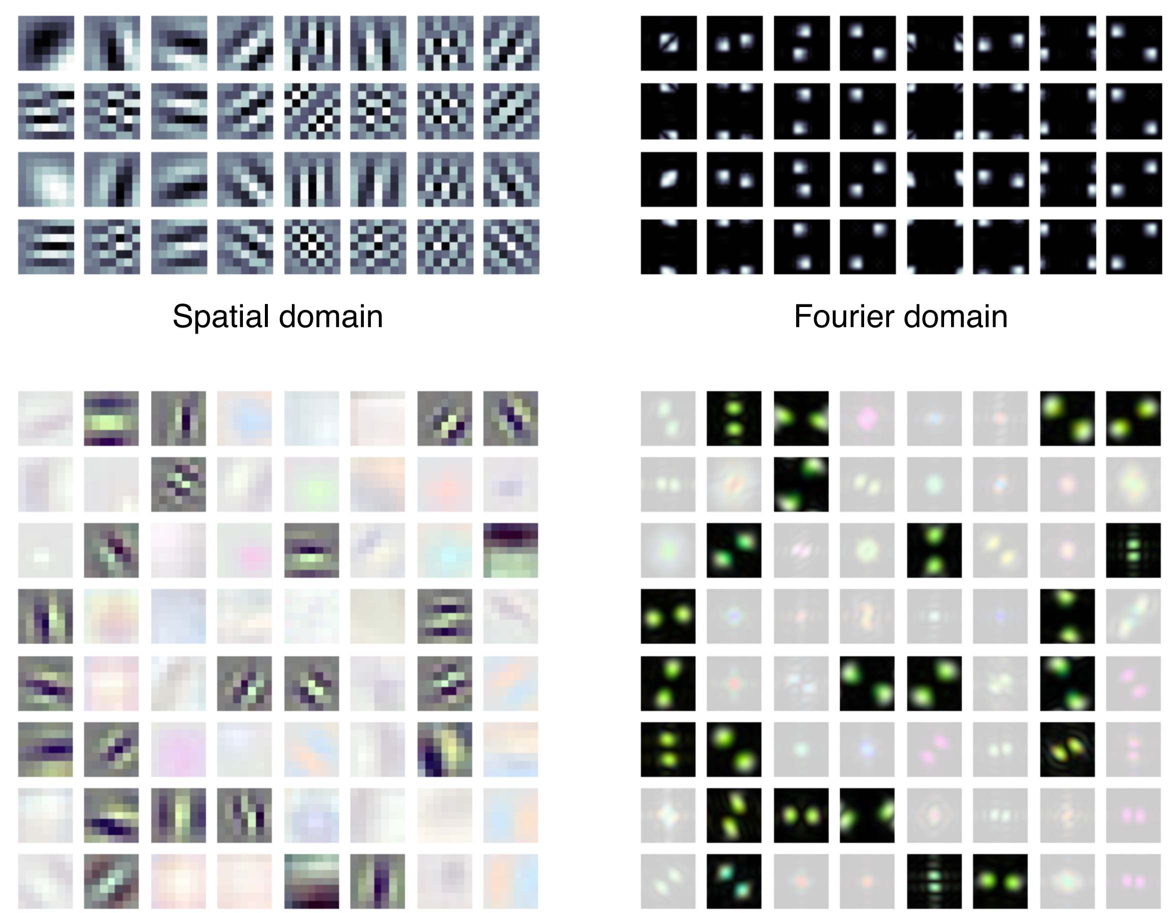

Experiments

- Filters generated by the DT-CWPT

Case $J = 3$ (three levels of dual-tree decomposition):
$\kappa = \pi/4$;
$m = 4$;
128 filters + complex conjugates.

Experiments

- Filters generated by the DT-CWPT

Case $J = 3$ (three levels of dual-tree decomposition):
$\kappa = \pi/4$;
$m = 4$;
128 filters + complex conjugates.

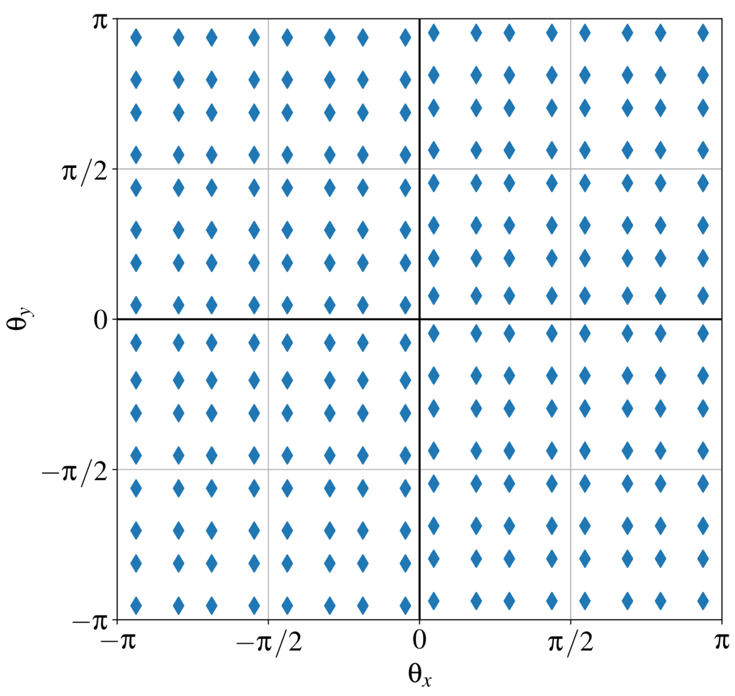

Experiments

- Filters generated by the DT-CWPT

Case $J = 3$ (three levels of dual-tree decomposition):

$\kappa = \pi/4$;

$m = 4$;

128 filters + complex conjugates.

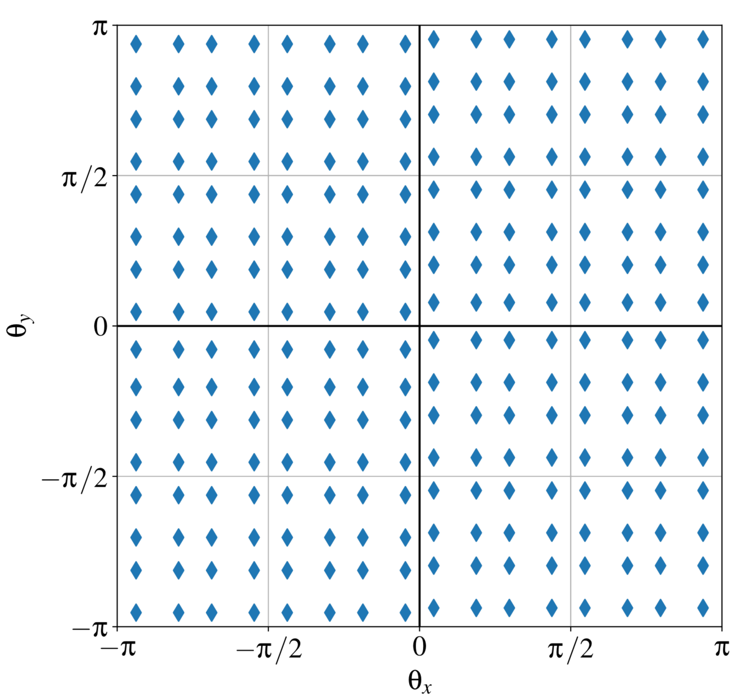

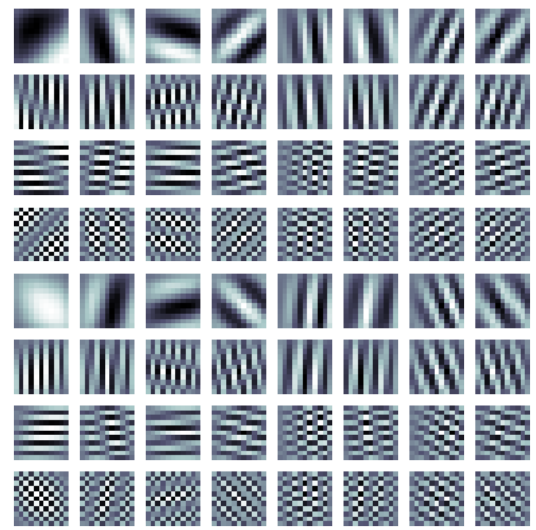

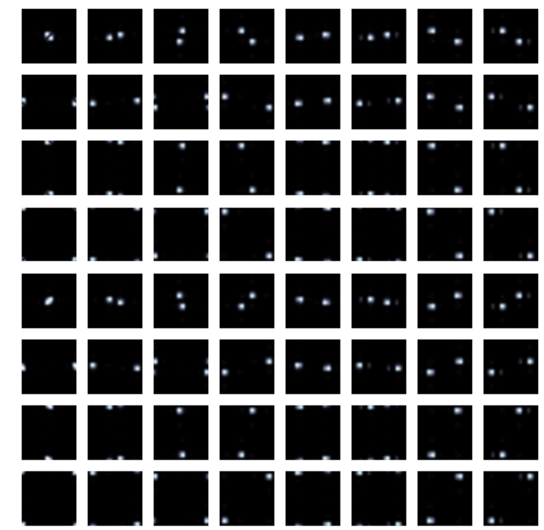

DT-$\mathbb{C}$WPT (subset, real part only)

Experiments

- Filters generated by the DT-CWPT

Case $J = 3$ (three levels of dual-tree decomposition):
$\kappa = \pi/4$;
$m = 4$;
128 filters + complex conjugates.

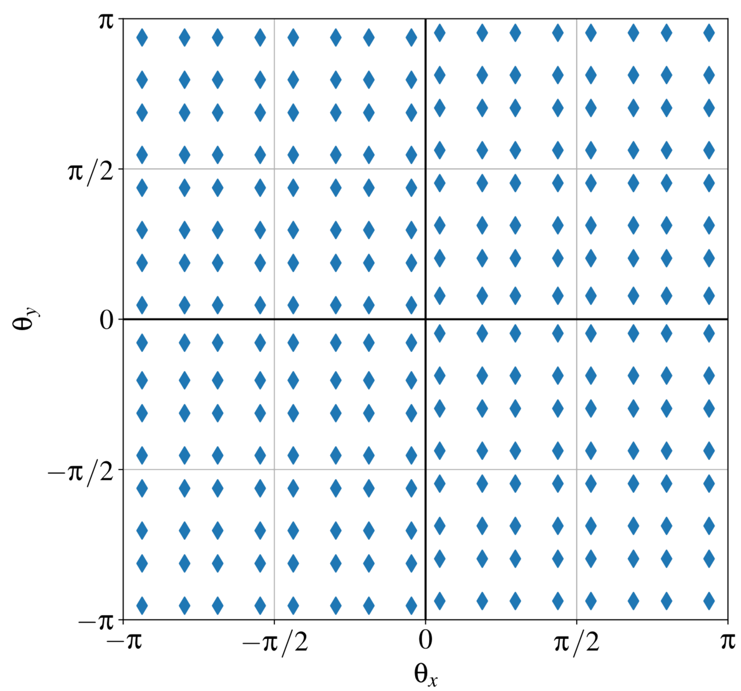

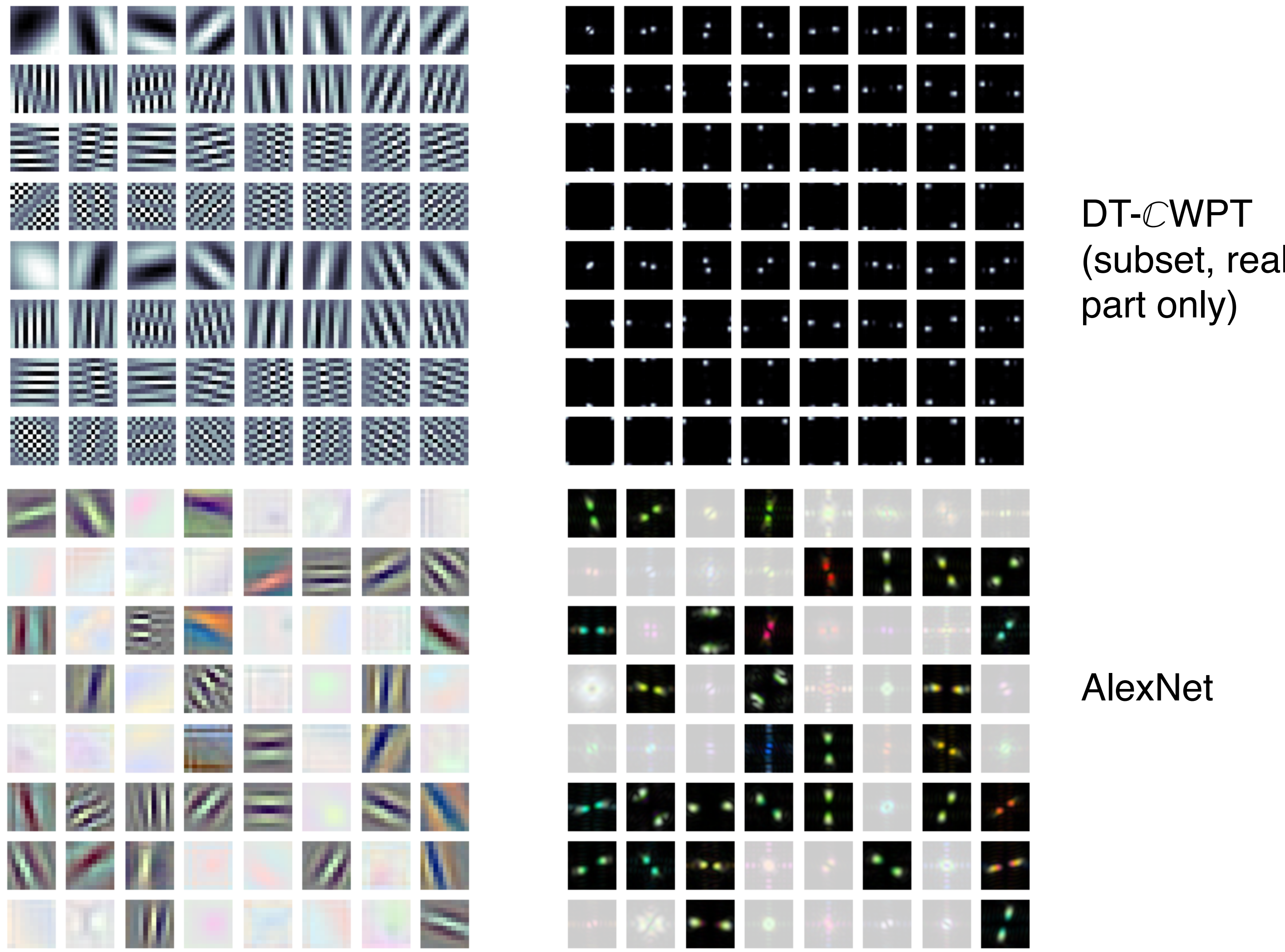

Spatial domain

Fourier domain

Experiments

- Normalized MSE between $\mathbb{C}$**Mod** and $\mathbb{R}$**Max**

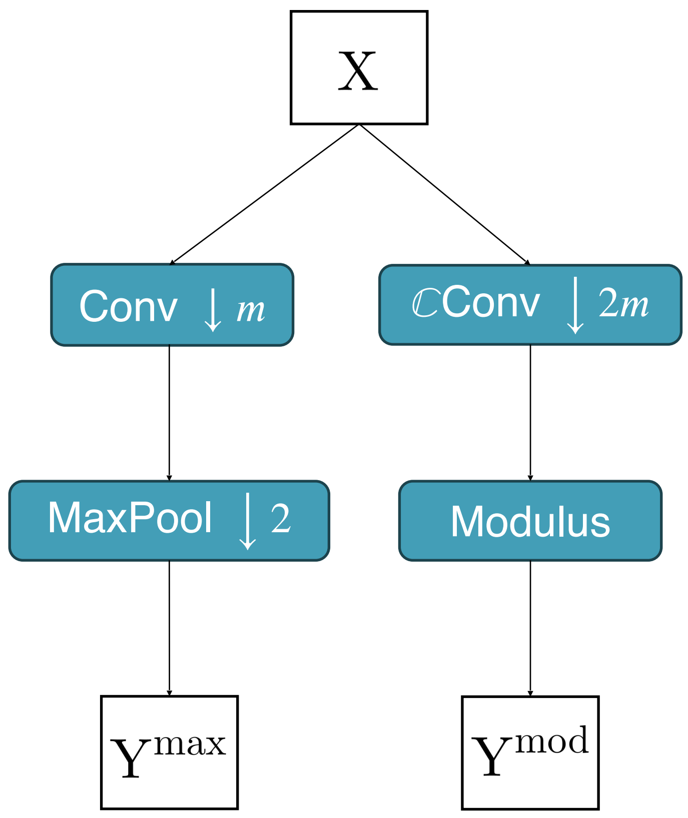

Experiments

- Normalized MSE between $\mathbb{C}$**Mod** and $\mathbb{R}$**Max**

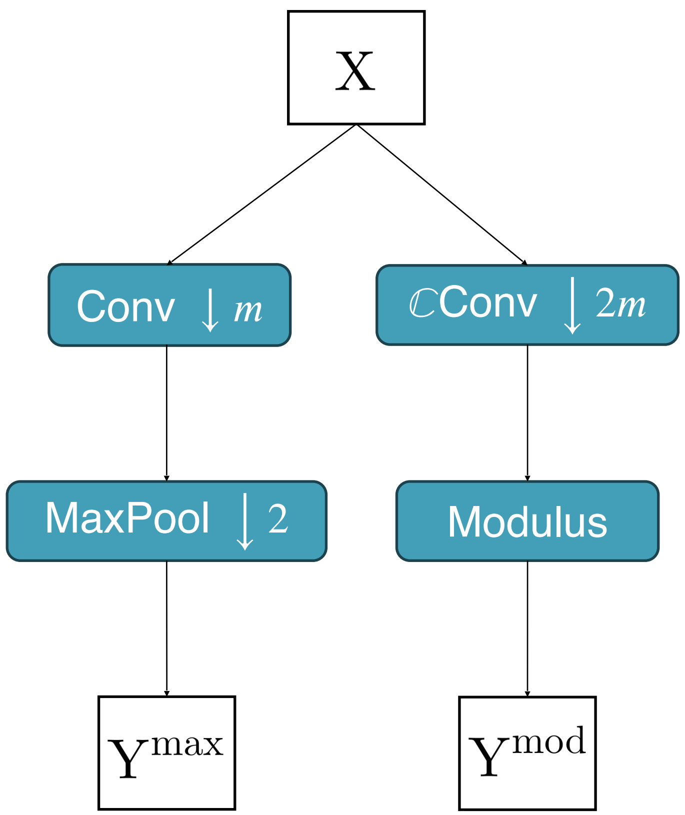

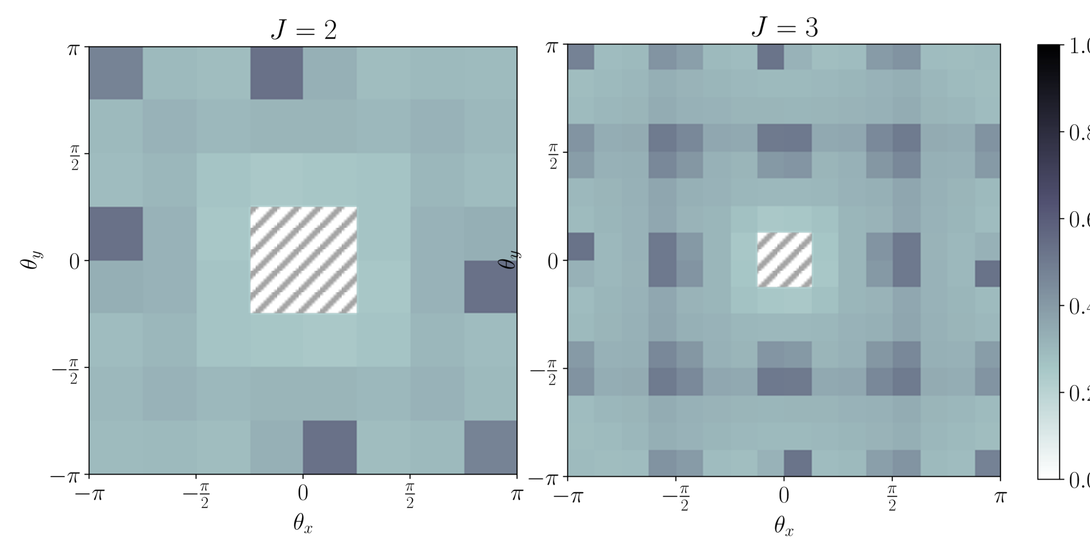

$$\rho^2 = \frac{\left\|\mathrm{Y}^{\max} - \mathrm{Y}^{\mathrm{mod}}\right\|_2^2}{\left\|\mathrm{Y}^{\mathrm{mod}}\right\|_2^2}$$

Experiments

- Normalized MSE between **ℂMod** and **ℝMax**

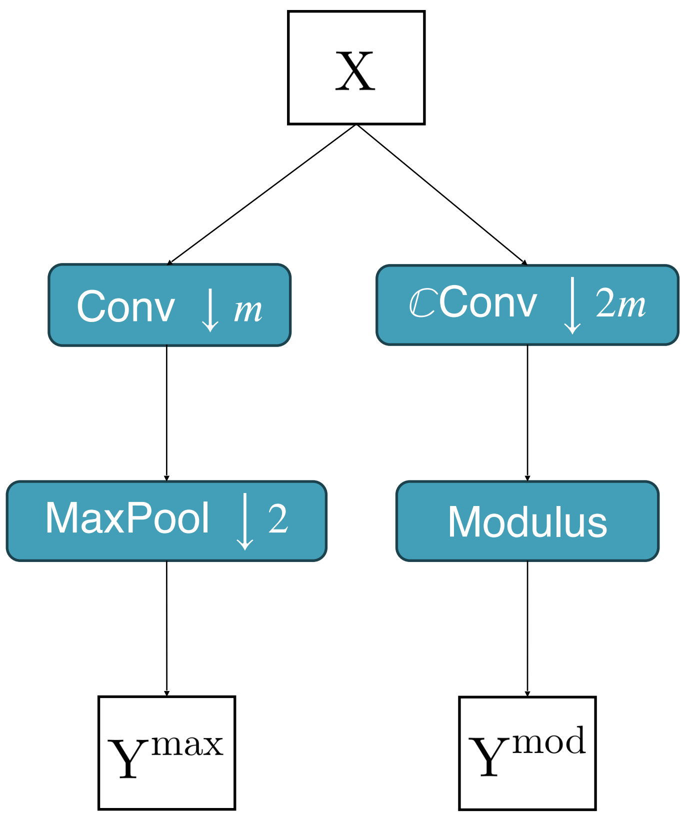

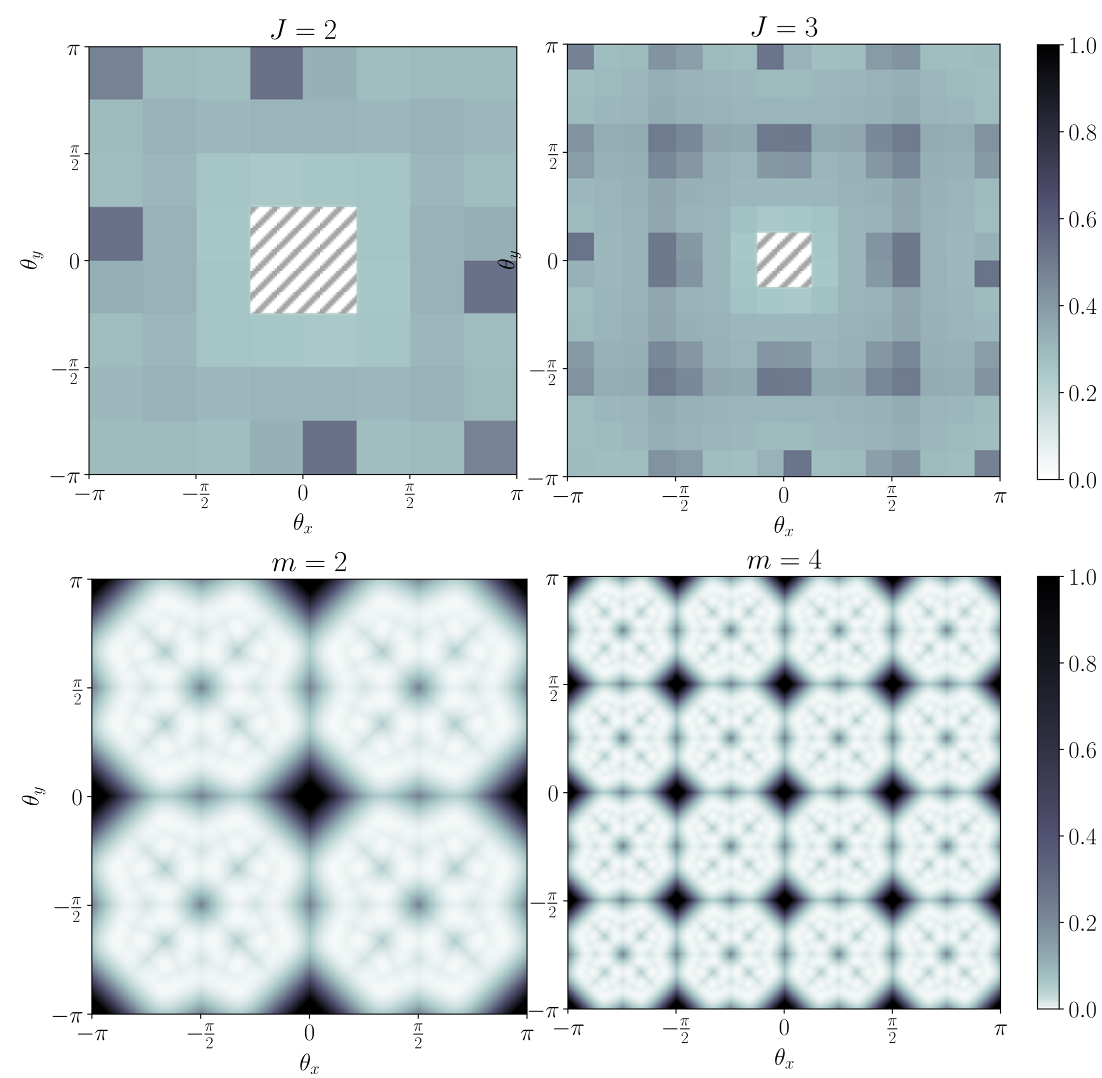

$$\rho^2 = \frac{\left\| \mathrm{Y}^{\max} - \mathrm{Y}^{\mathrm{mod}} \right\|_2^2}{\left\| \mathrm{Y}^{\mathrm{mod}} \right\|_2^2}$$

$$\boldsymbol{\theta} \mapsto \gamma_q(m\boldsymbol{\theta})^2$$

Experiments

- Normalized MSE between $\mathbb{C}$**Mod** and $\mathbb{R}$**Max**

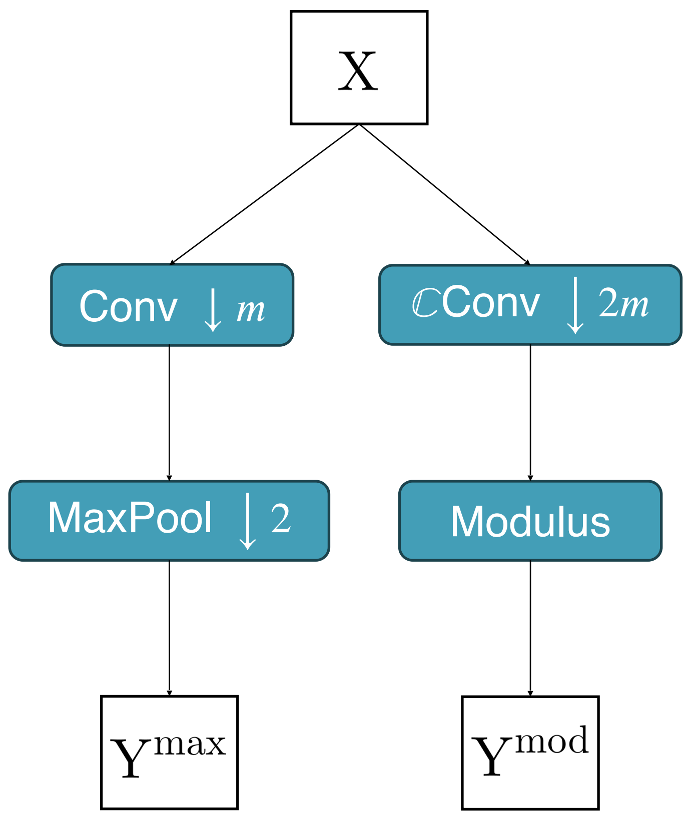

Outside the scope of our study (low-pass filters)

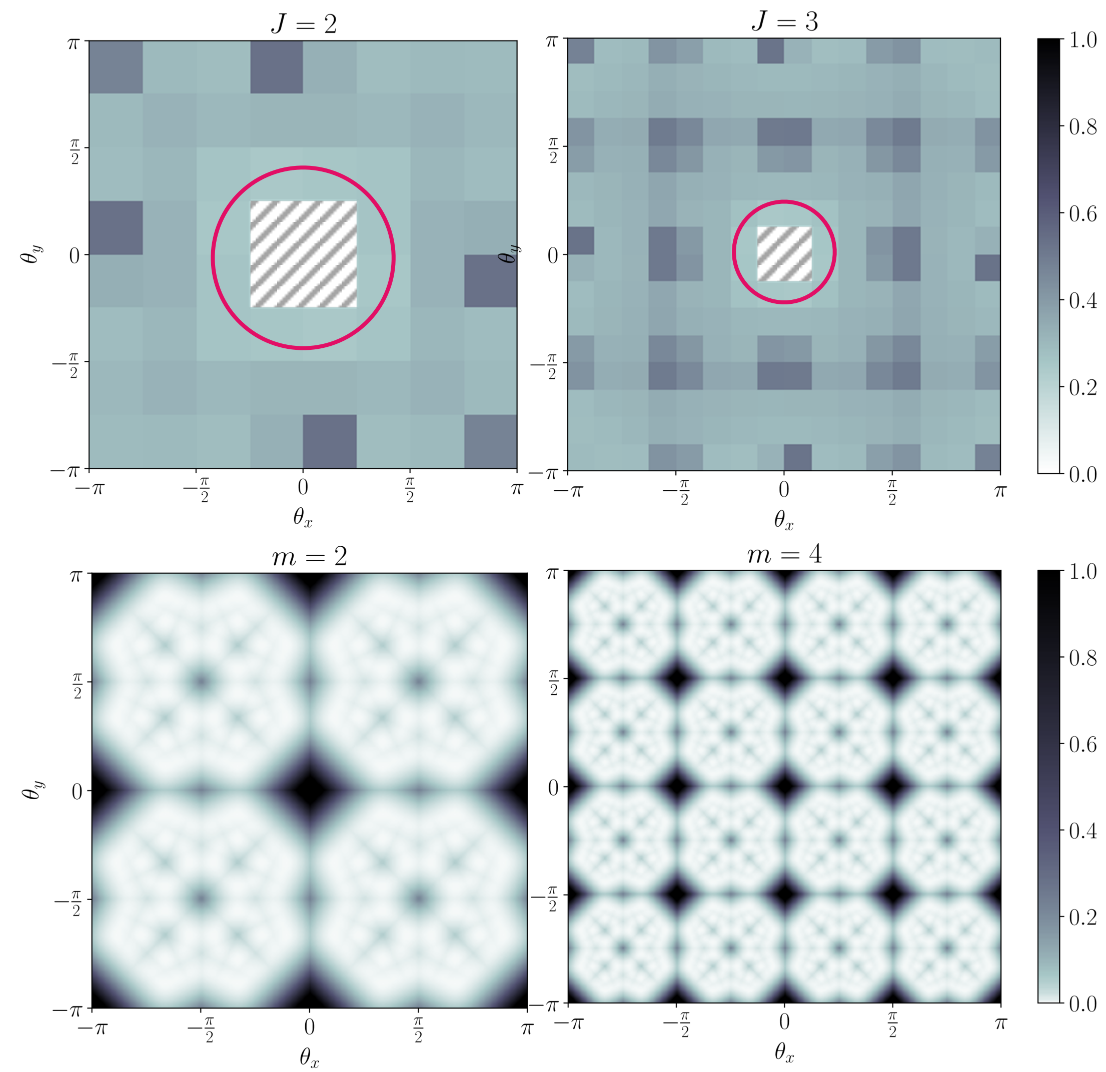

$$\rho^2 = \frac{\left\| \mathrm{Y}^{\max} - \mathrm{Y}^{\mathrm{mod}} \right\|_2^2}{\left\| \mathrm{Y}^{\mathrm{mod}} \right\|_2^2}$$

$$\boldsymbol{\theta} \mapsto \gamma_q(m\boldsymbol{\theta})^2$$

Experiments

- Normalized MSE between $\mathbb{C}$**Mod** and $\mathbb{R}$**Max**

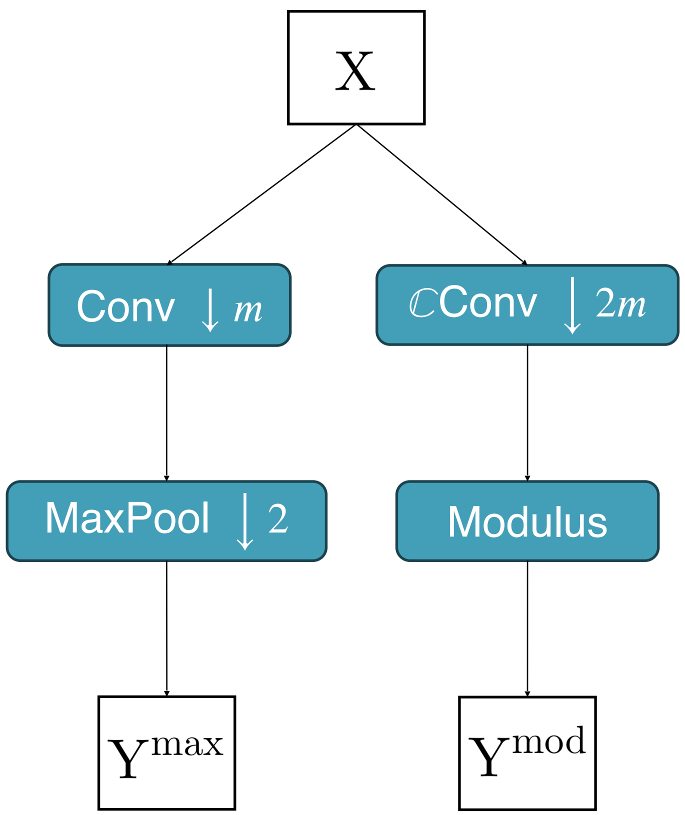

ResNet-like scenario
$J = 2,\ m = 2,\ \kappa = \pi/2$

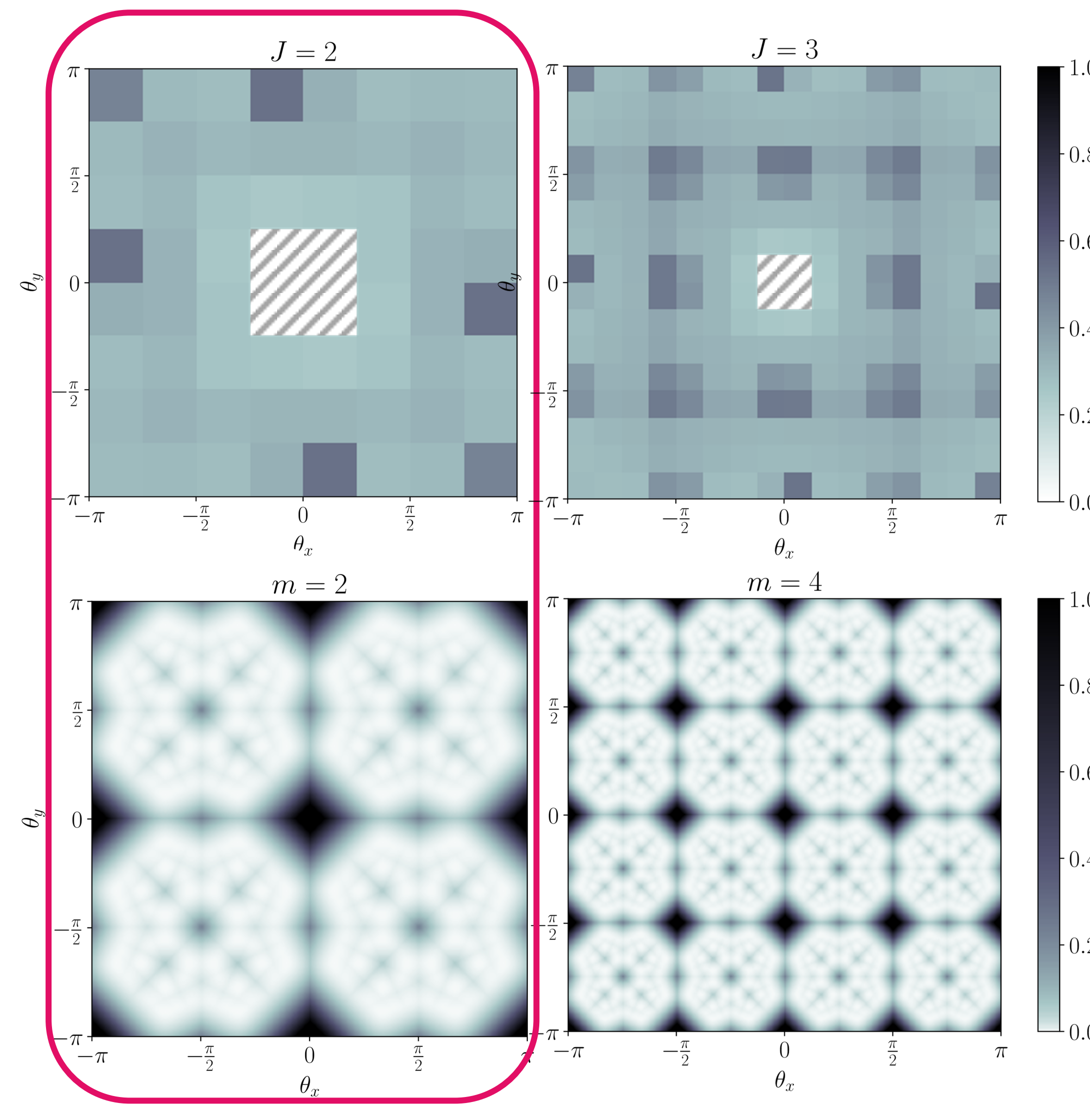

$$\rho^2 = \frac{\left\| Y^{\max} - Y^{\mathrm{mod}} \right\|_2^2}{\left\| Y^{\mathrm{mod}} \right\|_2^2}$$

$$\boldsymbol{\theta} \mapsto \gamma_q(m\boldsymbol{\theta})^2$$

Experiments

- Normalized MSE between $\mathbb{C}$**Mod** and $\mathbb{R}$**Max**

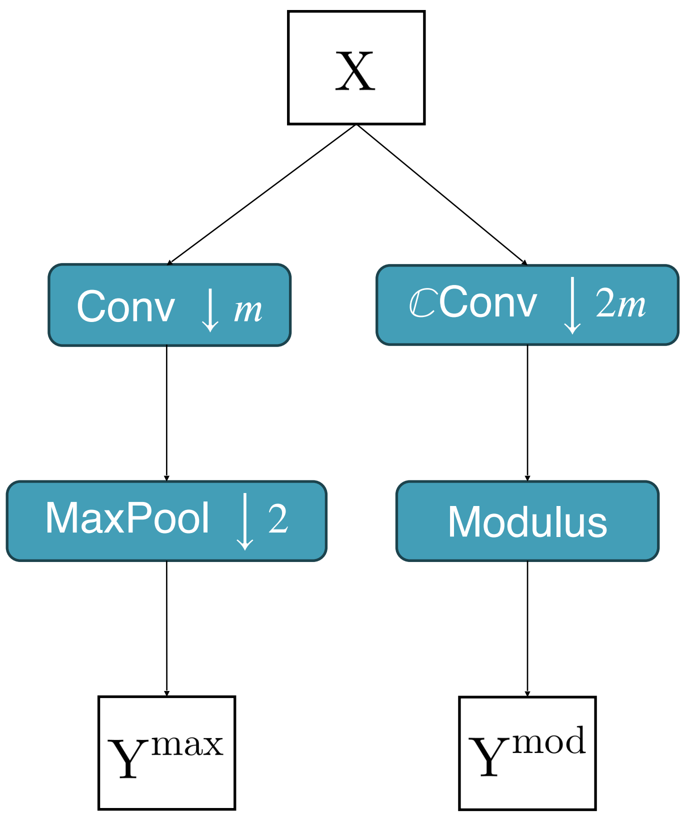

AlexNet-like scenario
$J = 3,\ m = 4,\ \kappa = \pi/4$

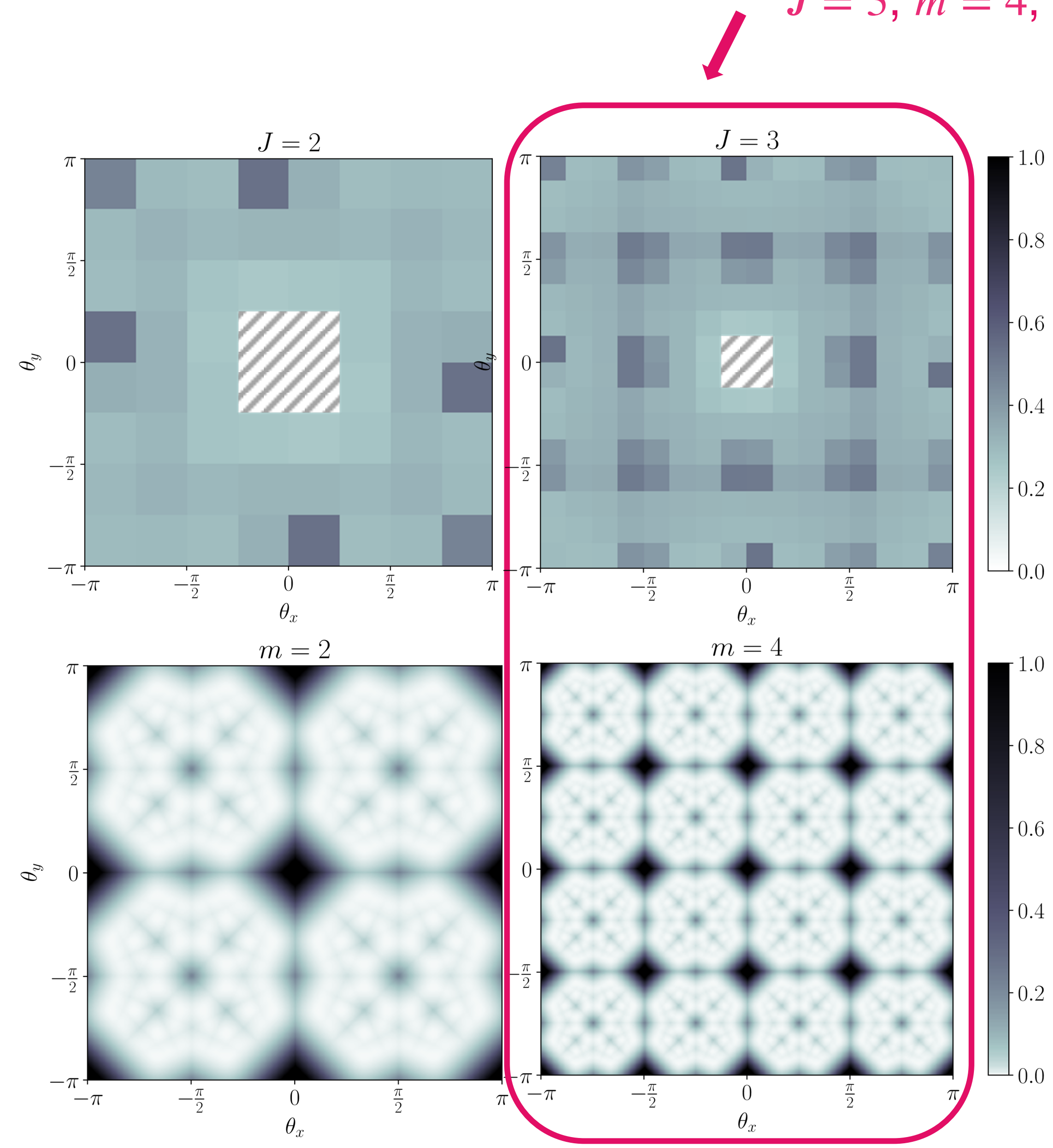

$$\rho^2 = \frac{\left\|\mathrm{Y}^{\max} - \mathrm{Y}^{\mathrm{mod}}\right\|_2^2}{\left\|\mathrm{Y}^{\mathrm{mod}}\right\|_2^2}$$

$$\boldsymbol{\theta} \mapsto \gamma_q(m\boldsymbol{\theta})^2$$

Experiments

- Shift-invariance of $\mathbb{R}$**Max** outputs

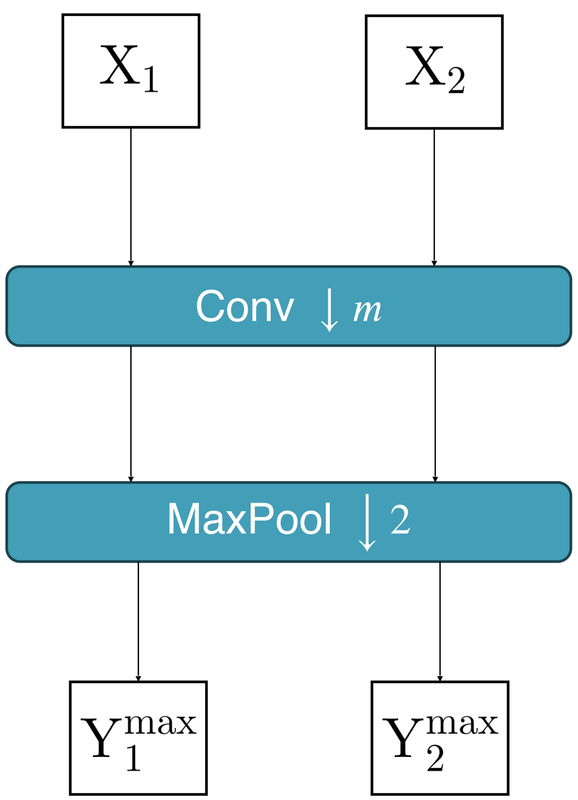

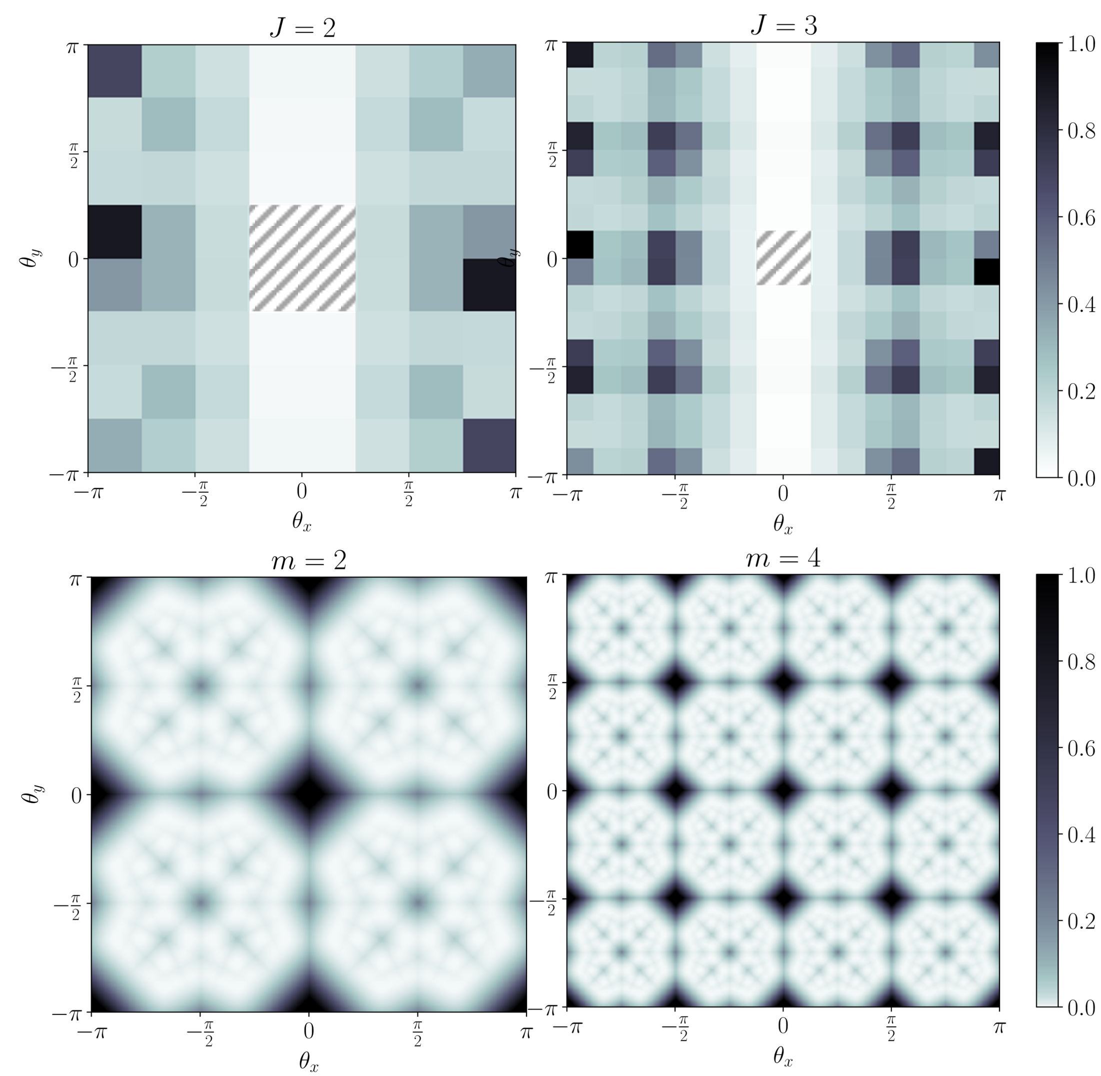

$$\rho^{\max} = \frac{\left\| \mathrm{Y}_1^{\max} - \mathrm{Y}_2^{\max} \right\|_2}{\left\| \mathrm{Y}_1^{\mathrm{mod}} \right\|_2}$$

$$\boldsymbol{\theta} \mapsto \gamma_q(m\boldsymbol{\theta})^2$$

Experiments

- Shift-invariance of $\mathbb{R}$**Max** outputs

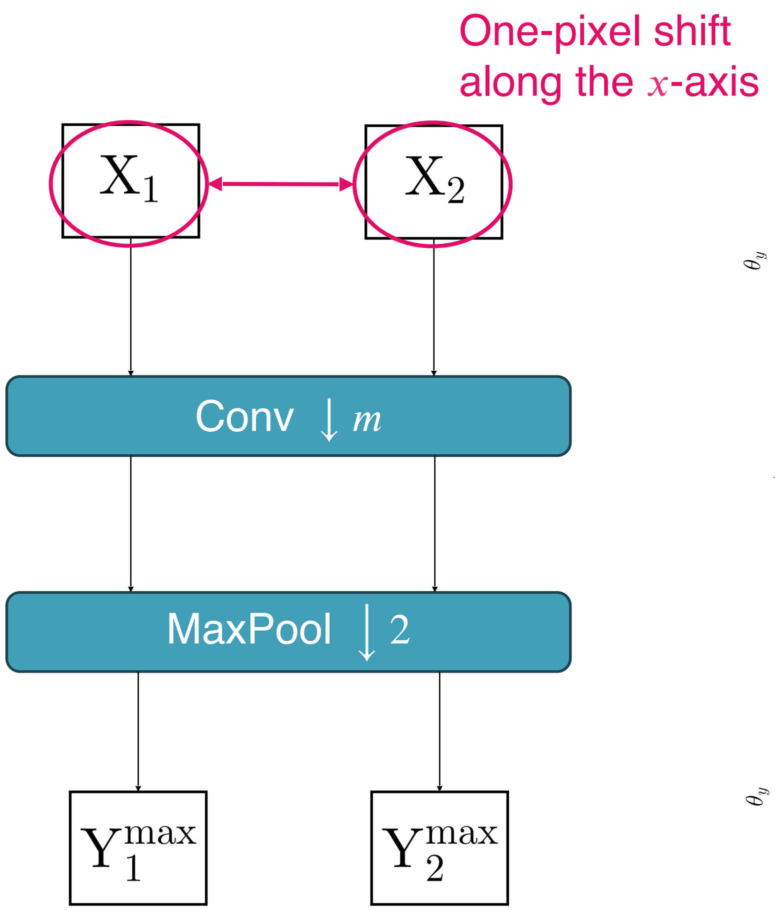

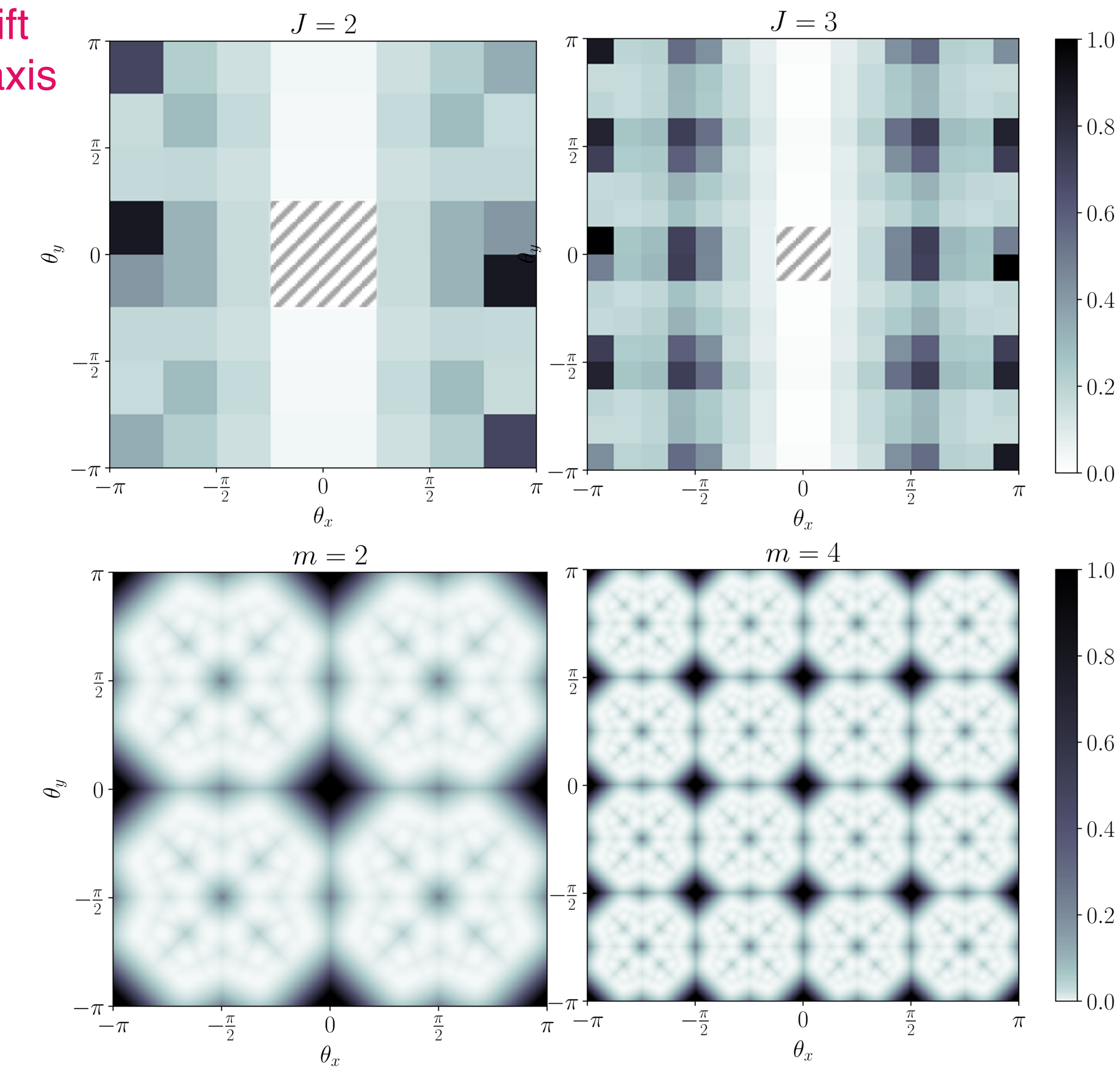

$$\rho^{\max} = \frac{\left\| Y_1^{\max} - Y_2^{\max} \right\|_2}{\left\| Y_1^{\mathrm{mod}} \right\|_2}$$

$$\boldsymbol{\theta} \mapsto \gamma_q(m\boldsymbol{\theta})^2$$

Conclusion

Conclusion

- Exploration of the shift invariance properties captured by the max pooling operator, when applied on the first layer.

Conclusion

- Exploration of the shift invariance properties captured by the max pooling operator, when applied on the first layer.

- Bridge between complex and standard real CNNs.

Conclusion

- Exploration of the shift invariance properties captured by the max pooling operator, when applied on the first layer.
- Bridge between complex and standard real CNNs.
- Study of the discrete case in a probabilist framework.

Conclusion

- Exploration of the shift invariance properties captured by the max pooling operator, when applied on the first layer.
- Bridge between complex and standard real CNNs.
- Study of the discrete case in a probabilist framework.
- Establish a validity domain for near-shift invariance.

Conclusion

- Exploration of the shift invariance properties captured by the max pooling operator, when applied on the first layer.
- Bridge between complex and standard real CNNs.
- Study of the discrete case in a probabilist framework.
- Establish a validity domain for near-shift invariance.
- Experimental setting based on the dual-tree complex wavelet packet transform

Conclusion

- Exploration of the shift invariance properties captured by the max pooling operator, when applied on the first layer.
- Bridge between complex and standard real CNNs.
- Study of the discrete case in a probabilist framework.
- Establish a validity domain for near-shift invariance.
- Experimental setting based on the dual-tree complex wavelet packet transform
- $\mathbb{C}\mathbf{Mod}$ operator can serve as a stable proxy for $\mathbb{R}\mathbf{Max}$ enabling to improve shift invariance in CNNs architecture while preserving high-frequency information.

Publications

- Hubert Leterme, Kévin Polisano, Valérie Perrier, Karteek Alahari. **Modélisation Parcimonieuse de CNNs avec des Paquets d'Ondelettes Dual-Tree**. ORASIS 2021 - Journées francophones des jeunes chercheurs en vision par ordinateur, Centre National de la Recherche Scientifique [CNRS], Sep 2021, Saint Ferréol, France. pp.1-9. ⟨hal-03339792v2⟩

- Hubert Leterme, Kévin Polisano, Valérie Perrier, Karteek Alahari. **On the Shift Invariance of Max Pooling Feature Maps in Convolutional Neural Networks**. 2023. ⟨hal-03779434v2⟩

- Hubert Leterme, Kévin Polisano, Valérie Perrier, Karteek Alahari. **From CNNs to Shift-Invariant Twin Models Based on Complex Wavelets**. 2023. ⟨hal-03880520v2⟩

UGA Université Grenoble Alpes

Inria

LJK Laboratoire Jean Kuntzmann
Mathématiques appliquées - Informatique

PERSYVAL-Lab

MIAI Grenoble Alpes

Thank you!